

**Molecular mechanisms of PARP inhibitor sensitivity in
primary triple negative breast cancer**

Neha Chopra

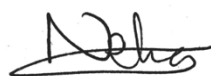
**Breast Cancer Now Centre
The Institute of Cancer Research
University of London**

**Submitted for the degree of MD (Res)
September 2020**

Declaration of originality

I declare that the work presented in this thesis is my own.

Any work that is not mine has been referenced and any data originating from collaborative work has clearly been identified.

A handwritten signature in black ink, appearing to read 'Neha', with a horizontal line underneath.

Neha Chopra

Abstract

Triple negative breast cancer (TNBC) encompasses molecularly different subgroups, with a subgroup harbouring evidence of defective homologous recombination (HR) DNA repair. At present there are no biomarkers available in the clinic to identify this subgroup and hence the mainstay of treatment remains to be chemotherapy.

The objectives of the work presented here were to:

- Identify biomarkers of homologous recombination deficiency in TNBC
- Assess the response activity of PARP inhibition in primary sporadic TNBC

Initial validation work used samples from the ChemoNEAR study to optimise a functional biomarker of HR deficiency using RAD51 immunohistochemistry (IHC). Using next generation sequencing techniques, a *BRCA1* and *RAD51C* methylation multiplex was designed using bisulfite sequencing in breast cancer samples from the ChemoNEAR study. Taking these two techniques forward into the RIO trial (EudraCT 2014-003319-12), a phase 2 window clinical trial, along with HRDetect a mutational-signature based classifier, a subgroup of HR deficient TNBC was identified.

Whether this subgroup of TNBC, representing the phenotype BRCAness can demonstrate activity to PARP inhibition, was assessed using tissue and liquid derived biomarkers, Ki67 and circulating tumour DNA (ctDNA) respectively. Although Ki67 was not an effective biomarker of response activity, ctDNA dynamics were able to demonstrate response to activity with PARP inhibition in germline *BRCA* and HR deficient TNBC patients.

The identification of HR deficient TNBC is of vital clinical importance if treatment for this aggressive breast cancer subtype is to improve. The work presented here shows that a subgroup of HR deficient TNBC can be identified using functional and genomic biomarkers. PARP inhibition is a promising

treatment in this cohort of patients and using ctDNA dynamics, changes in response to treatment can be assessed. This needs further validation in larger clinical trials to ascertain the most useful biomarker for HRD prediction to guide treatment decisions.

Publications

Chopra N, Tovey H, Pearson A, Cutts R, Toms C, Proszek P, Hubank M, Dowsett M, Dodson A, Daley F, Kriplani D, Gevensleben H, Davies HR, Degasperi A, Roylance R, Chan S, Tutt A, Skene A, Evans A, Bliss JM, Nik-Zainal S, Turner NC. Homologous recombination DNA repair deficiency and PARP inhibition activity in primary triple negative breast cancer. *Nat Commun.* 2020 May 29; 11(1):2662.

Garcia-Murillas I*, **Chopra N***, Comino-Méndez I, Beaney M, Tovey H, Cutts RJ, Swift C, Kriplani D, Afentakis M, Hrebien S, Walsh-Crestani G, Barry P, Johnston SRD, Ring A, Bliss J, Russell S, Evans A, Skene A, Wheatley D, Dowsett M, Smith IE, Turner NC. Assessment of Molecular Relapse Detection in Early-Stage Breast Cancer. *JAMA Oncol.* 2019 Aug 1; 5(10):1473-8.

* **Joint first authors**

Acknowledgements

Nick Turner – Group Leader, Molecular Oncology Group, The Institute of Cancer Research

Nick was the overall supervisor of the project and chief investigation of the RIO trial. During the project Nick provided guidance, direction and review of writing.

Alex Pearson – Senior Scientific Officer, Molecular Oncology Group, The Institute of Cancer Research

Alex co-supervised the project, providing technical oversight, assistance with assay development and guidance of the lab and infrastructure support. Alex supported with strategic input, critique of analyses and review of writing.

Ros Cutts – Senior Bioinformatician, Molecular Oncology Group, The Institute of Cancer Research

Ros performed the alignment, copy number and variant calling for all the sequencing data, including methylation and expression analyses.

Clinical Trials and Statistics Unit - Institute of Cancer Research

Under the guidance of Judith Bliss, the CTSU team conducted the trial analyses of primary and secondary endpoints. Specific acknowledgement to Holly Tovey for her statistic support and Christy Toms and Lynsey Houlton for their trial management.

Histopathology, Breast Cancer Now Research Laboratory, The Royal Marsden Hospital

Frances Daley (Pathology Core Facility Manager) optimised the RAD51 IHC protocol and conducted the RAD51 IHC and immunofluorescence staining. She prepared tissue slides for DNA and RNA extraction. Divya Kriplani (pathology fellow) was involved in optimisation and scoring of RAD51 IHC. She also assisted with the analysis of RAD51 IHC validation. Heidi Gevensleben (pathologist) for help with the optimisation of RAD51 immunohistochemistry and review of Ki67 data. David Robertson (Senior

Scientific Officer, Molecular Cell Biology) performed the immunofluorescence assays and taught me how to use the confocal microscope for scoring.

Academic Department of Biochemistry – The Royal Marsden Hospital

Under the guidance of Prof Mitch Dowsett the Academic Department of Biochemistry team conducted the Ki67 and apoptosis assessments as part of the RIO trial. They also stored the RIO samples and assisted with ensuring the samples were blinded. Specific acknowledgement to Andrew Dodson, Vera Martins, Arjun Naginlal Modi and Kally Sidhu.

Serena Nik-Zainal – CRUK Advanced Clinician Scientist, MRC Cancer Unit University of Cambridge

Serena with the assistance of Helen Davies (Senior Research Associate) conducted the HRDetect assay with samples from the RIO trial. They performed whole genome sequencing and analysis in accordance to the HRDetect protocol to deliver the HRDetect score.

Molecular Oncology Group, The Institute of Cancer Research

As a group, the Molecular Oncology team regularly reviewed and discussed data at meetings, making contributions to the direction and development of the project. They further provided a generously supportive environment in which the work was conducted, with help and advice as required.

Ben O’Leary gave advice and direction with methylation sequencing and ctDNA analysis.

Funding

This work was funded by a Cridlan Fellowship from the Cridlan foundation, Clovis Oncology Inc., Cancer Research UK (CRUK; CRUK Ref A15777) core funding to the ICR Clinical Trials and Statistics Unit, Breast Cancer Now to the Breast Cancer Now Research Centre at The Institute of Cancer Research, and NHS funding to the NIHR Royal Marsden Biomedical Research Centre. HRDetect was funded by a CRUK Grand Challenge Award (C38317/A24043).

Abbreviations

μ L	microlitre
μ M	micromolar
pM	picomolar
bp	base pair
BRCA1	breast cancer 1
BRCA2	breast cancer 2
BSA	bovine serum albumin
CDR15	circulating DNA ratio at day 15
CpG	A 5'-CG-3' dinucleotide
cfDNA	cell free DNA
ctDNA	circulating tumour DNA
DSB	double strand breaks
DAPI	4',6-diamidino-2-phenylindole
ddPCR	digital droplet PCR
DNA	Deoxyribonucleic acid
EDTA	Ethylenediaminetetraacetic acid
EOT	End of Treatment
ER	Oestrogen receptor
FAM	6-carboxyfluorescein
FBS	Foetal bovine serum
FFPE	Formalin fixed paraffin embedded
GMNN	Geminin
H&E	Haematoxylin and Eosin
HER2	Human epidermal growth factor receptor 2
HEX	5' hexachloro-fluorescein
HR	Homologous recombination
HRD	Homologous recombination deficiency
HRR	Homologous recombination repair
HS	High sensitivity
IFF	1% BSA, 2% FBS in PBS
IHC	Immunohistochemistry

LOH	Loss of heterozygosity
mg	milligrams
mL	millilitres
mt	mutant
NAC	Neoadjuvant chemotherapy
NFR	Nuclear fast red
NGS	next generation sequencing
ng	nanograms
NTC	No template control
PALB2	Partner and localizer of BRCA2
PAM50	Prosigna Breast Cancer Prognostic Gene Signature Assay
PARP	Poly (ADP-ribose) polymerase
PBS	Phosphate buffered saline
PCR	Polymerase chain reaction
PFA	4% (w/v) paraformaldehyde in PBS
PR	Progesterone receptor
RIO	Window study of the PARP inhibitor rucaparib in patients with primary triple negative or BRCA1/2-related breast cancer
RNA	Ribonucleic acid
rpm	Revolutions per minute
RPPH1	Ribonuclease P RNA Component H1
STRECK	Cell-free DNA blood collecting tubes
TNBC	Triple negative breast cancer
VIC	VIC dye for probes
WGS	Whole genome sequencing
WHO	World health organisation

Table of Contents

Abstract	3
Publications	5
Acknowledgements	6
Abbreviations	8
Table of Contents	10
List of Figures	15
List of Tables	17
Chapter 1 Introduction	18
1.1 Landscape of triple negative breast cancer	18
1.2 Neoadjuvant Treatment	20
1.3 DNA Double strand break repair	21
1.4 Homologous Recombination Repair and Deficiency	22
1.5 Identifying BRCAness with predictive biomarkers	23
1.5.1 Functional assessment of HRD	24
1.5.2 DNA Methylation associated with breast cancer	25
1.5.3 Mutational Signatures associated with breast cancer.....	26
1.6 PARP Inhibition in breast cancer	26
1.7 Biomarkers of response	29
1.7.1 Ki67 as a biomarker of response	30
1.7.2 Apoptosis as a biomarker of response	30
1.7.3 ctDNA as a biomarker of response	31
1.7.4 Technical approaches associated with ctDNA application	32
1.8 Summary	34
1.9 Hypothesis and Aims	35
Chapter 2 Materials and Methods	36
2.1 RIO trial	36

2.2	RAD51 Immunohistochemistry.....	38
2.2.1	Validation of RAD51: ChemoNEAR Study Samples.....	38
2.2.2	Immunohistochemistry for RAD51/ GMNN double staining.....	39
2.2.3	Immunofluorescence for RAD51/GMNN double staining.....	39
2.2.4	Scanning and uploading of slides onto Hamamatsu Nanozoomer and PathXL.....	40
2.2.5	Scoring RAD51/GMNN for immunohistochemistry: Hamamatsu Nanozoomer and Path XL.....	40
2.2.6	Scoring RAD51/GMMM for Immunofluorescence: Confocal Microscope.....	42
2.2.7	Scoring calculations.....	42
2.3	Processing of tissue for tumour assessment and dissection from RNALater™	42
2.4	DNA extraction from fresh frozen tissue	43
2.5	Processing of plasma and buffy coat DNA	43
2.6	Automated DNA extraction from plasma	43
2.7	DNA extraction from buffy coat	44
2.8	DNA quantification by droplet digital polymerase chain reaction (ddPCR).....	44
2.9	Analysis of digital PCR data	45
2.10	Targeted Tissue sequencing	46
2.11	AVENIO Sequencing	47
2.12	Primer Probe assay design	48
2.13	Optimisation of patient specific dPCR assays.....	50
2.14	Circulating tumour DNA mutational analysis.....	52
2.15	HRDetect	53
2.16	DNA Methylation Method.....	54
	Bisulfite conversion of DNA.....	54
	DNA Quantification by Qubit® 3.0 fluorometer	54
	PCR Amplification	55
	Library Preparation.....	55
	Library assessment with Bioanalyser Chip.....	56
	Library Quantification.....	56
	Sequencing on the Illumina MiniSeq	57
	Bioinformatic sequencing analyses	57

2.17 RNA Sequencing.....	58
RNA Extraction.....	58
RNA Quantification.....	58
RNA quality assessment with bioanalyser chip	58
RNA Sequencing	59
Bioinformatic RNA sequencing analysis.....	59
Chapter 3 RAD51 Immunohistochemistry Validation	60
3.1 Introduction.....	60
3.2 Hypothesis.....	62
3.3 Aims	62
3.4 Acknowledgements.....	62
3.5 Results	63
3.5.1 Validation of RAD51: ChemoNEAR Study Samples.....	63
3.5.2 Immunohistochemistry for RAD51/ GMNN double staining.....	65
3.5.3 Immunofluorescence for RAD51/GMNN double staining	70
3.5.4 Validation between immunohistochemistry and Immunofluorescence	72
3.5.5 Validation of assessing total cells/ field versus 100 cells/ field	76
3.5.6 Validation of number of RAD51 foci to count	77
3.5.7 Correlation between scorers	78
3.5.8 Number of tumour cells and GMNN cells to be counted for validity of sample	79
3.5.9 RAD51 score based on subtypes	80
3.5.10 Cut off to determine Homologous Recombination Deficiency (HRD).....	81
3.5.11 Final criteria for RAD51 Scoring	82
3.6 Discussion	83
Chapter 4 BRCA1 and RAD51C Methylation Validation	86
4.1 Introduction.....	86
4.2 Hypothesis.....	89
4.3 Aims	89
4.4 Acknowledgements.....	89
4.5 Results	90
4.5.1 Validation of <i>BRCA1</i> and <i>RAD51C</i> methylation primers	90

4.5.2	Validation of <i>BRCA1</i> and <i>RAD51C</i> methylation multiplex	93
4.6	Discussion	98
Chapter 5	Predictive biomarkers of homologous recombination deficiency (HRD) in TNBC	100
5.1	Introduction.....	100
5.2	Hypothesis.....	104
5.3	Aims	104
5.4	Acknowledgements.....	104
5.5	Results	105
5.5.1	HRDetect as a predictive biomarker of HRD.....	105
5.5.2	Identification of <i>BRCA1</i> and <i>RAD51C</i> Methylation in sporadic TNBC.....	108
5.5.3	<i>RAD51</i> Immunohistochemistry as a functional HRD biomarker.....	111
5.5.4	Sensitivity of predictive HRD biomarkers	117
5.6	Discussion	119
Chapter 6	Assessment of response activity in primary TNBC treated with rucaparib	123
6.1	Introduction.....	123
6.2	Hypothesis.....	127
6.3	Aims	127
6.4	Acknowledgements.....	127
6.5	Results	128
6.5.1	A fall in Ki67 as an assessment of response to rucaparib in primary TNBC.....	129
6.5.2	Apoptosis induction after treatment with rucaparib in primary TNBC	130
6.5.3	Mutation detection using targeted and whole genome sequencing and assay optimisation.....	131
6.5.4	ctDNA as a biomarker of response to rucaparib	137
6.6	Discussion	141
Chapter 7	Conclusions	146
Chapter 8	References	151
Appendix 1	Rad51 GMNN double staining on FFPE	178

Appendix 2 Immunofluorescence for RAD51/GMNN	180
Appendix 3 SOP 031 RAD51 IHC.....	183
Advanced preparation for immunohistochemistry staining	185
Preparation of samples	186
Rad51/gmmn staining with immunohistochemistry	186
Upload of slides to hamamatzu nanozoomer.....	187
Upload of slides to path xl xplore	188
Counting on path xl xplore	189
Appendix 4 Ki67 Protocol	192
Thanks	211

List of Figures

Figure 1 RIO Trial Design.....	37
Figure 2 ChemoNEAR Study Schema	38
Figure 3 RAD51/GMNN Immunohistochemistry using PathXL Xplore	41
Figure 4 ChemoNEAR Study Design	63
Figure 5 Consort of RAD51/GMNN immunohistochemistry.	64
Figure 6 RAD51/ GMNN IHC negative control	66
Figure 7 RAD51/ GMNN IHC at baseline	67
Figure 8 RAD51/ GMNN IHC positive control.....	68
Figure 9 RAD51/ GMNN IHC at 24-48 hours after 1 st cycle of chemotherapy	69
Figure 10 RAD51/GMNN IF.....	71
Figure 11 Validation of proliferation fraction and RAD51 score.....	73
Figure 12 Image from PathXL digital imaging platform.	75
Figure 13 Correlation between number of tumour cells scored.....	76
Figure 14 Number of RAD51 foci and timepoint assessed.....	77
Figure 15 Correlation between scorers	78
Figure 16 Minimum requirement for total tumour cells and GMNN positive cells.....	79
Figure 17 Rad51 score based on subtype.....	80
Figure 18 RAD51 score to determine HRD	81
Figure 19 <i>BRCA1</i> and <i>RAD51C</i> methylation sequences	90
Figure 20 Optimisation of <i>BRCA1</i> methylation primers	91
Figure 21 Optimisation of <i>RAD51C</i> methylation primers.....	92
Figure 22 Bioanalyzer tracing of multiplex PCR methylation primers.....	94
Figure 23 Optimum number of PCR cycles	95
Figure 24 Comparison of column versus beads for PCR clean up.....	96
Figure 25 <i>BRCA1</i> and <i>RAD51C</i> methylation status of individual CpG sites	97
Figure 26 Consort diagram to determine predictive biomarkers of HRD.....	105
Figure 27 Biomarkers of homologous recombination (HR) repair deficiency	107
Figure 28 <i>BRCA1</i> and <i>RAD51C</i> Methylation of BRCA versus non BRCA	110
Figure 29 RAD51 EOT IHC images.....	112
Figure 30 RAD51 EOT IHC images.....	113
Figure 31 Assessment of functional RAD51 deficiency.....	116
Figure 32 Association HRDetect score Other HRD markers.....	117

Figure 33 Individual gene analysis, HRDetect, HRD index and RAD51 IHC	118
Figure 34 Consort diagram to determine biomarkers of response	128
Figure 35 Ki67 staining	129
Figure 36 Effect of rucaparib on Ki67 expression.....	130
Figure 37 Effect of rucaparib on cleaved PARP expression.....	131
Figure 38 Mutations identified on targeted sequencing.....	132
Figure 39 RIO target sequencing compared to MSKCC cBioPortal and WGS	133
Figure 40 Temperature gradient of sample 28 with a TP53 mutation c.273G>A ...	134
Figure 41 An optimised multiplex for patient 22 using tumour tissue.	135
Figure 42 Correlation of allele frequency between	136
Figure 43 Baseline mutant copies/ml of patients with ctDNA detected	136
Figure 44 Example digital PCR ctDNA analysis plot	138
Figure 45 Change in circulating tumour DNA (ctDNA)	139
Figure 46 Associations of ctDNA change	140

List of Tables

Table 1 ABC-Bio Targeted Panel	46
Table 2 Roche AVENIO ctDNA Targeted Panel (17 genes)	47
Table 3 Roche AVENIO ctDNA Expanded Panel (77 genes).....	47
Table 4 Primer design parameters for dPCR	49
Table 5 Probe design parameters for dPCR	49
Table 6 20X Primer-probe cocktail mix.....	49
Table 7 RIO Trial dPCR assays	51
Table 8 PCR Mastermix	52
Table 9 PCR reaction	52
Table 10 PCR mix for DNA methylation	55
Table 11 Library Preparation PCR reaction.....	56
Table 12 Tumour cells/ field	76
Table 13 Apoptosis induction	130

Chapter 1 Introduction

Triple negative breast cancer (TNBC) represent 10-17% of breast cancers and are characterised by tumours that do not express oestrogen receptor (ER), progesterone receptor (PR) and are not HER-2 amplified¹. TNBC is highly proliferative, aggressive, has a disproportionately high risk of metastasis and has a shorter median time to relapse and death in comparison to other subtypes of breast cancer². Poor outcomes are compounded by a lack of suitable targeted agents and chemotherapy is the only systemic treatment available³.

The advancement and widespread use of scientific technology has allowed understanding of the heterogeneity of TNBC. Current research has shown TNBC is not just one entity of breast cancer but encompasses a variety of molecularly distinct diseases which may ultimately require different treatments^{4,5}. Despite these scientific advances the clinical management of TNBC still relies on the assessment of ER, PR and HER2 status and treatment is limited to chemotherapy. Identifying biomarkers, the establish the subgroups of TNBC could enable the use of target treatments with or without chemotherapy to improve the outlook for this disease.

PARP inhibition has shown great promise in *BRCA1/2* mutated tumours and olaparib is licenced for advanced *BRCA1/2* mutated ovarian cancer and activity has been seen in *BRCA1/2* mutated breast cancer^{6,7}. There is strong evidence suggesting a subset of TNBC behaves similarly to *BRCA1/2* mutated breast cancer and has the potential to be sensitive to PARP inhibition⁸⁻¹⁰, however clinical trials to date have not shown a benefit with PARP inhibitors in non-biomarker selected TNBC⁷. The aim of this thesis is to identify biomarkers in TNBC that may identify a subset of TNBCs that are sensitive to PARP inhibition and to assess response activity.

1.1 Landscape of triple negative breast cancer

TNBC tends to occur in younger patients, be larger in size, have a higher grade, lymph node involvement and are more biologically aggressive than hormone receptor positive tumours. Although they are more likely to respond to chemotherapy in the early setting, they still have a high risk of early metastases and death^{4,5,11,12}.

The current histological classification of TNBC includes a collection of tumour subtypes and this overarching characterisation includes a spectrum of less aggressive tumours such as secretory or adenoid cystic and more aggressive metaplastic tumours. As TNBCs are classified as one disease entity and with the lack of individualised molecular characterisation, treatment options other than chemotherapy are limited^{5,12}.

Since the early 2000s there has been an increase in knowledge about the heterogeneity of TNBC and gene expression analyses have shown that it is not one disease entity and can be classified into six separate subtypes; basal-like 1 and basal like 2 (BL-1, BL2), mesenchymal and mesenchymal stem-like (M and MSL), immunomodulatory group (IM) and a luminal androgen receptor group (LAR)^{13,14}. Lehmann *et al* went on to show that different molecularly targeted treatments can be effective in treating the different TNBC gene expression subtypes⁵. Additionally using this classification, a retrospective study concluded there were differences in responses to neoadjuvant chemotherapy depending on the TNBC subtype, increasing the likelihood that biomarkers to identify the subtypes of TNBC are essential to ensure the correct molecularly target treatments are available¹⁵.

The microenvironment of breast cancer includes tumour infiltrating lymphocytes (TILs) which has shown to have a prognostic and predictive benefit in early stage TNBC. A metaanalysis involving 37 studies in TNBC indicated that a high TIL level significantly increased pCR rates (OR 2.14, 95% CI 1.43–3.19), disease free survival (HR 0.66, 95% CI 0.57–0.76) and overall survival (HR 0.58, 95% CI 0.48–0.71)¹⁶. Recent data in HR deficient and *BRCA1/2*-mutant high grade serous ovarian cancer demonstrated enrichment of immune cell infiltration and it was hypothesised that the increase in TIL may increase the production of neoantigens and provide a rationale to combine treatment strategies^{17,18}. However, in a pooled analysis in TNBC, patients treated with neoadjuvant platinum based chemotherapy, TIL density was not significantly associated with HRD status¹⁸. It was suggested that TIL and HRD were distinct and in early stage TNBC tumour immunogenicity is an independent phenomenon¹⁸.

1.2 Neoadjuvant Treatment

Neoadjuvant therapy, also known as preoperative therapy or primary systemic therapy, refers to administration of systemic therapy in patients before surgery, as opposed to after surgery (adjuvant)¹⁹. Dating back to the 1970s, studies have shown benefit of primary chemotherapy in patients with unresectable locally advanced breast cancer leading to complete responses, and in the early 2000s studies confirmed similar clinical outcomes advocating the role for neoadjuvant versus adjuvant therapy in high risk patients^{20–25}. Along with reducing the extent of surgery, neoadjuvant therapy offers a valuable platform to monitor individual tumour response. Pre- and mid-treatment biopsies can be utilised for gene expression, whole genome or exome sequencing identifying predictive biomarkers of response providing valuable insights about therapeutic potential of a drug or tumour response^{26–28}. This has shifted the management of early breast cancer to utilise this window of opportunity in neoadjuvant therapy. It allows the study of novel agents and therapeutic strategies identifying markers that can differentiate patients who may benefit from continuing or changing their current treatment, enabling a more personalised treatment^{19,29}.

Neoadjuvant chemotherapy (NAC) for TNBC now plays an integral part in treatment of this disease, to downstage tumours aimed at reducing the impact of surgery and to explore the response of chemotherapy. Given the benefit of PARP inhibitors in gBRCA-positive metastatic breast cancer, PARP inhibitors have been evaluated in the neoadjuvant setting for early breast cancer. The I-SPY 2, phase 2 multi-centre adaptively randomised trial evaluated the neoadjuvant combination of the PARP inhibitor veliparib with carboplatin and paclitaxel, followed by anthracycline and cyclophosphamide compared to the standard taxane and anthracycline regime in stage II-III HER2-negative breast cancers³⁰. The estimated pCR rate was 33% versus 22% in favour of the addition of veliparib to chemotherapy and in the TNBC population this was 51% to 26% respectively. This led to the phase 3 study BRIGHTNess which evaluated three neoadjuvant strategies; paclitaxel alone, paclitaxel plus carboplatin and paclitaxel, carboplatin and veliparib³¹. Patients who received carboplatin had a higher pCR although this was not improved with the addition of veliparib. Whether this was due to veliparib not being a strong PARP inhibitor remains to be explored and further clinical trials are under way to evaluate the PARP inhibitor and chemotherapy

combination. It does need to be considered that the combination of chemotherapy and PARP inhibition has a challenge of overlapping toxicities and whether PARP inhibition alone is able to achieve the same response rate needs to be determined.

An initial pilot study at the MD Anderson Cancer Centre evaluated 2 months of talazoparib prior to neoadjuvant chemotherapy in gBRCA-positive patients with stage I-III disease³². The study was able to recruit 13 patients within 8 months and found a radiological response with a median decrease in tumour volume of 88% (30-98%). This led to a further study using 6 months on talazoparib in the neoadjuvant setting to assess pathological response³³. Pathological complete response was observed in 53% of patients and toxicities were manageable and a phase 2 study is currently ongoing (ClinicalTrials.gov identifier: NCT03499353).

The neoadjuvant setting is becoming a significant platform for exploring response to systemic therapy prior to primary surgery. Studies are in progress to establish PARP inhibitors in this setting and should they show improved response rates to chemotherapy it is possible to change the paradigm of patients care.

1.3 DNA Double strand break repair

DNA is subjected to endogenous (metabolic reactions and replication stress) and exogenous (radiation and chemotherapeutics) insults throughout a cell's life cycle that impair DNA replication and correct chromosome segregation³⁴. There are various types of DNA damage such as base lesions, intra- and inter-strand cross links, DNA protein cross-links and single- and double-strand breaks (DSBs)³⁴. Many lesions inhibit replication fork progression and result in replication fork collapse and DSB formation³⁵.

DSBs are cytotoxic lesions that threaten genomic integrity and occur when the phosphate backbone of the two complementary DNA strands are broken simultaneously^{34,36-38}. They are one of the most cytotoxic lesions and it is therefore paramount that they are repaired promptly and accurately to prevent mutation formation or larger scale genomic instability which can have tumorigenic potential or lead to apoptosis³⁹. Due to the implications of DSBs, eukaryotic cells have developed

complex and highly conserved systems to rapidly and efficiently identify the lesions and instigate their repair and arrest of the cell cycle or undergo apoptosis³⁹.

When a DSB is detected, close to the break site, the histone variant H2AX is phosphorylated to γ H2AX and serves as a molecular beacon signalling the presence of damage⁴⁰. γ H2AX plays a central role in linking the damaged chromatin to the DNA repair machinery, directing the recruitment of multiple DNA repair and signalling proteins into repair centres⁴⁰.

DSB repair can involve four mechanisms; classical nonhomologous end joining, homologous recombination (HR), alternative end joining and single-strand annealing. Alternative end joining and single-strand annealing are DSB repair pathways but are error-prone and can result in harmful genomic consequences³⁶. Classical nonhomologous end joining and HR are both cell cycle dependent.

1.4 Homologous Recombination Repair and Deficiency

Homologous recombination repair (HRR) is a series of interrelated pathways for the critical support for DNA replication and eventual DNA recovery leading to the repair of DSBs and failure of this repair pathway leads to genomic instability contributing to cancer aetiology⁴¹. HRR occurs after DNA replication in order to utilise the identical sister chromatid as a template for repair and is restricted to the S/G2 phases of the cell cycle. To reduce the likelihood of errors, cells have evolved mechanisms controlling HR ensuring it is invoked at the right time and location. HRR is a high-fidelity process initiated when the DSB is resected generating a single stranded DNA 3'-overhang for which the RAD51 recombinase attaches and invades the homologous sequence to use as a template for DNA repair⁴⁰. The RAD51 proteins are central to HRR, forming the nucleofilament scaffold and mediates the attraction of other HR proteins including BRCA2; the main mediator of the RAD51 nucleofilament formation, PALB2 and BRCA1⁴².

Homologous recombination is the principle DSB repair mechanism and cancers with a defective HR pathway, due to defective BRCA1, BRCA2 or other pathway components, compensate by activating an alternative pathway for which the cancer is dependent on for survival⁴³. DNA is either repaired with error prone pathways such as

NHEJ or SSA leading to DNA alterations including deletion of genetic material or not and all, both of which leads to genomic instability^{43–46}.

Homologous recombination deficiency (HRD) was initially described in cancers with germline mutations of the tumour suppressor genes *BRCA1* and *BRCA2* and has driven the development of PARP inhibitors. This cohort of breast cancers are highly sensitive to PARP inhibitors, that target the underlying HR DNA repair defect in these cancers, with the recent FDA approval for olaparib and talazoparib in advanced germline *BRCA1/2* mutated patients with HER2-negative locally advanced or metastatic breast cancer^{47,48}.

1.5 Identifying BRCAness with predictive biomarkers

The term ‘BRCAness’ has been attributed to sporadic tumours with molecular and phenotypic characteristics similar to *BRCA*-mutated cancers and in theory should be susceptible to PARP inhibitors^{43,49,50}. A phase 2 clinical study in women with germline or somatic *BRCA1* or *BRCA2* mutant ovarian cancer showed a benefit from maintenance olaparib therapy improving progression free survival by 7 months⁵¹. This led to the approval of olaparib by the US Food and Drug Administration (FDA) and European Medicines Agency (EMA) as maintenance therapy in ovarian cancer making it the first targeted treatment for a somatic *BRCA1/2* mutated cancer, paving the way to targeted treatment for BRCAness⁴⁵.

However, a clinical trial in an unselected heavily pre-treated advanced TNBC population showed no activity with the PARP inhibitor olaparib⁷. Within the neoadjuvant setting the BRIGHTNess study³¹, failed to demonstrate a benefit with the addition on veliparib. Therefore, the extent as to whether PARP inhibitor efficacy may translate to sporadic TNBC is unknown, as is the best way to select HR deficient/ BRCAness cancers.

Over 80% of hereditary *BRCA1* breast cancers are triple negative, and sporadic TNBCs show similar histological and transcriptomic characteristics to *BRCA1*-mutation carriers, suggesting that *BRCA1* inactivation may have a role in sporadic TNBCs^{49,52–55}. Over the last decade, several methods have been utilised to identify

'BRCAness' within sporadic tumours. Rapid development of next generation sequencing (NGS) shows TNBC has a diverse array of defects in HR DNA repair, through germline mutations in *BRCA1*, *BRCA2* and *PALB2*, somatic mutations in *BRCA1* and *BRCA2*, promoter methylation of *BRCA1* and *RAD51C*, and likely in other as yet to be identified mechanisms⁵⁶⁻⁵⁹. With this array of information several different HRD tests, mainly based on specific genomic or transcriptomic patterns, have been designed to identify this patient cohort^{53,54,60-65}, however no gold standard test for predicting response to PARP inhibitors has been established. Although these tests provide a vast amount of data it remains to be determined whether they can reflect the real-time HR status of a tumour which will ultimately affect the clinical response to PARP inhibition⁶⁶.

1.5.1 Functional assessment of HRD

Many of the HRD markers to date are based of genomic patterns or transcriptomic predictors of BRCAness measuring the accumulation of mutational and chromosomal aberrations over time, but they fail to assess the real time HR status. Independent of the underlying cause for HRD, the HR phenotype can be assessed functionally, precisely detecting patients who may benefit from PARP inhibition at the time treatment is required.

RAD51 nuclear foci do not form in cells that lack functional *BRCA1/2* or other functional HRR components. A functional HRD assay was first described by Graeser *et al* who used immunofluorescence to detect RAD51 foci formation in breast tumours 24 hours after anthracycline treatment, providing evidence that RAD51 focus formation can serve as a predictive biomarker of HRD⁶⁷. Further efforts to validate a functional assay for clinical use have been made and some are still in clinical trials using fresh tumour biopsies and ascities^{66,68-72}. A Dutch group have validated a functional assay, the Repair Capacity (RECAP) test, on tumour tissue exploiting the formation of RAD51 foci in proliferating cells after *ex vivo* irradiation of fresh breast cancer tissue^{71,72}. This immunofluorescence based test detected HRD in 19% (24/125) of primary breast cancer, of which 29% (7/24) were not related to a *BRCA1/2* mutation⁷². The HRD tumours were significantly associated with an increase in tumour infiltrating lymphocytes ($p=0.023$)⁷².

The group also postulated RECAP has the ability to detect reversion of the HRD phenotype in *BRCA*-deficient tumours that have been previously treated with DNA damaging chemotherapies inducing resistance, an important aspect to consider in the metastatic setting⁶⁶.

1.5.2 DNA Methylation associated with breast cancer

DNA methylation is an epigenetic mechanism that regulates gene expression by adding or removing a methyl group at the fifth carbon of the pyrimidine ring of cytosine to form 5-methyl-cytosine. The human genome contains about 30,000 5'-C-phosphate-G-3' (CpG) islands and many occur at gene promoters and are usually unmethylated^{73,74}. DNA methylation of the CpG islands is associated with the dysregulation of DNA pathways and genomic instability and is evident by reversible modification of DNA and gene silencing⁷³. Although these alterations are reversible they are very stable and can exert significant impact on gene expression mimicking the effect of deleterious mutations of tumour suppressor genes causing their silencing and can serve as the first or second hit in Knudson's model for tumour development^{73,75,76}. Methylation of the *BRCA1* and *RAD51C* promoter denotes BRCAness and HRD in TNBC^{49,57,73,77,78}.

The *BRCA1* gene is located on chromosome 17q12-21 and is a classical tumour suppressor gene, playing a crucial role in DNA repair, homologous recombination, checkpoint cell cycle control and transcription. Although germline mutations account for the majority of *BRCA1* associated breast cancers there is evidence for epigenetic silencing of *BRCA1* leading to decreased gene expression with a prevalence ranging from 5% to 65% in sporadic breast cancers⁷⁹⁻⁸⁴. A meta-analysis associated *BRCA1* promoter methylation with triple negative phenotype (OR = 2.79, 95%CI 1.74-4.48, $P < 0.001$) and a decrease in *BRCA1* protein expression⁸⁵. Preclinical studies with *BRCA1* mutated and *BRCA1* methylated tumours conferred similar sensitivity to PARP inhibitors⁸⁶⁻⁸⁸.

RAD51C acts with *RAD51* at sites of DNA damage to assist repair through the HR repair pathway, and depletion of *RAD51C* leads to impaired function of *RAD51* and ultimately decreased DNA repair, evidenced by impaired *RAD51* foci formation⁸⁹.

Polak *et al* were able to demonstrate epigenetic silencing of *RAD51C* in basal-like breast cancer reflected by reduced gene expression and the characteristic HRD signature, cementing its importance as a cause for HRD in tumours⁵⁷. Preclinical models with *RAD51C*-deficient cancer cells have shown sensitivity to PARP inhibitors indicating its translational importance in patient stratification for targeted HRD agents⁸⁹.

1.5.3 Mutational Signatures associated with breast cancer

Over the last decade, advances in whole genome sequencing (WGS) have led to the identification of mutational processes that leave a characteristic imprint, a mutational signature on the cancer genome. These have revolutionised our understanding of cancer and have the capability to improve diagnosis and treatment of cancer^{90,91}. Cancers with defects in HR based DNA repair have characteristic chromosomal changes reflecting the use of alternative error-prone repair pathways imprinting a 'genomic scar'⁹². This has led to the discovery of specific mutation profiles associated with an indicative HR defect, specifically signature 3^{57,90,91}. Measures of genomic instability; loss of heterozygosity, telomeric allelic imbalance and large-scale state transitions can accurately identify *BRCA1/2* tumours⁶⁰⁻⁶², and their combination to form the HRD Score has allowed identification of HR-deficient tumours (HRD Score >42), independent of *BRCA1/2* deficiency within a sporadic TNBC population⁶³.

Recent work has identified WGS signatures of HR deficiency with *BRCA1/2* deficient tumours associated with distinct mutational signatures. The mutational signatures and chromosomal instability markers of HR deficiency have been aggregated into the HRDetect score, robustly identifying *BRCA1/2* tumours with potential greater accuracy than indices such as HRD-score^{64,93}. Additionally, within the TNBC population HRDetect is more specific than current substitution signature and copy number aberration assays, notably HRD score, expanding the proportion of HRD tumours within TNBC⁵⁹.

1.6 PARP Inhibition in breast cancer

The poly (ADP-ribose) polymerases (PARPs) are a family of 18 enzymes that have the ability to catalyse the transfer of ADP-ribose to target protein, and PARP1 and 2 are the only ones known to play a role in the DNA damage repair of single strand breaks

via the base excision repair pathway⁹⁴. PARP1 binds at sites of DNA damage on single strand breaks causing a catalyst of changes for its activation via its zinc-finger DNA-binding domain creating polymers of poly(ADP-ribose) and recruitment of DNA effectors such as DNA ligase III, DNA polymerase beta, and the XRCC1 protein^{95,96}.

Cells deficient in either PARP or BRCA are viable, however the loss of both results in a lethal phenotype, known as 'synthetic lethality'. The concept of synthetic lethality was developed from studies in *Drosophila* and *Candida* nearly a century ago and subsequently entered into cancer therapeutics⁹⁷⁻¹⁰¹. In 2005, two seminal papers described the interaction between PARP inhibition and *BRCA1/2* mutated tumours resulting in synergistic cell death^{8,102}. The interaction was 1000 times more potent compared to BRCA-wild type tumours, and instigated the first clinical trials of single agent PARP inhibitors⁸.

It was initially thought the mechanism underlying synthetic lethality was the accumulation of SSBs due to PARP inhibition causing stalling of the DNA replication forks, subsequently leading to DNA DSB formation¹⁰³. However, this model was modified from data suggesting that PARP inhibitors 'trap' PARP1 onto DNA preventing autoPARylation and PARP1 release from the site of damage interfering with the catalytic cycle of PARP1 and causing a cytotoxic lesion⁴³. In HR deficient tumour cells DSB repair is forced to alternative error prone repair mechanisms resulting in chromatid instability, cell cycle arrest and eventual apoptosis¹⁰⁴. Notably PARP1/2 have other roles in transcription, apoptosis and immune function which also may lead to their anti-tumour effects of PARP inhibition and is important to acknowledge in the era of combination therapy and the advent of immunotherapy¹⁰⁵.

The understanding of PARP 1 and 2 function led to the development of PARP1/2 inhibitors originally for the sensitisation of tumour cells to conventional treatments; chemotherapy and radiotherapy. The first PARP inhibitor formulated 40 years ago, nicotinamide, inhibited PARylation, enhanced the cytotoxic effects of DNA damaging agents¹⁰⁶, and subsequently led to the discovery of clinical PARP inhibitors veliparib, rucaparib, olaparib and niraparib and more recently talazoparib⁴³.

Currently there is no rationale to choose one PARP inhibitor over another based on efficacy and safety data. For future direction it is important to understand the activity of individual PARP inhibitors to aid clinical decision making. Of the four approved PARP inhibitors, niraparib has been shown to be more selective for PARP1 and PARP2 compared to olaparib, rucaparib and talazoparib which show broader pan-PARP activity, however this does not explain the clinical differences between the 4 inhibitors¹⁰⁷.

It has been postulated that the higher the potency of PARP trapping the better the efficacy. In vitro studies have found PARP trapping to be more cytotoxic than unrepaired single-strand breaks caused by PARP depletion thought to be because trapped PARP is more likely to cause stalled replication forks and double-strand DNA breaks^{108,109}. Talazoparib demonstrates the highest PARP trapping with veliparib the weakest although currently efficacy and monotherapy activity does not correlate with PARP trapping potency¹¹⁰. However, a study performed at MD Anderson Cancer Centre has demonstrated single agent neoadjuvant talazoparib for 6 months achieved a 53% pathological complete response (pCR). If this is confirmed in the ongoing phase 2 study it may change the thought behind the importance of PARP trapping³³.

To date there has not been a head to head study between PARP inhibitors but Stemmer et al conducted systematic review and network meta-analysis between rucaparib, olaparib and niraparib in metastatic ovarian cancer¹¹¹. There was no difference in clinical outcomes, although niraparib was associated with higher risk of adverse events¹¹¹. Overall the toxicity between the PARP inhibitors is similar with nausea and fatigue being most common and grade 3/4 haematological effects in about 10% of patients. Rucaparib specifically has an higher rate of transaminitis occurring in a third of patients.

Over the years it has become clearer, the synthetic lethal approach with PARP inhibitors is not solely limited to germline *BRCA1/2* mutant cancers but extends to other germline and somatic deficiencies within the HR pathway. This led to the initial Food and Drug administration (FDA) approval in the USA of olaparib in germline *BRCA1/2* in advanced pre-treated ovarian cancer¹¹² and subsequently European Medicines Agency (EMA) approval in germline and somatic *BRCA1/2* ovarian

cancer^{51,113,114}. In breast cancer the first study by Tutt *et al* revealed an overall response rate of 41% with olaparib 400mg in advanced germline *BRCA1/2* breast cancer⁶, however this was not replicated in TNBC possibly due to the heavy pre-treatment of these patients⁷.

Extensive work has been done to identify the BRCAness population within cancers to establish molecularly targetable tumours. Patients with a positive BRCAness-scar have displayed longer progression free survival (PFS) compared to BRCAness-scar negative patients^{63,115–118}. Current breast clinical trials have focused on the germline *BRCA1/2* status for treatment with PARP inhibition^{119–121}, but with increasing data on identifying a HRD population that can benefit from PARP inhibitors, there is scope to extend the use of PARP inhibition within breast cancer, notably in TNBCs with a HR deficiency.

1.7 Biomarkers of response

According to the World Health Organisation, ‘a biomarker is any substance, structure or process that can be measured in the body or its products and influence or predict the incidence of outcome or disease’¹²². The first recognised test for cancer was reported in 1965 by Dr Joseph Gold who discovered the carcinoembryonic antigen in colon cancer and by the 1980s Ca19-9, Ca125 and Ca15-3 were discovered for pancreatic, ovarian and breast cancers respectively^{123,124}.

Two decades ago, reclassification of the subtypes of breast cancer using tissue samples altered clinical practice leading to the development of diagnostic, predictive and prognostic biomarkers^{13,14,125–129}. With the rapid evolution of genomic profiling technologies and molecular targeted therapies there is an increasing demand to identify molecular biomarkers to individualise cancer management based on the molecular features rather than the histological subtype of the tumours. Single-, or multi-gene signature based assays have been developed to measure specific molecular pathways, aiming to guide therapeutic decisions and may have the capability to change practice guidelines¹³⁰. Unfortunately, only 0.1% of potential biomarkers successfully reach clinical translation due to the challenges in the multiple processes involving initial discovery, validation and finally clinical implementation^{130,131}.

Immunohistochemistry (IHC) characterises intracellular proteins of various cell surfaces in all tissues. The technique utilises the staining of histological specimens and is widely used in clinical practice for diagnostic purposes and forms the basis of some prognostic and predictive biomarkers¹³². In breast cancer the most common IHC markers include ER, PR, HER2 and Ki67 and are available in routine clinical practice worldwide¹³². However, the disadvantage of dependency on tissue biopsy samples are it being an invasive technique, the uncertainty of the presence of tumour tissue within the sample and the lack of capturing the heterogeneity of the tumour. With the emergence of genomics and proteomics there has been a rapid development of biomarkers and there is growing evidence for the use of a panel of biomarkers rather than just one to ascertain the molecular portrait of a cancer.

1.7.1 Ki67 as a biomarker of response

Cell proliferation is a tightly regulated process and when uncontrolled, leads to hyperplasia and ultimately carcinogenesis. Nearly three decades ago Ki67 was discovered as nuclear non-histone protein¹³³, and with universal expression in proliferating tissues, Ki67 became a marker of cell proliferation¹³⁴. Ki67 levels are low in G1-early S phase of the cell cycle, as discrete foci in the karyoplasm; becoming large nucleolar foci in G2 and peaking at mitosis when the nuclear membrane disrupts showing Ki67 as an intense expression in the cytoplasm, followed by a rapid decline during anaphase and telophase¹³⁴.

Immunohistochemical expression of Ki67 is assessed using mindbomb E3 ubiquitin protein ligase 1 antibody (MIB1) and current visual reporting of nuclear staining is incorporated into the Ki67 score which is defined as the percentage of positively stained cells among the total number of malignant cells scored¹³⁵. There has been wide variability in the analytical practice of Ki67 and in 2011 a working group was set up to standardise Ki67 analysis and more recently there has been a drive to automate the scoring to advocate standardisation, reproducibility and throughput^{135,136}.

1.7.2 Apoptosis as a biomarker of response

Apoptosis, also known as programmed cell death, is an active process controlled by inducers and repressors and their balance determines whether a cell enters

proliferation of the apoptotic pathway; an imbalance can result in tumourigenesis or tumour progression¹³⁷. Cancerous cell populations exhibit abnormally high cell proliferation and enhanced apoptotic cell death¹³⁷. The enzyme poly ADP polymerase (PARP) is important in the repair of single-strand breaks in DNA. In apoptosis, PARP is cleaved by caspase enzymes (principally caspase-3) into small polypeptide fragments. The IHC demonstration of these cleaved-PARP fragments is a reliable indicator of the apoptotic pathway. The number of apoptotic bodies seen when compared to the total number of cells present gives the rate of apoptosis, known as the Apoptotic Index¹³⁸.

1.7.3 ctDNA as a biomarker of response

Over 70 years ago and 5 years before the discovery of the double helical structure of DNA Mandel and Métais identified the presence of nucleic acids in human blood of normal subjects and in those with various diseases¹³⁹. This was further validated 20 years later in patients with systemic lupus erythematosus, arthritis and hepatitis¹⁴⁰. It was not until 1975 when Leon *et al* found circulating DNA in higher levels in cancer patients (mean 180ug/ml) when compared to non-malignant patients (mean 13ug/ml)¹⁴¹. Although there was no association with tumour site or size, there was correlation with increased amounts of circulating DNA in metastatic disease versus localised disease¹⁴¹. On average, solid tumours have up to 80 somatic mutations¹⁴² with the potential to serve as highly specific biomarkers¹⁴³.

Release of intact cells and subsequent lysis into the bloodstream or apoptosis and necrosis have been proposed mechanisms of release of circulating free DNA (cfDNA), thus both tumour and normal cfDNA circulates in the bloodstream of cancer patients^{140,144,145}. The amount of cfDNA attributed to a tumour depends on the size and the presence of metastases; for a patient with a 100g tumour up to 3.3% of the tumour DNA may enter the bloodstream every day¹⁴³ and its elimination from the circulation via the liver and kidneys is approximately 2 hours^{146,147}.

Tumour-derived mutant DNA can be found in the blood of cancer patients and can be used as a biomarker to track the evolution of the disease. Known as a 'liquid biopsy', it negates the need for repeat tumour biopsies to trace the natural course of the

disease or monitor response during treatment¹⁴⁸. However, despite varied reports of the amount of circulating tumour DNA (ctDNA) in patients with cancer, ranging from 0.01% to 93%, the overall consensus is that the levels are low, challenging its reliable and consistent detection^{143,144,149}. Over the last decade technological advances have overcome these restrictions making it possible to identify both genetic and epigenetic aberrations in ctDNA although standardisation is still required if this is to be taken forward into routine clinical practice¹⁵⁰.

The quantity and quality of ctDNA can vary dramatically between cancers and patients, and hence the detection of ctDNA in the circulation for the detection of tumour-specific genetic aberrations requires specialised equipment. The majority of studies referencing ctDNA as a biomarker are in metastatic disease and hence the advocacy of use of ctDNA in early stage disease has been met with hesitation. In early disease, the low tumour burden of micrometastases raises concern of the adoption of ctDNA as the optimal DNA concentration required for the detection of mutations is approximately 30ng/ml in plasma which can be challenging to obtain^{143,151–153}.

There has been a positive correlation between disease burden and change in ctDNA levels¹⁵⁴ and ctDNA dynamics has been shown to predict response in metastatic breast cancer^{155,156}. This has been recently evaluated in 10 breast cancer patients receiving neoadjuvant chemotherapy¹⁵⁷. Butler et al used a patient specific hybrid capture sequencing panel and followed patients with ctDNA during their treatment. Patients who had a decline in ctDNA levels achieved a pCR at surgery and those failed to show a pCR showed evidence of residual ctDNA. Although this is a very small study it demonstrates the utility of ctDNA dynamics in early breast cancer and will need further validation¹⁵⁷.

1.7.4 Technical approaches associated with ctDNA application

Technological advances, specifically in digital PCR and next generation sequencing (NGS) have increased the sensitivity ctDNA analysis, making it possible to understand the heterogeneous landscape of cancer using a blood sample.

Digital PCR enables the absolute quantification of nucleic acids in a sample through the combination of a limiting dilution, end-point PCR and Poisson statistics^{158,159}. However, its initial adoption was limited by low throughput using microwells or more expensive BEAMing technology¹⁶⁰. With the advent of droplet digital PCR (ddPCR) using water-in-oil droplets, being a high throughput process with low costs associated and allowing for the detection of a single copy of mutant template with levels of detection lower than 0.01% tumour content, dependent on input amount increased acceptance of the utility of digital PCR^{160,161}. However, its main limitation is the detection of a limited number of genomic targets and necessitates the prior knowledge of mutations, limiting its use for primary mutational discovery but is a powerful validation tool¹⁶².

Improvements in NGS have allowed massive parallel sequencing to obtain maximal tumour genomic assessment of DNA by whole-genome, whole-exome and targeted sequencing and RNA sequencing facilitating gene expression analysis¹⁶³. It substantially improves on the traditional sequencing methods, facilitating high throughput by simultaneously sampling multiple genomic regions in multiple samples, reducing time to analysis, a vital component when considering utilisation into clinical practice and importantly reducing the amount of DNA or RNA required¹⁶³. Rosenfeld *et al* were able to discover mutations with allele frequencies as low as 2% strengthening the use of NGS to determine the genomic architecture of ctDNA¹⁶⁴.

Determining which NGS model is required for a specific question requires understanding of the advantages and disadvantages of each process. Whole genome sequencing (WGS) is able to give a comprehensive view without requiring prior knowledge of mutations allowing for more complex analyses such as identifying mutational signatures⁹¹ and identification of structural variants. However, WGS is expensive, requires large amounts of DNA and has challenges in obtaining sufficient depth. Using WES or targeted sequencing although requires prior knowledge of mutations can be conducted using multiplex PCR or hybrid capture with oligonucleotide probes, enabling larger depth and higher coverage of a specific variant, with the ability to detect mutations down to an allele fraction of 1%^{164–166,167}.

A fundamental limitation of NGS are errors introduced during sample preparation and sequencing¹⁶⁸. In order to improve the limits of detection the advocacy of using replicates, bioinformatic strategies to reduce background noise and molecular indices; 'barcoding' the starting molecules with a unique identifier, has improved the sensitivity of the techniques^{166,167,169–171}.

With rapid technical advances in digital PCR and NGS and the combined efforts to improve sensitivity and lower cost has made these techniques possible in clinical studies with the likely future prospect of entering routine clinical practice.

1.8 Summary

Identification of HRD biomarkers is of vital importance in the treatment of TNBC with HRD. The use of functional and genomic biomarkers has the ability to change the landscape of TNBC and ultimately altering treatment options and possibly increasing survival. The ability to assess response early can ensure the correct treatment is adopted for each individual patient.

1.9 Hypothesis and Aims

The extent to which PARP inhibitor efficacy may translate to sporadic TNBC is unknown as is the best way to identify HR-deficient TNBC. Using the RIO trial (CCR4109, REC ID: 14/LO/2181), a translational clinical trial, the objective of this thesis was to examine the following hypotheses:

1. Functional and genomic biomarkers can accurately detect HRD in sporadic TNBC.
2. Ki67, cPARP and ctDNA dynamics can be used to assess rucaparib activity in early TNBC.

The specific aims were:

1. To validate IHC as a reliable method to assess RAD51 foci in primary breast cancer.
2. To develop an assay for *BRCA1* and *RAD51C* promoter methylation using bisulfite conversion and next generation sequencing.
3. To determine if HRDetect can detect HRD in sporadic TNBC in patients with or without an underlying epi(genetic) HR defect.
4. To determine if promoter methylation of *BRCA1* and *RAD51C* can be identified in tumours with HRD.
5. To assess the effect of rucaparib on RAD51 formation in sporadic TNBC.
6. To assess if HRDetect positive cancers have an underlying functional defect in HR DNA repair.
7. To assess Ki67 change in baseline and D12-14 samples as a surrogate of activity to rucaparib.
8. To establish the proportion of patients with sporadic TNBC with apoptosis induction on rucaparib.
9. To assess ctDNA levels in baseline and D12-14 plasma samples and associated changes as a marker of response.

Chapter 2 Materials and Methods

2.1 RIO trial

RIO (CCR4109, REC ID: 14/LO/2181) is a single-group, open-label, phase II window of opportunity study assessing rucaparib efficacy in patients with triple negative or *BRCA1/2* mutant breast cancer prior to commencing primary treatment (neoadjuvant chemotherapy or surgery). Patients were recruited from 10 centres in the United Kingdom.

Patients received 12-14 days of rucaparib and baseline bloods (EDTA and STRECK) and core biopsies (FFPE and RNAlater™) were collected at time of diagnostic biopsy or following study entry. End of treatment (EOT) bloods (STRECK) and biopsies (FFPE and RNAlater™) were taken at surgery or prior to neo-adjuvant chemotherapy within 24-48 hours of the last rucaparib dose (Figure 1).

Key eligibility criteria included breast tumour size ≥ 2 cm or < 2 cm with cytologically/histologically confirmed axillary lymph nodes, WHO performance status 0-2, no prior history of ipsilateral breast cancer within 5 years and no prior treatment with PARP inhibitors. Patients received rucaparib 600mg twice daily for 12-14 days. The primary endpoint was Ki67 response from baseline to EOT defined as a $\geq 50\%$ decrease. Secondary and exploratory endpoints were change in ctDNA levels between baseline and day 12-14, assessment of a genomic predictor of HR deficiency, *BRCA1* methylation, RAD51 focus deficiency in the end of treatment biopsy, apoptosis, and safety and tolerability of rucaparib.

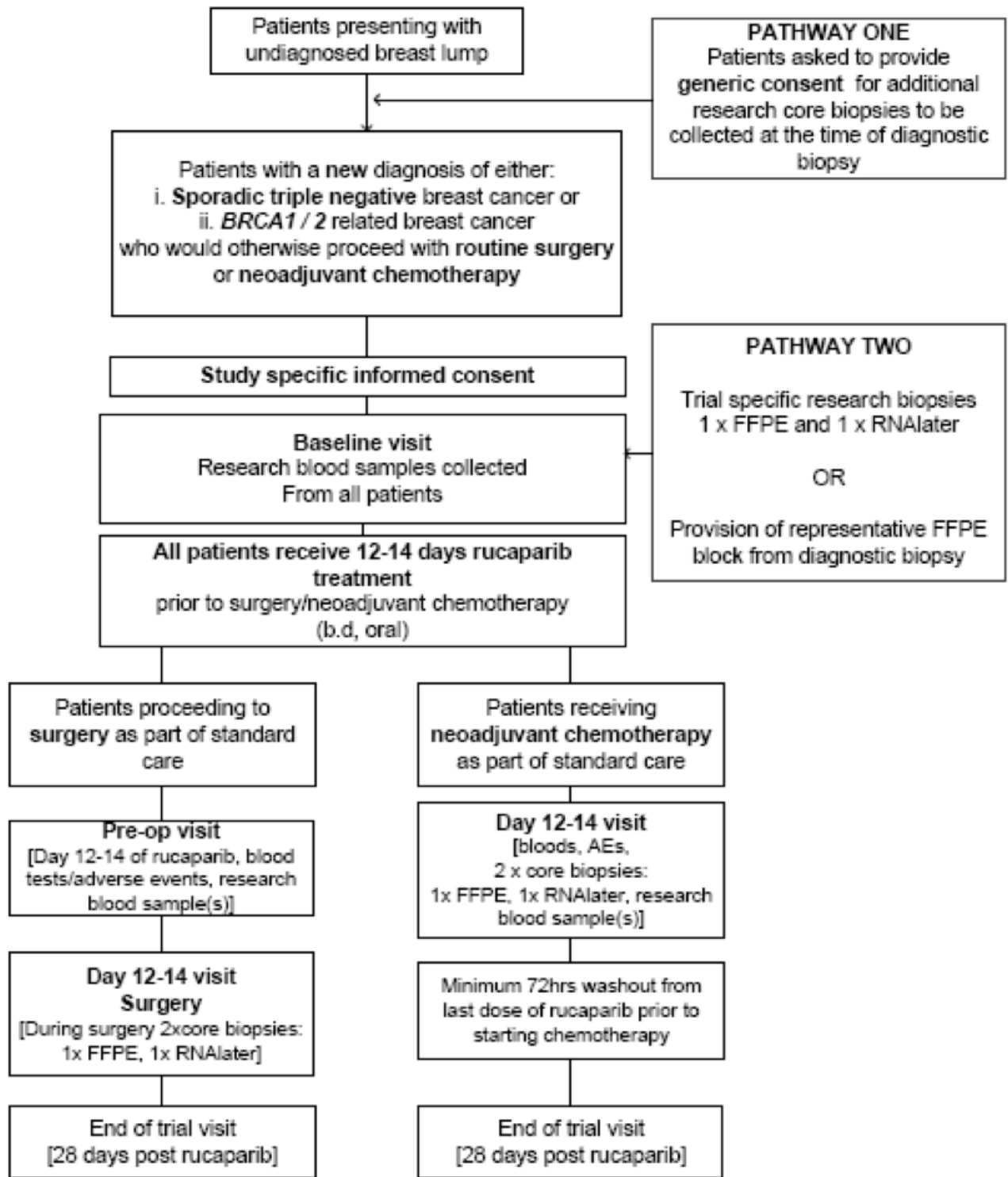


Figure 1 RIO Trial Design

2.2 RAD51 Immunohistochemistry

2.2.1 Validation of RAD51: ChemoNEAR Study Samples

To validate RAD51 IHC, samples from the ChemoNEAR study (CCR3449, REC ID: 11/EE/0063), a multicentre breast cancer tissue collection research study were utilised. All patients irrespective of hormone/ HER2 status undergoing neoadjuvant chemotherapy for primary breast cancer were included in the study. Research biopsies were collected at baseline (B), 24-48 hours post 1st cycle of chemotherapy (H; optional) and prior to the 2nd cycle (C) (Figure 2). Samples were processed at local centres by formalin fixation and paraffin embedding (FFPE) before being sent to and stored at The Royal Marsden Hospital.

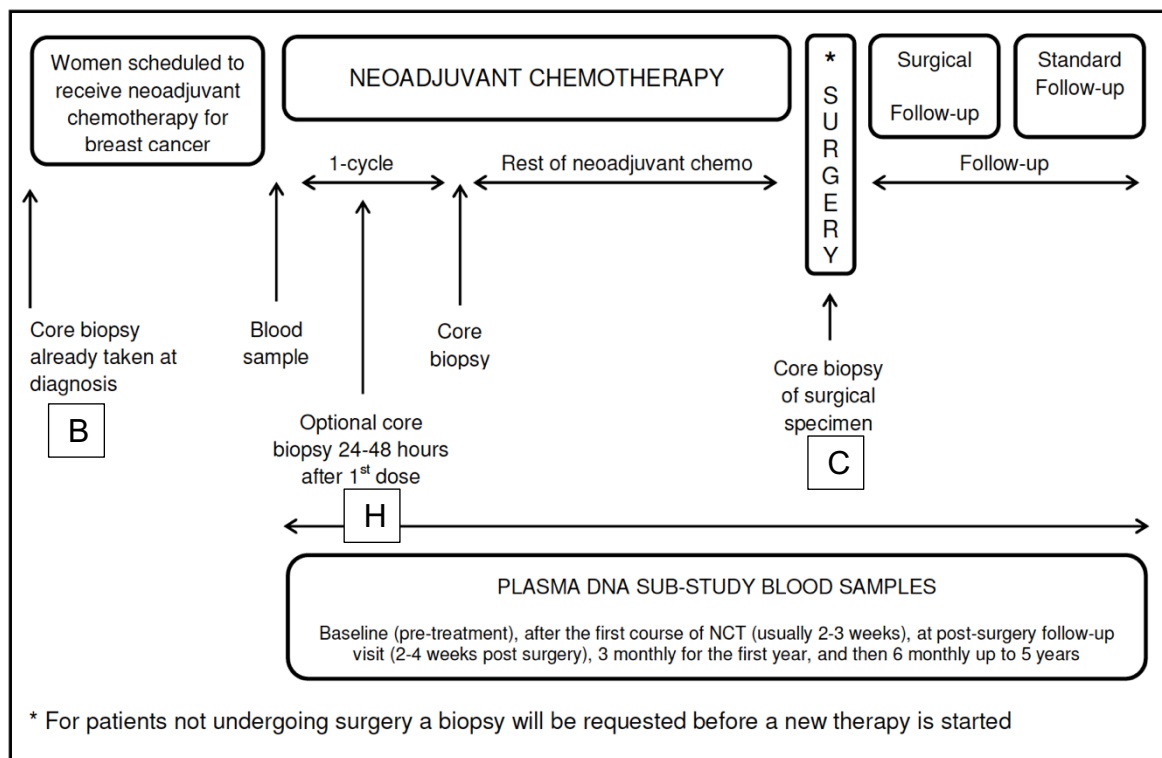


Figure 2 ChemoNEAR Study Schema

2.2.2 Immunohistochemistry for RAD51/ GMNN double staining

Immunohistochemistry was performed by Frances Daley at Breast Cancer Now Core Facility. Two sections of FFPE samples were cut, deparaffinised, rehydrated and stained with either haematoxylin and eosin (H&E) or double stained with GMNN and RAD51. Pre and post radiotherapy induced squamous cell carcinoma were used as negative and positive controls for DNA damage.

Antigen retrieval was performed and RAD51 primary antibody (mouse monoclonal, Genetex, GTX70230) was diluted 1/200 in Dako antibody diluent (K8006) and applied for 1 hour at room temperature. Slides were incubated with Dako Envision Flex HRP (K8002). GMNN antibody (rabbit polyclonal, Proteintech 10802-1-AP) diluted 1/1500 in Dako antibody diluent was applied and incubated with Dako Envision Flex HRP (K8002). Sections were incubated with Vector TMB blue (SK4400) and counterstained with Gills 1 haematoxylin, air dried and dehydrated in xylene before mounted and coverslipped with Vectamount (appendix 1).

2.2.3 Immunofluorescence for RAD51/GMNN double staining

Immunofluorescence was performed by David Robertson at Breast Cancer Now. Antigen retrieval was performed using micro-waving at pH 9 (DAKO pH 9 buffer) for 18 min, let stand for 20 min on deparaffinised and rehydrated 3 μ m sections. Sections were permeabilised with Triton 0.2% for 20 minutes at room temperature, washed in PBS and blocked with IFF (PBS + 1% BSA + 2% FBS). Sections were incubated with anti-GMNN antibody (rabbit polyclonal, Proteintech 10802-1-AP) diluted in 1/400, and anti-rabbit 488 conjugate (Invitrogen A32731, 1/1000 in IFF) added. Sections were incubated with anti-mouse RAD51 antibody (diluted 1/200; Genetex–clone 14B4) and further incubated with anti-mouse 555 conjugate (Invitrogen A-21422, 1/1000 dilution in IFF). Sections were counterstained with DAPI (1/10000 in PBS) and fixed with 4% PFA. Stained sections were rinsed in water and coverslips mounted using Vectashield (appendix 2).

2.2.4 Scanning and uploading of slides onto Hamamatsu Nanozoomer and PathXL

Slides were scanned using the Hamamatsu Nanozoomer-XR digital slide scanner at 40X magnification. Images were uploaded onto PathXL Xplore, an image and data management system. Folders were created for H&E slides, immunohistochemistry and immunofluorescence. To allow for blinded 2 person scoring separate folders were created for each scorer. PathXL Xplore was not used for immunofluorescence scoring as images could not be collected at 40X.

2.2.5 Scoring RAD51/GMNN for immunohistochemistry: Hamamatsu Nanozoomer and Path XL

Five random fields at 40X magnification were identified and marked in PathXL for immunohistochemistry (Figure 3). GMNN positive cells (blue/green staining) were identified and scored for presence of brown RAD51 nuclear foci. Scoring was done independently by 2 scorers blinded to each other, time point and clinical details.

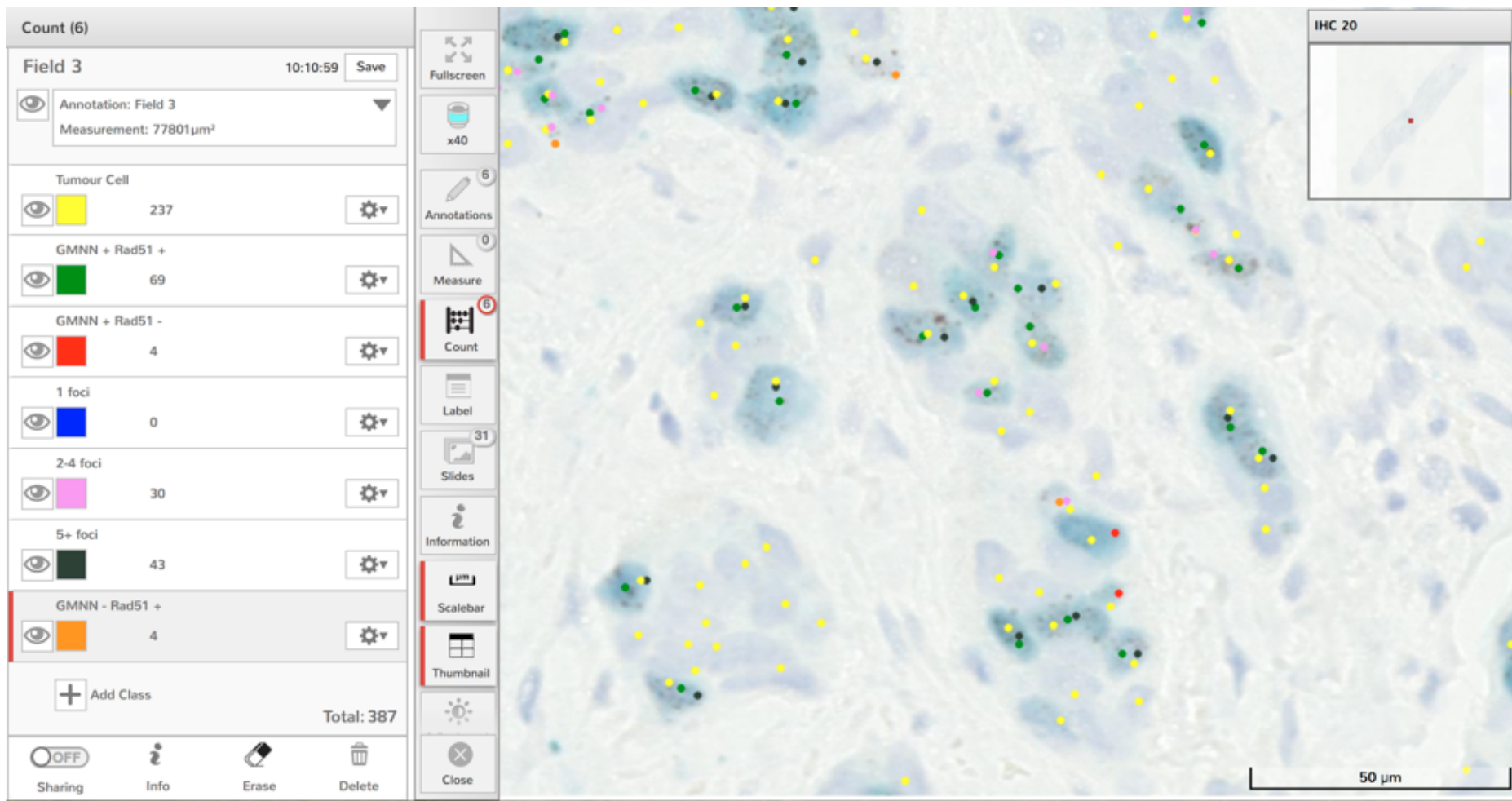


Figure 3 RAD51/GMNN Immunohistochemistry using PathXL Xplore

Immunohistochemistry double stain with RAD51/GMNN from PathXL Xplore using coloured dots to identify tumour cell, GMNN positive cell, RAD51 foci and number of foci. GMNN green stain, RAD51 brown foci

2.2.6 Scoring RAD51/GMMN for Immunofluorescence: Confocal Microscope

Immunofluorescence images were captured on a Leica TCS confocal microscope at 40X magnification over 5 fields. Tumour cells identified by the H&E section were cross referenced with cells positive for DAPI, a nuclear stain (blue) and were counted. Cells positive for GMNN stained green and cells with RAD51 foci had red nuclear foci. Eight samples were scored manually from images captured on the confocal and on the Nanozoomer NDP viewer. PathXL Xplore was not used for immunofluorescence scoring as images could not be collected at 40X magnification using the Nanozoomer automated scanner. Scoring was done by 2 scorers blinded to each other, time point and clinical details.

2.2.7 Scoring calculations

The number of tumour cells, GMNN positive cells and RAD51 positive cells (presence of 5+ foci) were counted. Raw data were collected and the proliferation fraction ((no. of GMNN positive cells/ total number of tumour cells) x100) and RAD51 score ((no. of RAD51 positive cells/ no. of GMNN positive cells) x100) were calculated (appendix 3).

2.3 Processing of tissue for tumour assessment and dissection from RNALater™

All samples were processed by the central laboratory as part of the RIO trial. Fresh tumour samples were collected in RNALater™ tubes, processed within 24-48 hours and stored at -80°C until required for extraction. Baseline biopsies were sectioned using a cryostat. One section was cut for H&E at 4µm and 16 sections were cut at 8µm and counterstained with Nuclear Fast Red (NFR). A second H&E section was cut at the end of the series. A pathologist reviewed and marked the H&E sections and assessed tumour content. If the baseline biopsy did not contain tumour the EOT biopsy was used.

2.4 DNA extraction from fresh frozen tissue

DNA was extracted using the Qiagen DNeasy Blood and Tissue kit (Qiagen.cat# 69504) following the manufacturer's guidelines. NFR sections were micro dissected from tumour using the marked H&E sections for guidance and tissue was placed in a 1.5mL microcentrifuge tube with 180µl buffer ATL and 20µl proteinase K. The sample was vortexed and incubated at 56°C overnight on a heat block with interval mixing at 700 rpm for 10 seconds every 90 minutes. After overnight incubation an additional 20µl proteinase K was added and left to incubate on the heat block at 56°C for 1 hour. 4µl RNase A (100mg/mL) was added and incubated at room temperature for 2 minutes. 200µL buffer AL was added to the sample and mixed by vortexing. 200µL ethanol (96-100%) was added to the sample, vortexed and centrifuged briefly, before being transferred to a Mini Spin column and centrifuged at >6000 x g for 1 minute. The Mini Spin column was put into a new collection tube and the lysate was discarded. 500µL of wash buffer AW1 was added and centrifuged at >6000 x g for 1 minute. This was repeated for buffer AW2 and was centrifuged for 3 minutes at >10,000 x g. The Mini Spin column was placed in a clean, labelled 1.5mL microcentrifuge tube and the sample was eluted into 50µL pre heated buffer AE (42°C) twice to have a final elution of 100µL. The sample was stored at -20°C before quantification by ddPCR (see section 1.8).

2.5 Processing of plasma and buffy coat DNA

Blood collected in STRECK and EDTA tubes were processed within 24 hours of sample collection. Tubes were inverted 8-10 times before centrifugation at 1600 x g for 20 minutes on a horizontal rotor at 4°C. Plasma and buffy coat were collected separately and stored in labelled 2mL cryogenic tubes. The samples were at stored -80°C until DNA extraction.

2.6 Automated DNA extraction from plasma

Cell free DNA (cfDNA) was extracted, from up to 4mLs of archived plasma, using the automated MagMax™ Cell-Free DNA Isolation Kit (containing the MagMax™ cell free DNA binding solution, magnetic beads, wash and elution solutions; Thermo Cat # A29319) and Thermo Scientific™ KingFisher™ Flex Purification System. Samples with less than 4mLs of plasma were made up to 4mLs with PBS. Samples were thawed and

60µl of proteinase K (STRECK tubes only) and 200µl of SDS 20% solution were added, incubated for 20 minutes at 60°C on a Eppendorf™ Thermomixer™ and cooled on ice for 5 minutes. The Thermo Scientific™ KingFisher™ Flex Purification System was loaded with plates containing the sample, MagMax™ cell free DNA binding solution, MagMax™ cell free DNA magnetic beads, MagMax™ cell free DNA solution, 80% ethanol, and a tip comb plates. The Thermo Scientific™ KingFisher™ Flex Purification System was run on programme: MagMAX cfDNA-4mL-Flex-V2-100. DNA was eluted into 100µL MagMax™ cell free DNA elution solution and stored at -20°C.

2.7 DNA extraction from buffy coat

Buffy coat extraction was performed using the Qiagen DNeasy blood and tissue kit (Cat no. 69504, QIAGEN). Inputs of 50µL of buffy coat was added to 20µL proteinase K and 4µL of RNase A stock solution (100mg/ml; Qiagen Cat # 19101) to a 1.5mL microcentrifuge tube and vortexed. This was combined with 200µL buffer AL then briefly vortexed. The sample was incubated at 56°C for 10 minutes, combined with 200µL ethanol (96-100%) and briefly vortexed. This mixture was moved to a QIAmp Mini spin column and centrifuged at >10,000 x g for 1 minute and the filtrate discarded. Subsequently 500µL buffer AW1 was added to the spin column and centrifuged at >10,000 x g for 1 minute and the filtrate discarded. This step was repeated with 500µL buffer AW2 and centrifuged at >10,000 x g for 3 minutes. The filtrate was discarded and the Mini spin column centrifuged for a further minute to remove any remaining traces of ethanol. The Mini spin column was placed in a new labelled 1.5mL microcentrifuge tube and the DNA was eluted into 100µL pre-heated (42°C) buffer AE and stored at -20°C prior to quantification.

2.8 DNA quantification by droplet digital polymerase chain reaction (ddPCR)

DNA was quantified by ddPCR on a Bio-Rad QX-200™ ddPCR system using RNase P as the reference gene. PCR reactions consisted of 10µL ddPCR Supermix for probes (Bio-Rad), 1µL of TaqMan Copy Number Reference Assay, human, RNase P (*RPPH1*, Thermo Fisher Scientific 4403326) 1µL of DNA eluate and nuclease free water made up to reach a total volume of 20µL. The reaction was emulsified in 70µL of droplet generator oil into approximately >20,000 droplets per sample using the manual droplet generator (BioRad QX200™ droplet generator). Emulsified PCR reactions were

transferred on to a 96 well plate and heat-sealed with foil. All experiments were run with at least one non template control (NTC). PCR reactions were run on a G-Storm Quad thermocycler incubating the plates at 95°C for 10 min followed by 40 cycles at 95°C for 15 sec and 60°C for 60 secs, followed by 10 min incubation at 98°C. Plates were read on a Bio-Rad QX200 droplet reader, with signal identifying FAM, VIC or HEX channels in each droplet. The output files were stored as .qlp files for later processing.

2.9 Analysis of digital PCR data

QLP files were analysed using QuantaSoft software v1.7.4 from Bio-Rad. Droplets were manually gated according to population clustering as positive or negative compared to the population of 'empty' droplets. The estimated DNA concentration was quantified by ddPCR using the *RPPH1* reference assay to calculate copies/ well and multiplying by the c-value (3.3pg), an estimate of the mass of a single haploid human genome.

2.10 Targeted Tissue sequencing

Paired buffy coat DNA and RNALater™ tissue DNA were sent to the Centre of Molecular Pathology at The Royal Marsden Hospital for sequencing using a targeted capture-based approach designed to detect mutations and amplifications frequently seen in breast cancer. The targeted panel, “ABC-Bio” panel, has been validated in the ABC-Bio (molecular screening for patients with advanced breast cancer) trial and comprises of 41 genes commonly mutated in breast cancer (Table 1).

Genes for this panel were selected from an analysis of several breast cancer sequencing studies^{172–174}. Genes were selected based on either being frequently mutated in breast cancer or rare but potentially targetable. The designed panel could detect single nucleotide variants at >5% allele frequency with >99% sensitivity (95% CI) and >98% specificity (95% CI). Small indels could be detected at >5% variant allele frequency with sensitivity >95% (95% CI) and specificity >81% (95% CI). The panel is capable of detecting high-level gene amplifications (>8 copies) in samples with >30% neoplastic nuclei.

Genes for mutations and copy number		Genes for mutation only	Hotspots only	Fusion Genes
BRCA1	FGFR2 (hotspot regions in FGFR1/2/3)	AKT1	AKT2	FGFR1
BRCA2	IGF1R	ATM	AKT3	FGFR2
CCND1	KIT	CDKN1B	BRAF	FGFR3
CCNE1	MAP2K4	ERBB3	KRAS (exon 2)	
CDH1	MCL1	GATA3	KRAS (exon 3)	
CDH4	MDM2	MAPK3K1	KRAS (exon 4)	
CDKN1A	MET	NF1	NRAS (exon 2)	
CDKN2A	MYC	PIK3CA	NRAS (exon 3)	
CDKN2B	PDGFRA	PIK3R1	NRAS (exon 4)	
EGFR	PTEN	SF3B1		
ERBB2	RB1			
ESR1	TP53			
FGFR1 (hotspot regions in FGFR1/2/3)				

Table 1 ABC-Bio Targeted Panel

2.11 AVENIO Sequencing

Samples from the RIO trial that had inadequate amount of tumour tissue available for sequencing on the ABC-Bio targeted panel had plasma from EDTA tubes sent to Roche for sequencing using the AVENIO ctDNA targeted tumour profiling kit (Roche Sequencing). A total of 4 samples were sequenced on the AVENIO ctDNA 17 gene targeted kit (Table 2) and 2 samples were run on the AVENIO ctDNA 77 gene expanded kit (Table 3).

Gene	
ALK	KRAS*
APC	MET*
BRAF	NRAS
BRCA1*	PDGFRA
BRCA2*	RET
DPYD	ROS1
EGFR*	TP53*
ERBB2*	UGT1A1
KIT	

Table 2 Roche AVENIO ctDNA Targeted Panel (17 genes)

* denotes all coding regions

Gene						
ABL1	CCND2*	ERBB2*	GNA11	MAP2K1	PDCD1LG2*	RNF43
AKT1	CCND3*	ESR1*	GNAQ	MAP2K2	PDGFRA	ROS1
AKT2	CD274*	EZH2	GNAS	MET*	PDGFRB	SMAD4*
ALK	CDK4*	FBXW7*	IDH1	MLH1*	PIK3CA	SMO*
APC	CDK6	FGFR1	IDH2	MLH2*	PIK3R1	STK11*
AR*	CKDN2A*	FGFR2	JAK2	MSH6*	PMS2*	TERT promoter
ARAF	CSF1R	FGFR3	JAK3	MTOR	PTCH1	TP53*
BRAF	CTNNB1	FLT1	KDR	NF2*	PTEN*	TSC1
BRCA1*	DDR2	FLT3	KEAP1*	NFE2L2	RAF1	TSC2
BRCA2*	DPYD	FLT4	KIT	NRAS	RB1*	UGT1A1
CCND1*	EGFR*	GATA3	KRAS*	NTRK1	RET	VHL*

Table 3 Roche AVENIO ctDNA Expanded Panel (77 genes)

* denotes all coding regions

2.12 Primer Probe assay design

For each RIO trial subject, ddPCR assays were specifically designed for the mutations identified by targeted sequencing. The region of interest in the mutation sequence was identified and primers and probes were designed in ThermoFisher Scientific Primer Express™ software v3.0.1 or Primer 3 (<http://bioinfo.ut.ee/primer3/>) with specific parameters (Table 4 and Table 5). Primer pair specificity to the amplicon was checked using UCSC ePCR tool (<http://genome.ucsc.edu/cgi-bin/hgPcr?command=start>). Primer-probe dimer formation was checked in an oligoanalyser (<http://eu.idtdna.com/analyzer/Applications/OligoAnalyzer/>) to ensure no self- or hetero dimerization. The free energy noted by DeltaG of all individual and combinations should be more positive than -9kcal.mol to avoid primer pair problems as directed by the IDT manufacturer (<https://www.idtdna.com/pages/support/faqs/how-do-i-use-the-oligoanalyzer-tool-to-analyze-possible-hairpins-and-dimers-formed-by-my-oligo>). Primers and probed were ordered from Integrated DNA Technologies. Primers were desalted and probes contain a 5' dye (FAM for the mutant allele and HEX for the wild-type allele) and a 3' non-fluorescent quencher (Iowa Black® FQ).

Primer Parameters	
Amplicon length	Less than 150bp
Tm of primers	52-62°C, ideally 57-60°C for both primers
Primer length	Less than 30bp, ideally 18-24bp
3' end of primers	The five nucleotides at the 3' end should have less than three G and/ or C residues
GC content of primers	Between 20-80%, ideally 40-60%

Table 4 Primer design parameters for dPCR

Probe Design	
Tm	2-8°C above the Tm of the primer pair
5' end	The 5' end should not contain a guanosine (G) residue. A guanosine residue at the 5' end will quench some of the fluorescence even after hydrolysis.
GC content of probe	Between 20-80%, ideally 40-60%

Table 5 Probe design parameters for dPCR

Primers and probes were prepared to a 20X assay cocktail and aliquoted in 100µL and stored at -20°C (Table 6).

	Volume (µL)
Forward Primer (100µM)	18
Reverse Primer (100µM)	18
Probe 1 (100µM)	5
Probe 2 (100µM)	5
Nuclease Free Water	54

Table 6 20X Primer-probe cocktail mix

2.13 Optimisation of patient specific dPCR assays

Each patient in the RIO trial who had at least one mutation identified on sequencing (ABC-Bio, Avenio, HRDetect) had personalised dPCR assays designed. If more than one mutation was identified multiple assays were designed and optimised.

Assays were tested on patient's tumour DNA to ensure the mutation was present. Temperature gradients (52.1 – 60.2°C) were conducted to determine the optimum annealing temperature for the PCR conditions. Validation of the mutation in tumour was conducted by ddPCR on tumour DNA, negative controls, buffy coat and NTCs. Assays validated are listed in Table 7.

Sample	Gene	Nucleotide Change	Seq Primer F	Seq Primer R	WT probe Sequence	5' modification	3' modification	Mutant Probe Sequence	5' modification	3' modification	ddPCR ann/ ext Temp (C)	Amplicon Length (bp)
R01001	SF3B1	c.3028A>G	GTGAACAAAAGTTGCAATCAAATG	GGTGAGTCTAGGCAGCAGATCTTA	ATGCATAAGATGACTCC	HEX	lowa Black FQ	ATGCATAAGATG G CTC	6-FAM	lowa Black FQ	52	103
R01001	TP53	c.713G>A	TTGGCTCTGACTGTACCACAT	CCGCCATGCAGGAACT	CACTACAACACTCATGTGTAA	HEX	lowa Black FQ	CACTACAACACTCAT G TATA	6-FAM	lowa Black FQ	52	60
R01002	SIK	c.1189G>C	TGAGGCTGCTGCGATCTG	GCAGCTCCCGCTGACA	TCCAACGTGGAGGC	HEX	lowa Black FQ	CCAACGTGCGAGC	6-FAM	lowa Black FQ	52	87
R01003	TP53	c.1024C>T	GGCGTGAGCGCTTCGA	GCTGGGCATCCTGAGTT	ATGTTCCGAGAGCTG	HEX	lowa Black FQ	ATGTT C TGAGAGCTGAA	6-FAM	lowa Black FQ	52	63
R01003	ERBB2	c.734C>T	ACTGACTGCTCCATAGACA	CACATGGGCACAAGCAG	TGCACGGGCCCAA	HEX	lowa Black FQ	TGCATGGGCCCAA	6-FAM	lowa Black FQ	53	92
R01004	CND1	c.433G>C	CCCTGTGTTCCGAGCAAT	CGGCCAGGTTCCACTGA	AGCTGTCTGGTGTG	HEX	lowa Black FQ	TGCTCTG C TGAACA	6-FAM	lowa Black FQ	52	60
R01004	TP53	c.773A>G	AACCCGAGGCCATCCT	TGTGCAGGGTGGCAAGTG	CATCACACTGGAAGAC	HEX	lowa Black FQ	CATCACACTGG G AGAC	6-FAM	lowa Black FQ	52	70
R01006	MET	c.3938A>T	CTCTGGGAGCTGATGACAAG	TGGGCAGTATTCGGGTTGTA	AGTGT T ACTGTTGCAAGGG	HEX	lowa Black FQ	ACTGTT T CTGTTGCAAGGG	6-FAM	lowa Black FQ	52	111
R01006	BRCA1	c.5282delT	CACCAAGGTCCAAAGCGAG	GATCTGTGGCATGTTGGTG	CAGAAAGATCTCAGGGGGCT	HEX	lowa Black FQ	CAGAAAGATCTCAGGGGGCT	6-FAM	lowa Black FQ	52	100
R01008	TP53	c.273G>A	CACCAGCAGCTCCTACAC	GCTGCCCTGGTAGGTTT	TCCTGGCCCTGTCTCTTGT	HEX	lowa Black FQ	TCCTG A CCCTGTCTCTTGT	6-FAM	lowa Black FQ	53	92
R01009	GATA3	c.829C>T	AGAAGGCAGGGAGTGTGAA	CAGGCGTTGCAGGTAAGTGT	ACTGTGGCGCGAG	HEX	lowa Black FQ	ACTGTGGCGG T GAGA	6-FAM	lowa Black FQ	53	64
R01009	TP53	c.1024delC	GGCGTGAGCGCTTCGA	CAGCCTGGGCATCCTGA	ATGTTCCGAGAGCTGAAT	HEX	lowa Black FQ	ATGTT C GAGAGCTGAATGA	6-FAM	lowa Black FQ	53	66
R01010	TP53	c.637C>T	TTTGGTGTGGAGTATTTGGAT	CTCATAGGGCACCACCACACT	ACAGAAACACTTTTCGAC	HEX	lowa Black FQ	ACAGAAACACTTT T GAC	6-FAM	lowa Black FQ	53	63
R01011	TP53	c.394A>C	TGTCTCTCTCTCTCTACAGTACTC	GCTGCACAGGGCAGGTCTT	CCCTCAACAAGATG	HEX	lowa Black FQ	TGCCCTCAAC A GAGA	6-FAM	lowa Black FQ	52	80
R01012	TP53	c.596G>T	GGCCCTCCTCAGACTCT	ATCAAATACTCCAACGCAAA	TCCGAGTGGAAAGAAATT	HEX	lowa Black FQ	TCCGAGTGGAA G TAA	6-FAM	lowa Black FQ	52	57
R02001	TP53	c.372C>A	GCATTCTGGGACAGCCAAGT	CAGGCATTGAAGTCTCATGGAA	TGACTTGCACGGTCACT	HEX	lowa Black FQ	TGACTT G AACGGTCA	6-FAM	lowa Black FQ	53	78
R02002	BRCA2	BRCA2 (Sub + Del)	GCATTGGAGGAATATCGTAGGT	GTCAATACTCTTGTGGTAG	CATTTTTGAAATTTTAAAGACAC	HEX	lowa Black FQ	CATTTTT A GAAATTTTAAAGACAC	6-FAM	lowa Black FQ	52	70
R02004	TP53	c.356_360delCCAAG	GTCCTGGGCTTCTGCATTCT	GCCAGCATTGAAGTCTCAT	ACAGCCAAGTCTGTGACTTGCACGGTCTAT	HEX	lowa Black FQ	ACAG T CTGTGACTTGCACGGTCTAT	6-FAM	lowa Black FQ	53	93
R02005	TP53	c.972_975delTGGGA	CTCTCCCCAGCAAGAAGA	AACCGCATTTTGAAGTGTAGAC	ACTGGATGGGAATAT	HEX	lowa Black FQ	ACT GG AGAATATTTCT	6-FAM	lowa Black FQ	52	115
R02005	ERBB2	c.2264T>C	AGGGCATCTGGATCCCTGAT	CGTCTAAGATTTCTTGTGGCTTTGG	ATCAAAGT T TGAGGGGA	HEX	lowa Black FQ	TGGCCATCAAAGT T CGA	6-FAM	lowa Black FQ	52	102
R02005	PIK3CA	c.3140A>G	TGAGCAAGAGGCTTTGGAGT	TCAGTTCAATGATGCTGTTT	AATGATGCAC A TCATGGTGGCT	VIC	NFQMB	AATGATGCAC G TCATGGTGGCT	6-FAM	NFQMB	52	115
R02006	TP53	c.375+1G>-	TCTTGCATTCTGGGACAGC	AGAAATGCAGGGGGATACG	AGTCTGTGACTTGCACGGT	HEX	lowa Black FQ	AGTCTGTGACTT G AGGTC	6-FAM	lowa Black FQ	52	104
R02007	TP53	c.659A>G	TTGGATGACAGAAACCTTTTCGAC	AGACCCAGTTGCAAAACCA	TGGTGCCCT A TGAGCC	HEX	lowa Black FQ	TGGTGCCCT G TGAGCC	6-FAM	lowa Black FQ	52	79
R02007	PIK3CA	c.3140A>G	TGAGCAAGAGGCTTTGGAGT	TCAGTTCAATGATGCTGTTT	AATGATGCAC A TCATGGTGGCT	VIC	NFQMB	AATGATGCAC G TCATGGTGGCT	6-FAM	NFQMB	52	115
R02008	TP53	c.421T>C	CTCAACAAGATGTTTTGCCAATG	GGGTGTGGAAATCAACCCACA	CAAGACTGCCTGTG	HEX	lowa Black FQ	CAAGAC CC CGCCCTGT	6-FAM	lowa Black FQ	52	66
R02009	TP53	c.715A>G	TCTGACTGTACCACCATCCAATA	CATGCCGCCATGCA	CTACATGTGTAACAGTTC	HEX	lowa Black FQ	CATGTGTGACAGTTC	6-FAM	lowa Black FQ	52	60
R03001	TP53	c.993+1T>G	GAAGAAACCACTGGATGAGAAATATT	CCACTTGATAAGAGTCCCAAGA	CACCTTCAGGTC	HEX	lowa Black FQ	CACCTTCAGG G ACT	6-FAM	lowa Black FQ	52	67
R03005	TP53	c.560-1G>A	CCAGCCCTCTGATTCCTCACT	CCTTCCACTCGGATAAAGATGCT	ATTGCTCTTAGGTCTG	HEX	lowa Black FQ	ATTGCTCT A AGTCTGG	6-FAM	lowa Black FQ	53	69
R03007	TP53	c.527G>A	AGCATGACGAGGTTGT	TGCTCACCATCGTCTATCTGA	AGGCGCT G CCCCAC	HEX	lowa Black FQ	AGGCGCT A CCCCAC	6-FAM	lowa Black FQ	52	66
R03008	TP53	c.839G>A	GCTTTGAGGTTGCGTGTGTTG	TGGGAGATCTCTCTCTCTG	CCTGGGAGAGACCG	VIC	NFQMB	CCTGGGAAAGACCG	6-FAM	NFQMB	60	66
R03009	TP53	c.742C>T	AACTACATGTGTAACAGTTCTGCAT	GAGTCTCCAGTGTGATGATGGT	TGGGCTCCGTTCA	VIC	NFQMB	TGGGCTCCAGT T CA	6-FAM	NFQMB	52	77
R04001	TP53	c.376-1G>T	TGACTTCAACTCTGCTCCTCCT	CAGTTGGCAAAACATCTGTTGAG	TTCTACAGTACTCCC	HEX	lowa Black FQ	TTCTACAT T ACTCCCT	6-FAM	lowa Black FQ	52	70
R06001	TP53	c.715A>G	TCTGACTGTACCACCATCCAATA	CATGCCGCCATGCA	CTACATGT T AACAGTTC	HEX	lowa Black FQ	CATGTG T GACAGTTC	6-FAM	lowa Black FQ	52	59
R06002	TP53	c.323_331delGTTTCCGTCinsTG	TGTCCTTCCAGAAAACCT	CAGGCATTGAAGTCTCATGGA	TTT CCGCTGGG CGCTTCTTG	HEX	lowa Black FQ	ACG TG TGGGCTTCTGCA	6-FAM	lowa Black FQ	52	133
R06003	NF1	c.2409+1G>C	AACTATCCAAAAGCCAAATGGAA	GCAGATCAGTTAACAAGCAAAAGTCAA	TGGCCA G TAAAGTCTGTAA	HEX	lowa Black FQ	TGGCCA G TAAAGTCTGTAA	6-FAM	lowa Black FQ	52	73
R06004	ATM	c.8293G>A	GCTGAATGATGATCAATGCTCTTT	TCACCAATGGGACAGTTC	CAGCGAAGTGGTGTCTTGA	HEX	lowa Black FQ	CAGCGAAG T AGTGTCTTGA	6-FAM	lowa Black FQ	57.5	133
R06005	TP53	c.659A>G	TTGGATGACAGAAACACTTTTCGAC	AGACCCAGTTGCAAAACCA	AGACCCAGTTGCAAAACCA	HEX	lowa Black FQ	TGGTGCCCTGTGAGCC	6-FAM	lowa Black FQ	52	79
R06006	TP53	c.713G>A	TTGGCTCTGACTGTACCACAT	CCGCCATGCAGGAACT	CACTACAACACTCATGTGTAA	HEX	lowa Black FQ	CACTACAACACTAT G TTA	6-FAM	lowa Black FQ	52	61
R06007	TP53	c.665delC	TGGATGACAGAAACACTTTTCGA	GCCACTGACAACCCCTTAAAC	CCCTATGAGCGCT	HEX	lowa Black FQ	CCCTATGAG C GCC	6-FAM	lowa Black FQ	52	112
R06008	TP53	c.814G>T	GCTTCTCTTCTTCTCTGAGTAGTG	CCGAGCAGGACACAACA	AACAGCTTTGAGTGC	HEX	lowa Black FQ	AACAGCTTTGAG T GC	6-FAM	lowa Black FQ	52	77

Table 7 RIO Trial dPCR assays

Once the assays were optimised, further mutation analysis was done on extracted DNA from patient's plasma taken at baseline and EOT. DNA was taken from 100µl DNA (4mL plasma equivalent) and divided equally into 4 wells from each time point. DNA was dried at 60 degrees for 100 minutes before preparing the PCR reactions to a volume of 20µl (Table 8 and Table 9). Three NTCs and a negative control of the patient's buffy coat DNA were included for each ddPCR assay. To ensure no contamination between time points, baseline and EOT samples were set up on different plates.

Reagent	Volume (µl)
DNA	Dried
Primer Probe Mix	1
Supermix	10
Water	9
Total	20

Table 8 PCR Mastermix

Heated lid 105°C microplate pressure	
95°C 10 min (Temp. Ramp increment 2.5C/sec)	
95°C 15 sec (Temp. Ramp increment 2.5C/sec)	X40
Assay specific temp 10 min (Temp. Ramp increment 2.5C/sec)	
98°C 10 min (Temp. Ramp increment 2.5C/sec)	
10°C indefinite	

Table 9 PCR reaction

2.14 Circulating tumour DNA mutational analysis

Only paired samples with at least 4 positive droplets in baseline samples were analysed for change in ctDNA levels between baseline and EOT. The circulating DNA ratio at day 15 (CDR15) was assessed as a ratio of the ctDNA copies/ml at EOT copies/mL compared to ctDNA copies/mL at baseline. Where more than one mutation was tracked a weighted mean of ctDNA change was calculated. The CDR15 cut off <0.25 for ctDNA suppression, was pre-specified determined in a separate study¹⁵⁶.

2.15 HRDetect

Extracted DNA from fresh frozen tissue with >20% tumour content with >200ng quantifiable DNA and paired germline DNA from buffy coat were identified and sent to the Sanger Institute, Cambridge, UK. In collaboration with Serena Nik-Zainal, samples were sent for whole genome sequencing and analysis using the HRDetect assay⁶⁴ as described below.

500bp insert genomic libraries were constructed according to Illumina library protocols and 150bp paired-end sequencing performed on an Illumina HiSeq X Ten, to an average sequence depth of 38.5X for both tumour and normal. The resulting reads were aligned to the reference human genome (GRCh37) using Burrows-Wheeler Aligner, BWA) (0.7.16a (r1181)). Mutation calling was performed as described previously⁹³. CaVEMan (Cancer Variants Through Expectation Maximization: <http://cancerit.github.io/CaVEMan/>) was used for calling somatic substitutions. Indels in the tumour and normal genomes were called using a modified Pindel version 2.0. (<http://cancerit.github.io/cgpPindel/>). Structural variants were discovered using a bespoke algorithm, BRASS (BReakpoint AnalySiS) (<https://github.com/cancerit/BRASS>). All annotation was to Ensembl build 75. Allele-specific copy number analysis of tumours was performed using ASCAT (v2.1.1) applied to next-generation whole genome sequencing data as described previously^{64,93}. Copy number values and estimates of aberrant tumour cell provided by ASCAT were input into the CaVEMan substitution algorithm. In addition, ASCAT segmentation profiles were used to establish the presence of copy number changes and loss of heterozygosity across the *BRCA1*, *BRCA2* and *PALB2* genes.

The predominant mutational signatures present in breast cancer have been identified in a large WGS study involving 560 breast cancers. These comprise 12 substitution signatures and 6 structural rearrangement signatures. The contributions of these consensus mutational signatures were estimated in the 27 RIO trial WGS samples as described previously^{93,175}. In addition, the contribution of small insertions and deletion at regions of micro-homology or repeats and HRD LOH index were estimated⁶⁰.

Mutational signature contributions for substitution signatures 3 and 8, rearrangement signatures 3 and 5, deletions at microhomology and HRD LOH index were calculated for each sample as input into the weighted model, HRDetect. The HRDetect algorithm was run as described previously⁶⁴.

2.16 DNA Methylation Method

Bisulfite conversion of DNA

Extracted DNA was subjected to bisulfite sequencing (Zymo Research Methylation Gold spin column kit D5005) as per manufacturer's instructions. In a PCR tube 130µl of CT conversion reagent was added to 20µl of DNA and incubated for 10 minutes at 98°C, followed by 64°C for 2.5 hours. The DNA sample along with 600µl M-binding buffer were added to a Zymo™ spin IC column and inverted several times followed by centrifuge at >10,000 x g for 30 seconds. The sample was washed with 100µl M-wash buffer and M-Desulphonation buffer was added and incubated for 15-20 minutes before centrifuging for 30 seconds at >10,000 x g. The sample was then washed twice before being eluted into 10µl of M-Elution Buffer and quantified using Qubit® 3.0 fluorometer.

DNA Quantification by Qubit® 3.0 fluorometer

DNA was quantified using the Qubit dsDNA HS assay from Qubit (Q32854, Thermo Fisher Scientific, Waltham, USA). Qubit working solution was prepared by diluting Qubit dsDNA HS reagent 1:200 with Qubit dsDNA HS buffer. Standards were prepared in clear 0.5mL PCR tubes using 190µL of working solution and 10µL of Standard #1 and Standard #2 respectively. Similarly, samples were prepared using 1-10µL made up to 200µL with Qubit working solution. Standards and samples were incubated for 2 minutes at room temperature and concentration of DNA assessed using a Qubit 3.0 Fluorometer. The measured fluorescence (QF value) was then interpolated from the standard curve to determine DNA concentration of the samples.

PCR Amplification

A minimum of 2ng of bisulfite converted DNA was amplified by PCR with *BRCA1* (forward-TATTTTGAGAGGTTGCTGTTTAG and reverse-CTAAAAAACCCCACAACCTATCCC) and *RAD51C* (forward-TGGTAATTGGTTAGTGTGTGT and reverse-TCCTCATCAAATATACACCCTAACT) methylation primers and AccuPrime™ Taq DNA polymerase (Table 10). (See Chapter 4).

Reagent	Volume for a 10µl reaction
10XReaction Buffer II	1
<i>BRCA1</i> Fwd Primer (10uM)	0.2
<i>BRCA1</i> Rev Primer (10uM)	0.2
<i>RAD51C</i> Fwd Primer (10uM)	0.2
<i>RAD51C</i> Rev Primer (10uM)	0.2
Bisulfite DNA (variable)	2
Accuprime Taq DNA Polymerase	0.04
ddH2O	6.16

Table 10 PCR mix for DNA methylation

The modified DNA was desulphonated using the Qiagen QIAquick PCR Purification Kit and resuspended in 10mMTris-Cl, pH 8.5. Samples were quantified using Qubit® 3.0 fluorometer as previously described.

Library Preparation

Samples were subjected to Illumina NebNext Ultra II library preparation (E76455, New England Bio Labs). End repair of the PCR products was performed in a 60µL reaction with 3µL NEBNext Ultra II End Prep Enzyme Mix, 7µL NEBNext Ultra II End Prep Reaction Buffer, then incubated for 30 minutes at 20°C and a further 30mins at 65°C. Adapters were ligated by adding 30µL of NEBNext Ultra II Ligation Master Mix, 1µL of NEBNext Ligation Enhancer and 2.5µL of NEBNext Adaptor for Illumina at 1.5µM. This volume was then incubated at 20°C for 15 minutes, 3µL of USER enzyme was added

followed by a further incubation at 37°C for 15 minutes. A 2X AMPure XP bead clean up with two 80% ethanol washes was then performed with elution into 17µL 0.1XTE and recovery of 15µL. PCR enrichment with addition of P5 and P7 adapters was performed by adding the 15µL of products to 25µL NEBNext Ultra II Q5 Master Mix, 5µL of Index Primer/i7 Primer and 5µL of Universal PCR Primer/i5 Primer and using the following program in a thermal cycler (Table 11 **Error! Reference source not found.**).

Initial activation	98°C	30 seconds	Hold
Denaturation	98°C	10 seconds	4-6 x cycles
Annealing	65°C	75 seconds	
Final extension	65°C	5 minutes	Hold

Table 11 Library Preparation PCR reaction

A final 2X AMPure XP bead clean up with two 80% ethanol washes was then performed with elution into 17µL 10mM Tris-HCl and recovery of 15µL, before quantification.

Library assessment with Bioanalyser Chip

Libraries were assessed using an Agilent Bioanalyzer™ using High-sensitivity DNA chips (5067-4626, Agilent). A gel-dye mix was prepared by mixing 385µL of High Sensitivity DNA gel matrix with 15µL High Sensitivity DNA dye concentrate at room temperature, vortexing, then centrifuging through the provided spin filter at 2240g for 15 minutes. DNA chips were then loaded with gel-dye mix, marker and ladder as per the manufacturer's protocol and 1µL of sample added to each well. The chip was vortexed at 2400rpm for 1 minute and then loaded on to the Agilent 2100 Bioanalyzer.

Library Quantification

All Illumina-compatible libraries were quantified using the KAPA Illumina Library Quantification Kit (Roche; KK-4835). Duplicate reactions of library dilutions were set up with 6µL KAPA SYBR® FAST qPCR Master Mix containing Primer Premix and 4µL

of library dilution. Six standards in descending orders of magnitude from 20pM, along with NTC wells were run in duplicate. Reactions were loaded onto a QuantStudio 6 flex (ThermoFisher) and run with the below program.

Initial activation	95°C	5 minutes	Hold
Denaturation	95°C	30 seconds	35 x cycles
Annealing	60°C	45 seconds	

Sequencing on the Illumina MiniSeq

Pooled Illumina-compatible libraries were diluted to 1nM using 0.1XTE. The 1nM library pool in a 5µL volume was then combined with 5µL of 0.1XTE, vortexed and incubated for 5 minutes at room temperature, then 5µL 200mM Tris-HCl, pH 7.0 added with a further vortex and 1 minute incubation at room temperature. A loading concentration of 1.8pM was achieved through dilution with Illumina Hybridization Buffer and PhiX control added with a concentration 1-10% depending on requirements, before loading onto a MiniSeq cartridge add instrument details.

Bioinformatic sequencing analyses

Bioinformatic analysis was performed by Dr Ros Cutts (Molecular Oncology Laboratory, ICR). Mean number of reads for *BRCA1* amplicon was 36909 (range 9654-60084) and *RAD51C* amplicon 48879 (range 28404- 71129) with a mean 47% of reads on target for the methylation sequencing run (range 37-50%). Bioinformatics analysis of methylation followed a similar workflow to previous studies¹⁷⁶. Paired overlapping reads were merged into a single sequence using flash¹⁷⁷ after adaptor trimming using trim-galore (https://www.bioinformatics.babraham.ac.uk/projects/trim_galore/). Each read was aligned using pairwise alignment to the *BRCA1* or *RAD51C* amplicons using Biostrings R¹⁷⁸ package with 90% identity. Reads with more than 1 mismatch in alignment were additionally removed. Reads with incomplete bisulphite conversion were removed by calculating the unconverted cytosine count at non-CG sites as well as reads where all CG sites in the read were not C or T. Reads were assessed as

being methylated when >90% of CpG sites in the amplicon were methylated. For *RAD51C* methylation, 2/8 sites in the *RAD51C* amplicon were not included in the analysis because they were found to be methylated in all samples.

2.17 RNA Sequencing

RNA Extraction

Paired RNAlater™ samples were identified and sectioned using a cryostat. One section was cut for H&E and 10 sections were cut and stained with nuclease-free Nuclear Fast Red. A second H&E section was cut at the end of the series. H&E sections were reviewed and marked by a pathologist for tumour and assessed for tumour content. NFR stained sections were micro-dissected and RNA was extracted using the Qiagen RNeasy Mini kit according to the manufacturer's instructions. RNA was eluted twice into separate 50µL aliquots using RNase free water and stored at -80°C before quantification.

RNA Quantification

RNA was quantified using the Qubit™ RNA HS Assay Kit (Q32852, ThermoFisher Scientific). Qubit working solution was prepared by diluting Qubit HS RNA reagent 1:200 with Qubit HS RNA buffer. Standards were prepared in clear 0.5mL PCR tubes using 190µL of working solution and 10µL of Standard #1 and Standard #2 respectively. Similarly, samples were prepared using 1-10µL made up to 200µL with Qubit working solution. Standards and samples were incubated for 2 minutes at room temperature and concentration of RNA assessed using a Qubit 3.0 Fluorometer. The measured fluorescence (QF value) was then interpolated from the standard curve to determine RNA concentration of the samples.

RNA quality assessment with bioanalyser chip

RNA quality was assessed on the Agilent Bioanalyzer RNA 6000 Nano Kit. A gel-dye mix was prepared by mixing 65µL of RNA filtered gel with 1µL RNA dye concentrate at room temperature, vortexing, then centrifuging through the provided spin filter at 13,000g for 10 minutes. RNA chips were then loaded with gel-dye mix, marker and

ladder as per the manufacturer's protocol and 1µL of sample added to each well. The chip was vortexed at 2400rpm for 1 minute and then loaded on to the Agilent 2100 Bioanalyzer.

RNA Sequencing

Extracted RNA (approximately 1ug) was sent to Eurofins Genetic Services Limited for RNA Exome sequencing. Total RNA was subjected to RiboZero depletion and Illumina TruSeq RNA Exome library preparation. Libraries were pooled and sequenced on an Illumina HiSeq 2500 (v4 chemistry).

Bioinformatic RNA sequencing analysis

Bioinformatic analysis was performed by Dr Ros Cutts (Molecular Oncology Laboratory, ICR). RNA sequencing data was aligned to the GChr37 genome using STAR aligner¹⁷⁹ with a mean of 44,117,169 reads per sample (range 14010752-91,470,225). Gene counts were established using htseq¹⁸⁰. DeSeq2¹⁸¹ was used to establish gene-wise normalisation and to look for differential expression between different sample groups. Gene set enrichment analysis was carried out using the R package fgsea¹⁸². PAM50 and TNBC subtypes were established using AIMS¹⁸³ and TNBCtype¹⁸⁴. Cibersort¹⁸⁵ was run in absolute mode using normalized gene counts.

Chapter 3 RAD51 Immunohistochemistry Validation

3.1 Introduction

Homologous recombination (HR) is an essential component to DNA double strand break repair and works in the S and G2 phase of the cell cycle and requires the protein RAD51 which plays an integral role along with BRCA1, BRCA2 and PALB2^{186,187}. Abnormalities in these genes impair homologous recombination repair (HRR) and leads to the accumulation of double strand DNA breaks and ultimately genomic instability^{186,188}.

Germline *BRCA1/2* mutated breast cancer is known to harbour defects in HRR. Pre-clinical through to phase III trials have shown effective use of PARP inhibitor therapy, leading to the clinical use of PARP inhibitors in this population^{6,8,47,102,189}. Cell lines with defects in HR genes other than *BRCA1/2* have shown sensitivity to PARP inhibitor therapy. Genetic defects in HRR genes have been identified in human breast cancers, including TNBCs with somatic mutations in HRR-related genes and epigenetic silencing of *BRCA1* and *RAD51C*^{57,190-192}. This increases the possible utilisation of PARP inhibitors. However, despite strong pre-clinical evidence no biomarker has been developed to identify this subpopulation of non-germline *BRCA* associated TNBCs^{49,57,71,193}.

There have been efforts made to identify this subpopulation of TNBC including use of mRNA expression signatures, analysis of genomic scars or individual analysis of genetic alterations in HRR-related genes. However, they lack the ability to detect tumours that may have restored their HRR function and are HR deficient (HRD) at the time of treatment^{57,60,64,92,194,195}. Therefore, there is an important unmet need to develop a marker that can accurately identify tumours that are HRD in a timescale suitable to clinical diagnostic requirements, if we are to change the way we treat TNBC from a blanket of chemotherapy to a more individualised therapy.

RAD51 is a 339-amino acid protein that plays a vital role in the HR of DNA during double strand break repair. Expression of RAD51 is cell-cycle regulated, being lowest in resting cells and peaking during the S/G2 phase of the cell cycle in proliferating cells¹⁹⁶. When cells are exposed to genotoxic agents or irradiation, RAD51 is recruited

from the cytosol to the nucleus¹⁹⁷. BRCA2 delivers RAD51 to the DNA double strand break where it accumulates and can be detected as foci in the nucleus. Subsequently, DNA strand exchange occurs with the undamaged sister chromatid which serves as the template for the new strand restoring the missing genetic information^{41,198}.

The HR proficiency of a cell is probably the most important factor to predict whether PARP inhibitor treatment will be effective⁷¹. Induction of RAD51 nuclear foci after neoadjuvant chemotherapy and PARP inhibition can measure the HRR functionality in breast cancer biopsies and can therefore be used as a convenient and informative marker of functional HR^{67,71,72,193,199}.

Studies have shown that cells with deficient BRCA1/2 or other HR deficient factors ineffectively form RAD51 foci which could be used as a marker for PARP inhibitor sensitivity and this has been explored in formalin fixation and paraffin embedding (FFPE) breast cancer tumours^{8,102,199}. The dynamics of DNA repair alter throughout tumour evolution and a functional RAD51 assay can be used as a dynamic readout of tumour HRR at the specific time for treatment decision-making^{71,92,200}. Current studies are using immunofluorescence (IF) on FFPE tumour samples which can be labour intensive and require use of a confocal microscope. We have validated an immunohistochemical RAD51 assay in a retrospective study, ChemoNEAR, and further used the assay in a prospective PARP inhibitor trial, RIO.

3.2 Hypothesis

IHC can reliably assess RAD51 foci in primary triple negative breast cancer.

3.3 Aims

1. To validate IHC as a reliable method to assess RAD51 foci in primary breast cancer.
2. To ascertain the proportion of homologous recombinant deficient triple negative breast cancer patients in the RIO trial as determined by IHC RAD51 foci assessment.

3.4 Acknowledgements

- Samples from the ChemoNEAR study were used in RAD51 IHC validation.
- Immunohistochemistry was performed by Frances Daley at Breast Cancer Now Core Facility.
- Immunofluorescence was performed by David Robertson at Breast Cancer Now.
- Analysis was performed by Neha Chopra and Divya Kriplani.

3.5 Results

3.5.1 Validation of RAD51: ChemoNEAR Study Samples

The ChemoNEAR study (CCR3449, REC ID: 11/EE/0063) is a multicentre breast cancer tissue collection research study. All patients irrespective of hormone/ HER2 status undergoing neoadjuvant chemotherapy for primary breast cancer were included. Research biopsies were collected at baseline (B), 24-48 hours post first cycle of chemotherapy (H; optional) and prior to the second cycle (C;

Figure 4). Samples were processed at local centres by FFPE before being sent to and stored at The Royal Marsden Hospital. Patients who had the optional 24-48 hour biopsy were identified and their corresponding baseline and second cycle core biopsies were retrieved for RAD51 analysis. A subset of samples underwent a RAD51 immunofluorescence (IF) assay.

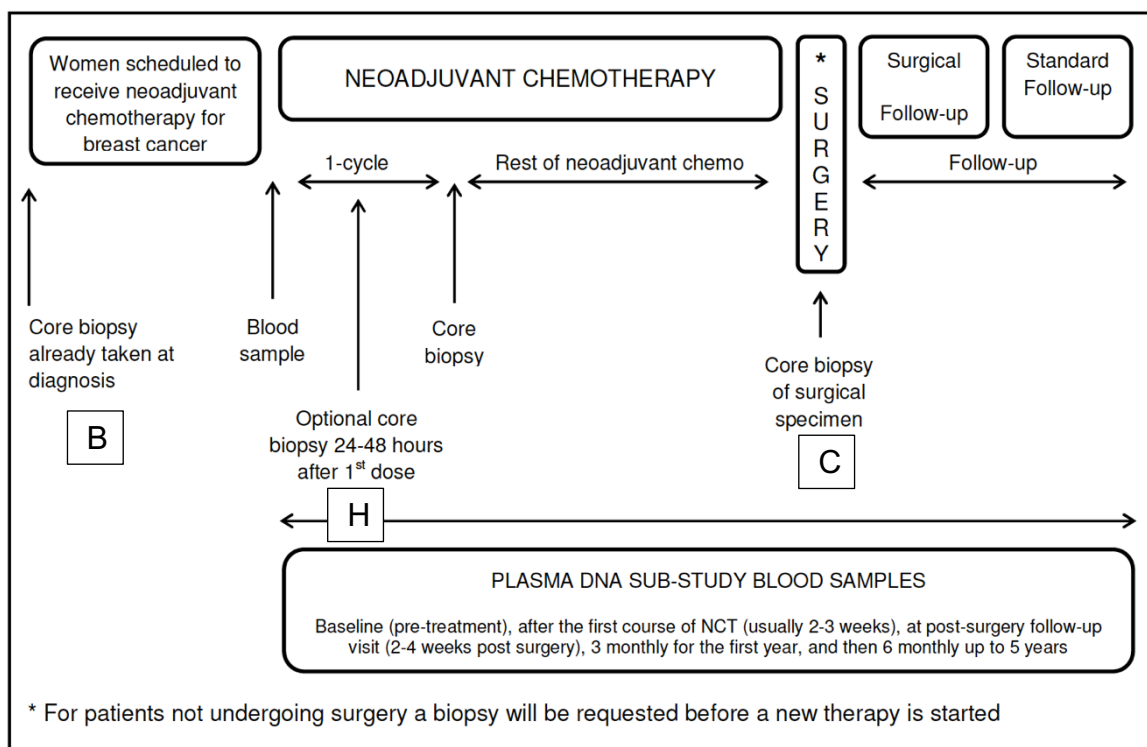


Figure 4 ChemoNEAR Study Design

The ChemoNEAR study was used as the validation set for RAD51. B refers to baseline samples taken before any treatment, H refers to a biopsy taken 24-48 hours after the 1st cycle of chemotherapy. C refers to a biopsy taken before the 2nd cycle of chemotherapy is administered.

A total of 27 patients were included in the validation cohort to assess whether RAD51 IHC could determine functional HR deficiency. There were 19 B, 27 H and 22 C samples available for RAD51 assessment and subsequently stained for GMNN and RAD51 foci (Figure 5) Twelve patients had core biopsies with sufficient tumour for all three-time points. Blocks that were missing were either because the sample had not been taken or the sample had been exhausted for other analyses within the ChemoNEAR study. Eight paired baseline and 24-48 hours post first cycle of chemotherapy FFPE samples underwent IHC and IF staining.

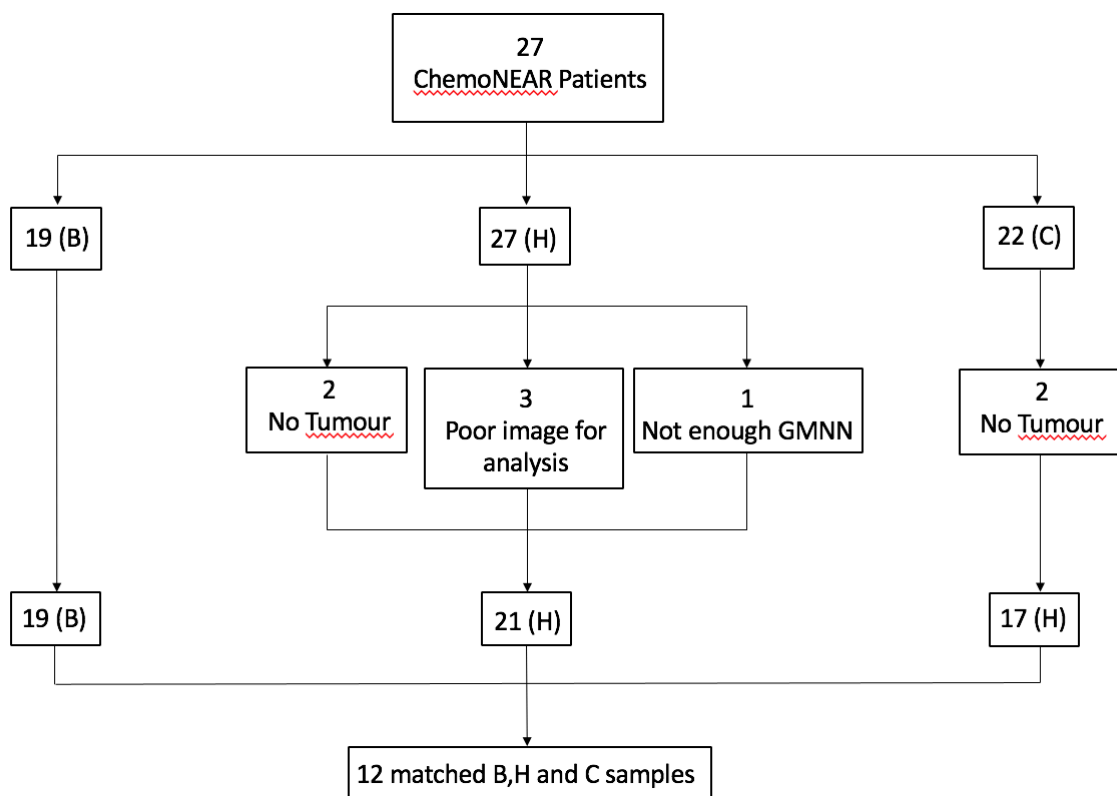


Figure 5 Consort of number of samples used for RAD51/GMNN immunohistochemistry.

A total of 27 patients were identified for the validation study. Samples were evaluated for amount of tumour assessable for RAD51 IHC. B - Baseline biopsy; H - 24-48 hours post first cycle chemotherapy; C - pre second cycle chemotherapy

3.5.2 Immunohistochemistry for RAD51/ GMNN double staining

Samples were stained with GMNN polyclonal antibody (Proteintech 10802-1-AP, rabbit) producing blue/green stained tumour cells indicating tumour cells in S/G2 phase of the cell cycle (Figure 6, Figure 7, Figure 8 and Figure 9). Cells undergoing homologous recombination repair (HRR) were determined by the presence of brown foci, RAD51 foci, in GMNN positive cells at x40 magnification (Figure 8 and Figure 9). Slides were scanned using a Hamamatzu NanoZoomer Digital Pathology Platform at x40 magnificationn.

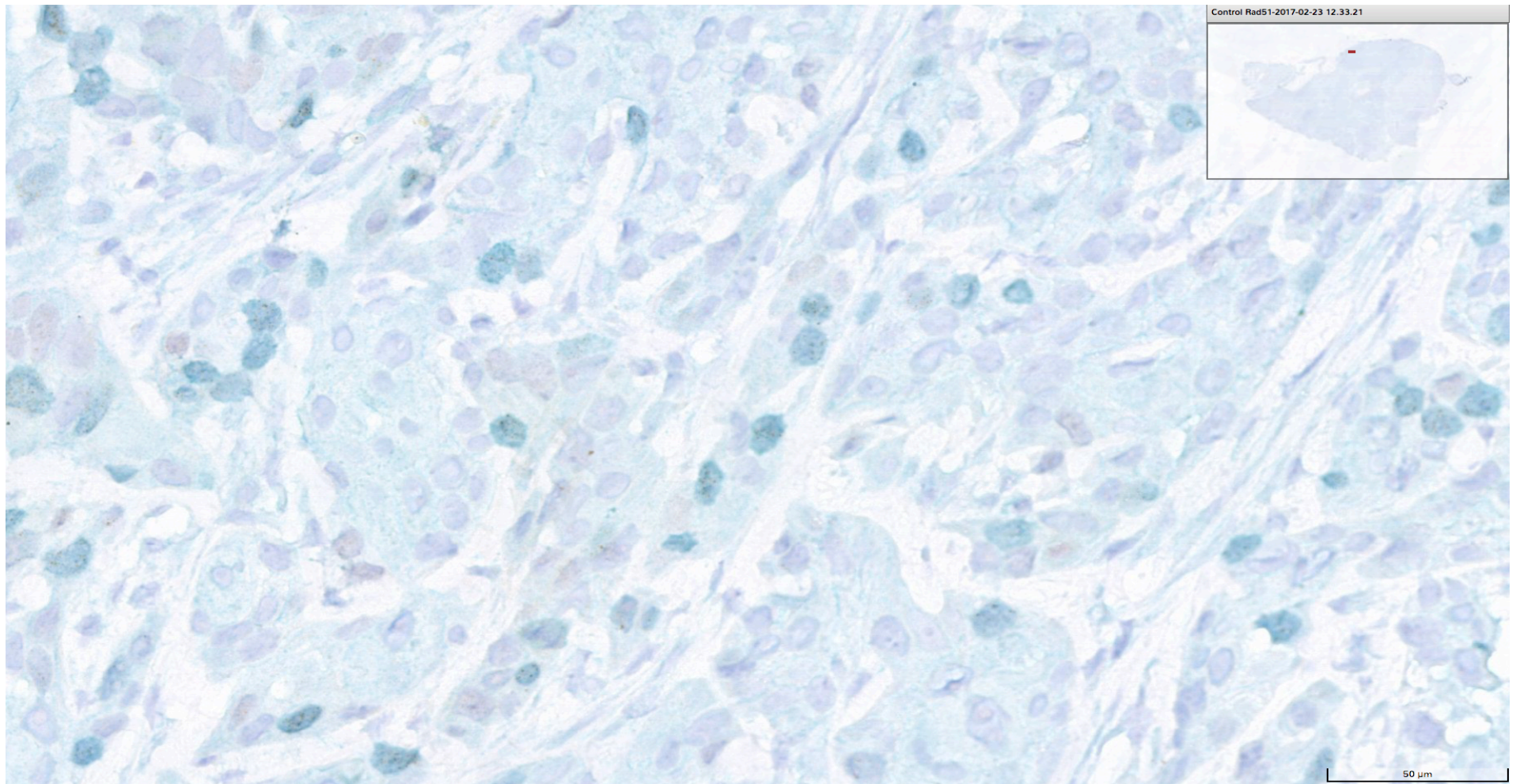


Figure 6 RAD51/ GMNN IHC negative control (Untreated SCC at x40 magnification)

GMNN staining of tumour cells in blue/ green represents S2/G phase of the cell cycle. No brown foci are presenting indicating no HRR is occurring. Scale bar 50μm.

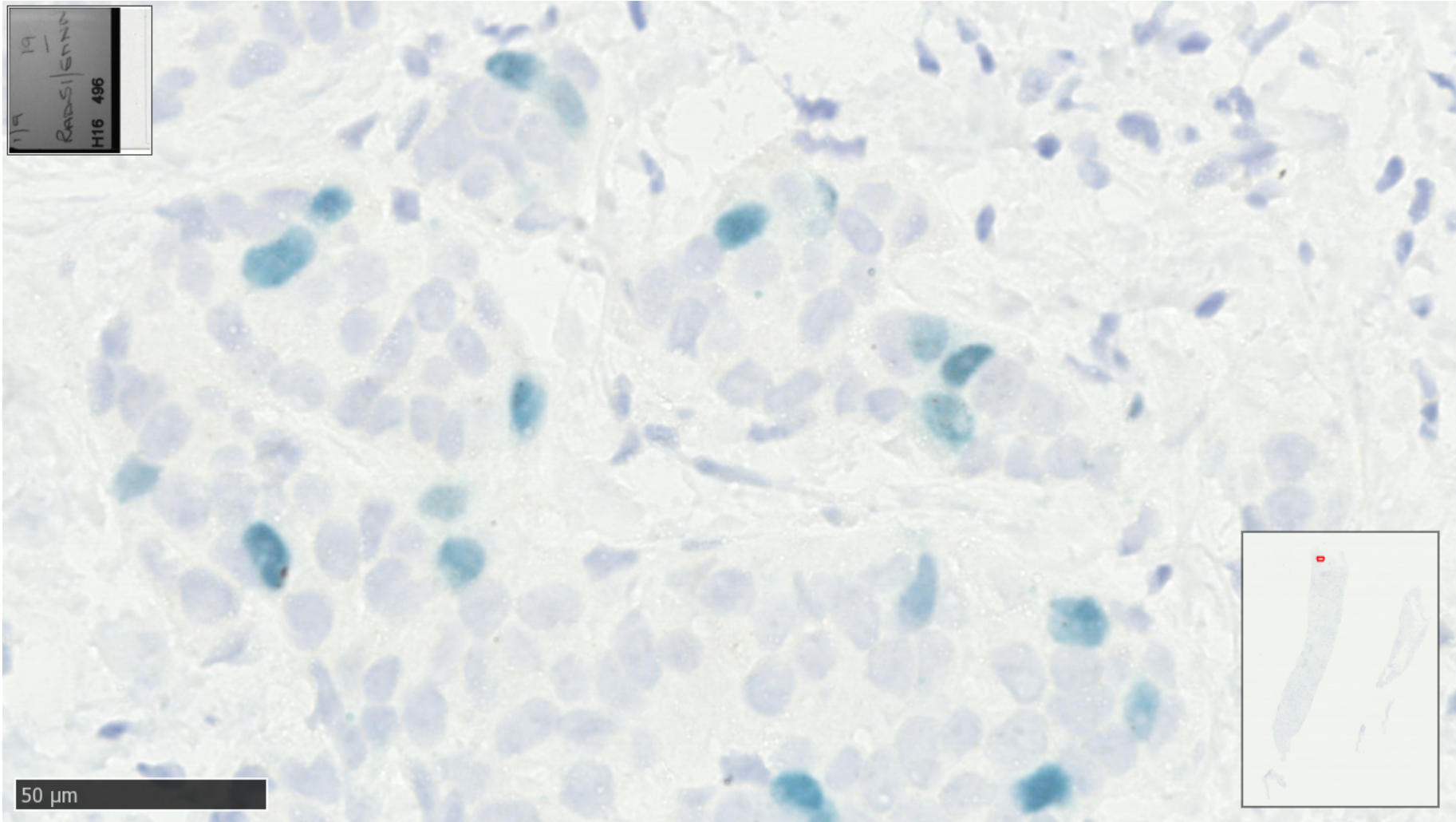


Figure 7 RAD51/ GMNN IHC from patient RMC 001 057 at baseline (B)

No treatment received. X40 magnification. GMNN staining of tumour cells in blue/ green. No brown foci are presenting indicating no HRR is occurring. Scale bar 50µm.

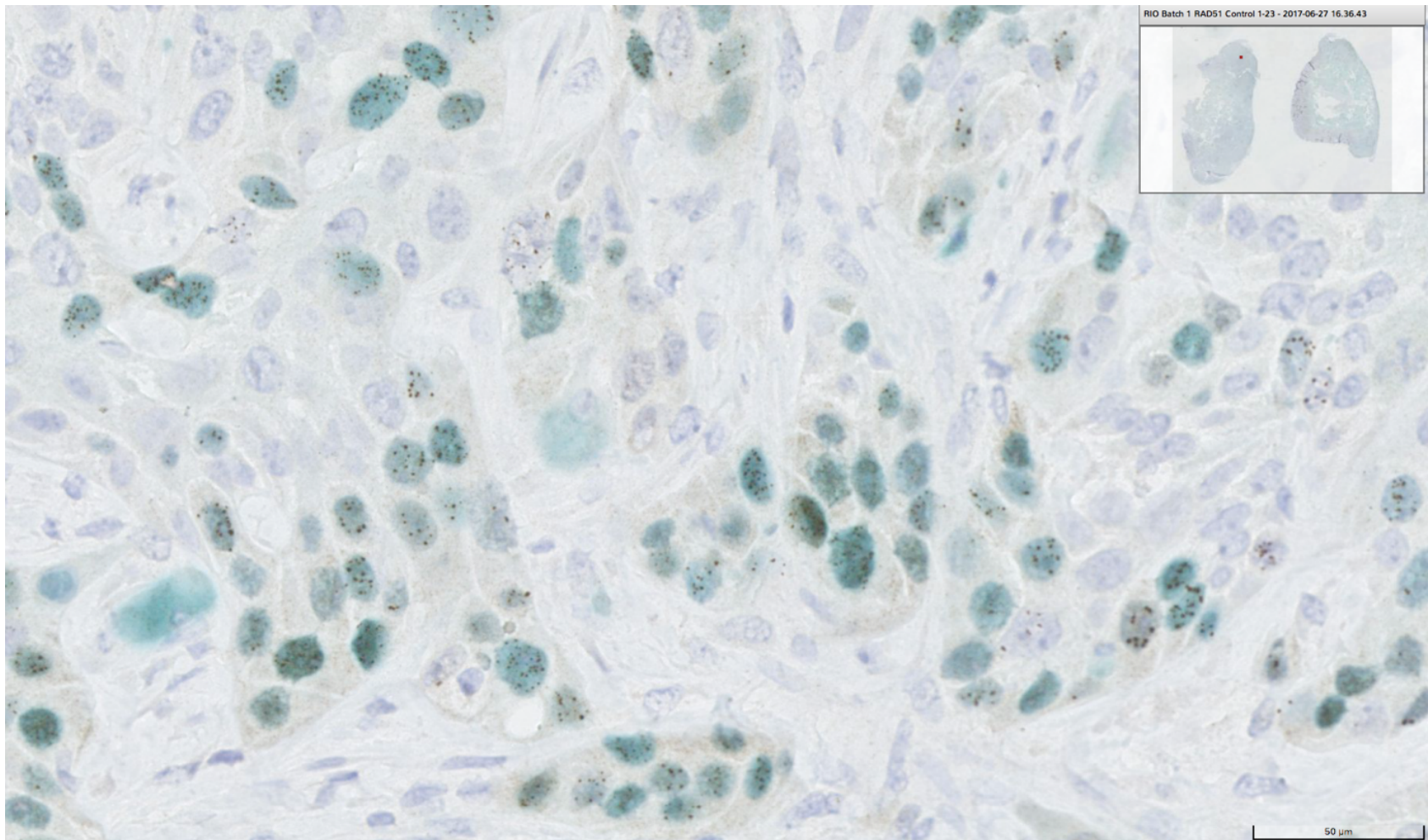


Figure 8 RAD51/ GMNN IHC positive control (Radiotherapy treated SCC at x40 magnification)

GMNN staining of tumour cells in blue/ green and brown foci of RAD51 indicating HRR is occurring. Scale bar 50μm.

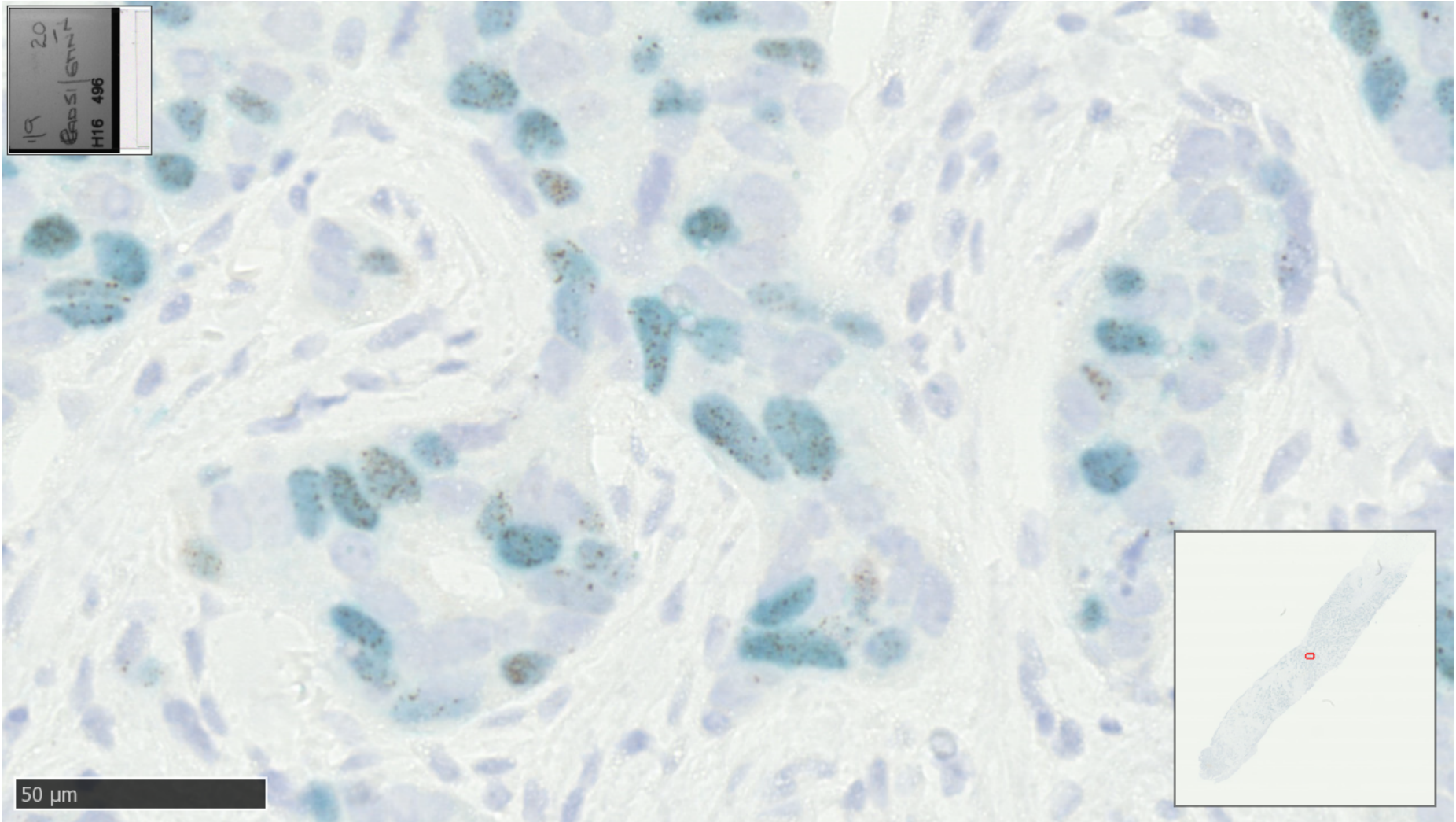


Figure 9 RAD51/ GMNN IHC from patient RMC 001 057 at 24-48 hours after 1st cycle of chemotherapy (H)

GMNN staining of tumour cells in blue/ green and brown foci of RAD51 foci at x40 magnification indicating HRR is occurring. Scale bar 50µm.

3.5.3 Immunofluorescence for RAD51/GMNN double staining

A subset of samples were stained by IF to allow comparison with IHC. Comparative to IHC, IF required an additional stain with DAPI to identify the cell nucleus (blue). GMNN stains the cell green and the presence of RAD51 foci is visualised as red foci (Figure 10). Two scoring methods were analysed; the Hamamatsu NanoZoomer digital slide scanner and the confocal microscope. Images uploaded onto the Hamamatsu were visualised at x40 magnification. Confocal images were able to be scanned up to x80 if required.

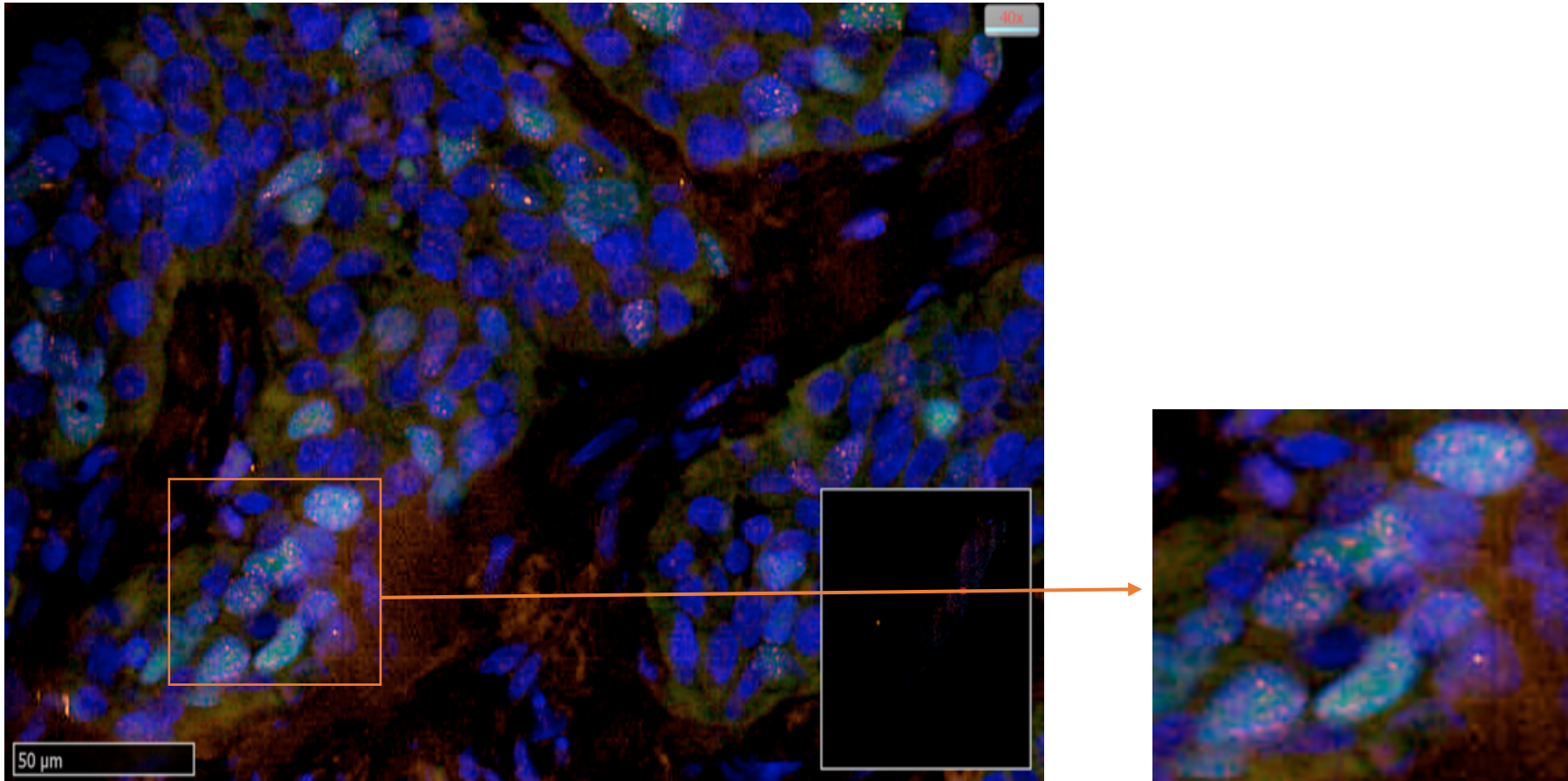


Figure 10 RAD51/GMNN IF

Patient RMC 001 057 taken at 24-48 hours after 1st cycle chemotherapy. IF stained with DAPI, RAD51 and GMNN. Image from Hamamatsu Nanozoomer digital slide scanner at x40 magnification. DAPI nuclear stain (blue), GMNN stain (green), RAD51 foci (red). The presence of rad51 foci indicated HR taking place.

3.5.4 Validation between immunohistochemistry and Immunofluorescence

Eight samples were used to compare the efficiency and accuracy of scoring between IHC and IF. All images were scanned using the Hamamatzu Nanozoomer digital slide scanner. IHC images were uploaded onto the digital imaging platform, PathXL and were able to be viewed at 40X. IF images were not able to be uploaded to PathXL due to a limitation in the magnification of 20X. Therefore, IF images were scored manually via NDP Nanozoomer digital pathology system (x40) and using the confocal microscope (x80). One sample did not have any tumour cells in the core biopsy and was excluded from analysis. There was good correlation between IHC and IF when scored for proliferation fraction and RAD51 score by digital imaging platforms (Figure 11).

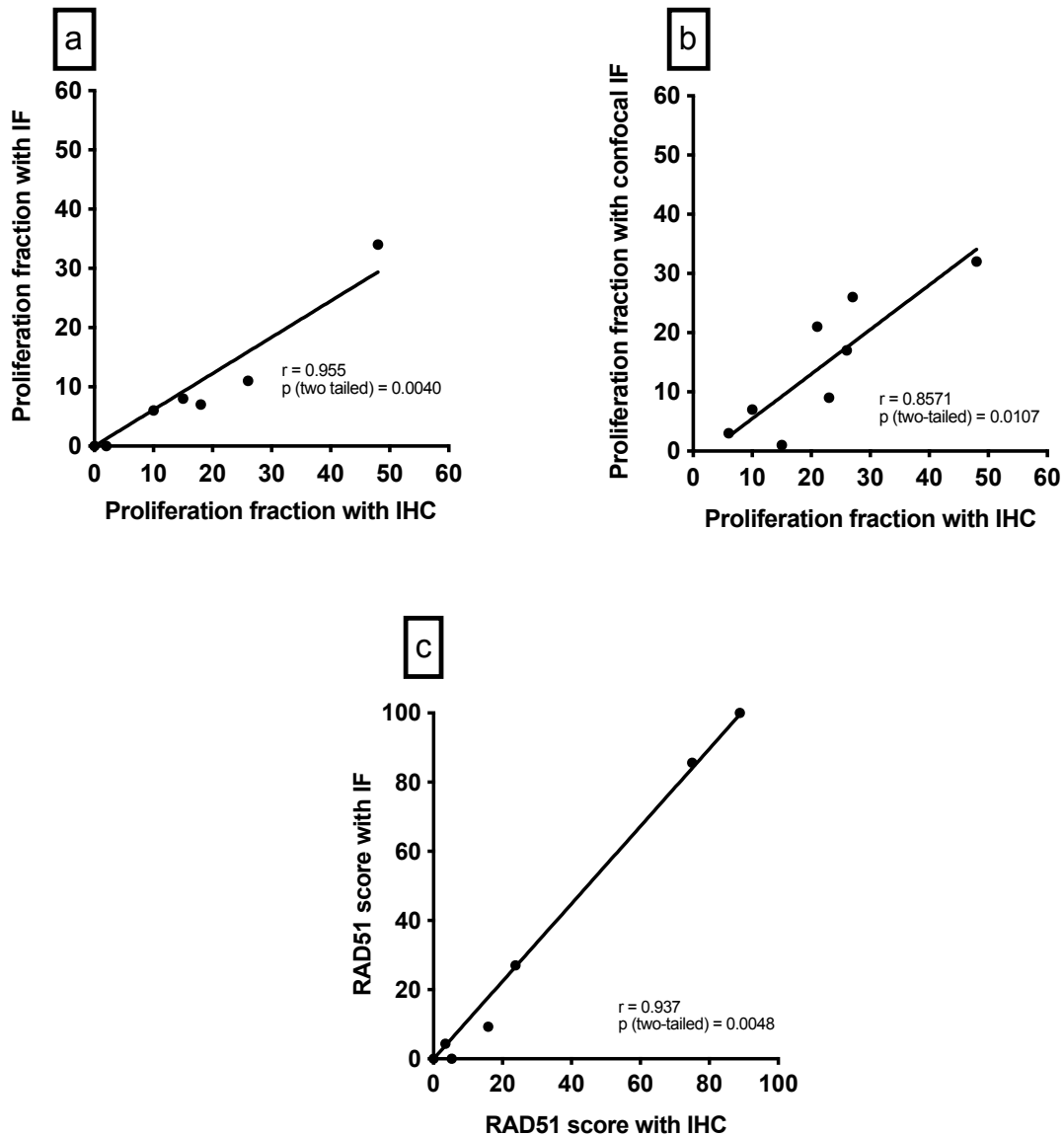


Figure 11 Validation of proliferation fraction and RAD51 score between immunohistochemistry and immunofluorescence RAD51

a) Comparison of proliferation fraction by immunohistochemistry (IHC) and PathXL vs IF (IF) and Hamamatsu Nanozoomer digital slide scanner for scoring (Spearman correlation: $r=0.955$, $p=0.0040$).

b) Comparison of proliferation fraction by immunohistochemistry (IHC) and PathXL vs IF (IF) and Confocal microscope for scoring (Spearman correlation: $r=0.8571$, $p=0.0107$).

c) Comparison of RAD51 score by immunohistochemistry (IHC) and PathXL vs IF (IF) and Hamamatsu Nanozoomer digital slide scanner for scoring (Spearman correlation: $r=0.937$, $p=0.0048$).

In regards to accuracy of scoring and time efficiency, the use of PathXL as a digital platform was superior. This platform allowed images along with the scoring to be stored for future validation (Figure 12). The good correlation between IHC and IF, and the ease of use of the digital platform PathXL, validated the use of IHC and scoring with PathXL for the remaining sample validation set.

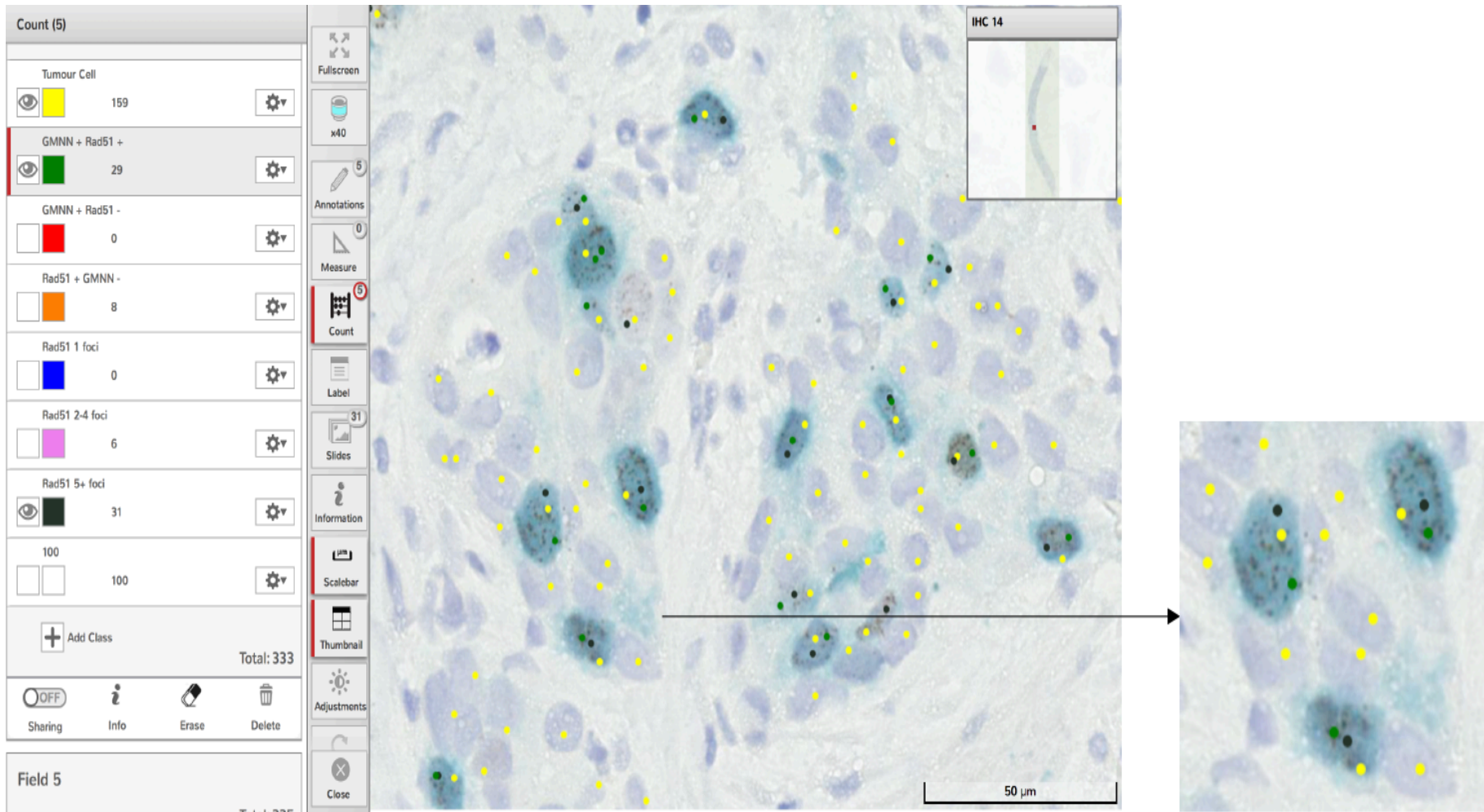


Figure 12 Image from PathXL digital imaging platform.

Software allows manual allocation of identifiers. Tumour cell identified with yellow dot; GMNN +ve/RAD51+ve identified with green dots; Rad51 5+ foci represented with black dots.

3.5.5 Validation of assessing total cells/ field versus 100 cells/ field

Initially, all the tumour cells were counted in each sample. However, there was a wide range in the total cells/ field (Table 12 ; mean 982.5; range 382-1570). Therefore, establishing whether a 100 cells/field would achieve similar results without affecting accuracy and improve efficiency was sort. Twelve paired baseline (B) and 24-48 hour post 1st cycle of chemotherapy (H) samples were used to assess the validity of counting all tumour cells in the field versus 100 cells per field.

	100/field	Total cells/ field
Min	382	382
Max	500	1570
Mean	467.4	982.5

Table 12 Tumour cells/ field

There was good correlation comparing 100 cells/ field and total cells for proliferation fraction (Figure 13A **Error! Reference source not found.** Spearman correlation: $r=0.9753$, $p<0.0001$) and RAD51 score (Figure 13B Spearman correlation: $r=0.993$, $p<0.0001$). Using 100 cells/field improved efficiency without compromising accuracy and hence ongoing analyses were performed using 100 cells per field in 5 random fields.

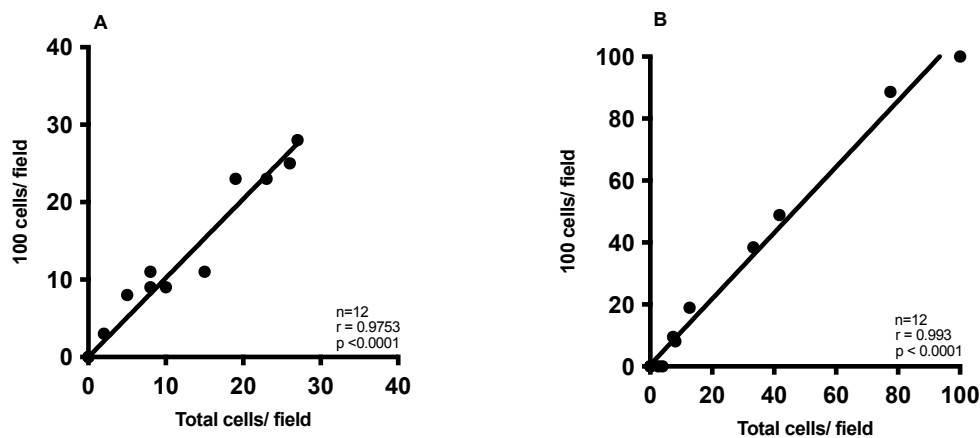


Figure 13 Correlation between number of tumour cells scored.

Correlation between total tumour cells counted per field versus 100 tumour cells per field for proliferation fraction (A) and RAD51 score using 5+ foci (B) (Spearman correlation; A: $r=0.9753$, $p<0.0001$; B: $r=0.993$, $p<0.000$, $n=12$).

3.5.6 Validation of number of RAD51 foci to count

Next, the RAD51 score was assessed in twelve patients that had assessable samples for RAD51/GMNN IHC at all three time points, to determine the threshold for the number of RAD51 foci/cell to reliably identify cells positive for foci formation. Samples were assessed on the basis of having 1+, 2+ and 5+ foci per cell (Figure 14). There was a significant difference between the H sample (24h post chemotherapy) and the 2 other time points for 1+, 2+ and 5+ foci, consistent with the induction of DNA damage by chemotherapy, showing that counting cells with 5+ foci provided the greatest sensitivity and discrimination between timepoints to assess HRR (Figure 14c, B vs H $p=0.0001$; H vs C $p=0.0033$; 95% confidence interval, non-parametric Friedman test with Dunn's multiple comparisons test).

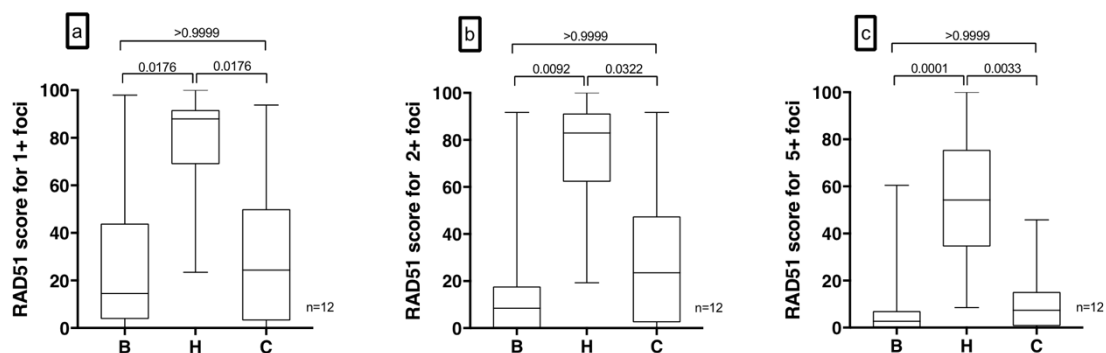


Figure 14 Number of RAD51 foci and timepoint assessed.

The RAD51 score for A) 1+, B) 2+, and C) 5+ foci, at the three time points – Baseline (B), 24-48 hours post 1st cycle of chemotherapy (H) and prior to the 2nd cycle of chemotherapy (C). Box = 5th and 95th percentile and median, error bars = minimum and maximum values. Statistical analysis with non-parametric Friedman test and Dunn's multiple comparisons test.

3.5.7 Correlation between scorers

Having established thresholds for number of tumour cells (100 cells/ field in 5 fields) and number of foci to call positivity for RAD51 foci formation, all samples were scored independently by 2 scorers (one clinician and one pathologist), using these conditions. There was good correlation between the scorers for proliferation fraction and RAD51 score counting 5+ foci and using the H time point (Figure 15; Spearman correlation: a: $r=0.9338$, $p<0.0001$; b: $r=0.862$, $p<0.0001$). One sample was excluded, as there were less than 10 GMNN positive cells in the sample causing discrepancy between the scorers.

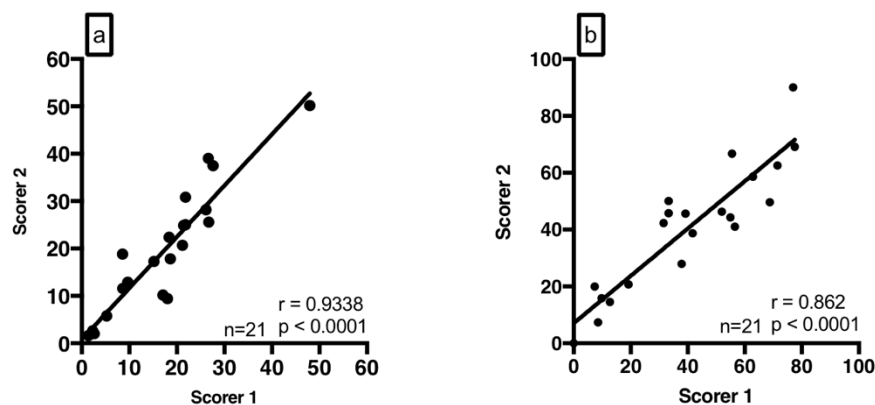


Figure 15 Correlation between scorers

Correlation between 2 scorers for (a) proliferation fraction and (b) RAD51 score counting 5+ foci at H time point (Spearman correlation; a: $r=0.9338$, $p<0.0001$; b: $r=0.862$, $p<0.0001$).

3.5.8 Number of tumour cells and GMNN cells to be counted for validity of sample

Due to one sample having a discrepancy between the scorers it was determined whether a minimum number of tumour cells and GMNN positive cells should be counted to ensure the samples are scored accurately. Using eight samples of the chemoNEAR cohort the RAD51 score was variable when less than 300 tumour and 30 GMNN positive cells were counted (Figure 16). These were used as the minimum required for an acceptance of a sample for RAD51 scoring.

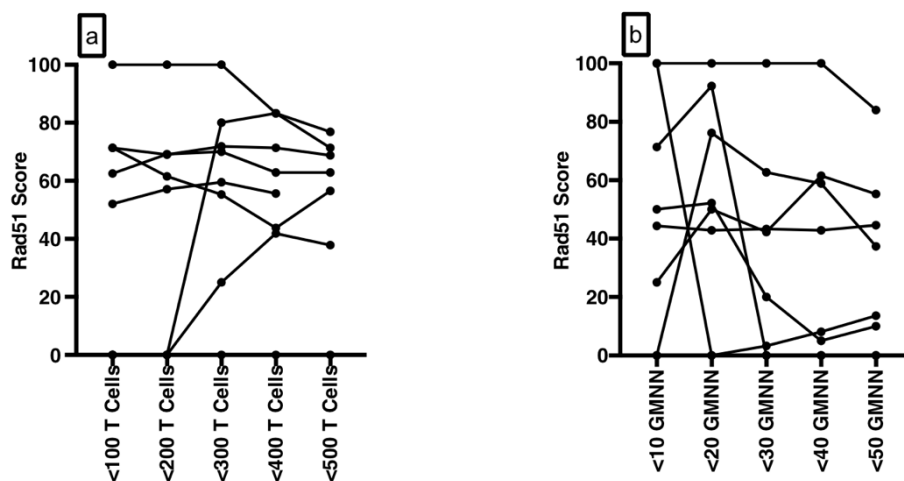


Figure 16 Minimum requirement for total tumour cells and GMNN positive cells.

Calculating the variability of the RAD51 score based on (a) number of tumour cells or (b) number of GMNN positive cells counted in a sample.

3.5.9 RAD51 score based on subtypes

Using samples from the ChemoNEAR study the H time point and 5+ foci were used to determine the differences in RAD51 score between breast cancer subtypes (Figure 17). There were a total of 21 samples, 1 patient was excluded due to no clinical information. 4 patients were ER+/HER2, 5 patients were ER+/HER2+, 7 patients were ER-/HER2+, 6 patients were TNBC. Patients with TNBC had a lower RAD51 score in comparison to the other breast cancer subtypes although this was not significant (Mann Whitney Test: $p=0.0639$).

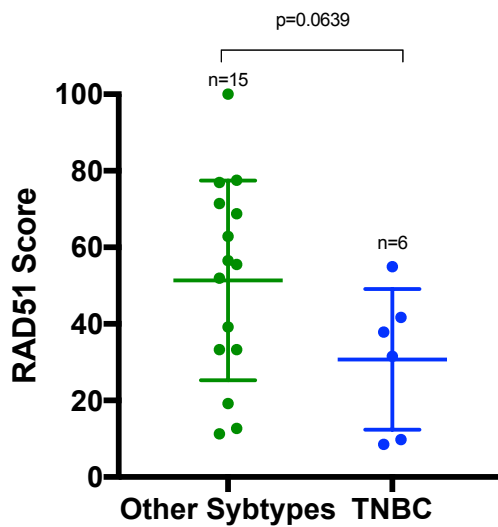


Figure 17 Rad51 score based on subtype.

RAD51 score using the H time point and 5+ foci for scoring to determine the difference between TNBC (n=6) and other breast cancer subtypes (n=15; Mann Whitney Test: $p=0.0639$).

3.5.10 Cut off to determine Homologous Recombination Deficiency (HRD)

The RAD51 score at the H timepoint was used to determine whether a functional HRD was present. A RAD51 score of 20 was determined based on 75% of samples with a RAD51 score less than 20 were TNBCs and comparatively, 24% of high RAD51 score were TNBCs (Figure 18). There were no known *gBRCA1/2* patients in this cohort.

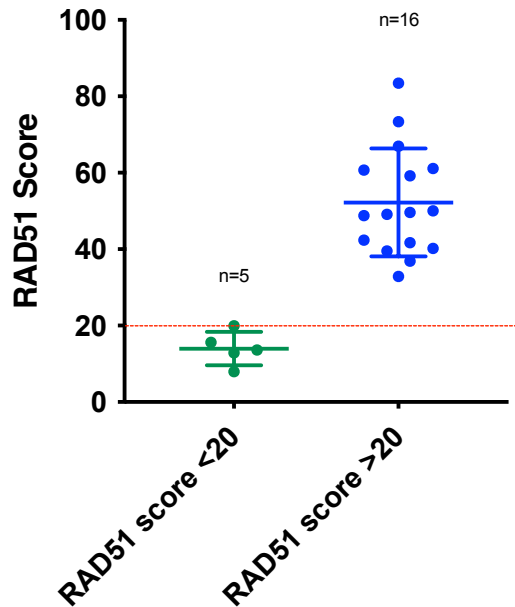


Figure 18 RAD51 score to determine HRD

3.5.11 Final criteria for RAD51 Scoring

1. Double staining IHC with RAD51 and GMNN.
2. Scoring using PathXL, a digital imaging platform.
3. The 24-48 hour sample taken after treatment is the most reliable for RAD51 assessment within this study.
4. 100 cells per field in 5 random fields.
5. 5+ RAD51 foci per GMNN positive nucleus.
6. A minimum of 300 tumour cells in a total sample (if 100 cells per field is not possible).
7. A minimum of 30 GMNN cells in a total sample.
8. If criteria 4-7 are not met another sample should be stained and analysed. If the criteria are not met after repeating IHC the sample should be recorded as insufficient.

(Appendix 3)

3.6 Discussion

A cell with RAD51 foci present will have an intact HR pathway, and cells which have a failure to show RAD51 foci represent HR deficiency. Detection of cells with HR deficiency, may identify a subset of TNBC that can respond to PARP inhibition. Currently there is an unmet need to design a marker to identify these patients. Studies to date have used IF RAD51 assays and a clinical trial is investigating the use of a RAD51 IF assay for clinical development^{67,71,72,193,199}. To date there is no published data using IHC as a method of RAD51 foci assessment. If a marker is to be utilised in the clinical setting it must be accurate and have the ability to be high throughput. Using the ChemoNEAR study as a validation set, we have validated an IHC protocol for FFPE tissue to detect RAD51 foci as a surrogate for HR deficiency.

The IHC RAD51 assay is shown to be reliable and consistent allowing interpretation of RAD51 foci to establish the presence of DNA repair after DNA damaging chemotherapy in the case of the ChemoNEAR validation set. RAD51 foci can be seen as brown foci in the nucleus and double staining with blue/ green GMNN confirms that the cell is in the correct phase of the cell cycle for HRR. This dataset shows IHC can be used with similar results to IF therefore showing that RAD51 foci detection by IHC maybe a useful marker to detect HRD in the clinical setting.

Assessment was consistent between 2 independent scorers showing that the data is reproducible. Using IHC and PathXL for scoring was more time efficient than the IF RAD51 assay in conjunction with either the confocal microscope or Hamamatsu NanoZoomer digital scanner reinforcing it is an adoptable marker for the clinic. Using the confocal microscope did yield a higher sensitivity to detect RAD51 foci but overall, there was no difference in the overall HR assessment of the samples concluding that IHC staining for RAD51 is worth pursuing for further assessment.

Currently there is no standard guideline for IHC RAD51 foci assessment. We therefore used the IF criteria from the literature as a guide to create guidelines for IHC^{67,71,193}. Most studies accept counting 5+ foci per nucleus as a marker for HRD, however, there are discrepancies in studies between the number of RAD51 foci to count and the timepoint which best assess HRD^{67,199}. Therefore, we explored whether the presence

of 1, 2 or 5 foci and at which timepoint; baseline, 24-48 hours after chemotherapy or before the second cycle of chemotherapy most accurately determine HRD. The validation study showed that using 5+ foci at the 24-48 hours post chemotherapy was the most accurate. This is in keeping with Meijer *et al* who have validated a functional HR assay, RECAP, exploiting the formation of RAD51 foci in GMNN positive cells after ex vivo irradiation of metastatic breast cancer tissue⁶⁶. However, a recent paper by Castroviejo-Bermejo *et al* reported RAD51 foci assessment at baseline was possible due to the high amount of endogenous DNA damage¹⁹³. This is somewhat surprising as it contrasts with several other studies and the data presented in this chapter that have shown no or minimal RAD51 foci formation at baseline^{67,71,72}.

To get an overall assessment of the tumour, 100 tumour cells in 5 different fields was representative rather than counting all the tumour cells. This led to the requirement of achieving a minimum of 300 tumour cells and 30 GMNN positive cells to reduce the variability and improve the accuracy of the test and is similar to the studies looking at IF^{71,193,199}.

Although not significant in the validation study, likely due to the low number of patients, there was a preference for a low RAD51 score in the TNBC subtype of breast cancer. This is consistent with data published from Graeser *et al* and Naipal *et al* who both show TNBC subtype with low RAD51 score confirming HRD^{67,71}. Interestingly in Naipal *et al* two out of the five HR-deficient cases were not caused by mutations in the *BRCA1* and *BRCA2* genes but by *BRCA1* promoter hypermethylation indicating the importance not to solely rely on germline mutations when determining who should be classed as HR deficient.

Most IF assays use a <10% RAD51 score to determine HR deficiency based on Graeser *et al*^{67,193}. In the validation dataset a <10% cut off was not specific enough and excluded samples which may show HRD. A cut off of <20%, was consistent with the RECAP test that has recently shown to be effective in ascertaining HRD in metastatic breast tumours treated with ionising radiation⁶⁶.

To develop this assay further a larger sample set would need to be required, and with the absence of response data in the ChemoNEAR study did not allow for further

correlation with histological subtypes. The RAD51 IHC functional assay presented here can determine the HR status at the time of treatment which could increase the number of patients eligible of PARP inhibitor treatment. The opportunity to use IHC in this setting rather than IF could be more time and cost effective.

Chapter 4 BRCA1 and RAD51C Methylation Validation

4.1 Introduction

Epigenetic mechanisms of gene inactivation are now well recognised as a potential alternative to genetic mutation in the silencing of tumour suppressor genes⁴⁹. DNA promoter methylation has been investigated for breast cancer detection, prognosis and treatment and there is mounting evidence that methylation status of CpG islands in cancer-related gene promoters, especially tumour suppressor genes, is distinct in breast cancer patients compared with healthy women or patients with benign breast disease⁸⁵.

DNA methylation is a naturally occurring event in eukaryotes and functions in the regulation of gene expression. Aberrant DNA methylation is a widespread phenomenon in cancer and may be among the earliest changes to occur during oncogenesis^{201,202}. DNA methylation consists of the addition of a methyl group to the fifth carbon position of the cytosine pyrimidine ring via a methyltransferase enzyme only at cytosines located at 5' to guanosine in the CpG dinucleotide^{203,204,205}. About 80% of all 5'-CpG-3' dinucleotides are found to be methylated, however the majority of the 20% percent that remain unmethylated are within CpG 'rich' areas, known as CpG islands in the promoters region²⁰⁵. Promoter methylation associates with a change in the activity of the DNA segment without changing the sequence ultimately silencing the gene in transcription. If the promoters of DNA repair genes are silenced this can lead to the accumulation of errors and ultimately mutations that give rise to cancer^{206,207}.

The ability to detect and quantify DNA methylation efficiently and accurately has become essential for the study of cancer. To date, a number of methods have been developed to detect/ quantify DNA methylation including: high-performance capillary electrophoresis and methylation-sensitive arbitrarily primed PCR^{205,208,209}. However, the most common technique used today remains the bisulfite conversion method where sodium bisulfite chemically reacts with and deaminates only unmethylated cytosines, while not reacting with methylated cytosines²¹⁰. This process was initially

done by Sanger sequencing of cloned PCR products. As bisulfite-converted DNA works well with sequencing-based approaches and with the rapid development of next generation sequencing (NGS) platforms, bisulfite sequencing is playing an important role in epigenetics²¹¹. Once converted, the methylation profile of the DNA can be determined by PCR amplification followed by DNA sequencing²⁰⁵.

BRCA1 is a “classical” tumour suppressor gene, represented by loss-of-function mutations accompanied by loss of heterozygosity (or gene inactivation by epigenetic mechanisms such as methylation); mutation in inherited syndromes that predispose to cancer; somatic mutation in spontaneous tumours; and the ability to inhibit the growth of transformed cells *in vitro*²¹². Numerous studies have demonstrated the methylation status of CpG islands in the promoter regions of *BRCA1* gene is abnormal in approximately 11-14% of patients⁴⁹. This is seen with sporadic breast cancer, notably TNBC, compared with normal healthy breast tissue and results in complete silencing of gene expression.^{13–16} Methylation can be associated with loss of heterozygosity (LOH) at the *BRCA1* locus signifying a situation where one allele is lost by deletion and expression of the remaining allele lost by promoter methylation.⁴⁹

It is suggested that sporadic tumours with *BRCA1* methylation have similar expression patterns to germline-*BRCA1* mutated tumours hence exploiting the theory of BRCAness which may add value in their response to PARP inhibition.^{76,216} Pre-clinical studies have demonstrated that *BRCA1* hypermethylation confers sensitivity for PARP inhibition and platinum derived drugs similar to *BRCA1* mutated tumours.^{86–88} Translated into the clinical setting there is conflicting data regarding the sensitivity of platinum and PARP inhibitor treatment associated with *BRCA1* methylation. Xu *et al* and Swisher *et al* reported that *BRCA1*-methylated tumours patients were sensitive to adjuvant chemotherapy and PARP inhibitor treatment respectively.^{217,218} However this conflicts with data showing patients with *BRCA1* promoter hypermethylation do not respond to platinum-based chemotherapy to the same degree as those with *BRCA* mutations.^{76,217} Possible reasoning for the conflict in data could be due to the reactivation of *BRCA1* mRNA expression through demethylation of the *BRCA1* promoter during tumourigenesis as methylation can be a transient event.⁷⁶

RAD51C is a paralog of *RAD51* that has an important role in maintaining genomic stability by acting with *RAD51* at the DNA damage site.²¹⁹ The prevalence of methylated *RAD51C* gene promoter in breast cancer has been reported at 0.5%.⁷³ Decreased expression of *RAD51C* can lead to impairment in HRR and hence tumours with low *RAD51C* may be responsive to treatment with PARP inhibitors similar to *BRCA1/2* deficient tumours. Min *et al* were the first to show that silencing *RAD51C* sensitises cancer cell lines to PARP inhibitor treatment and restoration of *RAD51C* expression decreased sensitivity *in vivo* and *in vitro*.²¹⁹ Recently *RAD51C*-promoter methylation has correlated with downregulation of gene expression in basal-like breast tumours independent of *BRCA1/2* events.⁵⁷ With the evolving data on *RAD51C* promoter methylation it opens another avenue to investigate to widen the patient selection who can benefit from PARP inhibition.

4.2 Hypothesis

BRCA1 and *RAD51* promoter methylation can be accurately identified with bisulfite sequencing.

4.3 Aims

1. To develop an assay for *BRCA1* and *RAD51C* promoter methylation using bisulfite conversion and next generation sequencing.
2. To validate the promoter methylation assays of *BRCA1* and *RAD51C* in tumour samples.

4.4 Acknowledgements

- Samples from the ChemoNEAR study were used for *BRCA1* and *RAD51C* methylation optimization.
- *BRCA1* and *RAD51C* methylation optimisation was performed by Neha Chopra.
- Bioinformatics for *BRCA1* and *RAD51C* methylation was performed by Ros Cutts.

4.5 Results

4.5.1 Validation of *BRCA1* and *RAD51C* methylation primers

An optimum bisulfite conversion and PCR optimisation assay was developed preceding next generation sequencing (NGS). *BRCA1* primers were identified from previously used primers in the Molecular Oncology Laboratory. *RAD51C* primers were designed using the methods discussed in Chapter 2 Methods and Materials. The *BRCA1* amplicon included 11 CpG sites and the *RAD51C* amplicon had 8 CpG sites (Figure 19).

<i>BRCA1</i>	<p>5'TATTTTGAGAGGTTGTTGTTTAGCGGTAGTTTTTTGGTTTTCGTGGCACG</p> <p>GAAAAGCGCGGGAATTATAGATAAATTACGAATTGCGCGGCGTGAG</p> <p>TTCGTTGAGATTTTTGGCGGGGGATAGGTTGTGGGGTTTTTAG3'</p>
<i>RAD51C</i>	<p>5'TGGTAATTGGTTAGTGTGTGTCGTTCGTTTATTATTTTTATTCGAGATTA</p> <p>TTTTTATTAATGATTTTGAGTTTTATTTAATAGGTTACGGTGGAGGTAAGGA</p> <p>AATGTGGCGTGGAGAATTTATTGGGTTTGGTTTTCGTTTTATGGTTTTCGTT</p> <p>TATCGTTTTATAGTTAGGGTGTATATTTGATGAGGA3'</p>

Figure 19 *BRCA1* and *RAD51C* methylation sequences

BRCA1 and *RAD51C* amplicons showing the CpG sites in the amplicon (red). Amplicon length is 148 and 190 bases respectively. Bold underlined bases showing consensus site for the methylation primers. Red highlighted CG sites showing the CpG sites.

Initial workup of primers involved the determination of the optimum annealing temperature by temperature gradient PCR. A thermostable Taq with a proof-reading enzyme was used to ensure primer-specific hybridisation and increase precision of PCR amplification. Using predesigned bisulfited DNA oligonucleotides both *BRCA1* and *RAD51C* primers were tested at 55°C, 60°C and 65°C and PCR product was analysed on an Agilent Bioanalyzer 60°C was the optimum temperature for *BRCA1* and *RAD51C* methylation primers allowing for the possibility of a multiplex (Figure 20 and Figure 21).

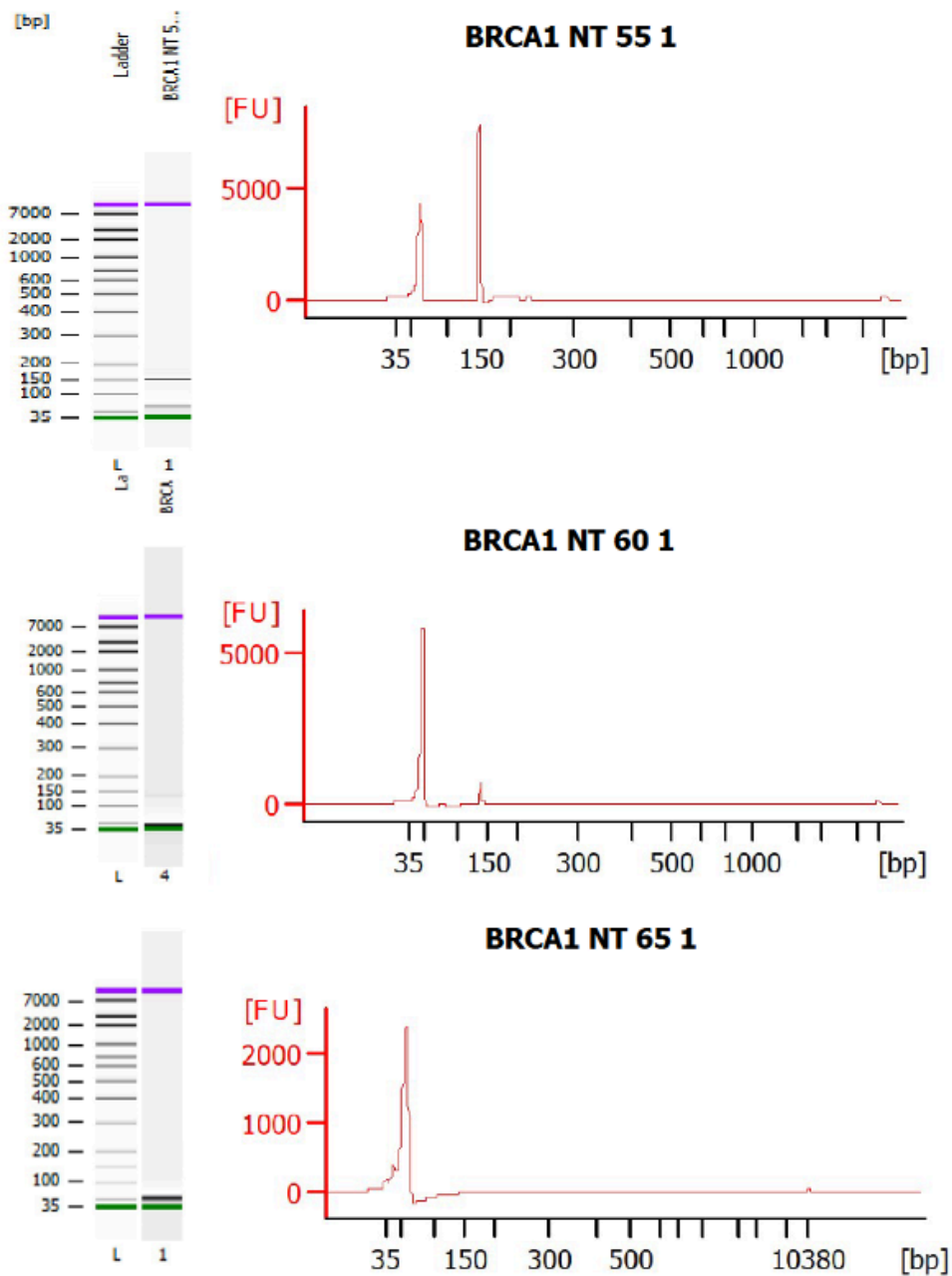


Figure 20 Optimisation of *BRCA1* methylation primers

Identical PCR reactions at increasing temperatures; 55°C, 60°C and 65°C. Using Agilent's Bioanalyzer instrument each reaction was analysed for presence or absence of PCR product. 3 Bioanalyzer traces with corresponding ladders using predesigned bisulfite treated DNA to ascertain the optimum temperature for *BRCA1* methylation primers. 60°C was the optimum temperature for *BRCA1* methylation primers.

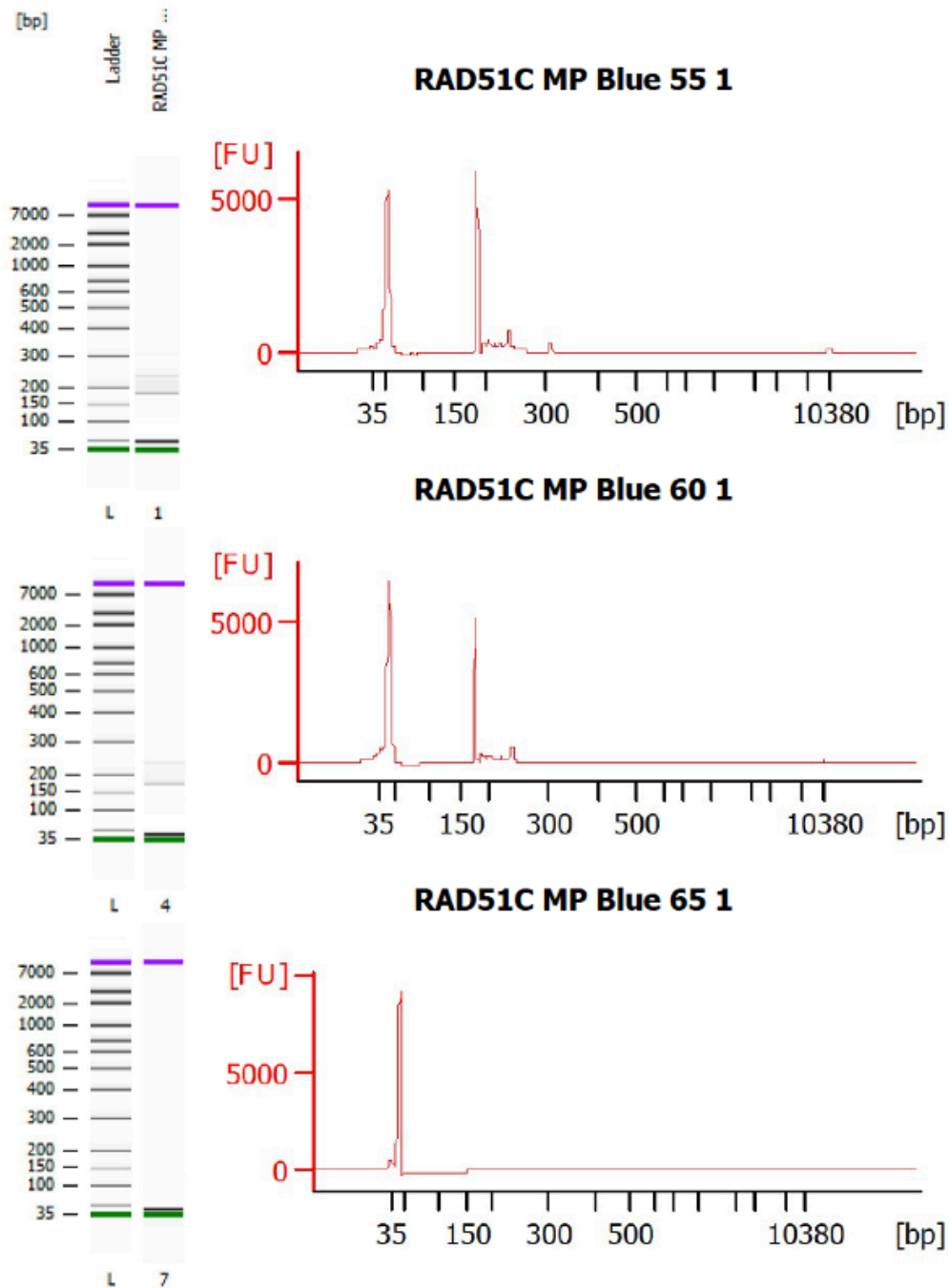


Figure 21 Optimisation of *RAD51C* methylation primers

Identical PCR reactions at increasing temperatures; 55°C, 60°C and 65°C. Using Agilent's Bioanalyzer instrument each reaction was analysed for presence or absence of PCR product. 3 Bioanalyzer traces with corresponding ladders using predesigned bisulfite DNA to ascertain the optimum temperature for *RAD51C* methylation primers. 60°C was the optimum temperature for *RAC51C* methylation primers.

4.5.2 Validation of *BRCA1* and *RAD51C* methylation multiplex

A minimum amount of DNA required to detect both *BRCA1* and *RAD51C* methylation in tumour samples is favorable. As both primers were optimised at 60°C and have different amplicon lengths, we designed a multiplex assay for *BRCA1* and *RAD51C*. Using the Agilent Bioanalyzer two peaks were visible identifying *BRCA1* at 150bp and *RAD51C* at 200bp (Figure 22).

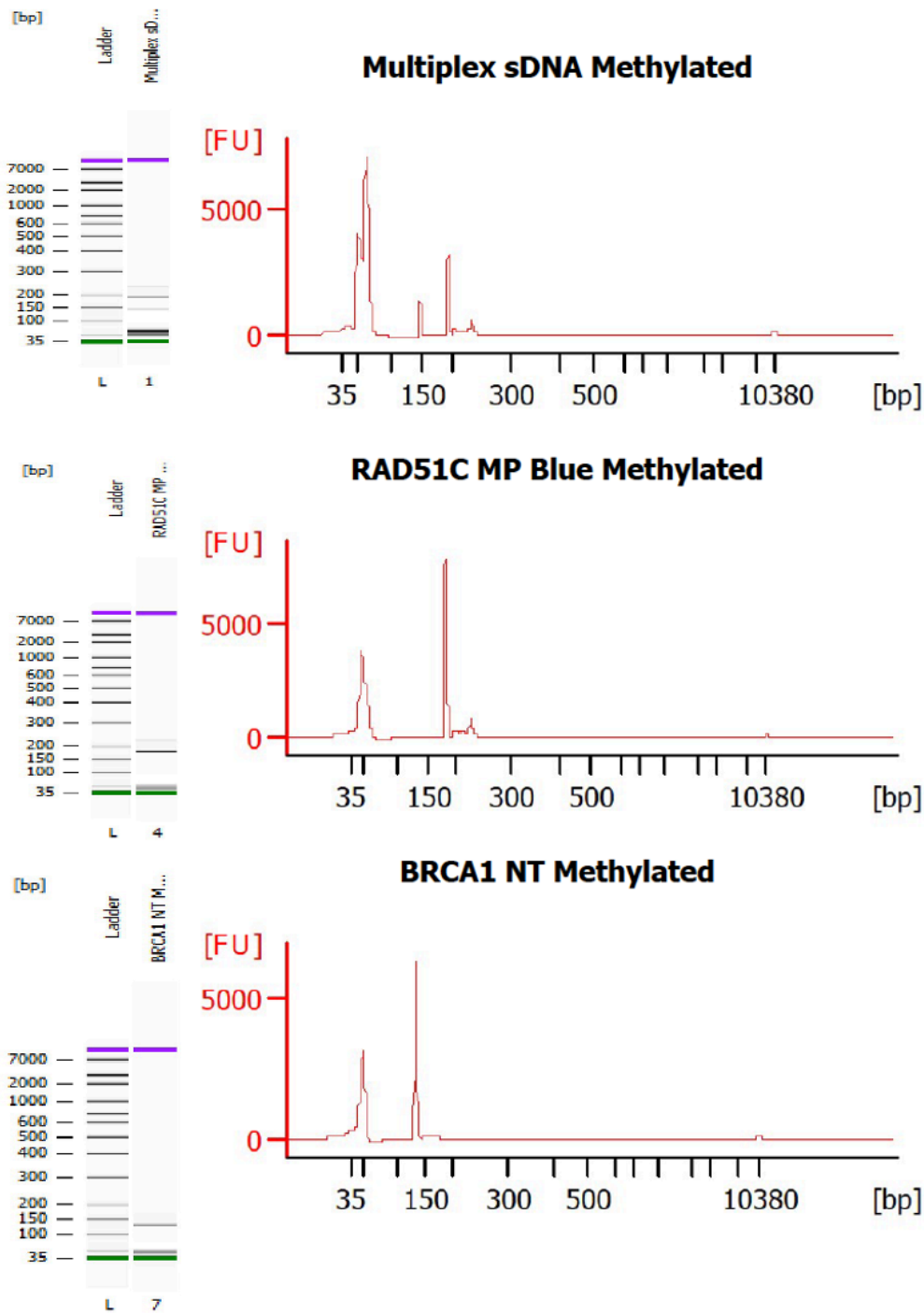


Figure 22 Bioanalyzer tracing of multiplex PCR with *BRCA1* and *RAD51C* methylation primers

Combining *BRCA1* and *RAD51C* after bisulfite treatment in a PCR is possible. The top tracing shows the multiplex assay with a clear distinction between the two primer pairs. The middle and bottom Bioanalyzer tracing are of *RAD51C* singleplex and *BRCA1* singleplex respectively.

Initially PCR was conducted with 40 cycles producing a large amount of PCR product. To reduce PCR error and ensure ample target enrichment the optimum number of PCR cycles was determined. The multiplex PCR was subjected to an increasing number of PCR cycles in triplicate and subsequently run on an agarose gel (Figure 23a). The total DNA amount produce at each interval PCR cycle is shown in Figure 23b. A steady amount of PCR product was produced at 34 cycle and correlated with the agarose gel and as a result 34 cycles was taken as the optimum number of cycles for the multiplex assay.

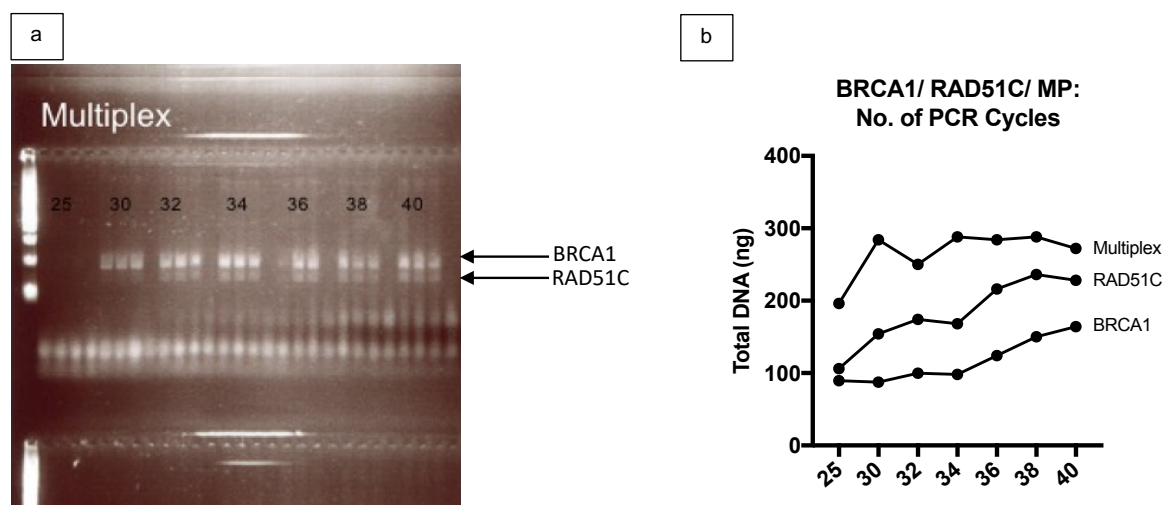


Figure 23 Optimum number of PCR cycles

- A. To ensure the optimum number of PCR cycles was determined an agarose gel was run to ensure both *BRCA1* and *RAD51C* products were amplified. *BRCA1* and *RAD51C* primers showed adequate target enrichment at 34 cycles.
- B. Represents the amount of PCR product produced from the PCR amplification. *BRCA1*, *RAD51C* and the multiplex PCR were run to ensure ample amplification of both products in the multiplex. 34 cycles showed an approximate doubling of PCR product and target enrichment.

Cleaning the PCR product by either columns or beads was evaluated along with determining the optimum elution volume to assess DNA concentration. Due to less user involvement it was determined columns produced the least variability in the amount of PCR product and the higher yield along with a lower elution volume (Figure 24). Going forward post PCR DNA was cleaned using columns and with a 50 μ L elution volume.

Post PCR Clean Up Beads vs Columns

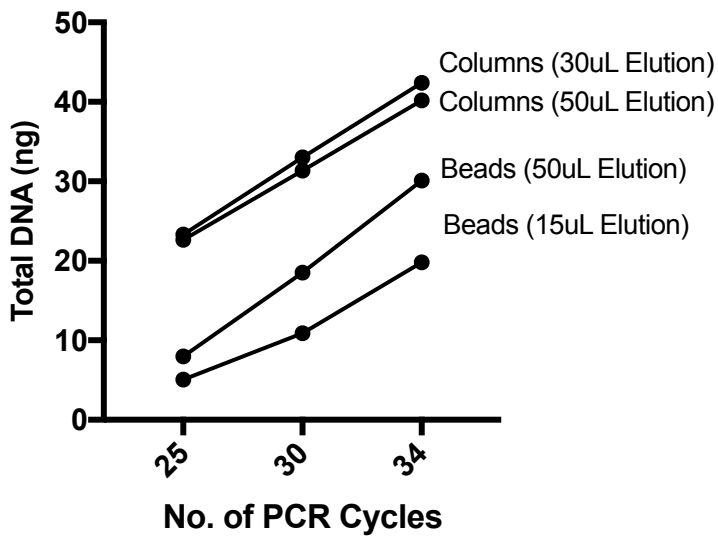
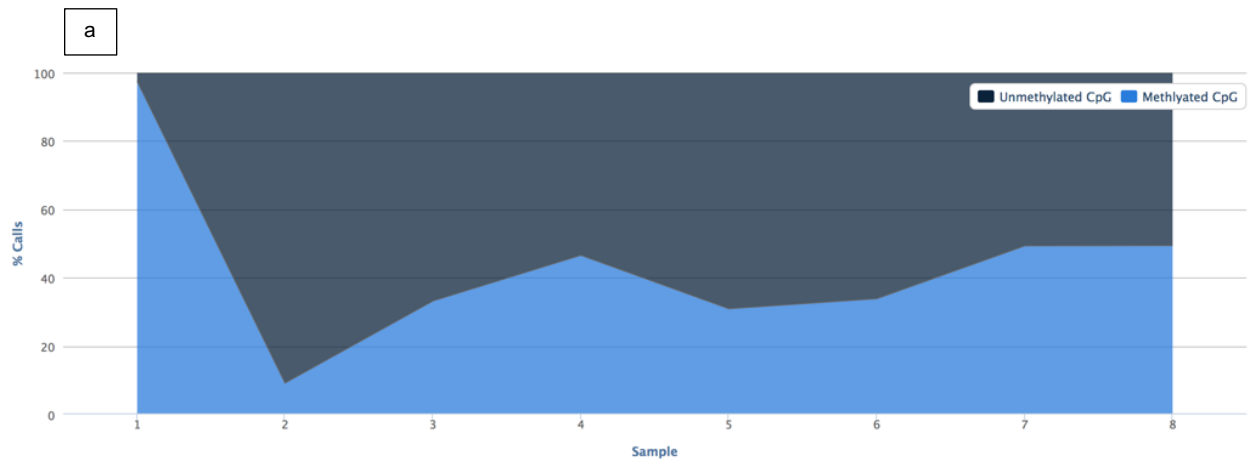


Figure 24 Comparison of column versus beads for PCR clean up and elution volume.

Total DNA comparisons between method of PCR clean up, columns versus beads and elution volumes. PCR clean up with columns and in an elution of 50µl was used.

To validate the *BRCA1* and *RAD51C* methylation multiplex on tumour samples a pilot run of synthetic methylated and unmethylated DNA, and DNA extracted from 4 TNBC and 2 *gBRCA1* RNA Later tissue samples from the ChemoNEAR study underwent DNA quantification, bisulfite modification, PCR as described in Chapter 2 methods and materials. PCR products were subjected to NGS sequencing using an Illumina Miniseq to detect CpG sites within the amplicons.

NGS clearly delineated between methylated and unmethylated synthetic DNA (Figure 25a) and was also able to accurately identify the 11 and 8 CpGs in the *BRCA1* and *RAD51C* gene promoter amplicons respectively. Methylation of *BRCA1 promoter* was homogenous throughout all CpG sites in a sample simplifying whether a sample would be identified as methylated or not (Figure 25b). In contrast, in keeping with previous data^{220,221}, the *RAD51C* promoter showed a heterogeneous pattern of methylation across the CpG sites with island number 5 being constantly methylated (Figure 25c).



		Island No	Pos	Neg	TNBC	TNBC	TNBC	TNBC	gBRCA	gBRCA
<i>BRCA1</i>	1	0.96	0.12	0.10	0.33	0.10	0.04	0.36	0.28	
	2	0.97	0.10	0.10	0.33	0.09	0.04	0.36	0.28	
	3	0.95	0.10	0.09	0.34	0.09	0.04	0.35	0.25	
	4	0.97	0.11	0.09	0.35	0.09	0.04	0.37	0.28	
	5	0.97	0.11	0.10	0.36	0.09	0.03	0.36	0.28	
	6	0.97	0.11	0.09	0.35	0.10	0.04	0.37	0.27	
	7	0.98	0.11	0.09	0.33	0.09	0.04	0.36	0.26	
	8	0.97	0.11	0.09	0.36	0.10	0.04	0.36	0.27	
	9	0.98	0.11	0.09	0.35	0.10	0.03	0.35	0.19	
	10	0.97	0.11	0.09	0.35	0.09	0.04	0.36	0.27	
	11	0.96	0.11	0.09	0.35	0.09	0.04	0.32	0.27	

		Island No	Pos	Neg	TNBC	TNBC	TNBC	TNBC	gBRCA	gBRCA
<i>RAD51C</i>	1	0.98	0.01	0.35	0.41	0.37	0.48	0.46	0.69	
	2	0.98	0.01	0.65	0.66	0.63	0.79	0.73	0.91	
	3	0.98	0.01	0.31	0.37	0.24	0.47	0.39	0.43	
	4	0.98	0.02	0.72	0.69	0.66	0.83	0.66	0.85	
	5	0.98	0.01	0.94	0.88	0.95	0.95	0.91	0.97	
	6	0.98	0.01	0.54	0.68	0.61	0.74	0.72	0.83	
	7	0.98	0.01	0.40	0.56	0.45	0.63	0.56	0.65	
	8	0.98	0.01	0.29	0.41	0.32	0.47	0.46	0.38	

Figure 25 *BRCA1* and *RAD51C* methylation status of individual CpG sites

- a. Analysis from Bismark (<https://www.bioinformatics.babraham.ac.uk/projects/bismark/>) – a tool to map bisulfite converted sequence reads and determine cytosine methylation states. This shows the % of calls for methylation states for each sample. 1 – Synthetic methylated DNA, 2 – Synthetic unmethylated DNA, TNBC samples 3-6, *gBRCA1* samples 7-8.
- b. NGS using the MiniSeq shows all CpG islands for *BRCA1* were identified in all 6 samples. There was positive identification of the methylated and unmethylated samples. The methylation cut off was set as 0.9 as per previous data.¹⁷⁶ There were no methylated tumour samples identified in this set. Pos – positive control for methylation (green); Neg – negative control for methylation (red); TNBC – triple negative breast cancer; gBRCA – germline *BRCA*.
- c. NGS using the MiniSeq shows all the islands either methylated or unmethylated in the positive and negative controls confirming the assay works. In the tumour samples the proportion of methylation of CpG islands in a sample is not homogenous. Island 5 is always methylated. The variability of methylation at individual CpG sites is consistent with results from the TCGA database. No expression data was available for this dataset. Pos – positive control for methylation (green); Neg – negative control for methylation (red); TNBC – triple negative breast cancer; gBRCA – germline *BRCA*

4.6 Discussion

Promoter methylation is a well-characterised mechanism leading to gene silencing and can be utilised to identify patients sensitive to PARP inhibition²¹⁸. Research shows methylation of *BRCA1* and *RAD51C* causes gene silencing, leading to downregulation of mRNA, protein expression and ultimately functional HRD.^{57,73,218–220}

Identification of DNA methylation at CpG islands by bisulfite sequencing remains the gold standard, however the method is inefficient with large DNA losses and it is imperative to preserve DNA for other molecular analyses^{210,222}. We have developed a multiplex assay using both *BRCA1* and *RAD51C* primers which can identify methylated and unmethylated CpG sites in breast tumours. Both gene promoters' amplicons had similar annealing temperatures and as the amplicon sizes were different they were able to be distinguished during PCR and ultimately NGS.

The *BRCA1* promoter was homogeneously methylated in a sample clearly identifying whether a sample was methylated or unmethylated (Figure 25B). However, in comparison *RAD51C* promoter methylation was heterogeneously associated and one CpG island was found to be permanently methylated; island 5 (Figure 25C). Although there is not much data in the literature in regards to the patterns of methylation in specific genes^{57,176}, interrogation of the TCGA database confirms our findings.

Analysis of the pilot data was limited in determining gene function as no expression data was available. However, determination of whether the multiplex was effective in detecting methylation CpG sites was possible. Bismark, a program to align bisulfite treated reads to a reference genome and perform methylation calls was used to determine the methylation status.²²³ Further interpretation of the gene methylation status, bases at CpG sites were counted and the % methylated at each CpG site was calculated per sample. This was possible using IGV genome browser²²⁴.

The methylation PCR method involving bisulfite sequencing validated in this chapter is a reliable method to determine the methylation status of *BRCA1* and *RAD51C* using

a multiplex assay. Although gene expression data was not available to determine the impact of methylation in this dataset, this will be evaluated within the RIO trial.

Chapter 5 Predictive biomarkers of homologous recombination deficiency (HRD) in TNBC

5.1 Introduction

Cancer is a disease of the genome and throughout the lifecycle of a cancer cell, the genome acquires genomic alterations due to various mutational, endogenous and exogenous processes, resulting in genomic instability and subsequently a 'genomic scar'^{225,226}. These genomic scars portray the life history of the cancer and potentially allow tumours to be classified into subtypes⁷⁶. Initially, three independent DNA-based measures of genomic instability, including loss of heterozygosity, telomeric allelic imbalance and large-scale state transitions, accurately identified *BRCA1/2* tumours^{60–62}. However their combination to form the HRD Score allowed HR-deficient tumours (HRD Score >42), independent of *BRCA1/2* deficiency, to be identified within a sporadic TNBC population⁶³.

With the drive to identify these scars, the advent of massive parallel sequencing and the reducing cost of genomic analysis, it has been feasible to classify cancers according to their underlying mutations⁷⁶. Each mutational process leaves a characteristic imprint known as a mutational signature on the cancer genome^{56,227}. Next generation sequencing (NGS) has identified numerous driver mutations implicated in tumorigenesis^{56,228} and with further development in sequencing technology, identification of passenger mutations and their importance in tumorigenesis as scars of biological processes has increased the need to develop models to encompass all the information available for a cancer to develop⁵⁶. Advances in next-generation sequencing (NGS) have revealed the genomic complexity and heterogeneity of TNBC which is molecularly distinct from other types of breast cancer²²⁹.

Breast cancers with *BRCA1* and *BRCA2* germline mutations are highly sensitive to PARP inhibitors, that target the underlying HR DNA repair defect^{47,48}. A subgroup of *BRCA1/2* wild type TNBC are known to harbor defective HR DNA repair, that is potentially targetable with PARP inhibitors^{4,12,230}. However the extent to which PARP inhibitor efficacy may translate to sporadic TNBC is unknown as, a clinical trial with heavily pre-treated

un-selected advanced showed no activity¹⁸⁹. The opportunity to use treatment naive tumours provides a platform to identify primary HR-deficient TNBC and investigate whether there is a response to PARP inhibitor in this population. Recent research has discovered defects in HR DNA repair in TNBC, through germline mutations in BRCA1, BRCA2 and PALB2, somatic mutations in BRCA1 and BRCA2 and promoter methylation of BRCA1 and RAD51C^{5,58,59,64}. Furthermore, Polak et al were able to show in patients with basal like breast cancer an association of RAD51C methylation with low RAD51C expression⁵⁷.

A pivotal study using the discovery of somatic mutations through tumour sequencing and a mathematical non-negative matrix factorisation model on 21 breast cancers, identified base substitutions relating to five mutational signatures(A-E), each representing a specific mutational process^{90,231}. This work was further validated in 30 different cancer types, where a further 16 substitution-based signatures were identified⁹¹. *BRCA1/2* mutant tumours were noted to be associated with signature 3 (previously known as signature D) and an excess of larger indels (>3bp) with microhomology present at breakpoint junctions^{90,93}. The authors noted that there were a higher proportion of signature 3 tumours than the expected 5-15% *BRCA1/2* tumours, advocating the presence of homologous recombination deficiency (HRD) in wild type *BRCA1/2* tumours⁹¹. Every signature serves as an imprint of a distinct DNA damage and repair process either at present or at some point during tumorigenesis. Most breast tumours have less than 20,000 substitutions and a small number will have a higher mutational burden, of up to 94,000 substitutions⁵⁶. Irrespective of the mutational burden, tumours can either be driven by one predominant signature or a multitude of signatures⁹³.

Further genomic analyses have discovered that mutational processes in human somatic cells are not restricted to producing base substitutions⁵⁶. DNA damage and repair processes can generate patterns of indels, large-scale chromosomal aberrations or structural variations²³². Some tumours have a large number of rearrangements that can be at a specific site or be widely distributed throughout the genome. Using the same mathematical model as first described by Alexandrov *et al*²³³, Nik-Zainal *et al* described six rearrangement signatures, 3 of which were associated with HR-deficient tumours⁹³.

HR DNA repair deficiency causes characteristic mutational signatures that result from error-prone repair of DNA⁵⁸. Using whole genome sequencing (WGS) 59% of 237 tumours derived from an unselected, population-based TNBC cohort were found to be HR deficient²³⁴. HRDetect, a novel biomarker, identifies six previously designated signatures of HR dysfunction; microhomology-associated small deletions, mutation signature 3 and 8, rearrangement signature 3 and rearrangement signature 5 as well as the LOH-based HRD score, outperforming copy number-based approaches such as Myriad's HRD score and individual signatures, giving an alternative to identifying *BRCA1/2* tumours and possibly sporadic TNBCs^{56,64}. HRDetect is able to identify a larger proportion of patients with *BRCA1/2* deficiency, not all with a germline mutation, opening the gate to identify new HR deficient mutations and pathways that may increase the number of patients who might benefit from HRD targeted treatments. HRDetect is sensitive at lower tumour cellularity, tumour sequencing depth and in FFPE samples, all important factors to consider when thinking about clinical utilisation. Whether mutational signatures, such as HRDetect, can be used to direct therapy in the clinic is unknown, in part as there is limited direct evidence that these cancers have a functional defect in HR.

The development of biomarkers that accurately and robustly predict treatment outcome is a key part of the drive towards personalised medicine. In the era of NGS with the rapid speed at which information is generated, how to best exploit the genomic alterations of TNBC for therapeutic options remains an important yet an unanswered problem. In the context of sporadic TNBC there is currently no biomarker that can ascertain those that have functional HRD and hence may respond to PARP inhibition. Therefore, the challenge remains to develop an efficient and coordinated strategy to identify effective biomarkers such that patients who are more likely to respond to drugs like the PARP inhibitors may be identified.

There is a drive for HRD assays and focus has been towards the genomic landscape assessing for BRCAness. However, whether these assays reflect the real-time HRD status of a tumour, is a valuable concern especially when committing a patient to a specific treatment pathway. The RECAP assay uses ex vivo irradiation followed by immunofluorescence of fresh clinical breast cancer samples to obtain a functional readout of a tumours HRD status. This gives the advantage of assessing functional

HR deficiency at the point of treatment but will require further validation in comparison to the genomic biomarkers⁶⁶.

The RIO trial (EudraCT 2014-003319-12) is a translational clinical trial with the objective of identifying biomarkers of PARP inhibitor activity in sporadic TNBC. Within the study we utilised clinical samples to identify both functional and genomic biomarkers to robustly identify HRD in sporadic TNBC. Here we will show how each individual biomarker can be used to detect HRD and the interplay between both genomic and functional biomarkers.

5.2 Hypothesis

Genomic and functional biomarkers can accurately detect HRD in sporadic TNBC.

5.3 Aims

1. To determine if HRDetect can detect HRD in sporadic TNBC in patients with or without an underlying epi(genetic) HR defect.
2. To determine if promoter methylation of *BRCA1* and *RAD51C* can be identified in tumours with HRD.
3. To assess the effect of rucaparib on RAD51 formation in sporadic TNBC
4. To assess if HRDetect positive cancers have an underlying functional defect in HR DNA repair.

5.4 Acknowledgements

- Samples in this chapter were used from the RIO trial
- HRDetect was performed by Serena Nik-Zainal with the assistance of Helen Davies (Senior Research Associate) with samples from the RIO trial.
- Immunohistochemistry was performed by Frances Daley at Breast Cancer Now Core Facility
- RAD51 IHC analysis was performed by Neha Chopra and Divya Kriplani
- *BRCA1* and *RAD51C* methylation was performed by Neha Chopra
- Bioinformatics for *BRCA1* and *RAD51C* methylation was performed by Ros Cutts

5.5 Results

The prevalence of HRD in primary TNBC was interrogated using multiple approaches in 38 patients from the RIO trial (Figure 26). DNA from RNA Later samples was extracted and utilised for WGS for HRDetect and discovery of the mutational status of *BRCA1*, *BRCA2* and *PALB2*. DNA and RNA was used for promoter methylation of *BRCA1* and *RAD51C* analysis and expression analysis. The functional assessment of HRD but RAD51 IHC used FFPE samples.

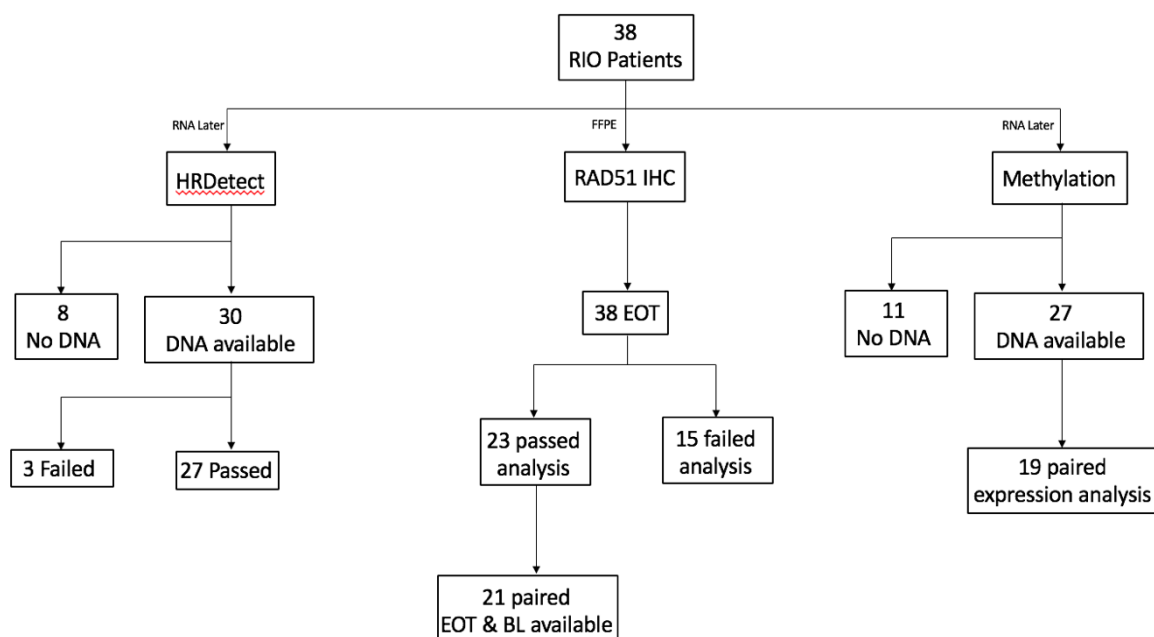


Figure 26 Consort diagram of the samples used to determine predictive biomarkers of HRD
 FFPE – formalin fixed paraffin embedded; IHC – immunohistochemistry; EOT – end of treatment; BL – baseline.

5.5.1 HRDetect as a predictive biomarker of HRD

HRD causes characteristic genomic aberrations reflecting error-prone repair of DNA and to encapsulate the imprint of HRD, we used the HRDetect assay, a score >0.7 was deemed HR deficient⁶⁴.

HRDetect identified HRD in 69% TNBC (18/26) as well as an additional control ER positive cancer with a known germline *BRCA2* mutation. Of the HRDetect +ve

cancers, 74% (14/19) had a detectable underlying mutation of *BRCA1/2* and *PALB2* or gene promoter hypermethylation of *BRCA1* or *RAD51C*. HRDetect identified all cancers with known HR pathway defects, as well as additional sporadic cancers with no single detectable defect. None of the eight HRDetect negative cancers had an underlying genetic/epigenetic defect ($p=0.001$, Fisher's exact test; Figure 27).

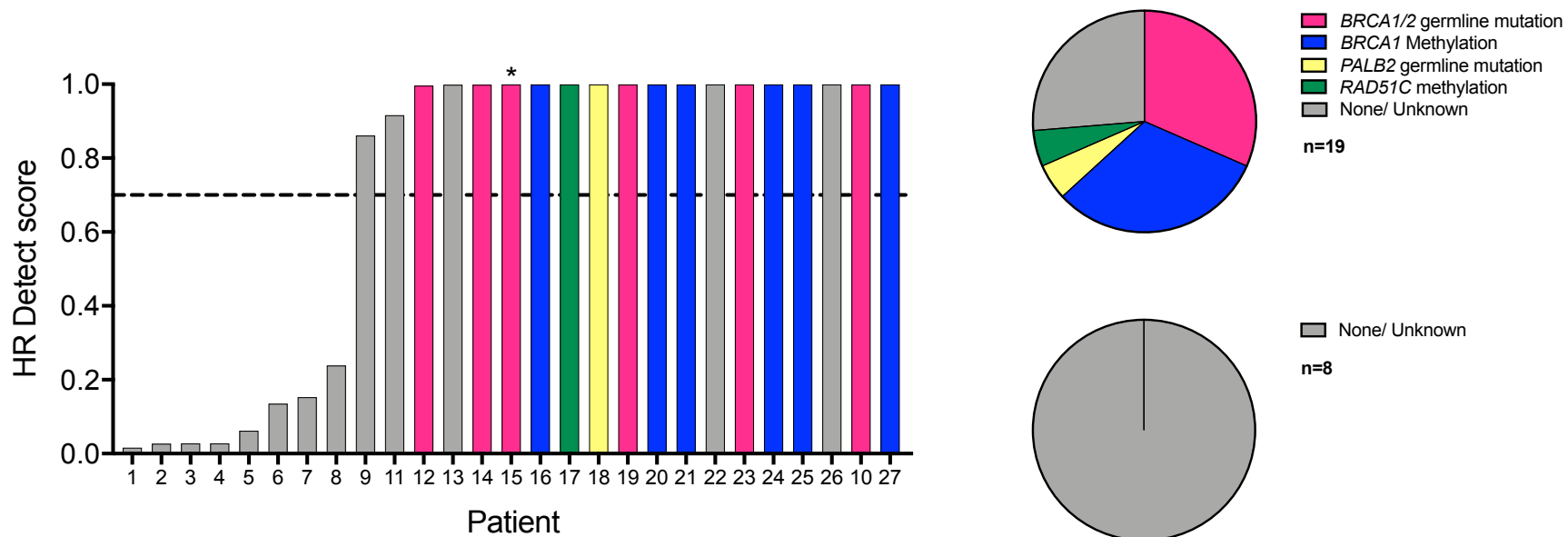


Figure 27 Biomarkers of homologous recombination (HR) repair deficiency in triple negative breast cancer

HRDetect positive cancers (HRDetect score >0.7) were enriched for inactivating mutations and promoter methylation of HR genes compared to HRDetect negative cancers (p=0.0006, Fisher's exact test). *An additional patient with ER positive breast cancer and *BRCA2* germline mutation is shown.

5.5.2 Identification of *BRCA1* and *RAD51C* Methylation in sporadic TNBC

Promoter methylation of *BRCA1* and *RAD51C* has been identified as a possible method of HR DNA repair deficiency and showed reduced gene expression^{57,58,228}. Identification of these tumours could increase the number of sporadic TNBCs susceptible to PARP inhibitor treatment. A multiplex methylation specific PCR method validated in an independent sample set to identify both *BRCA1* and *RAD51C* methylation was used (see Chapter 4 *BRCA1* and *RAD51C* Methylation Validation).

Extracted RNA was sent for RNA for expression analysis to determine whether methylation status altered expression values. Extracted DNA from 27 RIO RNA Later samples were subjected to bisulfite sequencing and the total DNA input ranged from 103-558ng.

The mean number of reads for *BRCA1* amplicon was 36909 (range 9654-60084) and *RAD51C* amplicon 48879 (range 28404- 71129) with a mean 47% of reads on target for the methylation sequencing run (range 37-50%). Using the germline *BRCA1/2* sub-cohort of the RIO trial *BRCA1* and *RAD51C* methylation limits were in agreement with previously published data^{57,176} and set the limits for the TNBC cohort (Figure 28). For *RAD51C* methylation, 2 sites in the *RAD51C* amplicon were removed as these were found to be methylated in all samples. Of the TNBC patients, 7 had *BRCA1* (Figure 28a) and 1 had *RAD51C* methylation and where expression data was available showed reduced expression levels (Figure 28b).

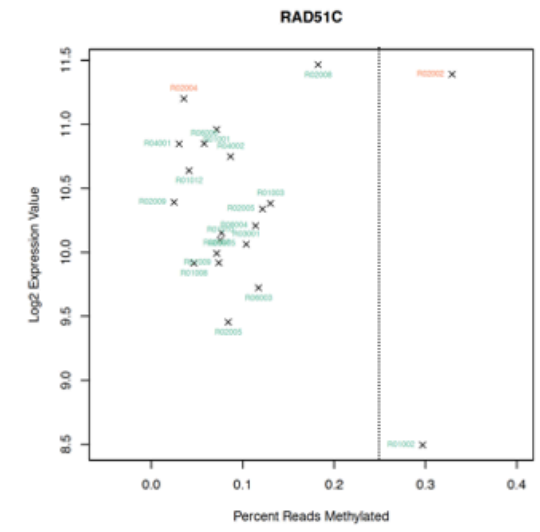
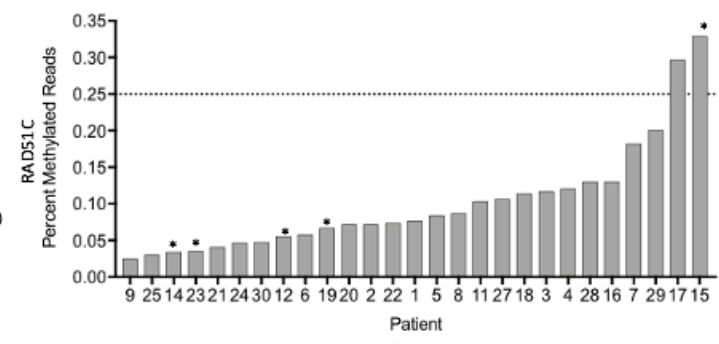
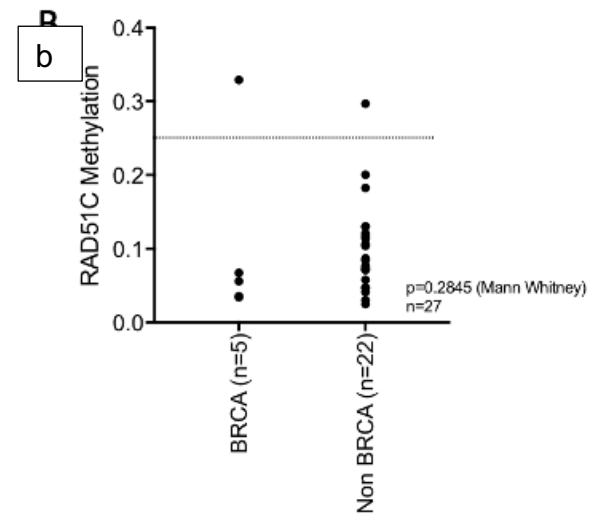
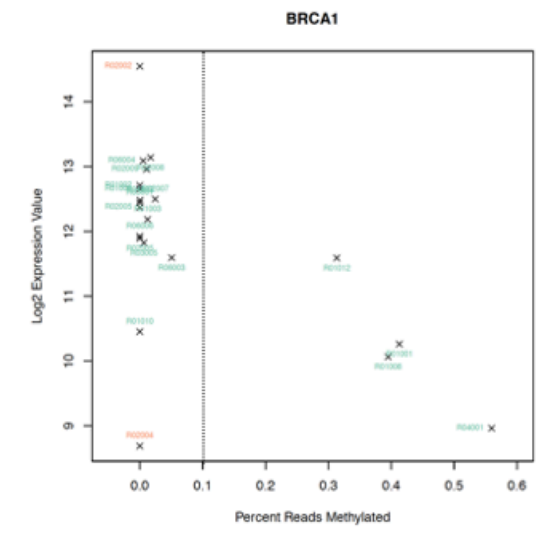
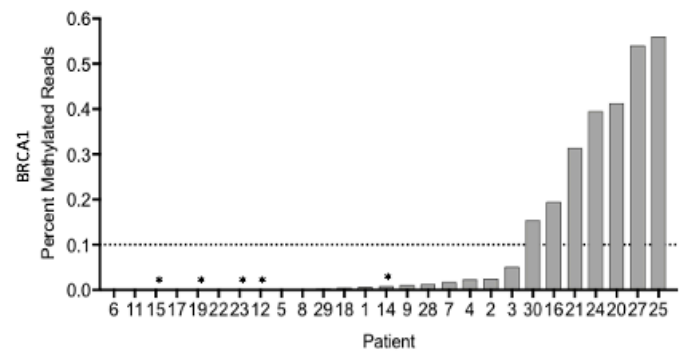
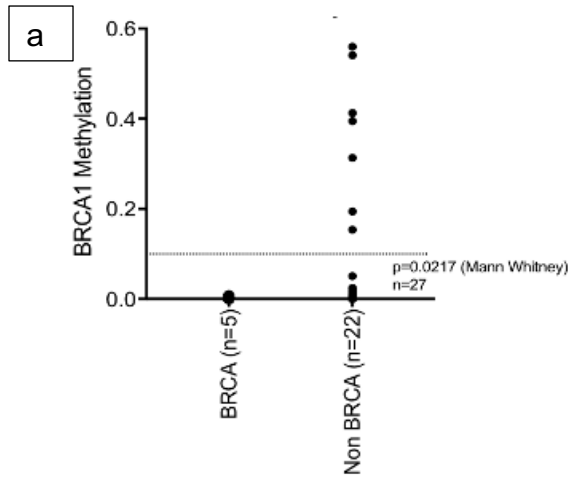


Figure 28 *BRCA1* and *RAD51C* Methylation of *BRCA* versus non *BRCA*

Using the *BRCA1/2* cohort of patients in the RIO trial, limits for determining *BRCA1* and *RAD51C* methylation were assessed and analysed with RNA expression data. Percent Reads methylated was determined by Number of CpGs methylated in read/ Number of CpGs methylated in read + Total reads.

a. *BRCA1* methylation was significantly different between the *BRCA* and non *BRCA* cohort ($p=0.0217$, Mann Whitney). Limit of detection was set at 10% of methylated reads. Seven patients were *BRCA1* methylated, none of which had a *BRCA* mutation. Four of the seven underwent expression analysis and were found to have lower *BRCA1* expression. Three samples did not have RNA sequencing data due to tumour availability. * denotes *BRCA1/2* germline mutation

b. *RAD51C* methylation was not significantly different between the *BRCA* cohort and non *BRCA* cohort ($p=0.2845$, Mann Whitney). Limit of detection was set at 25% of methylated reads. Two patients were *RAD51C* methylated, one had an additional *BRCA1* germline mutation and the other was a non *BRCA* patient which demonstrated low *RAD51C* expression. * denotes *BRCA1/2* germline mutation

5.5.3 RAD51 Immunohistochemistry as a functional HRD biomarker

To assess functional HRD the RAD51 IHC assay as discussed in Chapter 3 RAD51 immunohistochemistry validation was used and a RAD51 score <20% indicated HRD. Patients in the RIO trial had FFPE biopsies taken at baseline and after 12-14 days of treatment (EOT) with the PARP inhibitor, rucaparib. All samples were assessed for tumour content by a pathologist. A total of 23 EOT samples were available for RAD51 IHC assessment and 21 paired baseline and EOT samples were available for RAD51 IHC assessment.

RAD51 foci are visible at sites of DNA repair as a hallmark for HR-mediated repair by IHC. Examples of RAD51 foci negative and positive TNBC treated with rucaparib in the RIO trial are presented in Figure 29 and Figure 30.

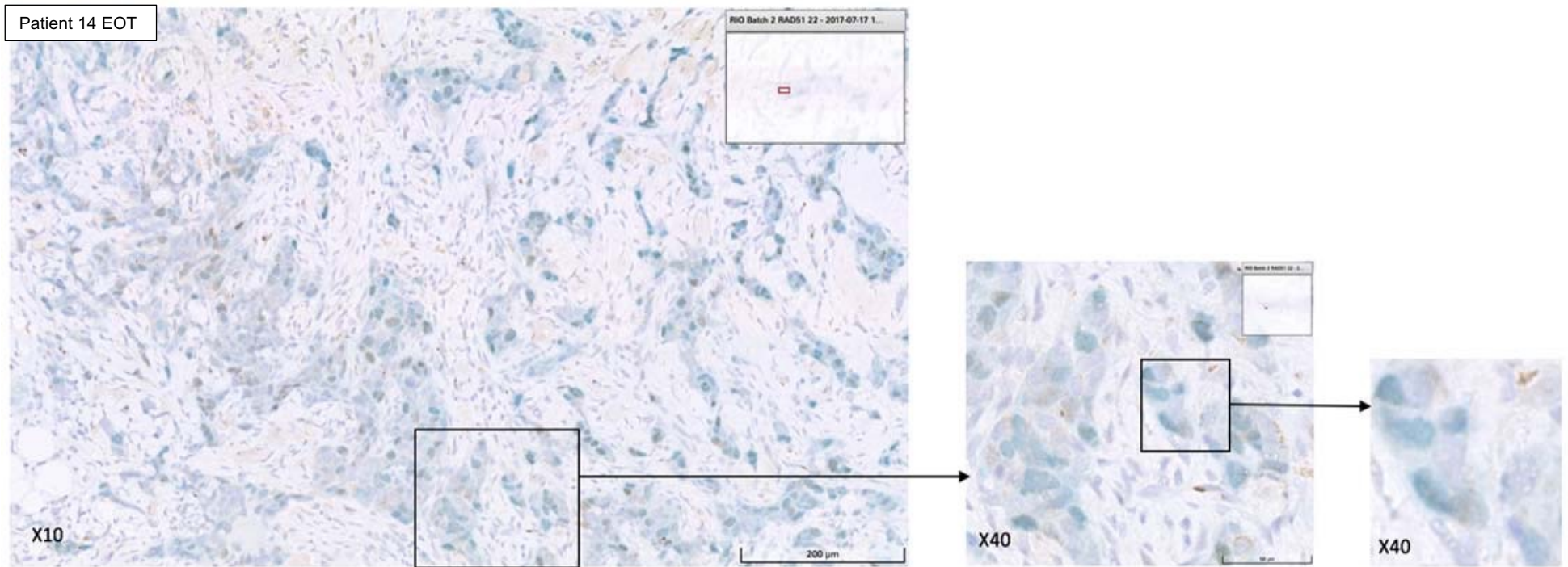


Figure 29 RAD51 EOT IHC images

RAD51 EOT IHC low (x10) and high (x40) -power field images from patient 14. No RAD51 foci were present indicating HRD. GMNN stained green/ blue to identify tumour cell S/G2 phase and RAD51 foci stained brown foci.

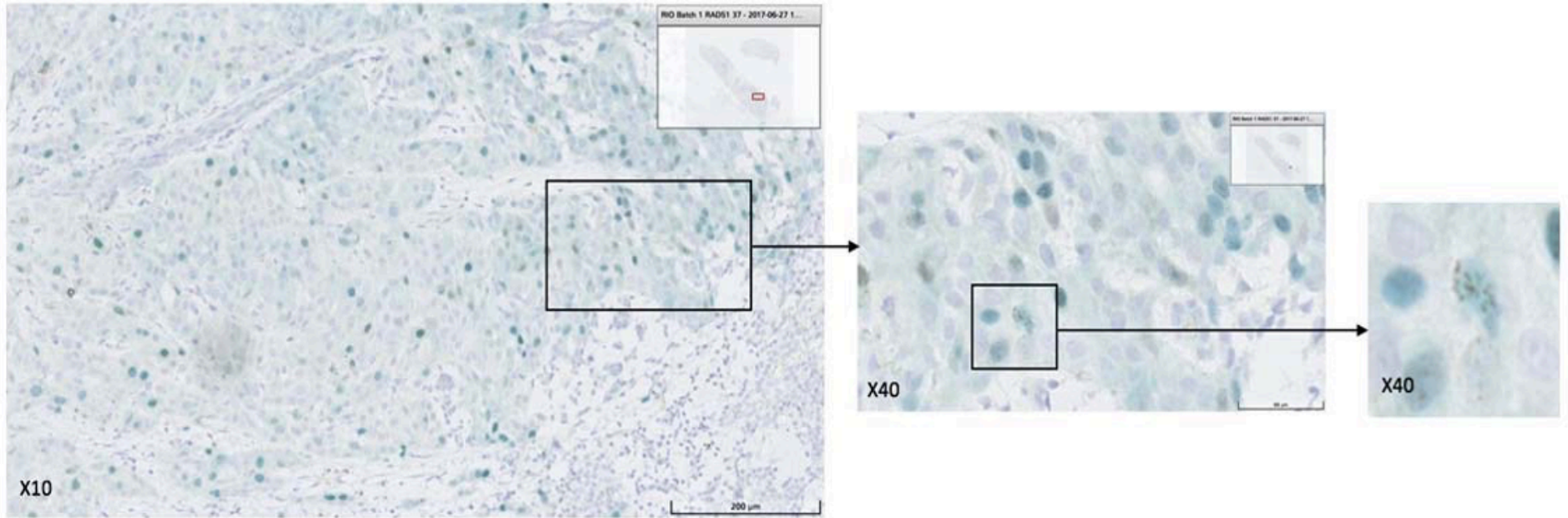


Figure 30 RAD51 EOT IHC images

RAD51 EOT IHC low (x10) and high (x40) -power field images patient 5 showing RAD51 foci indicating HR proficiency. GMNN stained green/ blue to identify tumour cell S/G2 phase and RAD51 foci stained brown foci.

The RAD51 IHC assay was able to detect RAD51 foci in baseline and EOT samples (n=21). There was a significant increase in RAD51 score from baseline to EOT indicating rucaparib induced DNA damage and RAD51-mediated repair (Wilcoxon test: $p=0.0006$, Figure 31a and b). The inability to form RAD51 foci after DNA damage may identify cancers with defective HR^{60,65}. We assessed functional HRD by the absence of RAD51 focus formation in the end of treatment (EOT) biopsy. RAD51 deficiency was identified in 78% (18/23) of patients including an ER positive *BRCA2* germline mutant and weakly positive PR control cancer. Of the twenty-one patients with TNBC 76% (16/21) had RAD51 foci deficiency (Figure 31c). There were 2 distinct groups in the TNBC cohort representing (Figure 31c). In the TNBC RAD51<20 group, indicating functional HRD, 4 patients had *BRCA1* methylation, 1 had *RAD51C* methylation, 1 *PALB2* genetic mutation and 8 had no other markers of HRD. None of the patients in the TNBC RAD51 >20 group has an underlying genetic/ epigenetic defect in HR (Figure 31c). Of the total number of RAD51 IHC-deficient cancers, 61% (11/18) had an underlying detectable HR defect compared to none (0/5) of RAD51 foci proficient cancers, $p=0.037$ Fisher's exact test (Figure 31d).

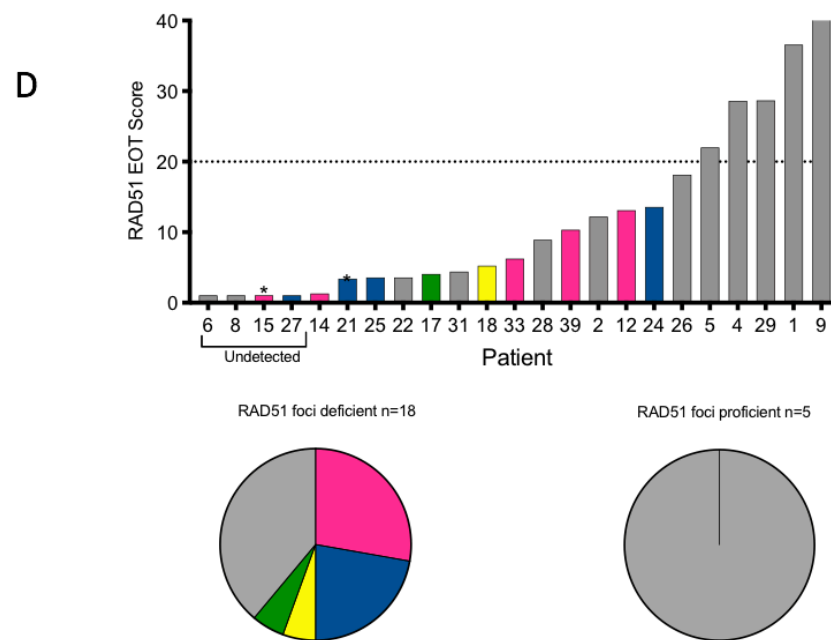
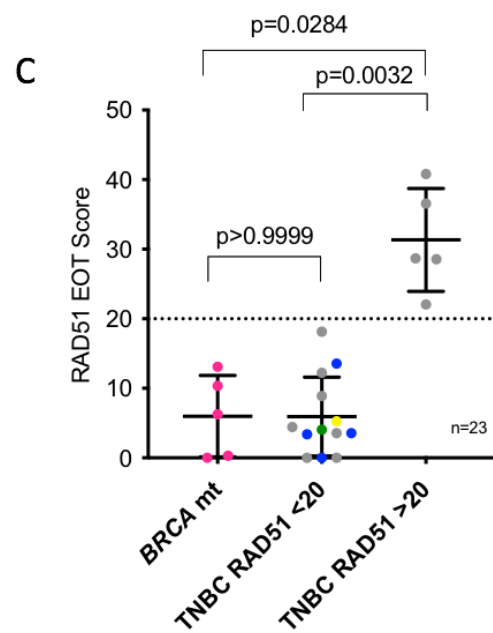
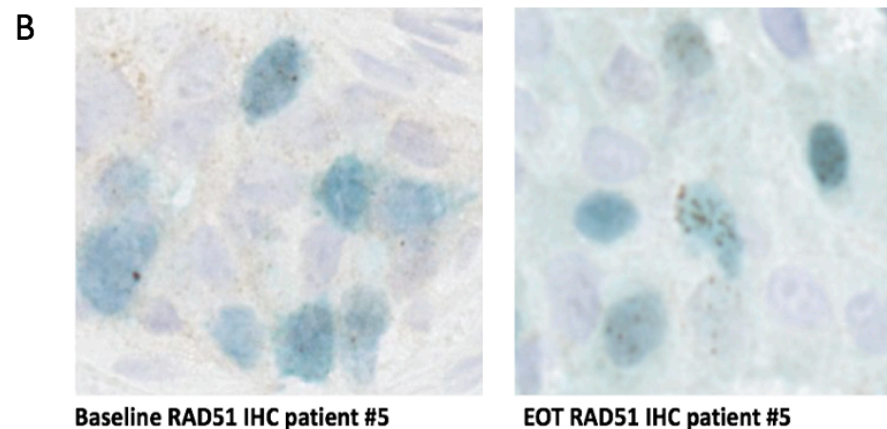
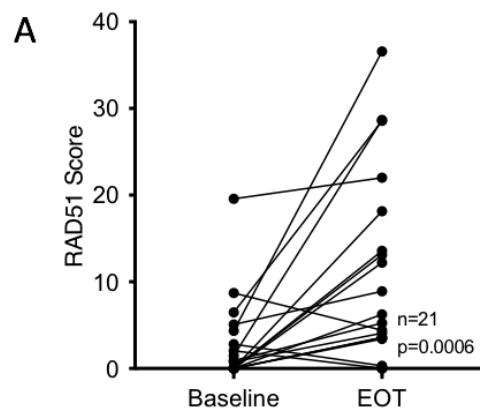


Figure 31 Assessment of functional RAD51 deficiency

- a: Paired baseline and EOT FFPE RAD51 scores (Wilcoxon test, $p=0.0006$, $n=21$)
- b: Images show the formation of RAD51 foci in baseline and EOT sample for patient 5.
- c: RAD51 EOT score based on *BRCA1/2* germline mutation versus TNBC; *BRCA* mutant (mt) $n= 5$, TNBC RAD51 <20 $n= 13$, TNBC RAD51 >20 $n=5$. *BRCA1/2* germline mutation patients were a control group to enable a reference for the TNBC patients. This figure shows a separation within the TNBC cohort of RAD51 foci deficiency (Kruskal Wallis multiple comparison; *BRCA* mt vs TNBC deficient $p>0.9999$; *BRCA* mt vs TNBC proficient $p=0.0284$).
- d: RAD51 EOT score for patients in the RIO trial. A score of 20 was the cuff off as determined in the validation trial. Four patients had undetected RAD51 foci. Cancers with RAD51 foci deficient are enriched for inactivating mutations and promoter methylation of HR genes compared to RAD51 proficient cancers ($p=0.037$ Fisher's exact test). *ER positive and *BRCA2* germline breast cancer and PR positive breast cancer mutation is shown.

5.5.4 Sensitivity of predictive HRD biomarkers

Cancers with RAD51 foci deficiency had significantly higher HRDetect scores than tumour samples that were RAD51 foci proficient (n=18, p=0.0118 Mann-Whitney test; Figure 32a). The Myriad HRD score identifies cancers with genomic instability but without rearrangement signatures and indels at microhomology. A score >42 using the Myriad HRD assay identifies homologous recombination deficiency. In this study, the Myriad HRD assay identified more cancers as HRD than HRDetect. None of the Myriad HRD score high but HRDetect low tumours had detectable pathway aberrations, suggesting that HRDetect was more specific (Figure 32b).

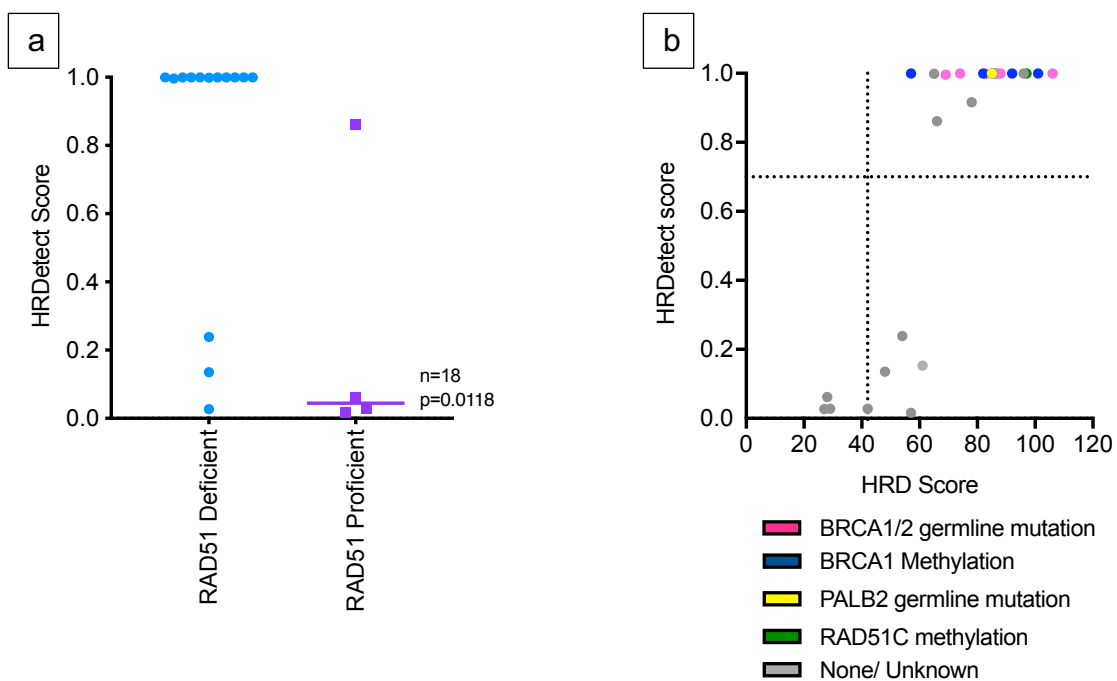


Figure 32 Association HRDetect score Other HRD markers

- HRDetect identifies tumours with a functional HRD. Association between RAD51 foci proficiency and HRDetect scores in 18 patients, p=0.0118 Mann Whitney U Test.
- Association of copy number based HRD Score and HRDetect score. Thresholds for both assays are indicated by dotted lines.

Multiple approaches have been used to predict HR defects in this cohort of sporadic TNBC patients including targeted gene analysis for *BRCA1*, *BRCA2* and *PALB2*, promoter methylation for *BRCA1* and *RAD51C*, HRDetect assay, RAD51 IHC assay and HRD score. Interrogating HRDetect, HRD Score and RAD51 IHC there was 67% (12/18) concordance between all three assays in both HR deficient and proficient group. Two samples had discrepancies in the HRD status, with agreement between HRDetect and HRD score but not with RAD51 IHC (Patient 2 and 9; Figure 33).

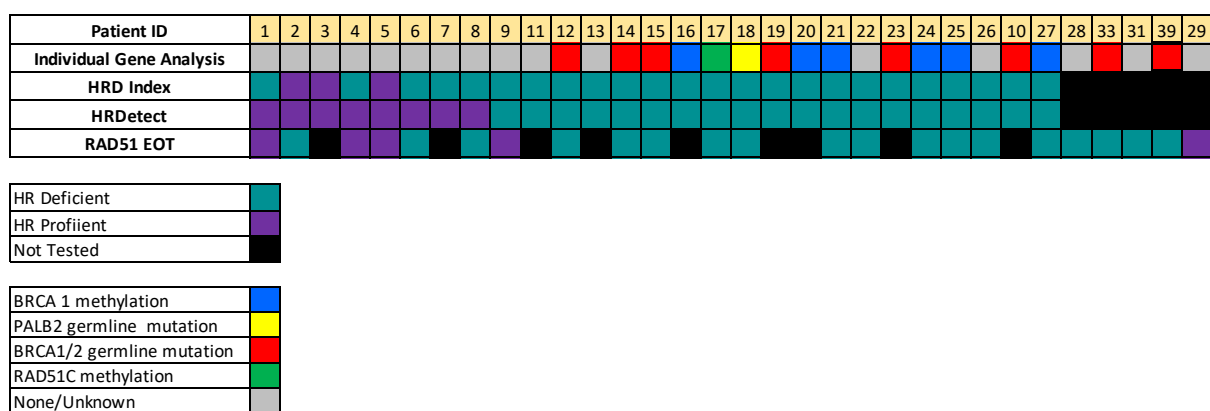


Figure 33 Individual gene analysis, HRDetect, HRD index and RAD51 IHC

Individual patient analysis by biomarker to assess HR. Individual gene analysis is coded as per the mutational process identified by WGS or promoter methylation analysis. HRD defined as; HRDetect >0.7; RAD51 EOT <20; HRD Score >42. Patients who were excluded from analysis are not shown.

5.6 Discussion

Clinically identifying and treating TNBC as a single entity is incorrect and needs to change to improve outcomes. Over the last decade there have been considerable improvements in molecular characterisation revealing the biologic heterogeneity of TNBC and furthermore the importance to ensure targetable aberrations can be treated appropriately²³⁵. The utilisation of gene expression has identified the heterogeneity within TNBC, however there is still a lack of biomarkers that can clearly identify targetable groups⁵. In this study, we have utilised HRDetect, RAD51 IHC, single gene and methylation analyses to identify HR deficient TNBC with the future prospects of targeted treatment in this subpopulation of TNBC.

Whole genome, targeted gene and methylation analyses identified individual gene defects, however incorporating all of these into clinical practice is impractical due to DNA requirements, logistics and cost. The HRDetect assay has shown to be a sensitive and specific assay to detect HRD in TNBC and could be utilised into clinical practice as a biomarker for HRD. HRDetect identified cancers with an identifiable gene defect and further HR deficient cancers that were not identified by targeted gene analysis demonstrating the clinical utility of HRDetect. The copy number variation based HRD score identified more cancers with HRD than HRDetect, with the HRD score identifying cancers with genomic instability but without rearrangement signatures and indels at microhomology. Five tumours indicating HRD by a high HRD score, failed to show detectable pathway aberrations. In contrast these patients were HR proficient using HRDetect suggesting that HRDetect was more specific. Of these 5 samples only 2 were assessable for RAD51 IHC, of which both were HR proficient in agreement with HRDetect. HRDetect was more specific to underlying HRD than HRD scores, the currently used clinical tool, suggesting that mutational signature assessment might be more accurate in identifying cancers that would benefit from platinum chemotherapy or PARP inhibition. Within the realm of the thesis the individual mutational signatures were not affiliated with samples although this would be an interesting area to review in future analyses.

The 3/30 samples that failed HRDetect, did so because of low tumour content, meaning there was not sufficient sensitivity in the WGS to identify somatic mutations

with confidence at 30-40X coverage. This made it difficult to make an accurate estimation of the mutational signature contributions and ultimately to produce a meaningful HRDetect score. In keeping with this, two of the samples also failed targeted sequencing for similar reasons. Further interrogation of these two samples revealed a large amount of tumour infiltrating lymphocytes in the tissue, potentially decreasing the relative tumour content of the sample, important for the genomic assessment of the sample. A reduced tumour content remains an ongoing concern with tissue biopsies. It raises the importance of retrieving adequate tissue samples for genomic analysis and questions the reliability of tissue samples for in-depth sequencing analysis.

A prospective study looking at pre-chemotherapy biopsies revealed that biopsies taken under ultrasound guidance had a higher tumour content²³⁶, and this was only mandated in a RIO protocol amendment during the trial. Aguilar-Mahecha et al reported in 15% of pre-chemotherapy biopsies there was no tumour and 63% failed to have $\geq 50\%$ tumour content²³⁶. Additionally within the study²³⁶ the use of RNA-later yielded less DNA than fresh frozen samples and recommended that at least 3 image-guided core biopsies should be obtained per sample and be freshly frozen. This is an avenue which could be further explored in future trials to reduce the chance of failed results.

We understand the presence of TILs has a positive impact on response to neoadjuvant treatment and is an independent factor in early stage TNBC. Although further analysis on TILs was not part of this thesis it could be a consideration for future research. In a post hoc analysis it was demonstrated that PARP inhibitors can induce a pro-inflammatory/ interferon response in HR-deficient TNBC, likely through the cGAS-cGAMP-STING pathway²³⁷.

Assessment of RAD51 using immunofluorescence for HRD has been shown to be a reliable marker, however, immunofluorescence is labour and time intensive^{67,193,199,238}. The utilisation of an IHC assay that can be subjected to batch assessment and possibly analysed digitally could bring this assay forward into the clinic and has been shown to be a reliable functional HRD marker^{71,72}. RAD51 IHC identified HR activity

after PARP inhibition evidence by the increased in RAD51 score from baseline to EOT. This demonstrates DNA damage when tumours are treated with PARP inhibitors^{193,199} and a positive indication that immunohistochemistry can assess functional HRD. Within this cohort of samples there is a clear group of tumours with lack of RAD51 IHC indicating a stall in HRR and hence HRD. The cutoffs used to determine functional HRD by RAD51 IHC is in line with data from Naipal et al⁷¹, and validates the use of IHC in this setting.

There are several methods used to identifying HRD in tumours,^{53,60,61,63,64,194} which are based on the genomic disturbances within a tumour, however whether a tumour is HRD at the point of treatment is important to establish⁶⁶. Within the RIO trial, HRDetect was able to identify 87% (13/15) of RAD51-deficient samples showing that HRDetect identifies cancer with a functional defect in HR as assessed by RAD51 foci formation.

Of the samples that were assessed for RAD51 IHC, the assay was robust, with the majority of samples scoring consistently between two independent scorers. However, one sample (patient ID 2) enlisted the patient both in HR deficient (RAD51 EOT score 3.65) and proficient (RAD51 EOT score 20.76) according to RAD51 IHC when scored by 2 independent reviewers. This sample was re assessed and an average was taken of the RAD51 scores and the sample was deemed HR deficient. Further assessment of the sample by an independent pathologist reported heterogeneity within the tumour affecting the scoring results. In contrast, this sample was deemed HR proficient by both HRDetect and HRD score.

The majority of primary sporadic TNBC were found to harbour defects in HR-based DNA repair. Cancers with HRD were robustly identified with the mutational signature assay HRDetect and further validated by a having functional HRD. HRDetect was more specific to underlying HRD than HRD scores, suggesting that mutational signature assessment might be more accurate in identifying cancers that would benefit from platinum chemotherapy or PARP inhibition.

The data here illustrates the potential of using both a functional biomarker and WGS mutational signatures to guide cancer treatment, advocating for prospective clinical trials of PARP inhibitors, in sporadic TNBC with HRD.

Chapter 6 Assessment of response activity in primary TNBC treated with rucaparib

6.1 Introduction

In the current clinical environment, a tissue biopsy is the gold standard to obtain essential information; histology and grade of tumours to diagnose and guide cancer treatment. Although this has been a vital part of cancer diagnosis, there has been increased scrutiny for its invasiveness causing pain and discomfort to patients, risk of infection, bruising, potentially delaying treatment and the high financial cost and logistical management²³⁹. Additionally, anatomically challenging tumours risk failure of diagnosis due to insufficient tissue and possible risk of seeding causing metastatic disease²⁴⁰.

One of the main causes that complicates treatment is tumour heterogeneity. Gerlinger *et al* published a pivotal study detailing intra-tumour heterogeneity and the underrepresentation of an entire tumour by a single biopsy, challenging the way we monitor cancer response and identify biomarkers²⁴¹. Tumours evolve over time and monitoring at intervals makes tumour biopsies an unfavourable option for both patient and physicians. Although serial imaging can give a visual impression, it fails to detect changes in tumour burden and is unable to give vital molecular information that can direct personalised therapy.

Current classification of breast cancer is in accordance to ER, PR and HER2 and treatment is dependent on this subclassification and currently is obtained by a single biopsy at diagnosis. However, with the development of transcription studies and genomic analysis the scope of further classifying breast cancer to personalise treatment is on the horizon. Over the last couple of decades TNBC has been divided into six subgroups; basal-like 1, basal-like 2, immunomodulatory, mesenchymal, mesenchymal stem-like and luminal androgen receptor subtype, demonstrating heterogeneity at a transcriptomic level has a different behaviour of disease and response to treatment⁵. Additionally, genomic studies at single cell level have shown genetic heterogeneity and extensive clonal diversity in breast cancer²⁴². These

developments extend the knowledge of a breast cancer and challenge our treatment pathways as we may steer away from a single biopsy and reveal that a patient's breast cancer is a multitude of cell populations that we can target. The best way to do this is still to be determined but when established will no doubt change the way we deliver treatment for breast cancer.

ctDNA, 'the liquid biopsy' allows for sensitive and specific serial sampling to be performed during the course of treatment giving more information regarding the patient's entire tumour burden, because the sample theoretically represents all the tumour DNA present in the circulation as opposed to the spatial limitations of a biopsy sampling a single lesion within a single anatomic site. ctDNA therefore tackles both intra-tumour heterogeneity and clonal evolution²⁴³. Currently several studies are underway in metastatic breast cancer to explore the clinical utility and feasibility of ctDNA. However, ctDNA is unlikely to completely replace a tissue biopsy for most diagnostic purposes but no doubt will complement and become a tool of choice for dynamic monitoring of patients on treatment or under active surveillance.

In breast cancer, Ki67 has been confirmed as an independent predictive and prognostic marker in early breast cancer, especially hormone positive breast cancer²⁴⁴. Breast cancers with a high Ki67 expression have been shown to respond better to chemotherapy although associated with a poorer prognosis, similar to the TNBC paradox; increased response to neoadjuvant chemotherapy but poorer overall survival^{245,246}. Pre-clinical studies with xenograft tumours showed a rapid decline of Ki67 within one week of treatment with oestrogen deprivation or antiestrogen hormonal treatments, along with an increase of apoptosis resulting in tumour regression^{247,248} and a decrease of Ki67 of 32-50% between two time-points was required to be able to attribute a treatment effect^{249,250}. Clinical studies have shown effective hormonal treatment can suppress Ki67 within 2 weeks of neoadjuvant endocrine treatment predicting favorable long-term outcome with greater suppression^{251,252}, however, absence of a decrease in Ki67 maybe evidence of therapeutic failure. TNBC is associated with higher Ki67 expression. High expression of Ki67 is predictive of pathological complete responses after neoadjuvant chemotherapy (NAC) indicating the importance of its inclusion in neoadjuvant clinical trials^{253,254,255}. Multiple studies have shown that change in Ki67 rather than the Ki67

value of the baseline tumour was a stronger prognostic factor^{256–259}. The RIO trial attempts to determine if it is possible to use a change in Ki67 as a biomarker after PARP inhibitor treatment in a TNBC population.

Apoptosis is a highly conserved mechanism stimulated by many signals including chemotherapeutic drugs. It enables the removal of defective cells through an orderly process without causing undesirable inflammatory responses²⁶⁰. Apoptosis provides a counterbalance to proliferation and has been reported to be positively correlated with Ki67 in breast cancer^{137,251,261,262}. In the IMPACT study both cell proliferation and apoptosis reduced with treatment with anastrozole and it was proposed that it was the dynamic change in Ki67 proliferation between the pretreatment and on treatment biopsy that would determine the apoptotic level²⁶².

Within the metastatic setting a number of studies have found that ctDNA suppression as early as the first cycle of therapy can identify a good prognosis group of patients in ovarian, melanoma, colorectal and lung cancer^{263–271}. The current biomarker to monitor metastatic breast cancer relies on the cancer antigen CA15-3 which has a sensitivity of approximately 60-70%. Dawson *et al* showed the benefit of using ctDNA as a biomarker increasing sensitivity to 85% vs 59% (95% confidence interval [CI], 11 to 37; $P < 0.002$), and ctDNA fluctuated according to treatment responses shown on imaging, advocating its use as a biomarker for response activity¹⁵⁴.

Most of the data on ctDNA early response to targeted treatment has arisen from *EGFR* mutated lung cancer^{269,270,272}. In early breast cancer, TNBC has been shown to have higher levels of ctDNA at diagnosis (median, 4.96copies/mL; IQR, 0-17.0copies/mL)²⁷³ and ctDNA detection with serial follow up after neoadjuvant treatment accurately predicts distant recurrence²⁷⁴. Early changes in ctDNA dynamics represent an early biomarker of drug activity, as cancers that respond to treatment rapidly suppress the level of ctDNA in plasma^{155,156,275}. Hrebien *et al* showed within 4 weeks of treatment PFS improved in a phase I/II study using the ctDNA ratio (CDR) of 0.25¹⁵⁶. Furthermore, in the phase III study, PALOMA3, a drop in ctDNA levels after 15 days of treatment with fulvestrant and palbociclib strongly predicted for PFS (HR 3.94, 95% CI 1.61–9.64, log-rank $p = 0.0013$)¹⁵⁵.

The test for ctDNA detection needs to ensure a low false-positive rate to ensure it is a highly specific indicator of cancer. One challenge to maintain the specificity of ctDNA detection is to ensure the detection of cancer cells over normal biological variants. Clonal haematopoietic mutations of indeterminate potential (CHIP) are derived from the cell-free DNA of haematopoietic cells. These cells accumulate somatic mutations with age and drive the clonal expansion of cells without causing a malignancy causing a cofounding factor when interpreting ctDNA results²⁷⁶.

Analysis of ctDNA was prospectively planned as an exploratory marker of rucaparib activity, in part as Ki67 change has only been validated as an activity endpoint in endocrine based therapies²⁷⁷⁻²⁷⁹. Currently, there is no data for using ctDNA as a treatment response biomarker in early breast cancer making it an unmet clinical need with the increasing use of neoadjuvant treatment.

6.2 Hypothesis

Ki67, cPARP and ctDNA dynamics can be used to assess rucaparib activity in early TNBC.

6.3 Aims

1. To assess Ki67 change in baseline and D12-14 samples as a surrogate of activity to rucaparib.
2. To establish the proportion of patients with sporadic TNBC with apoptosis induction on rucaparib.
3. To assess ctDNA levels in baseline and D12-14 plasma samples and associated changes as a marker of response.

6.4 Acknowledgements

- Samples in this chapter were used from the RIO trial
- Ki67 and cPARP IHC and analysis was performed under the guidance of Prof Mitch Dowsett, the Academic Department of Biochemistry team
- Targeted sequencing was performed by The Centre of Molecular Pathology at The Royal Marsden Hospital
- Avenio sequencing was performed by Roche
- ctDNA analysis was performed by Neha Chopra
- Bioinformatics was performed by Ros Cutts

6.5 Results

To evaluate biomarker of response to PARP inhibition Ki67 and cPARP were assessed using paired baseline and end of treatment FFPE biopsies. Both samples required a minimum amount of tumour to be evaluable. To assess ctDNA response DNA was extracted from 32 RNA later samples and underwent targeted sequencing using the ABCBio panel. Samples that did not retrieve a mutation were sent for WGS. 6 patients did not have an RNA Later samples and therefore EDTA plasma was sent to Roche for targeted sequencing using their AVENIO panel (Figure 34).

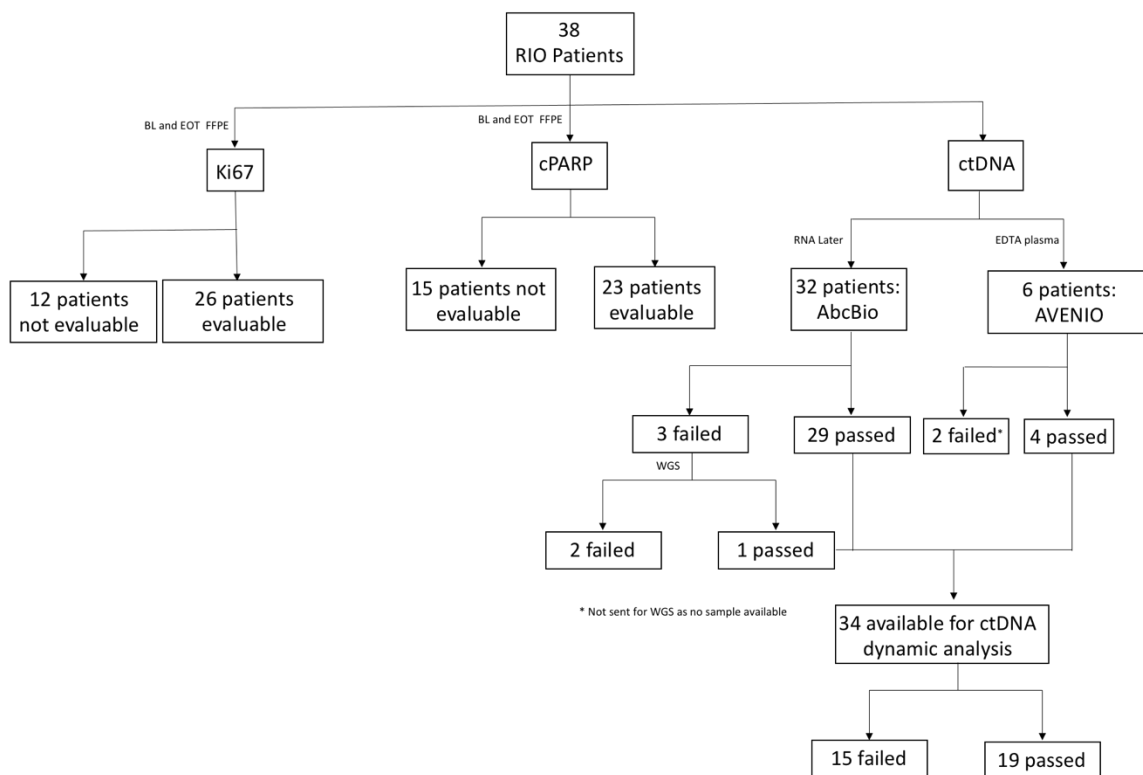


Figure 34 Consort diagram of the samples used to determine biomarkers of response to PARP inhibition

BL – baseline, EOT – end of treatment, FFPE – formalin fixed paraffin embedded, cPARP – cleaved PARP, ctDNA – circulating tumour DNA.

6.5.1 A fall in Ki67 as an assessment of response to rucaparib in primary TNBC

The primary endpoint of the RIO trial was a drop in Ki67 by 50% in triple negative patients without a known *BRCA1/2* mutation at trial entry. Ki67, a nuclear protein is only present in invasive tumour cells and exhibits a brown nuclear staining which are included in deriving the score (Figure 35). Tissue samples were taken at baseline and after 12-14 days of rucaparib treatment, and Ki67 was analysed if both samples were taken. On dissection of the tissue sample, tumour assessment was conducted to ensure adequate tumour cells were available for assessment and in accordance to the protocol (appendix 4). Analyses of all biomarkers of response (Ki67, apoptosis and ctDNA) included patients who had greater than 7 days of treatment with rucaparib.

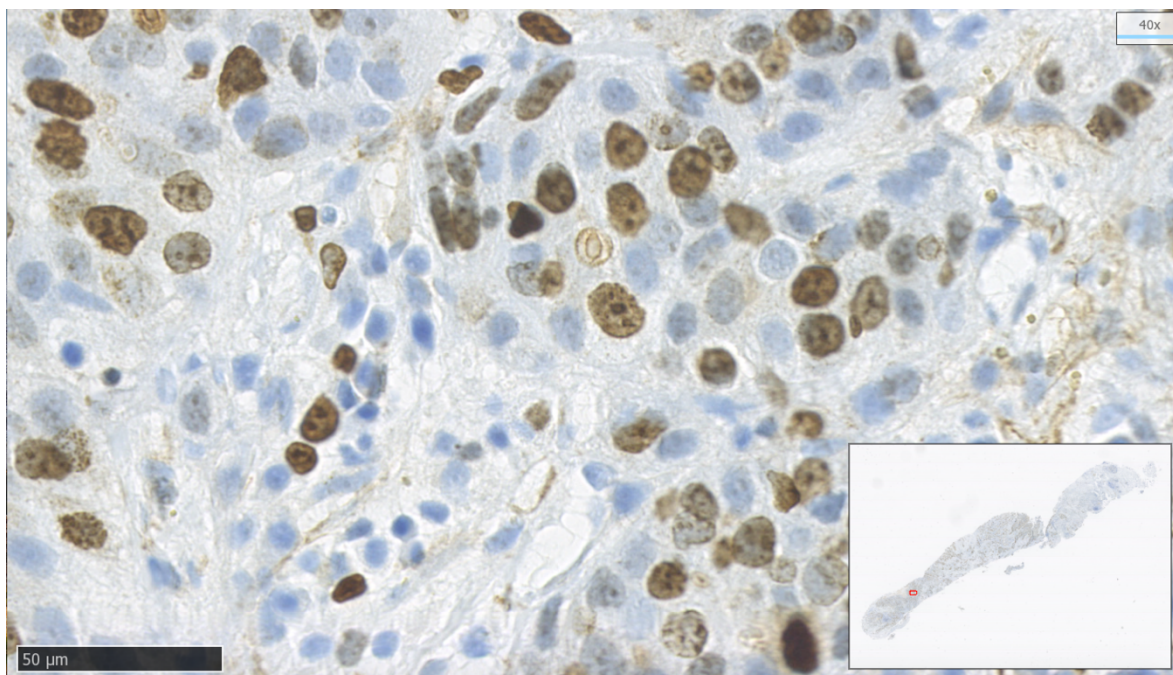


Figure 35 Ki67 staining

Ki67 IHC staining in high-power field (x40) from patient 5 in the RIO trial. Brown nuclear staining identifies Ki67 nuclear activity

A drop in Ki67 by 50% in the triple negative patients without a known *BRCA1/2* mutation at trial entry was seen in 12% tumours (2.5 – 31.2 95% CI; n= 3/25), one additional patient with known *BRCA* mutation at trial entry was assessed and did not have a 50% drop in Ki67 (Figure 36).

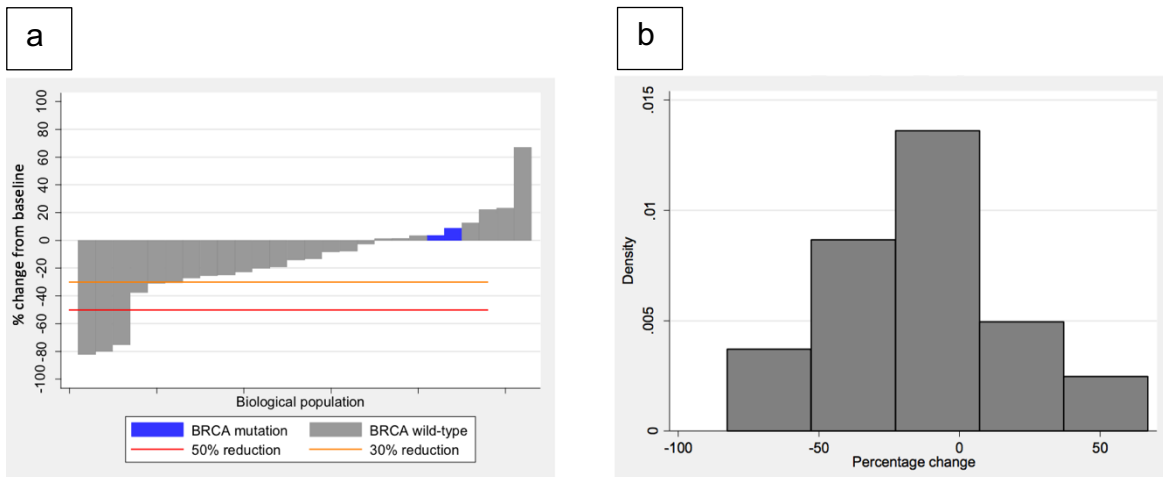


Figure 36 Effect of rucaparib on Ki67 expression assessed by immunohistochemistry.

- The change in proportion of tumour cells expressing Ki67 between baseline and D12-14, in patients that had assessable pairs of baseline and D12-14 samples. *BRCA* mutation cancers, blue bars, had no evidence of decreased Ki67.
- b. Distribution of percentage change in Ki67 (Shapiro-Wilk W test for normality: $p=0.229$)

6.5.2 Apoptosis induction after treatment with rucaparib in primary TNBC

Apoptosis induction was defined as any increase in apoptosis from baseline to day 12-14. Of the 23 evaluable pairs, no association was observed with cleaved PARP levels as a marker of apoptosis with *BRCA1/2* mutated cancers (Table 13 and Figure 37).

Apoptosis induction	N=23 evaluable	
	n	%
No	10	43.5
Yes	13	56.5

Table 13 Apoptosis induction

Proportion of patients with apoptosis induction = 56.5% (95% CI = 34.5-76.8)

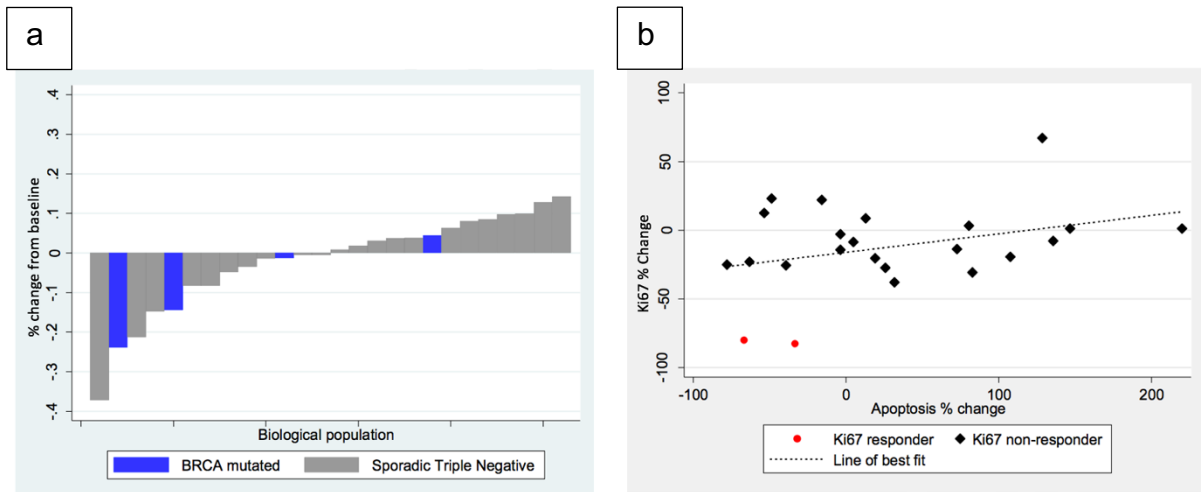


Figure 37 Effect of rucaparib on cleaved PARP expression assessed by immunohistochemistry, as a marker of apoptosis.

- The change in proportion of tumour cells expressing cleaved PARP between baseline and D12-14, in patients that had assessable pairs of baseline and D12-14 samples. *BRCA* mutation cancers had no evidence of increased cleaved PARP expression.
- Percentage change in Ki67 against percentage change in apoptosis (odds ratio 0.97; $p=0.208$; 95% CI 0.92-1.02)

6.5.3 Mutation detection using targeted and whole genome sequencing and assay optimisation

We individually determined the mutational status of 38 patients in the RIO trial. All patients entered into the study with either tissue or plasma available was sequenced. A total of 32 RNeasyTM tissue samples were sectioned and sequenced using the targeted ABCBio 41 gene panel and 6 samples with no tumour tissue available had ctDNA extracted from EDTA plasma and sent to ROCHE for either the AVENIOTM 17-gene or 77-gene targeted panel (see chapter 2).

Using targeted sequencing (ABCBio and AVENIO) a total of 63 mutations were detected in 38 samples and the total mutation detection rate was 86.8% (33/38). 17/38 (44.7%) patients had more than 1 mutation and the most common mutation was *TP53*, 30/38 (78.9%) (Figure 38), of which one patient had more than one *TP53* mutation (sample 14). Of the *PIK3CA* mutations detected c.3140A>G was present in 4/5 patients.

Mutations were not detected in 5/38 (13.2%) samples that underwent targeted sequencing, 3 of which underwent WGS using tumour derived DNA.

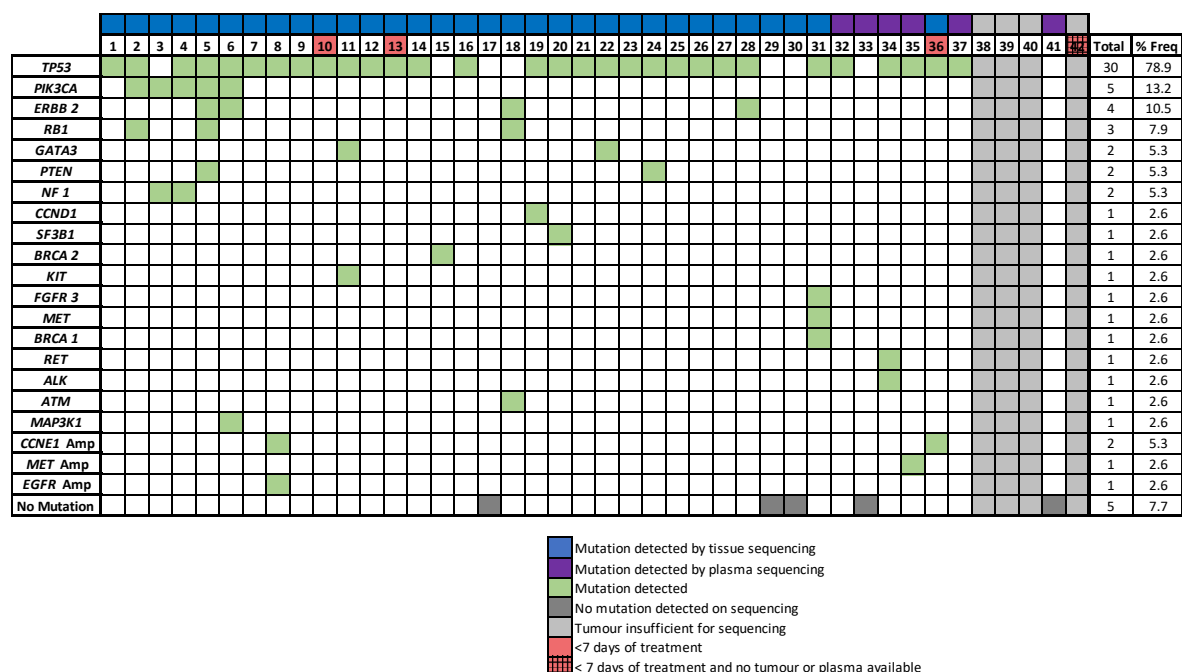


Figure 38 Mutations identified on targeted sequencing

Using targeted sequencing, mutations were identified using DNA extracted from RNA Later tissue or plasma. Table includes all patients entered into the study, patients 10, 13, 36 and 42 are excluded from further analyses. Sample 17 underwent further WGS analysis and had a SIK2 mutation which was deemed amenable for further ctDNA analysis

The frequency of mutations were in keeping with the MSKCC cBioPortal (<https://www.cbioportal.org>) although our database identified mutations not previously documented, for example in *RET*, *MET*, *FGFR3* and *KIT* (Figure 39a)^{280,281}. Targeted sequencing was compared with WGS, one sample which did not detect a mutation with targeted sequencing had mutations that were not part of the targeted panel detected with WGS, of which one mutation, SIK2, a tumour suppressor gene, was amenable to amplicon design for ctDNA analysis (sample 17). WGS sequencing identified a *PALB2* mutation which was not included in the targeted ABCBio sequencing panel (sample 18). Over eighty percent (40/48, 83%) of mutations detected with targeted sequencing were validated by WGS showing a good correlation between allele frequency (Figure 39b). Of the eight mutations that failed detection by WGS, 2 were from a sample that had a partial failure due to low tumour DNA and 6

had a low number of reads in WGS and failed to be called with the applied algorithm although were present on manual inspection. The allele frequencies of these mutations were low and ranged from 0.05-0.19.

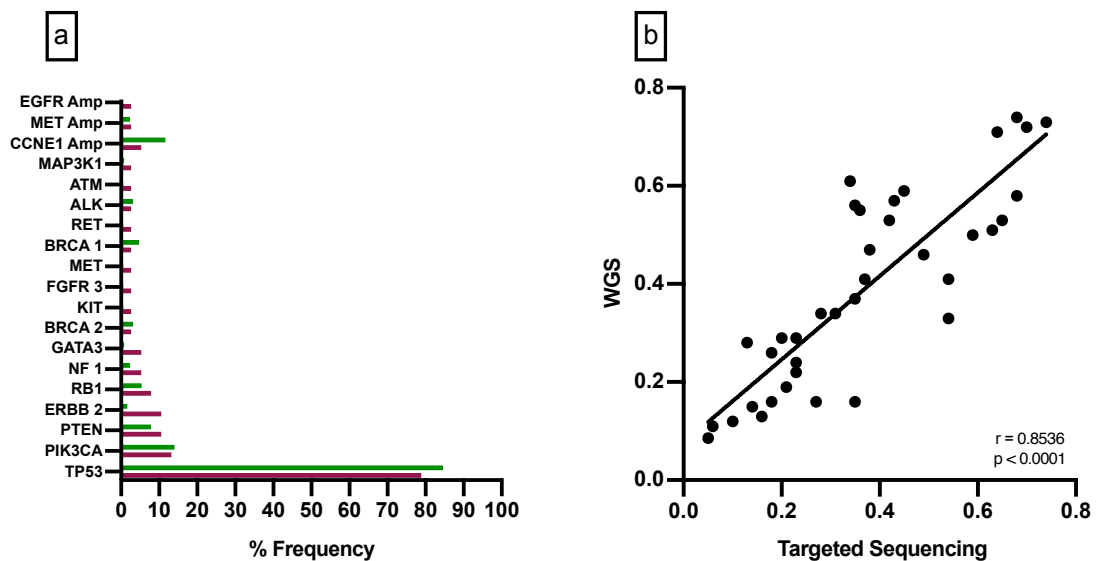


Figure 39 RIO target sequencing compared to MSKCC cBioPortal and WGS

- Mutations detected in the ABCBio targeted sequencing were cross referenced using the MSKCC cBioPortal. Criteria entered into the cBioPortal: Breast carcinoma; invasive ductal carcinoma, invasive lobular carcinoma, ER negative, HER2 negative, no hormonal therapy. Green bars represent the MSKCC cBioPortal and maroon lines represent ABCBio targeting sequencing in RIO trial
- Correlation between RIO trial targeted sequencing and whole genome sequencing (WGS). Validation of targeted sequencing by WGS; Mutations detected using the ABCBio targeted panel were cross referenced with the WGS data. Allele Frequency; Spearman correlation $r = 0.8536$, $p < 0.0001$.

For each trial subject, personalised ddPCR assays were designed and validated (40/47, 85.1%) for mutations identified by sequencing. Each mutation was validated by ddPCR using tissue derived DNA to determine the optimal annealing temperature for the assay which was subsequently used to detect ctDNA in plasma (Figure 40). Buffy coat DNA was analysed to control for clonal haematopoiesis of indeterminate potential (CHIP). If more than 1 mutation was identified for a patient a multiplex assay was optimised, the maximum number of mutations in a multiplex was 2 to ensure optimisation of the assay (Figure 41).

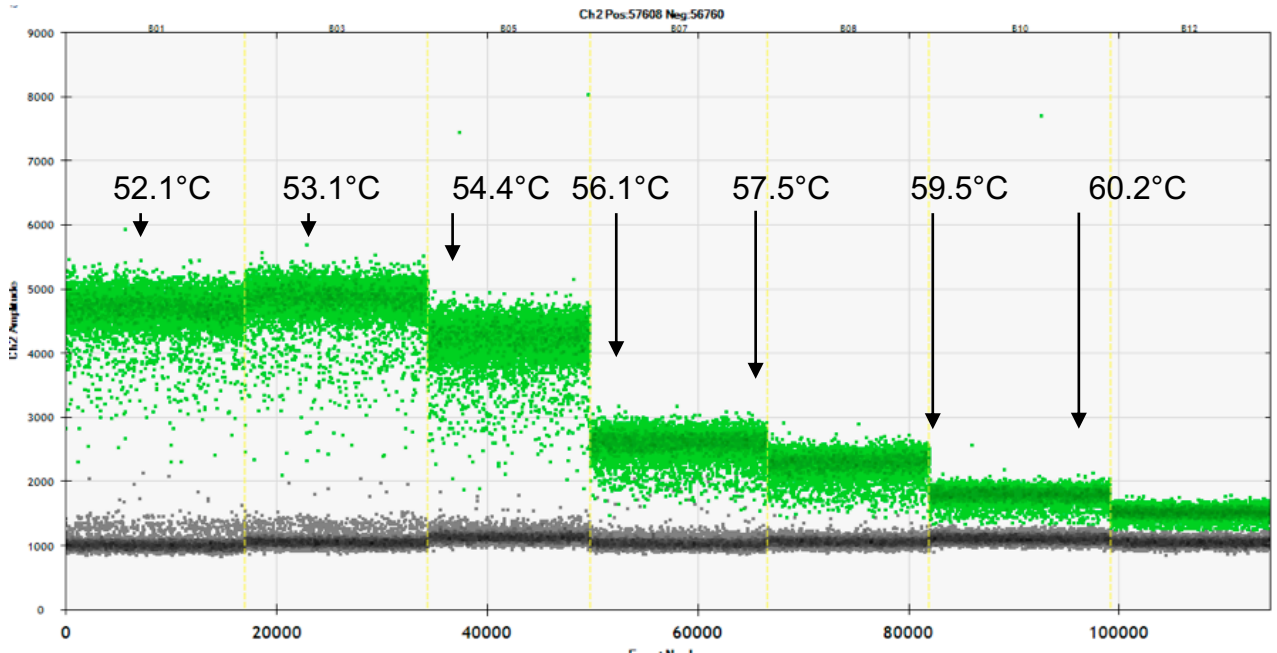
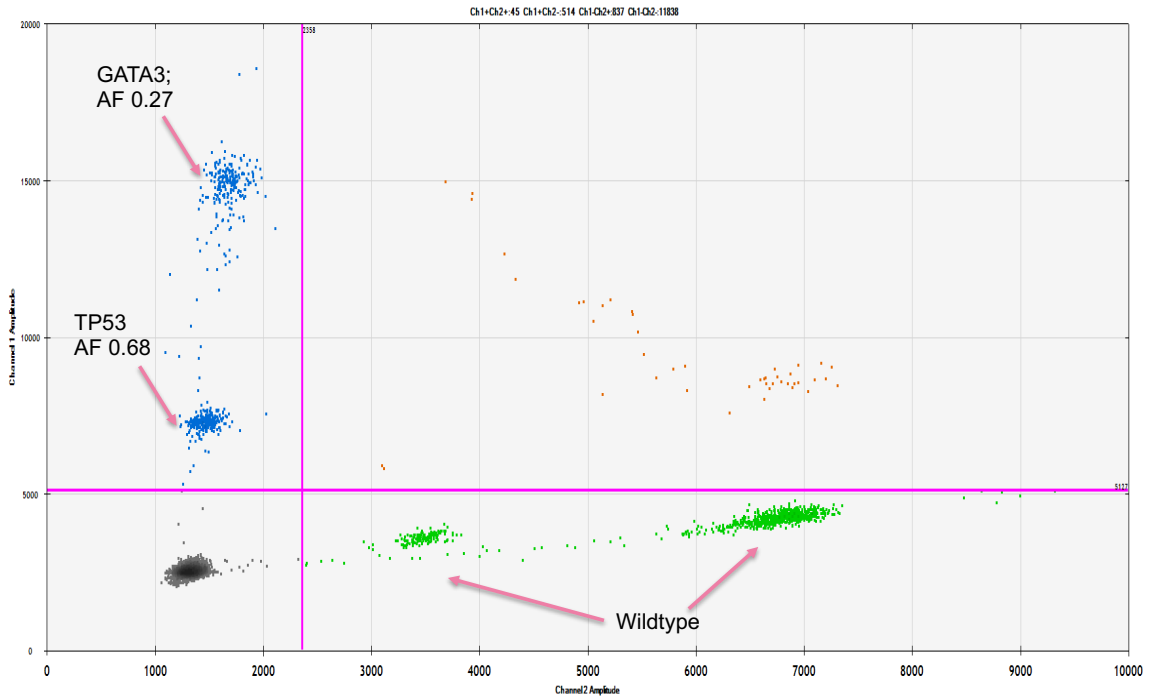


Figure 40 Temperature gradient of sample 28 with a TP53 mutation c.273G>A

Graph representing the wild type population (green droplets). As the temperature increases the number of wild type droplets reduces representing collapse of the assay. The correct assay temperature is determined based upon the temperature before the wild type population collapses. Black droplets represent empty droplets, green droplets represent wild-type HEX droplets.



AF = Allele Frequency

Figure 41 An optimised multiplex for patient 22 using tumour tissue.

ddPCR assay of two mutations: TP53 c.1024delC (0.68) and GATA3 c.829C>T (0.27), reflecting the abundance each mutation in the tumour and providing validation of the targeting sequencing. Black droplets represent empty droplets, blue droplets represent mutant FAM positive droplets, green droplets represent wild-type HEX droplets and orange droplets represent wild-type and mutant double positive droplets.

There was good correlation between allele frequency determined by ddPCR and tissue targeted sequencing (spearman correlation; $r=0.9804$, $p<0.0001$). This validated the use of ddPCR for the detection of ctDNA in plasma samples within the RIO trial (Figure 42). ctDNA was detected in 37/40 mutations (92.5%), the average mutant copies/ml of plasma was 10.23 copies/ml (IQR 0.1-110.85) (Figure 43) and samples with greater than 0.35 mutant copies/ml (≥ 4 positive HEX droplets) at baseline were eligible for assessment of ctDNA change.

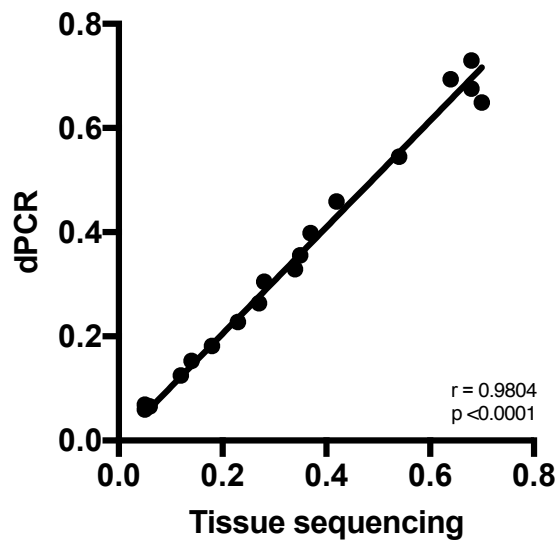


Figure 42 Correlation of allele frequency between targeted tissue sequencing and droplet digital PCR

Spearman correlation; $r=0.9804$, $p<0.0001$

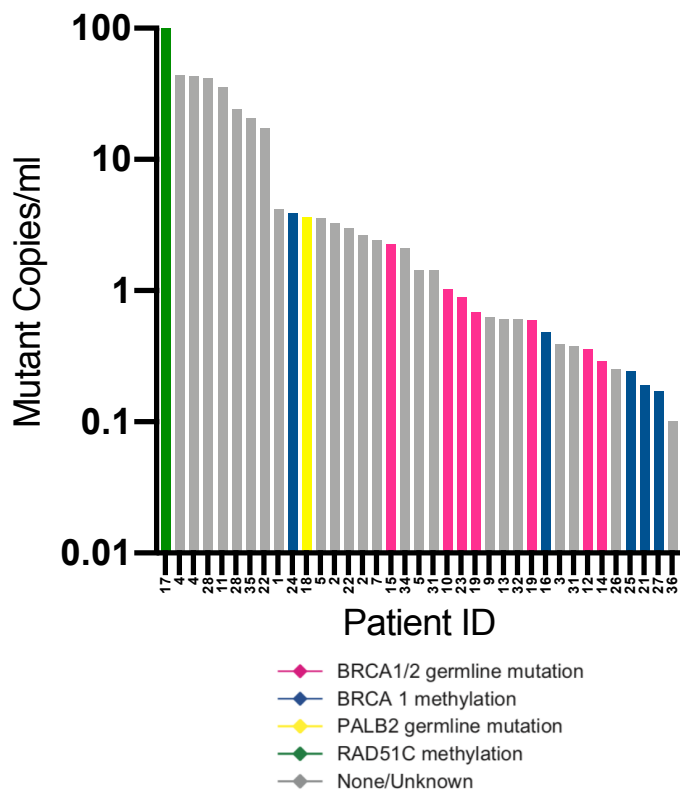


Figure 43 Baseline mutant copies/ml of patients with ctDNA detected

Patient baseline plasma ctDNA mutant copies/ml (log 10 scale). Average baseline copies/ml = 10.23

6.5.4 ctDNA as a biomarker of response to rucaparib

ctDNA from baseline and D12-14 plasma samples underwent ddPCR to determine whether a drop in ctDNA after treatment with rucaparib could be used as a biomarker of response (CDR15). The CDR15 was assessed as a ratio of the ctDNA copies/ml at D12-14 compared to ctDNA copies/ml at baseline. Where more than one mutation was tracked a weighted mean of ctDNA change was calculated. A threshold of $CDR < 0.25$ for ctDNA suppression, was pre-specified, having been determined in a separate study in metastatic breast cancer, that validated this cut-off to predict progression free survival on cytotoxic paclitaxel therapy¹⁵⁶. Although it would have been preferred to have a threshold from early disease there are currently no trials with a threshold for ctDNA dynamics in this setting. Figure 44 demonstrates a BRCA germline patients eliminating ctDNA from a baseline 8.01 mutant copies/ ml to 0 copies/ml after 2 weeks of rucaparib treatment.

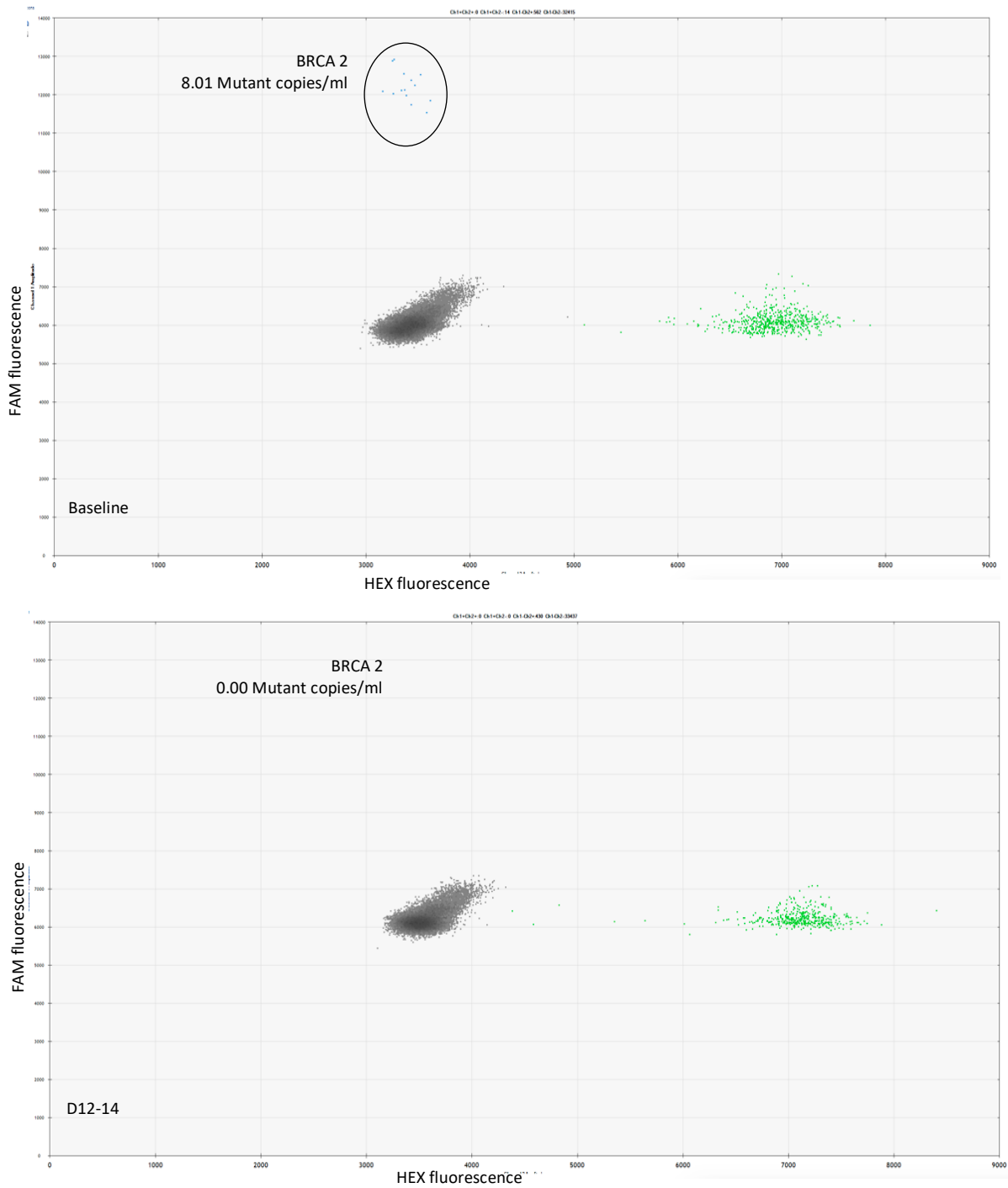


Figure 44 Example digital PCR ctDNA analysis plot

Plasma ddPCR of BRCA2 substitution and deletion in patient 11 with known BRCA1 and BRCA2 germline mutations. Baseline, 8.01 mutant copies/ml; D12-14, 0.000 mutant copies/ml. Black droplets represent empty droplets, blue droplets represent mutant FAM positive droplets, green droplets represent wild-type HEX droplets and orange droplets represent wild-type and mutant double positive droplets.

A baseline sample was considered positive when containing 4 or more mutant (HEX-positive) droplets per 4mLs of plasma. From the 38 patients that underwent targeted sequencing 19 (50%) were available for ctDNA analysis; 3 patients were excluded due no sample available (3) a further 12 patients were excluded due to not reaching the minimum of 4 mutant droplets at baseline (Figure 34). In contrast to tumour biopsy-based data, a substantial proportion of patients suppressed ctDNA after the two weeks rucaparib treatment (Figure 45). Patients with suppressed ctDNA after two weeks rucaparib (ctDNA ratio CDR <0.25, methods) were enriched for germline mutations of *BRCA1/2* and *PALB2* and gene promoter methylation of *BRCA1* and *RAD51C* (Figure 45).

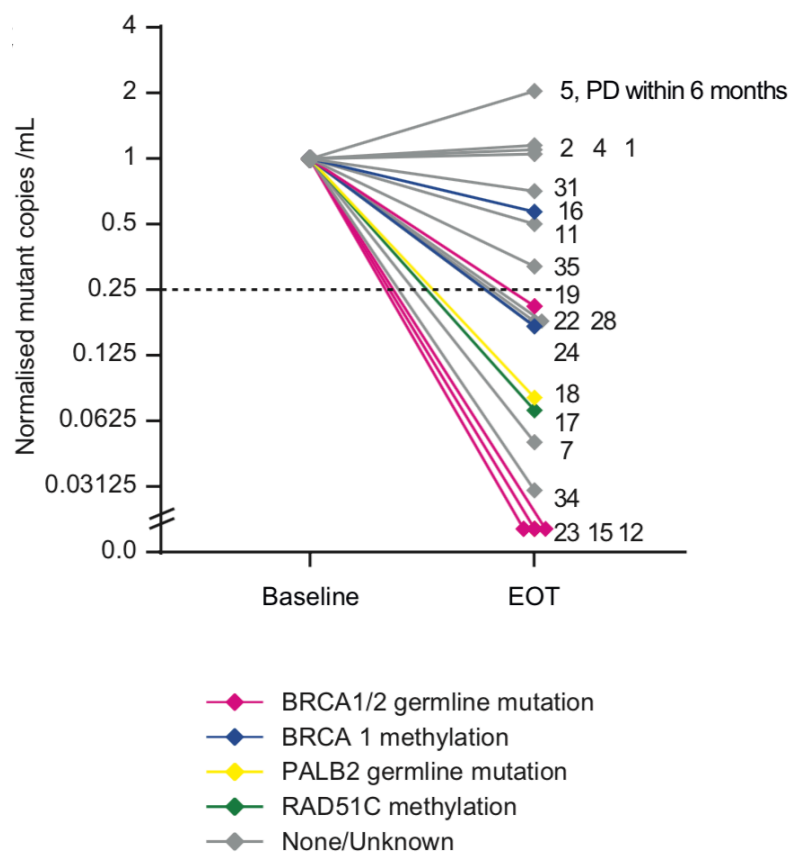


Figure 45 Change in circulating tumour DNA (ctDNA) copies/ml between baseline and end of treatment (EOT) after two weeks of rucaparib.

Patients with germline *BRCA1/2* mutations had a greater suppression of ctDNA than patients without germline mutations (n=19, p=0.021, Mann Whitney; Figure 46), validating ctDNA dynamics as a marker of rucaparib activity. Cancers with deficient

RAD51 foci formation (n=12, p=0.033, Mann Whitney; Figure 46) and HRDetect positive cancers had greater ctDNA suppression (n=15, p=0.027, Mann Whitney; Figure 46).

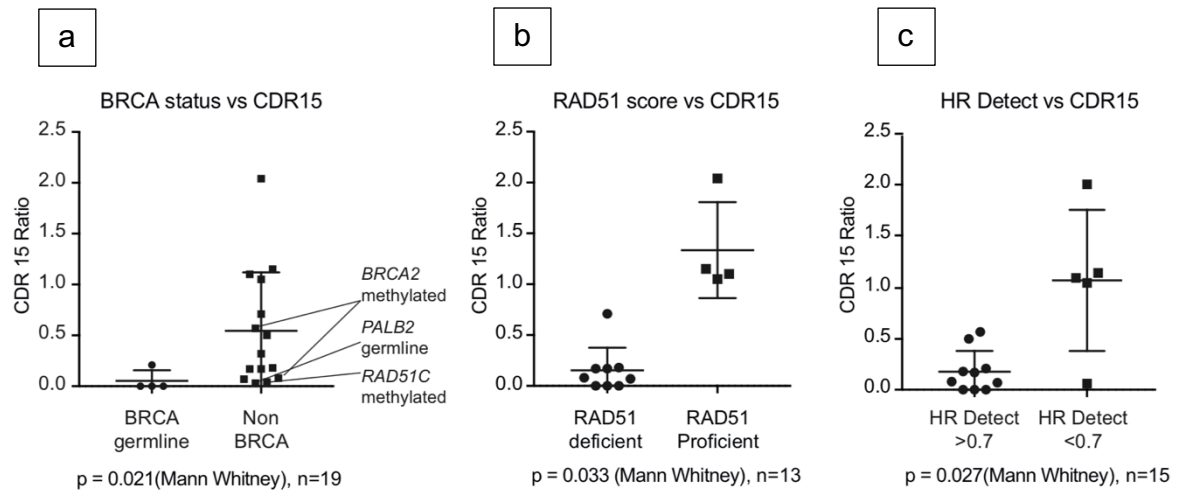


Figure 46 Associations of ctDNA change

- a. CDR15 in relation to BRCA germline status
- b. CDR15 in relation to RAD51 focus proficiency
- c. CDR15 in relation to HRDetect score

6.6 Discussion

This chapter has assessed the clinical utility of tissue and liquid biopsies as biomarkers of response to rucaparib. There is ongoing debate as to the validity of each of these biomarkers and with the increasing use of targeted treatment, the advent of biomarkers of response have an increasing role to assess the effectiveness of treatment earlier in the treatment pathway and ultimately guiding treatment. Several studies have demonstrated the use of ctDNA for identifying early metastatic disease and changes in ctDNA during treatment that can act as a potential predictor of response in metastatic cancer^{267,268,274,282,283}. In early breast cancer a prospective study using ddPCR showed 93% concordance between tumour tissue and mutations for PIK3CA in pre-surgical samples providing a proof-of-concept that ctDNA analysis is feasible in early breast cancer¹⁵³, however, this has yet to further validated.

The ideal ctDNA assay needs to be highly specific and sensitive and efficient to be applicable in the clinical setting to identify clinically relevant and actionable mutations. Currently, several techniques are available to detect ctDNA. If a single mutated region is known, digital PCR (dPCR) is sensitive to identify specific 'hotspot' mutated alleles and requires small amounts of DNA. Although multiple mutations can be detected the amount of DNA required would require sub-dividing the DNA the already small amount of DNA available^{284,285}. The amount of DNA available in early cancer is small and this is a concern when applying this technique in the clinical setting. With the advent of NGS, tagged-amplicon approach allows multiple genes to be interrogated with low frequency mutations. Enhanced Tam-Seq has demonstrated good concordance in metastatic breast cancer compared with dPCR^{275,286}. Furthermore, clinical application of NGS technologies has shown to detect multiple mutations in parallel, monitor tumour dynamics and identify de novo mutations. Although NGS currently is expensive over time this is likely to reduce with the vision to be incorporated into clinical practice. However, we need to be aware of the vast amount of information that will be obtained and how best to use it in the clinical setting for improved patient outcomes.

The primary endpoint of the study was a 50% decrease in Ki67, and aimed to be a biomarker of response based on studies involving ER+ve breast cancer showing it to be a strong predictor of clinical outcomes^{245,256–258,287}. Within the TNBC population

high Ki67 is associated with poor outcomes but whether a Ki67 change after a period of treatment remains to be determined²⁸⁸. Unfortunately, the RIO trial failed to meet its interim analysis of achieving 4/41 patients with a 50% drop in Ki67 in the triple negative population. Similarly, within the control *BRCA* population there were no samples that showed a greater than 50% drop in Ki67. There are several reasons for the primary endpoint not being reached, one being the study failed to meet its defined recruitment target. PARP inhibitors have yet to have proven efficacy in TNBC and may explain lower recruitment than was anticipated with patients preferring to start primary treatment without the possibility of delaying for short-term trial therapy. An amendment of the study protocol evaded the need for a baseline biopsy, enabling the use of the diagnostic biopsy, however this also failed to increase recruitment. Additionally, failure of tissue biopsies containing enough tumour impacted endpoint analyses for both Ki67 and apoptosis as paired biopsies were required to assess response. Only 25/40 (62.5%) of patient samples were included in the biological population as one of the biopsies were not evaluable due to lack of tumour, despite ultrasound guided biopsies. The hesitancy in using Ki67 in clinical practice has been the lack of standardised measurement methods and consistent cut-off values¹³⁵, although this has been challenged with an international collaboration to develop a global scoring method that is robust and reproducible²⁸⁹. Within the study, samples were assessed in batches and there was no evidence of a batch, observer or samples type effect although the sample numbers are small and any analysis would be underpowered. Although this study did not meet the recruitment target, within the *BRCA1/2* cohort Ki67 failed to show a decrease, doubting the utilisation of Ki67 as a predictive biomarker with PARP inhibition. No studies to date have assessed change in Ki67 with PARP inhibition.

Tissue derived biomarkers risk the potential of failure due to the lack of tumour available in the specimen with the literature reporting up to 65%²⁹⁰. In this study, FFPE samples were sectioned for Ki67 followed by apoptosis and RAD51 IHC. The failure rate due to no tumour available of paired Ki67 samples was 27% (10/37), paired apoptosis samples 42% (16/38) and RAD51 EOT IHC 32% (12/37). The interim analysis of the study identified one study centre which had a high number of samples with no tumour (5/7, 71%) and after collaborating with the study centre the trial protocol was amended to ensure all biopsies were taken under ultrasound guidance. This is possible within the remit of a clinical trial but would present an additional burden if this

was to be standardised for use in routine clinical practice. If this study centre was excluded the failure rate of paired Ki67 samples was halved (17%, 3/30), paired apoptosis reduced to 33% (10/30) and RAD51 EOT IHC decreased to 27% (8/30). The increase in failure of apoptosis and RAD51 EOT IHC is due to the lack of tissue available when sections are cut further into the sample.

The ongoing concern regarding tissue derived biomarkers was evident in the RIO trial and advocated a role for the exploration of ctDNA, a non-invasive biomarker to assess response to rucaparib activity. Initial assessment required tumour derived DNA to identify somatic mutations. This was a limiting step as some samples had low (<20%) or no tumour content. To assess patients without sufficient tumour sampling, we utilised the Roche AVENIO ctDNA kit which is a NGS liquid biopsy tumour profiling assay detecting allele fraction down to 0.1% with >99% sensitivity. Of the 6 samples that were sent, mutations were identified in 4 (67%). Using this method of genomic identification with liquid biopsy further validates the claim for the use of the liquid biopsy to identify genomic alterations of a tumour, although more work is required in this area.

Somatic mutations represented similar representation to previous studies and were able to be validated by ddPCR with good concordance in allele fraction^{280,281} with TP53 and PICK3CA the most commonly identified mutations 79% and 13% respectively (30/38 and 13/38 respectively)²⁸⁰. Using ctDNA for early cancer diagnosis is known to be challenging due to the low amount of tumour DNA released into the circulation and its dilution within DNA originating from non-tumour cells²⁹¹. However, it is assumed that the mutant copies/ml in early disease is likely to be lower than metastatic disease, hence the reserved approach in this study of although studies have suggested ≥ 2 droplets/ assay is adequate to eliminate false positive^{274,292}.

The RIO trial had a control subpopulation for *BRCA1/2* germline mutated patients, known responders to PARP inhibitor treatment, and ddPCR was able to show a clearance of mutant droplets after 12-14 days of treatment with rucaparib (Figure 44 and Figure 45). The RIO trial and Riva et al have shown no significant correlation between Ki67 and ctDNA response²⁹². Using ctDNA ddPCR as a biomarker of

response has several potential advantages over tissue derived biomarkers. It is non-invasive and has little discomfort for the patient. If a repeat sample is required this can be easily obtained. The data above illustrates the potential of ctDNA analysis to transform window trials, presenting a simple and robust assay of drug activity, without the potential sampling challenges involved with repeat biopsies. However, analytical challenges associated with low plasma DNA levels and low purity tumour samples, will benefit from further technological development. There is a growing need for larger studies to independently validate the use of ctDNA as a predictive biomarker in early TNBC, which will hopefully open new avenues for treatment in this poor prognostic group.

The future direction of utilising ctDNA is to determine the context of which modality to use; ddPCR or NGS and whether it can be used in early stage cancer. Within lung cancer there has been translational development in utilising ddPCR for the assessment of EGFR mutations on progression with tyrosine kinase inhibitors²⁹³ and more recently in detection of EGFR T790M in early lung cancer advocating the use of ctDNA in early disease²⁹⁴. In this setting the mutation is known and the low limit of detection of ddPCR makes this an appropriate clinical test. However, in the setting where mutations are still being identified ctDNA analysis there maybe benefit in using the more expensive NGS methods as long as data can be utilised effectively.

The role of tumour biopsies continues to have a role in clinical practice however, there are opportunities to use less invasive biomarkers to understand the clonal evolution of a tumour. We have demonstrated here that we can use ctDNA from plasma to sequence a patient's tumour. This is an area of active research with commercial assays already becoming available as demonstrated using the Roche AVENIO panel in the targeted sequencing of plasma samples in this study. Studies have used NGS in residual tumour after NAC to discover the genomic alterations, but whether this can be utilised earlier in the treatment pathway needs to be confirmed^{295,296}. Although currently this method is expensive and requires significant turnaround times, it is an area of future development. Using ctDNA sequencing during neoadjuvant treatment may determine whether treatment is responding and if there is knowledge of a larger pool of alterations could determine the next best course of treatment.

The study has demonstrated the advantage of non-invasive analysis, and the use of ctDNA as a potentially reliable and effective surrogate end point to assess response. This will require further validation in larger prospective trials.

Chapter 7 Conclusions

Triple negative breast cancer (TNBC) continues to have a poor prognosis and the lack of effective treatments demands the continued search for effective biomarkers to guide treatment and predict response. Recent studies have shown the neoadjuvant platform to be an optimal situation to investigate these biomarkers decreasing the time required to see a clinical impact¹⁹. Unfortunately, despite discovering a subset of breast cancers harbour BRCAness over a decade ago and with the advances in sequencing technology we are still a way from biomarkers that can identify HRD and assess response in the clinic^{8,102}. The work presented in this thesis has demonstrated that the majority of primary TNBCs have defects in HR-based DNA repair and that ctDNA dynamics can be used as an optimal biomarker to assess response to PARP inhibition. This was approached using tissue and plasma samples from the phase 2 RIO trial with the objective of identifying biomarkers of PARP inhibitor activity in sporadic TNBC.

At the outset of this work HRD could be tested using 3 main strategies; germline mutation, somatic mutation screening of genes related to HR repair and evaluation of a genomic scar with calculation of the HRD score. These strategies cannot encompass all of the potential aetiologies, hence functional evaluation of HRD is necessary. Induction of RAD51 nuclear foci after neoadjuvant chemotherapy and PARP inhibition can measure the homologous recombination functionality in breast cancer biopsies^{67,71,193,199,297}, with an association to loss of heterozygosity measures of HR deficiency^{193,298}. Studies have shown that cells with deficient BRCA1/2 or other HR proteins, do not efficiently form RAD51 foci which could be used as a marker for PARP inhibitor sensitivity using FFPE tumour samples^{8,102,199}. The dynamics of DNA repair alter throughout tumour evolution and a functional RAD51 assay can be used as a dynamic readout of tumour HR status at the specific time for treatment decision making^{41,71,225}. Current studies are using immunofluorescence (IF) on FFPE samples which can be labour intensive and require specialist protocols^{67,199,299}. In chapter 3, a RAD51 immunohistochemistry (IHC) protocol was developed using breast cancers treated with neoadjuvant chemotherapy and clearly showed DNA damage after one cycle of chemotherapy. The cut-off of GMNN positive cells with RAD51 foci (RAD51 score) <20% for HR deficiency is consistent with the RECAP test which has recently

shown to be effective in ascertaining HRD in metastatic breast tumours treated with ionising radiation²⁹⁷. However, whether the use of RAD51 IHC identified DNA damage in treatment with PARP inhibition was unknown. Using samples from the RIO trial as shown in chapter 5, DNA damage was identified after 2 weeks of treatment with rucaparib. This has yielded a novel technique that although will need further validation, if clinically validated could be a useful tool as it could automated making it an efficient biomarker for real-time clinical practice.

Genetic and somatic mutations cannot alone account for the majority of HR deficient breast cancers. Defects in epigenetic markers, such as modifications of CpG methylation at gene promoters, result in transcriptional silencing of active genes causing effects similar to those of gene mutations. Therefore, to address the role epigenetics in carcinogenesis it is important to identify epigenetic mutations which can serve as the first and/or the second hit in Knudson's model of tumour development. In sporadic breast cancers up to 20% display *BRCA1* promoter hypermethylation, mainly occurring in TNBC⁷³. More recently *RAD51C* methylation was shown to be enriched in basal-like breast cancers indicating its association with HRD^{57,200}. Using a validation cohort, bisulfite sequencing was interrogated using predesigned *BRCA1* and novel *RAD51C* methylation primers as a targeted multiplex methylation assay. This assay was subsequently validated in the RIO trial against gene expression data. *BRCA1* methylation was found in 32% (7/22) of sporadic TNBCs consistent with the 20-60% in published data³⁰⁰⁻³⁰⁴. *RAD51C* methylation was demonstrated in 5% (1/22) of sporadic TNBCs and is an important consideration with events comparable to the frequency to *BRCA2* germline events, with a predominance in basal-like breast cancers⁵⁷. The novel discovery of *RAD51C* methylation in basal type breast cancer may warrant consideration for including methylation analysis on larger patient populations to ascertain patients' risk of HRD. Methylation of *BRCA1* and *RAD51C* is associated with an increased risk of developing breast cancer^{73,305} but what remains to be determined is whether the methylation status of either *BRCA1* or *RAD51C* translates into clinical benefit from the use of DNA-damaging agents such as PARP inhibitors. In an Icelandic study involving over 1000 primary breast cancers, *BRCA1* promoter methylation was predictive of improved disease outcomes in patients receiving chemotherapy³⁰⁶. Further studies relating to methylation status and treatment response are required in this field. However, as different studies have used

different CpG sites and relied upon different techniques to determine methylation status it is difficult to define a universally valid threshold for gene silencing⁷³. In the first instance it may require creation of international criteria to standardised interpretation of methylation status to allow comparisons between studies.

The mutational-signature based classifier HRDetect can robustly identify HR deficiency in sporadic primary TNBC⁶⁴. Having a *BRCA1/2* cohort in the trial allowed validation of the assay by demonstrating HR deficiency in a *BRCA2* mutated patient. All tumours that were identified as having a defect in a component of the HR pathway through whole or targeted sequencing, and *BRCA1* and *RAD51C* methylation, were identified by HRDetect. None of the negative HRDetect (<0.7) tumours had a HR defect identified. HRDetect has shown HRD in other tumour types, notably ovarian and pancreatic cancer⁶⁴, and in a recent study, HRDetect high (>0.7) in advanced pancreatic cancer prognosticated improved survival with platinum treatment^{64,307}. In the study of the 57 patients with HRDetect high, 65% had an identifiable HR pathway defect. The authors report the remaining samples were false positives, however, it is not clear from the results whether these patients responded to treatment with platinum still making them HR deficient with the HR affected pathway unidentified. The work presented in chapter 5 compared the HRD score, which is an unweighted numeric sum of LOH, TAI, and LST and the HRDetect score, a weighted model based on six mutational signatures including LOH, TAI, and LST. HRDetect was more specific to underlying HR deficiency than the HRD score suggesting that mutational signature assessment might be more accurate in identifying cancers that would benefit from platinum chemotherapy or PARP inhibition.

Additionally, HRDetect was able to identify tumours with functional HR deficiency validating its role as a biomarker for HR to predict response to treatment. Currently HRDetect utilises WGS from tumour tissue requiring 1µg of tumour DNA (25uL at 40ng/uL) together with matched germline DNA. More studies are required to validate the current finding of HRDetect and should they continue to show HRDetect can encompass genetic, epigenetic and functional identification of HRD it could make it a valuable biomarker in the clinic. One suggestion could be the development of a tumour agnostic clinical trial focusing on identification of HR deficiency to direct treatment.

Whether identification of HR deficiency and subsequent treatment with PARP inhibition leads to response in treatment is still an area that requires further research. Currently, Ki67 is used to evaluate prognosis, guide adjuvant treatment and predict response to neoadjuvant treatment in hormone receptor positive (HR+) HER2 negative breast cancer (HER2-). Therefore, in the RIO trial, it was hypothesised that a change in Ki67 from baseline to end of treatment with the PARP inhibitor rucaparib could be used as a marker of response. However, this failed to show an association between Ki67 change with *BRCA1/2* mutated cancers and sporadic TNBC. Additionally, an ER positive *BRCA 2* germline mutated patient failed to show a drop in Ki67 from baseline to end of treatment. There was no association observed with cleaved PARP levels as a marker of apoptosis with *BRCA1/2* mutated cancers. Ki67 has been investigated primarily in HR+/HER2- breast cancer. In clinical studies the number of TNBC samples is small and a clear a uniform cut off has not been established in this cohort³⁰⁸, limiting the ability of Ki67 as a biomarker of response in TNBC. Secondly, what was evident in this work was the lack of tumour present in tissue biopsies making the assessment of Ki67 which requires paired biopsies challenging. This is an ongoing concern in tissue studies in both primary and metastatic setting and prompts further research in the use of non-tissue biomarkers as a marker of efficacy.

Liquid biopsy represents a non-invasive alternative for the characterisation of tumour heterogeneity and allows detection of dynamic changes during treatment. There is a positive correlation between disease burden and ctDNA levels with higher ctDNA levels in TNBC in comparison to other breast cancer subtypes³⁰⁹. In early stage breast cancer ctDNA can be detected, quantified and analysed with high sensitivity and specificity sequencing techniques³⁰⁹. The RIO trial utilised the use of ctDNA in early TNBC breast cancer and in contrast to the tumour biopsy-based data, revealed a substantial proportion of patients with suppressed ctDNA after rucaparib treatment. Patients with germline *BRCA1/2* mutations had a greater suppression of ctDNA than patients without germline mutations (n = 19, p = 0.021, Mann–Whitney) validating ctDNA dynamics as a marker of rucaparib activity. Cancers with deficient RAD51 foci formation (n = 12, p = 0.033, Mann–Whitney) and HRDetect+ve cancers had greater ctDNA suppression (n = 15, p = 0.027, Mann–Whitney) indicating patients with HRD respond to PARP inhibition within two weeks of treatment. Patients with suppressed

ctDNA (ctDNA ratio (CDR) <0.25, methods) were enriched for germline mutations of *BRCA1/2* and *PALB2* and gene promoter methylation of *BRCA1* and *RAD51C*. These data illustrate the potential of ctDNA analysis to transform window trials, presenting a simple and robust assay of drug activity, without the potential sampling challenges involved with repeat biopsies. ctDNA is a potentially reliable and effective surrogate end point to assess response but will require further validation.

Early ctDNA dynamics could be integrated into all phases of clinical trials to assess biomarker activity and aim to guide treatment depending on ctDNA changes earlier in a patient's treatment. Previous research has shown that early ctDNA changes can predict response with chemotherapy and targeted therapies^{155–157,310,311}. Although technologies for ctDNA are rapidly improving with increased sensitivity and specificity, clearly more evidence is required. Analytical challenges associated with low plasma DNA levels and low purity of tumour DNA in plasma samples, will benefit from further technological development. Additionally, majority of the work in ctDNA is in the metastatic setting but with improved techniques and sensitivity moving ctDNA dynamics into early cancer should be a priority.

In summary, the work presented here has identified a subset of TNBC that express HR deficiency and may be targetable by PARP inhibitors. Having a technique that can be translated from the laboratory to the clinic is vital to ensure early diagnosis and targeted treatment can be delivered to the patient. The novel RAD51 IHC score presented in this thesis can identify TNBC with a functional defect at the time of treatment. This assay although will need further validation, has the potential to be transferred to a clinical laboratory. With further development the assay could be assessed digitally increasing its sensitivity and specificity as a predictive test for HRD. Accompanying the functional HRD assay, the mutational-signature based classifier HRDetect, identifies cancers with genetic, somatic and functional deficiency in HR harnessing its role as a clinical biomarker for HR deficient.

Treatment with the PARP inhibitor rucaparib has shown evidence of activity using ctDNA analysis in sporadic TNBCs and explored the possible impact ctDNA dynamics could have during treatment, detecting response and changing the treatment pathway if required earlier in the patient's journey.

Chapter 8 References

1. Badve, S. *et al.* Basal-like and triple-negative breast cancers: A critical review with an emphasis on the implications for pathologists and oncologists. *Modern Pathology* (2011). doi:10.1038/modpathol.2010.200
2. Hudis, C. A. & Gianni, L. Triple-Negative Breast Cancer: An Unmet Medical Need. *Oncologist* (2011). doi:10.1634/theoncologist.2011-s1-01
3. Bianchini, G., Balko, J. M., Mayer, I. A., Sanders, M. E. & Gianni, L. Triple-negative breast cancer: Challenges and opportunities of a heterogeneous disease. *Nature Reviews Clinical Oncology* (2016). doi:10.1038/nrclinonc.2016.66
4. Bianchini, G., Balko, J. M., Mayer, I. A., Sanders, M. E. & Gianni, L. Triple-negative breast cancer: challenges and opportunities of a heterogeneous disease. *Nat Rev Clin Oncol* (2016). doi:10.1038/nrclinonc.2016.66
5. Lehmann, B. D. *et al.* Identification of human triple-negative breast cancer subtypes and preclinical models for selection of targeted therapies. *J. Clin. Invest.* (2011). doi:10.1172/JCI45014
6. Tutt, A. *et al.* Oral poly(ADP-ribose) polymerase inhibitor olaparib in patients with BRCA1 or BRCA2 mutations and advanced breast cancer: a proof-of-concept trial. *Lancet* **376**, 235–244 (2010).
7. Gelmon, K. A. *et al.* Olaparib in patients with recurrent high-grade serous or poorly differentiated ovarian carcinoma or triple-negative breast cancer: a phase 2, multicentre, open-label, non-randomised study. *Lancet Oncol* **12**, 852–861 (2011).
8. Farmer, H. *et al.* Targeting the DNA repair defect in BRCA mutant cells as a therapeutic strategy. *Nature* **434**, 917–921 (2005).
9. Bruna, A. *et al.* A Biobank of Breast Cancer Explants with Preserved Intra-tumor Heterogeneity to Screen Anticancer Compounds. *Cell* (2016). doi:10.1016/j.cell.2016.08.041
10. Evans, K. W. *et al.* A population of heterogeneous breast cancer patient-derived xenografts demonstrate broad activity of PARP inhibitor in BRCA1/2 wild-type tumors. *Clin. Cancer Res.* (2017). doi:10.1158/1078-0432.CCR-17-0615
11. Carey, L. A. *et al.* The triple negative paradox: Primary tumor chemosensitivity of breast cancer subtypes. *Clin. Cancer Res.* (2007). doi:10.1158/1078-

- 0432.CCR-06-1109
12. Hudis, C. A. & Gianni, L. Triple-negative breast cancer: an unmet medical need. *Oncologist* **16 Suppl 1**, 1–11 (2011).
 13. Perou, C. M. *et al.* Molecular portraits of human breast tumours. *Nature* (2000). doi:10.1038/35021093
 14. Sørlie, T. *et al.* Gene expression patterns of breast carcinomas distinguish tumor subclasses with clinical implications. *Proc. Natl. Acad. Sci. U. S. A.* (2001). doi:10.1073/pnas.191367098
 15. Masuda, H. *et al.* Differential response to neoadjuvant chemotherapy among 7 triple-negative breast cancer molecular subtypes. *Clin. Cancer Res.* (2013). doi:10.1158/1078-0432.CCR-13-0799
 16. Gao, G., Wang, Z., Qu, X. & Zhang, Z. Prognostic value of tumor-infiltrating lymphocytes in patients with triple-negative breast cancer: A systematic review and meta-analysis. *BMC Cancer* (2020). doi:10.1186/s12885-020-6668-z
 17. Strickland, K. C. *et al.* Association and prognostic significance of BRCA1/2-mutation status with neoantigen load, number of tumor-infiltrating lymphocytes and expression of PD-1/PD-L1 in high grade serous ovarian cancer. *Oncotarget* (2016). doi:10.18632/oncotarget.7277
 18. Telli, M. L. *et al.* Association of Tumor-Infiltrating Lymphocytes with Homologous Recombination Deficiency and BRCA1/2 Status in Patients with Early Triple-Negative Breast Cancer: A Pooled Analysis. *Clin. Cancer Res.* (2020). doi:10.1158/1078-0432.CCR-19-0664
 19. Bardia, A. & Baselga, J. Neoadjuvant Therapy as a Platform for Drug Development and Approval in Breast Cancer. *Clin. Cancer Res.* **19**, 6360–6370 (2013).
 20. De Lena, M., Zucali, R., Viganotti, G., Valagussa, P. & Bonadonna, G. Combined chemotherapy-radiotherapy approach in locally advanced (T3b-T4) breast cancer. *Cancer Chemother. Pharmacol.* (1978).
 21. Swain, S. M. *et al.* Neoadjuvant Chemotherapy in the Combined Modality Approach of Locally Advanced Nonmetastatic Breast Cancer. *Cancer Res.* (1987).
 22. Fisher, B. *et al.* Effect of preoperative chemotherapy on local-regional disease in women with operable breast cancer: Findings from national surgical adjuvant breast and bowel project B-18. *J. Clin. Oncol.* (1997).

- doi:10.1200/JCO.1997.15.7.2483
23. Hortobagyi, G. N. *et al.* Management of stage III primary breast cancer with primary chemotherapy, surgery, and radiation therapy. *Cancer* (1988). doi:10.1002/1097-0142(19881215)62:12<2507::AID-CNCR2820621210>3.0.CO;2-D
 24. Mauri, D., Pavlidis, N. & Ioannidis, J. P. A. Neoadjuvant versus adjuvant systemic treatment in breast cancer: A meta-analysis. *J. Natl. Cancer Inst.* (2005). doi:10.1093/jnci/dji021
 25. Rastogi, P. *et al.* Preoperative chemotherapy: Updates of national surgical adjuvant breast and bowel project protocols B-18 and B-27. *Journal of Clinical Oncology* (2008). doi:10.1200/JCO.2007.15.0235
 26. Ellis, M. J. *et al.* Whole-genome analysis informs breast cancer response to aromatase inhibition. *Nature* (2012). doi:10.1038/nature11143
 27. Baselga, J. *et al.* Phase II genomics study of ixabepilone as neoadjuvant treatment for breast cancer. *J. Clin. Oncol.* (2009). doi:10.1200/JCO.2007.14.2646
 28. Dowsett, M. *et al.* Prognostic value of Ki67 expression after short-term presurgical endocrine therapy for primary breast cancer. *J. Natl. Cancer Inst.* (2007). doi:10.1093/jnci/djk020
 29. Selli, C. & Sims, A. H. Neoadjuvant Therapy for Breast Cancer as a Model for Translational Research. *Breast Cancer: Basic and Clinical Research* (2019). doi:10.1177/1178223419829072
 30. Rugo, H. S. *et al.* Adaptive Randomization of Veliparib–Carboplatin Treatment in Breast Cancer. *N. Engl. J. Med.* (2016). doi:10.1056/nejmoa1513749
 31. Loibl, S. *et al.* Addition of the PARP inhibitor veliparib plus carboplatin or carboplatin alone to standard neoadjuvant chemotherapy in triple-negative breast cancer (BrighTNess): a randomised, phase 3 trial. *Lancet Oncol.* (2018). doi:10.1016/S1470-2045(18)30111-6
 32. Litton, J. K. *et al.* A feasibility study of neoadjuvant talazoparib for operable breast cancer patients with a germline BRCA mutation demonstrates marked activity. *npj Breast Cancer* (2017). doi:10.1038/s41523-017-0052-4
 33. Litton, J. K. *et al.* Neoadjuvant talazoparib for patients with operable breast cancer with a germline BRCA pathogenic variant. in *Journal of Clinical Oncology* (2020). doi:10.1200/JCO.19.01304

34. Mehta, A. & Haber, J. E. Sources of DNA double-strand breaks and models of recombinational DNA repair. *Cold Spring Harb. Perspect. Biol.* (2014). doi:10.1101/cshperspect.a016428
35. Aparicio, T., Baer, R. & Gautier, J. DNA double-strand break repair pathway choice and cancer. *DNA Repair (Amst)*. (2014). doi:10.1016/j.dnarep.2014.03.014
36. Ceccaldi, R., Rondinelli, B. & D'Andrea, A. D. Repair Pathway Choices and Consequences at the Double-Strand Break. *Trends in Cell Biology* (2016). doi:10.1016/j.tcb.2015.07.009
37. Lieber, M. R. & Karanjawala, Z. E. Ageing, repetitive genomes and DNA damage. *Nature Reviews Molecular Cell Biology* (2004). doi:10.1038/nrm1281
38. Lieber, M. R., Ma, Y., Pannicke, U. & Schwarz, K. Mechanism and regulation of human non-homologous DNA end-joining. *Nature Reviews Molecular Cell Biology* (2003). doi:10.1038/nrm1202
39. Jackson, S. P. Sensing and repairing DNA double-strand breaks. *Carcinogenesis* (2002). doi:10.1093/carcin/23.5.687
40. Chapman, J. R., Taylor, M. R. G. & Boulton, S. J. Playing the End Game: DNA Double-Strand Break Repair Pathway Choice. *Molecular Cell* (2012). doi:10.1016/j.molcel.2012.07.029
41. Li, X. & Heyer, W. D. Homologous recombination in DNA repair and DNA damage tolerance. *Cell Research* (2008). doi:10.1038/cr.2008.1
42. Wright, W. D., Shah, S. S. & Heyer, W. D. Homologous recombination and the repair of DNA double-strand breaks. *Journal of Biological Chemistry* (2018). doi:10.1074/jbc.TM118.000372
43. Lord, C. J. & Ashworth, A. PARP Inhibitors: The First Synthetic Lethal Targeted Therapy. *Science (80-.)*. (2017). doi:10.1126/science.aam7344
44. Javle, M. & Curtin, N. J. The role of PARP in DNA repair and its therapeutic exploitation. *British Journal of Cancer* (2011). doi:10.1038/bjc.2011.382
45. Rimar, K. J., Tran, P. T., Matulewicz, R. S., Hussain, M. & Meeks, J. J. The emerging role of homologous recombination repair and PARP inhibitors in genitourinary malignancies. *Cancer* (2017). doi:10.1002/cncr.30631
46. Keung, M., Wu, Y. & Vadgama, J. PARP Inhibitors as a Therapeutic Agent for Homologous Recombination Deficiency in Breast Cancers. *J. Clin. Med.* (2019). doi:10.3390/jcm8040435

47. Robson, M., Goessl, C. & Domchek, S. Olaparib for Metastatic Germline BRCA-Mutated Breast Cancer. *N Engl J Med* **377**, 1792–1793 (2017).
48. Litton, J. K. *et al.* Talazoparib in Patients with Advanced Breast Cancer and a Germline BRCA Mutation. *N Engl J Med* **379**, 753–763 (2018).
49. Turner, N., Tutt, A. & Ashworth, A. Hallmarks of ‘BRCAness’ in sporadic cancers. *Nat Rev Cancer* **4**, 814–819 (2004).
50. Hoppe, M. M., Sundar, R., Tan, D. S. P. & Jeyasekharan, A. D. Biomarkers for homologous recombination deficiency in cancer. *Journal of the National Cancer Institute* (2018). doi:10.1093/jnci/djy085
51. Ledermann, J. *et al.* Olaparib maintenance therapy in platinum-sensitive relapsed ovarian cancer. *N. Engl. J. Med.* (2012). doi:10.1056/NEJMoa1105535
52. Turner, N. C. *et al.* BRCA1 dysfunction in sporadic basal-like breast cancer. *Oncogene* (2007). doi:10.1038/sj.onc.1210014
53. Jooisse, S. A. *et al.* Prediction of BRCA1-association in hereditary non-BRCA1/2 breast carcinomas with array-CGH. *Breast Cancer Res. Treat.* (2009). doi:10.1007/s10549-008-0117-z
54. Jooisse, S. A. *et al.* Genomic signature of BRCA1 deficiency in sporadic basal-like breast tumors. *Genes Chromosom. Cancer* (2011). doi:10.1002/gcc.20833
55. Lips, E. H. *et al.* Triple-negative breast cancer: BRCAness and concordance of clinical features with BRCA1-mutation carriers. *Br. J. Cancer* (2013). doi:10.1038/bjc.2013.144
56. Nik-Zainal, S. & Morganella, S. Mutational Signatures in Breast Cancer: The Problem at the DNA Level. *Clin Cancer Res* **23**, 2617–2629 (2017).
57. Polak, P. *et al.* A mutational signature reveals alterations underlying deficient homologous recombination repair in breast cancer. *Nat Genet* **49**, 1476–1486 (2017).
58. Turner, N. C. Signatures of DNA-Repair Deficiencies in Breast Cancer. *N Engl J Med* **377**, 2490–2492 (2017).
59. Staaf, J. *et al.* Whole-genome sequencing of triple-negative breast cancers in a population-based clinical study. *Nature Medicine* (2019). doi:10.1038/s41591-019-0582-4
60. Abkevich, V. *et al.* Patterns of genomic loss of heterozygosity predict homologous recombination repair defects in epithelial ovarian cancer. *Br. J. Cancer* (2012). doi:10.1038/bjc.2012.451

61. Birkbak, N. J. *et al.* Telomeric allelic imbalance indicates defective DNA repair and sensitivity to DNA-damaging agents. *Cancer Discov.* (2012). doi:10.1158/2159-8290.CD-11-0206
62. Popova, T. *et al.* Ploidy and large-scale genomic instability consistently identify basal-like breast carcinomas with BRCA1/2 inactivation. *Cancer Res.* (2012). doi:10.1158/0008-5472.CAN-12-1470
63. Telli, M. L. *et al.* Homologous Recombination Deficiency (HRD) Score Predicts Response to Platinum-Containing Neoadjuvant Chemotherapy in Patients with Triple-Negative Breast Cancer. *Clin Cancer Res* **22**, 3764–3773 (2016).
64. Davies, H. *et al.* HRDetect is a predictor of BRCA1 and BRCA2 deficiency based on mutational signatures. *Nat Med* **23**, 517–525 (2017).
65. Lips, E. H. *et al.* Indicators of homologous recombination deficiency in breast cancer and association with response to neoadjuvant chemotherapy. *Ann. Oncol.* (2011). doi:10.1093/annonc/mdq468
66. Meijer, T. G. *et al.* Direct Ex Vivo Observation of Homologous Recombination Defect Reversal After DNA-Damaging Chemotherapy in Patients With Metastatic Breast Cancer. *JCO Precis. Oncol.* (2019). doi:10.1200/po.18.00268
67. Graeser, M. *et al.* A marker of homologous recombination predicts pathologic complete response to neoadjuvant chemotherapy in primary breast cancer. *Clin Cancer Res* **16**, 6159–6168 (2010).
68. Mukhopadhyay, A. *et al.* Development of a Functional Assay for Homologous Recombination Status in Primary Cultures of Epithelial Ovarian Tumor and Correlation with Sensitivity to Poly(ADP-Ribose) Polymerase Inhibitors. *Clin. Cancer Res.* **16**, 2344–2351 (2010).
69. Mukhopadhyay, A. *et al.* Clinicopathological features of homologous recombination-deficient epithelial ovarian cancers: Sensitivity to PARP inhibitors, platinum, and survival. *Cancer Res.* (2012). doi:10.1158/0008-5472.CAN-12-0324
70. Willers, H. *et al.* Utility of DNA repair protein foci for the detection of putative BRCA1 pathway defects in breast cancer biopsies. *Mol. Cancer Res.* (2009). doi:10.1158/1541-7786.MCR-09-0149
71. Naipal, K. A. *et al.* Functional ex vivo assay to select homologous recombination-deficient breast tumors for PARP inhibitor treatment. *Clin Cancer Res* **20**, 4816–4826 (2014).

72. Meijer, T. G. *et al.* Functional Ex Vivo Assay Reveals Homologous Recombination Deficiency in Breast Cancer Beyond BRCA Gene Defects. *Clin Cancer Res* **24**, 6277–6287 (2018).
73. Hansmann, T. *et al.* Constitutive promoter methylation of BRCA1 and RAD51C in patients with familial ovarian cancer and early-onset sporadic breast cancer. *Hum Mol Genet* **21**, 4669–4679 (2012).
74. Jeziorska, D. M. *et al.* DNA methylation of intragenic CpG islands depends on their transcriptional activity during differentiation and disease. *Proc. Natl. Acad. Sci. U. S. A.* (2017). doi:10.1073/pnas.1703087114
75. Łuczak, M. W. & Jagodziński, P. P. The role of DNA methylation in cancer development. *Folia Histochemica et Cytobiologica* (2006). doi:10.5603/4561
76. Lord, C. J. & Ashworth, A. BRCAness revisited. *Nat Rev Cancer* **16**, 110–120 (2016).
77. Lips, E. H. *et al.* Triple-negative breast cancer: BRCAness and concordance of clinical features with BRCA1-mutation carriers. *Br J Cancer* **108**, 2172–2177 (2013).
78. Timms, K. M. *et al.* Association of BRCA1/2 defects with genomic scores predictive of DNA damage repair deficiency among breast cancer subtypes. *Breast Cancer Res.* (2014). doi:10.1186/s13058-014-0475-x
79. Lux, M. P., Fasching, P. A. & Beckmann, M. W. Hereditary breast and ovarian cancer: Review and future perspectives. *Journal of Molecular Medicine* (2006). doi:10.1007/s00109-005-0696-7
80. Hasan, T. N., Leena Grace, B., Shafi, G. & Syed, R. Association of BRCA1 promoter methylation with rs11655505 (c.2265C>T) variants and decreased gene expression in sporadic breast cancer. *Clin. Transl. Oncol.* (2013). doi:10.1007/s12094-012-0968-y
81. Alkam, Y. *et al.* Protein expression and methylation of DNA repair genes hMLH1, hMSH2, MGMT and BRCA1 and their correlation with clinicopathological parameters and prognosis in basal-like breast cancer. *Histopathology* (2013). doi:10.1111/his.12220
82. Ignatov, T. *et al.* BRCA1 promoter methylation is a marker of better response to anthracycline-based therapy in sporadic TNBC. *Breast Cancer Res. Treat.* (2013). doi:10.1007/s10549-013-2693-9
83. Bal, A. *et al.* BRCA1-methylated sporadic breast cancers are BRCA-like in

- showing a basal phenotype and absence of ER expression. *Virchows Arch.* (2012). doi:10.1007/s00428-012-1286-z
84. Buyru, N., Altinisik, J., Ozdemir, F., Demokan, S. & Dalay, N. Methylation profiles in breast cancer. *Cancer Invest.* (2009). doi:10.1080/07357900802350814
 85. Zhang, L. & Long, X. Association of BRCA1 promoter methylation with sporadic breast cancers: Evidence from 40 studies. *Sci. Rep.* **5**, 17869 (2016).
 86. Veeck, J. *et al.* BRCA1 CpG island hypermethylation predicts sensitivity to poly(adenosine diphosphate)-ribose polymerase inhibitors. *J Clin Oncol* **28**, e563-4; author reply e565-6 (2010).
 87. Stefansson OA, Villanueva A, Vidal A, Martí L, E. M. BRCA1 epigenetic inactivation predicts sensitivity to platinum-based chemotherapy in breast and ovarian cancer. *Epigenetics* (2012).
 88. Cai, F. *et al.* Pyrosequencing analysis of BRCA1 methylation level in breast cancer cells. *Tumor Biol.* (2014). doi:10.1007/s13277-013-1508-2
 89. Min, A. *et al.* RAD51C-deficient cancer cells are highly sensitive to the PARP inhibitor olaparib. *Mol. Cancer Ther.* (2013). doi:10.1158/1535-7163.MCT-12-0950
 90. Nik-Zainal, S. *et al.* Mutational processes molding the genomes of 21 breast cancers. *Cell* **149**, 979–993 (2012).
 91. Alexandrov, L. B. *et al.* Signatures of mutational processes in human cancer. *Nature* (2013). doi:10.1038/nature12477
 92. Watkins, J. A., Irshad, S., Grigoriadis, A. & Tutt, A. N. Genomic scars as biomarkers of homologous recombination deficiency and drug response in breast and ovarian cancers. *Breast Cancer Res* **16**, 211 (2014).
 93. Nik-Zainal, S. *et al.* Landscape of somatic mutations in 560 breast cancer whole-genome sequences. *Nature* **534**, 47–54 (2016).
 94. Morales, J. C. *et al.* Review of poly (ADP-ribose) polymerase (PARP) mechanisms of action and rationale for targeting in cancer and other diseases. *Crit. Rev. Eukaryot. Gene Expr.* (2014). doi:10.1615/CritRevEukaryotGeneExpr.2013006875
 95. Satoh, M. S. & Lindahl, T. Role of poly(ADP-ribose) formation in DNA repair. *Nature* (1992). doi:10.1038/356356a0
 96. D'Amours, D., Desnoyers, S., D'Silva, I. & Poirier, G. G. Poly(ADP-ribosyl)ation

- reactions in the regulation of nuclear functions. *Biochemical Journal* (1999). doi:10.1042/0264-6021:3420249
97. DOBZHANSKY, T. Genetics of natural populations; recombination and variability in populations of *Drosophila pseudoobscura*. *Genetics* (1946).
 98. Lucchesi, J. C. Synthetic lethality and semi-lethality among functionally related mutants of *Drosophila melanogaster*. *Genetics* (1968).
 99. Kaiser, C. A. & Schekman, R. Distinct sets of SEC genes govern transport vesicle formation and fusion early in the secretory pathway. *Cell* (1990). doi:10.1016/0092-8674(90)90483-U
 100. Hennessy, K. M., Lee, A., Chen, E. & Botstein, D. A group of interacting yeast DNA replication genes. *Genes Dev.* (1991). doi:10.1101/gad.5.6.958
 101. Bender, A. & Pringle, J. R. Use of a screen for synthetic lethal and multicopy suppressor mutants to identify two new genes involved in morphogenesis in *Saccharomyces cerevisiae*. *Mol. Cell. Biol.* (1991). doi:10.1128/mcb.11.3.1295
 102. Bryant, H. E. *et al.* Specific killing of BRCA2-deficient tumours with inhibitors of poly(ADP-ribose) polymerase. *Nature* **434**, 913–917 (2005).
 103. Haber, J. E. DNA recombination: The replication connection. *Trends in Biochemical Sciences* (1999). doi:10.1016/S0968-0004(99)01413-9
 104. Yap, T. A., Sandhu, S. K., Carden, C. P. & de Bono, J. S. Poly(ADP-Ribose) polymerase (PARP) inhibitors: Exploiting a synthetic lethal strategy in the clinic. *CA. Cancer J. Clin.* (2011). doi:10.3322/caac.20095
 105. Krishnakumar, R. & Kraus, W. L. The PARP Side of the Nucleus: Molecular Actions, Physiological Outcomes, and Clinical Targets. *Molecular Cell* (2010). doi:10.1016/j.molcel.2010.06.017
 106. Clark, J. B., Ferris, G. M. & Pinder, S. Inhibition of nuclear NAD nucleosidase and poly ADP-ribose polymerase activity from rat liver by nicotinamide and 5'-methyl nicotinamide. *BBA Sect. Nucleic Acids Protein Synth.* (1971). doi:10.1016/0005-2787(71)90012-8
 107. Antolin, A. A. *et al.* The kinase polypharmacology landscape of clinical PARP inhibitors. *Sci. Rep.* (2020). doi:10.1038/s41598-020-59074-4
 108. Murai, J. *et al.* Trapping of PARP1 and PARP2 by Clinical PARP Inhibitors. *Cancer Res* **72**, 5588–5599 (2012).
 109. Caldecott, K. W. Protein ADP-ribosylation and the cellular response to DNA strand breaks. *DNA Repair (Amst)*. (2014). doi:10.1016/j.dnarep.2014.03.021

110. Murthy, P. & Muggia, F. PARP inhibitors: clinical development, emerging differences, and the current therapeutic issues. *Cancer Drug Resist.* (2019). doi:10.20517/cdr.2019.002
111. Stemmer, A., Shafran, I., Stemmer, S. M. & Tsoref, D. Comparison of poly (ADP-ribose) polymerase inhibitors (parpis) as maintenance therapy for platinum-sensitive ovarian cancer: Systematic review and network meta-analysis. *Cancers (Basel)*. (2020). doi:10.3390/cancers12103026
112. Kim, G. *et al.* FDA approval summary: Olaparib monotherapy in patients with deleterious germline BRCA-mutated advanced ovarian cancer treated with three or more lines of chemotherapy. *Clin. Cancer Res.* (2015). doi:10.1158/1078-0432.CCR-15-0887
113. Ledermann, J. *et al.* Olaparib maintenance therapy in patients with platinum-sensitive relapsed serous ovarian cancer: A preplanned retrospective analysis of outcomes by BRCA status in a randomised phase 2 trial. *Lancet Oncol.* (2014). doi:10.1016/S1470-2045(14)70228-1
114. Ledermann, J. A. *et al.* Overall survival in patients with platinum-sensitive recurrent serous ovarian cancer receiving olaparib maintenance monotherapy: an updated analysis from a randomised, placebo-controlled, double-blind, phase 2 trial. *Lancet Oncol.* **17**, 1579–1589 (2016).
115. González Martín, A. Progress in PARP inhibitors beyond BRCA mutant recurrent ovarian cancer? *The Lancet Oncology* (2017). doi:10.1016/S1470-2045(16)30621-0
116. Swisher, E. M. *et al.* Rucaparib in relapsed, platinum-sensitive high-grade ovarian carcinoma (ARIEL2 Part 1): an international, multicentre, open-label, phase 2 trial. *Lancet Oncol.* (2017). doi:10.1016/S1470-2045(16)30559-9
117. Mirza, M. R. *et al.* Niraparib maintenance therapy in platinum-sensitive, recurrent ovarian cancer. *N. Engl. J. Med.* (2016). doi:10.1056/NEJMoa1611310
118. Shapira-Frommer, R. *et al.* A phase II open-label, multicenter study of single-agent rucaparib in the treatment of patients with relapsed ovarian cancer and a deleterious BRCA mutation. *J. Clin. Oncol.* (2015). doi:10.1200/jco.2015.33.15_suppl.5513
119. Robson, M. *et al.* Olaparib for metastatic breast cancer in patients with a germline BRCA mutation. *N. Engl. J. Med.* (2017). doi:10.1056/NEJMoa1706450

120. Turner, N. C. *et al.* A phase II study of talazoparib after platinum or cytotoxic nonplatinum regimens in patients with advanced breast cancer and germline BRCA1/2 mutations (ABRAZO). *Clin. Cancer Res.* (2019). doi:10.1158/1078-0432.CCR-18-1891
121. Litton, J. K. *et al.* Talazoparib in Patients with Advanced Breast Cancer and a Germline BRCA Mutation. *N. Engl. J. Med.* **379**, 753–763 (2018).
122. WHO (World Health Organization). Biomarkers in risk assessment: validity and validation (EHC 222). *Environmental Health* (2001).
123. GOLD, P. & FREEDMAN, S. O. DEMONSTRATION OF TUMOR-SPECIFIC ANTIGENS IN HUMAN COLONIC CARCINOMATA BY IMMUNOLOGICAL TOLERANCE AND ABSORPTION TECHNIQUES. *J. Exp. Med.* (1965). doi:10.1084/jem.121.3.439
124. Chatterjee, S. K. & Zetter, B. R. Cancer biomarkers: Knowing the present and predicting the future. *Future Oncology* (2005). doi:10.1517/14796694.1.1.37
125. Cheang, M. C. U. *et al.* Ki67 index, HER2 status, and prognosis of patients with luminal B breast cancer. *J. Natl. Cancer Inst.* (2009). doi:10.1093/jnci/djp082
126. Rastelli, F. & Crispino, S. Factors predictive of response to hormone therapy in breast cancer. *Tumori* (2008). doi:10.1177/030089160809400314
127. Cardoso, F. *et al.* 70-Gene Signature as an Aid to Treatment Decisions in Early-Stage Breast Cancer. *N. Engl. J. Med.* **375**, 717–729 (2016).
128. Sparano, J. A. *et al.* Prospective validation of a 21-gene expression assay in breast cancer. *N. Engl. J. Med.* (2015). doi:10.1056/NEJMoa1510764
129. Dowsett, M. *et al.* Comparison of PAM50 risk of recurrence score with oncotype DX and IHC4 for predicting risk of distant recurrence after endocrine therapy. *J Clin Oncol* **31**, 2783–2790 (2013).
130. Goossens, N., Nakagawa, S., Sun, X. & Hoshida, Y. Cancer biomarker discovery and validation. *Translational Cancer Research* (2015). doi:10.3978/j.issn.2218-676X.2015.06.04
131. Poste, G. Bring on the biomarkers. *Nature* (2011). doi:10.1038/469156a
132. Zaha, D. C. Significance of immunohistochemistry in breast cancer. *World Journal of Clinical Oncology* (2014). doi:10.5306/wjco.v5.i3.382
133. Gerdes, J. *et al.* Immunobiochemical and molecular biologic characterization of the cell proliferation-associated nuclear antigen that is defined by monoclonal antibody Ki-67. *Am. J. Pathol.* (1991).

134. Urruticoechea, A., Smith, I. E. & Dowsett, M. Proliferation marker Ki-67 in early breast cancer. *Journal of Clinical Oncology* (2005). doi:10.1200/JCO.2005.07.501
135. Dowsett, M. *et al.* Assessment of Ki67 in breast cancer: recommendations from the International Ki67 in Breast Cancer working group. *J Natl Cancer Inst* **103**, 1656–1664 (2011).
136. Abubakar, M. *et al.* Prognostic value of automated KI67 scoring in breast cancer: A centralised evaluation of 8088 patients from 10 study groups. *Breast Cancer Res.* (2016). doi:10.1186/s13058-016-0765-6
137. Liu, S., Edgerton, S. M., Moore, D. H. & Thor, A. D. Measures of cell turnover (proliferation and apoptosis) and their association with survival in breast cancer. *Clin. Cancer Res.* (2001).
138. Potten, C. S. What is an apoptotic index measuring? A commentary. *Br. J. Cancer* (1996). doi:10.1038/bjc.1996.624
139. Mandel, P. & Métais, P. Les acides nucléiques du plasma sanguin chez l'homme (Nucleic acids in human blood plasma). *C R Acad Sci Paris* (1948). doi:10.1021/ol200486c
140. Gormally, E., Caboux, E., Vineis, P. & Hainaut, P. Circulating free DNA in plasma or serum as biomarker of carcinogenesis: Practical aspects and biological significance. *Mutation Research - Reviews in Mutation Research* (2007). doi:10.1016/j.mrrev.2006.11.002
141. Leon, S. A., Shapiro, B., Sklaroff, D. M. & Yaros, M. J. Free DNA in the Serum of Cancer Patients and the Effect of Therapy. *Cancer Res.* (1977).
142. Wood, L. D. *et al.* The genomic landscapes of human breast and colorectal cancers. *Science* (80-.). (2007). doi:10.1126/science.1145720
143. Diehl, F. *et al.* Circulating mutant DNA to assess tumor dynamics. *Nat. Med.* (2008). doi:10.1038/nm.1789
144. Jahr, S. *et al.* DNA fragments in the blood plasma of cancer patients: Quantitations and evidence for their origin from apoptotic and necrotic cells. *Cancer Res.* (2001).
145. Stroun, M., Lyautey, J., Lederrey, C., Olson-Sand, A. & Anker, P. About the possible origin and mechanism of circulating DNA: Apoptosis and active DNA release. in *Clinica Chimica Acta* (2001). doi:10.1016/S0009-8981(01)00665-9
146. Emlen, W. & Mannik, M. Effect of DNA size and strandedness on the in vivo

- clearance and organ localization of DNA. *Clin. Exp. Immunol.* (1984).
147. Diehl, F. *et al.* Detection and quantification of mutations in the plasma of patients with colorectal tumors. *Proc. Natl. Acad. Sci. U. S. A.* (2005). doi:10.1073/pnas.0507904102
 148. Schwarzenbach, H., Hoon, D. S. B. & Pantel, K. Cell-free nucleic acids as biomarkers in cancer patients. *Nature Reviews Cancer* (2011). doi:10.1038/nrc3066
 149. Hibi, K. *et al.* Molecular detection of genetic alterations in the serum of colorectal cancer patients. *Cancer Res.* (1998).
 150. Cresswell, G. D. *et al.* Mapping the breast cancer metastatic cascade onto ctDNA using genetic and epigenetic clonal tracking. *Nat. Commun.* (2020). doi:10.1038/s41467-020-15047-9
 151. Reinert, T. *et al.* Analysis of circulating tumour DNA to monitor disease burden following colorectal cancer surgery. *Gut* (2016). doi:10.1136/gutjnl-2014-308859
 152. Bettgowda, C. *et al.* Detection of circulating tumor DNA in early- and late-stage human malignancies. *Sci. Transl. Med.* (2014). doi:10.1126/scitranslmed.3007094
 153. Beaver, J. A. *et al.* Detection of cancer DNA in plasma of patients with early-stage breast cancer. *Clin. Cancer Res.* (2014). doi:10.1158/1078-0432.CCR-13-2933
 154. Dawson, S. J. *et al.* Analysis of circulating tumor DNA to monitor metastatic breast cancer. *N Engl J Med* **368**, 1199–1209 (2013).
 155. O’Leary, B. *et al.* Early circulating tumor DNA dynamics and clonal selection with palbociclib and fulvestrant for breast cancer. *Nat. Commun.* (2018). doi:10.1038/s41467-018-03215-x
 156. Hrebien, S. *et al.* Early ctDNA dynamics as a surrogate for progression-free survival in advanced breast cancer in the BEECH trial. *Ann. Oncol.* (2019). doi:10.1093/annonc/mdz085
 157. Butler, T. M. *et al.* Circulating tumor DNA dynamics using patient-customized assays are associated with outcome in neoadjuvantly treated breast cancer. *Cold Spring Harb. Mol. Case Stud.* **5**, 1–18 (2019).
 158. Sykes, P. J. *et al.* Quantitation of targets for PCR by use of limiting dilution. *Biotechniques* (1992).

159. Vogelstein, B. & Kinzler, K. W. Digital PCR. *Proc. Natl. Acad. Sci. U. S. A.* (1999). doi:10.1073/pnas.96.16.9236
160. Hindson, B. J. *et al.* High-throughput droplet digital PCR system for absolute quantitation of DNA copy number. *Anal. Chem.* (2011). doi:10.1021/ac202028g
161. Diaz, L. A. & Bardelli, A. Liquid biopsies: Genotyping circulating tumor DNA. *Journal of Clinical Oncology* (2014). doi:10.1200/JCO.2012.45.2011
162. Hrebien, S. *et al.* Reproducibility of digital PCR assays for circulating tumor DNA analysis in advanced breast cancer. *PLoS One* (2016). doi:10.1371/journal.pone.0165023
163. Serrati, S. *et al.* Next-generation sequencing: Advances and applications in cancer diagnosis. *OncoTargets and Therapy* (2016). doi:10.2147/OTT.S99807
164. Forshew, T. *et al.* Noninvasive identification and monitoring of cancer mutations by targeted deep sequencing of plasma DNA. *Sci. Transl. Med.* (2012). doi:10.1126/scitranslmed.3003726
165. Rothé, F. *et al.* Plasma circulating tumor DNA as an alternative to metastatic biopsies for mutational analysis in breast cancer. *Ann. Oncol.* (2014). doi:10.1093/annonc/mdu288
166. Newman, A. M. *et al.* An ultrasensitive method for quantitating circulating tumor DNA with broad patient coverage. *Nat. Med.* (2014). doi:10.1038/nm.3519
167. Newman, A. M. *et al.* Integrated digital error suppression for improved detection of circulating tumor DNA. *Nat. Biotechnol.* (2016). doi:10.1038/nbt.3520
168. Fox, E. J. & Reid-Bayliss, K. S. Accuracy of Next Generation Sequencing Platforms. *J. Next Gener. Seq. Appl.* (2014). doi:10.4172/2469-9853.1000106
169. Robasky, K., Lewis, N. E. & Church, G. M. The role of replicates for error mitigation in next-generation sequencing. *Nature Reviews Genetics* (2014). doi:10.1038/nrg3655
170. Xiong, Z. *et al.* ANP32E induces tumorigenesis of triple-negative breast cancer cells by upregulating E2F1. *Mol Oncol* **12**, 896–912 (2018).
171. Kinde, I., Wu, J., Papadopoulos, N., Kinzler, K. W. & Vogelstein, B. Detection and quantification of rare mutations with massively parallel sequencing. *Proc. Natl. Acad. Sci. U. S. A.* (2011). doi:10.1073/pnas.1105422108
172. Koboldt, D. *et al.* Cancer Genome Atlas Network. Comprehensive molecular portraits of human breast tumours. *Nature* (2012).
173. Stephens, P. J. *et al.* The landscape of cancer genes and mutational processes

- in breast cancer. *Nature* (2012). doi:10.1038/nature11017
174. Lawrence, M. S. *et al.* Discovery and saturation analysis of cancer genes across 21 tumour types. *Nature* (2014). doi:10.1038/nature12912
 175. Davies, H. *et al.* Whole-genome sequencing reveals breast cancers with mismatch repair deficiency. *Cancer Res.* (2017). doi:10.1158/0008-5472.CAN-17-1083
 176. Tutt, A. *et al.* Carboplatin in BRCA1/2-mutated and triple-negative breast cancer BRCAness subgroups: the TNT Trial. *Nat. Med.* **24**, 628–637 (2018).
 177. Magoč, T. & Salzberg, S. L. FLASH: Fast length adjustment of short reads to improve genome assemblies. *Bioinformatics* (2011). doi:10.1093/bioinformatics/btr507
 178. Pagès, H., Aboyoun, P., Gentleman, R. & DebRoy, S. Biostrings: Efficient manipulation of biological strings. *R package version 2.46.0* (2017).
 179. Dobin, A. *et al.* STAR: Ultrafast universal RNA-seq aligner. *Bioinformatics* (2013). doi:10.1093/bioinformatics/bts635
 180. Anders, S., Pyl, P. T. & Huber, W. HTSeq-A Python framework to work with high-throughput sequencing data. *Bioinformatics* (2015). doi:10.1093/bioinformatics/btu638
 181. Love, M. I., Huber, W. & Anders, S. Moderated estimation of fold change and dispersion for RNA-seq data with DESeq2. *Genome Biol.* (2014). doi:10.1186/s13059-014-0550-8
 182. Sergushichev, A. A. An algorithm for fast preranked gene set enrichment analysis using cumulative statistic calculation. *bioRxiv* (2016). doi:10.1101/060012
 183. Paquet, E. R. & Hallett, M. T. Absolute assignment of breast cancer intrinsic molecular subtype. *J. Natl. Cancer Inst.* (2015). doi:10.1093/jnci/dju357
 184. Chen, X. *et al.* TNBCtype: A subtyping tool for triple-negative breast cancer. *Cancer Inform.* (2012). doi:10.4137/CIN.S9983
 185. Newman, A. M. *et al.* Robust enumeration of cell subsets from tissue expression profiles. *Nat. Methods* (2015). doi:10.1038/nmeth.3337
 186. Denkert, C., Liedtke, C., Tutt, A. & von Minckwitz, G. Molecular alterations in triple-negative breast cancer-the road to new treatment strategies. *Lancet* **389**, 2430–2442 (2017).
 187. Lord, C. J. & Ashworth, A. The DNA damage response and cancer therapy.

- Nature* **481**, 287–294 (2012).
188. Belli, C., Duso, B. A., Ferraro, E. & Curigliano, G. Homologous recombination deficiency in triple negative breast cancer. *Breast* **45**, 15–21 (2019).
 189. Gelmon, K. A. *et al.* Olaparib in patients with recurrent high-grade serous or poorly differentiated ovarian carcinoma or triple-negative breast cancer: a phase 2, multicentre, open-label, non-randomised study. *Lancet Oncol.* **12**, 852–861 (2011).
 190. McCabe, N. *et al.* Deficiency in the repair of DNA damage by homologous recombination and sensitivity to poly(ADP-ribose) polymerase inhibition. *Cancer Res* **66**, 8109–8115 (2006).
 191. Lord, C. J., McDonald, S., Swift, S., Turner, N. C. & Ashworth, A. A high-throughput RNA interference screen for DNA repair determinants of PARP inhibitor sensitivity. *DNA Repair* **7**, 2010–2019 (2008).
 192. Turner, N. C. *et al.* A synthetic lethal siRNA screen identifying genes mediating sensitivity to a PARP inhibitor. *EMBO J* **27**, 1368–1377 (2008).
 193. Castroviejo-Bermejo, M. *et al.* A RAD51 assay feasible in routine tumor samples calls PARP inhibitor response beyond BRCA mutation. *EMBO Mol Med* **10**, (2018).
 194. Konstantinopoulos, P. A. *et al.* Gene expression profile of BRCAness that correlates with responsiveness to chemotherapy and with outcome in patients with epithelial ovarian cancer. *J. Clin. Oncol.* (2010). doi:10.1200/JCO.2009.27.5719
 195. Wagle, N. *et al.* High-throughput detection of actionable genomic alterations in clinical tumor samples by targeted, massively parallel sequencing. *Cancer Discov.* (2012). doi:10.1158/2159-8290.CD-11-0184
 196. Nogueira A Medeiros R, C. R. DNA Damage Repair and Cancer: The Role of RAD51 Protein and Its Genetic Variants. *DNA Repair Hum. Heal.* **Chapter 3**, 73–86 (2011).
 197. Haaf, T., Golub, E. I., Reddy, G., Radding, C. M. & Ward, D. C. Nuclear foci of mammalian Rad51 recombination protein in somatic cells after DNA damage and its localization in synaptonemal complexes. *Proc. Natl. Acad. Sci. U. S. A.* (1995).
 198. San Filippo, J., Sung, P. & Klein, H. Mechanism of Eukaryotic Homologous Recombination. *Annu. Rev. Biochem.* (2008).

doi:10.1146/annurev.biochem.77.061306.125255

199. Cruz, C. *et al.* RAD51 foci as a functional biomarker of homologous recombination repair and PARP inhibitor resistance in germline BRCA mutated breast cancer. *Ann Oncol* (2018). doi:10.1093/annonc/mdy099
200. Konstantinopoulos, P. A., Ceccaldi, R., Shapiro, G. I. & D'Andrea, A. D. Homologous recombination deficiency: Exploiting the fundamental vulnerability of ovarian cancer. *Cancer Discovery* (2015). doi:10.1158/2159-8290.CD-15-0714
201. Costello, J. F. & Plass, C. Methylation matters. *J. Med. Genet.* **38**, 285–303 (2001).
202. Stirzaker, C. *et al.* Extensive DNA methylation spanning the Rb promoter in retinoblastoma tumors. *Cancer Res.* **57**, 2229–37 (1997).
203. Adams, R. L. P. Eukaryotic DNA methyltransferases - structure and function. *BioEssays* **17**, 139–145 (1995).
204. Esteller, M. *et al.* Promoter hypermethylation and BRCA1 inactivation in sporadic breast and ovarian tumors. *J. Natl. Cancer Inst.* **92**, 564–9 (2000).
205. Herman, J. G., Graff, J. R., Myöhänen, S., Nelkin, B. D. & Baylin, S. B. Methylation-specific PCR: a novel PCR assay for methylation status of CpG islands. *Proc. Natl. Acad. Sci. U. S. A.* **93**, 9821–6 (1996).
206. Jin, B. & Robertson, K. D. DNA methyltransferases, DNA damage repair, and cancer. *Adv. Exp. Med. Biol.* **754**, 3–29 (2013).
207. Bernstein, C., Nfonsam, V., Prasad, A. R. & Bernstein, H. Epigenetic field defects in progression to cancer. *World J. Gastrointest. Oncol.* **5**, 43–9 (2013).
208. Fraga, M. F., Rodríguez, R. & Cañal, M. J. Rapid quantification of DNA methylation by high performance capillary electrophoresis. *Electrophoresis* **21**, 2990–4 (2000).
209. Gonzalgo, M. L. *et al.* Identification and characterization of differentially methylated regions of genomic DNA by methylation-sensitive arbitrarily primed PCR. *Cancer Res.* **57**, 594–9 (1997).
210. Frommer, M. *et al.* A genomic sequencing protocol that yields a positive display of 5-methylcytosine residues in individual DNA strands. *Proc. Natl. Acad. Sci. U. S. A.* **89**, 1827–31 (1992).
211. Laird, P. W. Principles and challenges of genome-wide DNA methylation analysis. *Nature Reviews Genetics* (2010). doi:10.1038/nrg2732

212. Clurman, B. & Groudine, M. Defining tumour-suppressor genes. *Nature* **389**, 123 (1997).
213. Jones, P. A. & Baylin, S. B. P.A. Jones, S.B. Baylin, The fundamental role of epigenetic events in cancer, *Nat. Rev./Genet.* **3** (2002) 415–428. *Nat. Rev./Genet.* **3** 415–428. (2002).
214. Catteau, A., Harris, W. H., Xu, C. F. & Solomon, E. Methylation of the BRCA1 promoter region in sporadic breast and ovarian cancer: Correlation with disease characteristics. *Oncogene* (1999). doi:10.1038/sj.onc.1202509
215. Jing, F. *et al.* CpG island methylator phenotype of multigene in serum of sporadic breast carcinoma. *Tumor Biol.* (2010). doi:10.1007/s13277-010-0040-x
216. Hedenfalk, I. A., Ringnér, M., Trent, J. M. & Borg, A. Gene expression in inherited breast cancer. *Advances in Cancer Research* (2002). doi:10.1016/S0065-230X(02)84001-5
217. Xu, Y. *et al.* Promoter methylation of BRCA1 in triple-negative breast cancer predicts sensitivity to adjuvant chemotherapy. *Ann. Oncol.* (2013). doi:10.1093/annonc/mdt011
218. Swisher, E. M. *et al.* BRCA1 and RAD51C promoter hypermethylation confer sensitivity to the PARP inhibitor rucaparib in patients with relapsed, platinum-sensitive ovarian carcinoma in ARIEL2 Part 1. *Gynecol. Oncol.* **145**, 5 (2017).
219. Min, A. *et al.* RAD51C-deficient cancer cells are highly sensitive to the PARP inhibitor olaparib. *Mol Cancer Ther* **12**, 865–877 (2013).
220. Azzollini, J. *et al.* Constitutive BRCA1 Promoter Hypermethylation Can Be a Predisposing Event in Isolated Early-Onset Breast Cancer. *Cancers (Basel)*. (2019). doi:10.3390/cancers11010058
221. TCGA. TCGA Wanderer: An interactive viewer to explore DNA methylation and gene expression data in human cancer. Available at: <http://maplab.imppc.org/wanderer/>. (Accessed: 21st March 2019)
222. Kint, S., De Spiegelaere, W., De Kesel, J., Vandekerckhove, L. & Van Criekinge, W. Evaluation of bisulfite kits for DNA methylation profiling in terms of DNA fragmentation and DNA recovery using digital PCR. *PLoS One* **13**, e0199091 (2018).
223. Babraham Bioinformatics - Publicly available projects. Available at: <https://www.bioinformatics.babraham.ac.uk/projects/>. (Accessed: 21st March

- 2019)
224. Broad Institute. IGV Genome Browser.
 225. Watkins, J. A., Irshad, S., Grigoriadis, A. & Tutt, A. N. J. Genomic scars as biomarkers of homologous recombination deficiency and drug response in breast and ovarian cancers. *Breast Cancer Res.* **16**, 211 (2014).
 226. Vanderstichele, A., Busschaert, P., Olbrecht, S., Lambrechts, D. & Vergote, I. Genomic signatures as predictive biomarkers of homologous recombination deficiency in ovarian cancer. *Eur. J. Cancer* (2017). doi:10.1016/j.ejca.2017.08.029
 227. Díaz-Gay, M. *et al.* Mutational Signatures in Cancer (MuSiCa): A web application to implement mutational signatures analysis in cancer samples. *BMC Bioinformatics* (2018). doi:10.1186/s12859-018-2234-y
 228. Stephens, P. J. *et al.* The landscape of cancer genes and mutational processes in breast cancer. *Nature* **486**, 400–404 (2012).
 229. Shi, Y., Jin, J., Ji, W. & Guan, X. Therapeutic landscape in mutational triple negative breast cancer. *Mol Cancer* **17**, 99 (2018).
 230. Badve, S. *et al.* Basal-like and triple-negative breast cancers: a critical review with an emphasis on the implications for pathologists and oncologists. *Mod Pathol* **24**, 157–167 (2011).
 231. Nik-Zainal, S. *et al.* The life history of 21 breast cancers. *Cell* (2012). doi:10.1016/j.cell.2012.04.023
 232. Helleday, T., Eshtad, S. & Nik-Zainal, S. Mechanisms underlying mutational signatures in human cancers. *Nature Reviews Genetics* (2014). doi:10.1038/nrg3729
 233. Alexandrov, L. B., Nik-Zainal, S., Wedge, D. C., Campbell, P. J. & Stratton, M. R. Deciphering Signatures of Mutational Processes Operative in Human Cancer. *Cell Rep.* (2013). doi:10.1016/j.celrep.2012.12.008
 234. Staaf, J. *et al.* The impact of whole-genome-sequencing in a population-based study of triple negative breast cancers collected through routine clinical diagnostic settings. *Nat.* (*in submission*)
 235. Yam, C., Mani, S. A. & Moulder, S. L. Targeting the Molecular Subtypes of Triple Negative Breast Cancer: Understanding the Diversity to Progress the Field. *Oncologist* (2017). doi:10.1634/theoncologist.2017-0095
 236. Aguilar-Mahecha, A. *et al.* The identification of challenges in tissue collection for

- biomarker studies: The Q-CROC-03 neoadjuvant breast cancer translational trial experience. *Mod. Pathol.* (2017). doi:10.1038/modpathol.2017.82
237. Chopra, N. *et al.* Homologous recombination DNA repair deficiency and PARP inhibition activity in primary triple negative breast cancer. *Nat. Commun.* (2020). doi:10.1038/s41467-020-16142-7
238. Gachechiladze, M., Škarda, J., Soltermann, A. & Joerger, M. RAD51 as a potential surrogate marker for DNA repair capacity in solid malignancies. *Int. J. Cancer* **141**, 1286–1294 (2017).
239. Marrugo-Ramírez, J., Mir, M. & Samitier, J. Blood-based cancer biomarkers in liquid biopsy: A promising non-invasive alternative to tissue biopsy. *International Journal of Molecular Sciences* (2018). doi:10.3390/ijms19102877
240. Robertson, E. G. & Baxter, G. Tumour seeding following percutaneous needle biopsy: The real story! *Clinical Radiology* (2011). doi:10.1016/j.crad.2011.05.012
241. Gerlinger, M. *et al.* Intratumor heterogeneity and branched evolution revealed by multiregion sequencing. *N Engl J Med* **366**, 883–892 (2012).
242. Wang, Y. *et al.* Clonal evolution in breast cancer revealed by single nucleus genome sequencing. *Nature* (2014). doi:10.1038/nature13600
243. Merker, J. D. *et al.* Circulating tumor DNA analysis in patients with cancer: American society of clinical oncology and college of American pathologists joint review. *Archives of Pathology and Laboratory Medicine* (2018). doi:10.5858/arpa.2018-0901-SA
244. Sheri, A. & Dowsett, M. Developments in Ki67 and other biomarkers for treatment decision making in breast cancer. *Ann Oncol* **23 Suppl 1**, x219-27 (2012).
245. Wang, R. X., Chen, S., Jin, X. & Shao, Z. M. Value of Ki-67 expression in triple-negative breast cancer before and after neoadjuvant chemotherapy with weekly paclitaxel plus carboplatin. *Sci. Rep.* (2016). doi:10.1038/srep30091
246. Carey, L. A. *et al.* The triple negative paradox: primary tumor chemosensitivity of breast cancer subtypes. *Clin Cancer Res* **13**, 2329–2334 (2007).
247. Detre, S. *et al.* Time-related effects of estrogen withdrawal on proliferation and cell death-related events in MCF7 xenografts. *Int. J. Cancer* (1999). doi:10.1002/(SICI)1097-0215(19990412)81:2<309::AID-IJC23>3.0.CO;2-S
248. Johnston, S. R. D. *et al.* Idoxifene antagonizes estradiol-dependent MCF-7

- breast cancer xenograft growth through sustained induction of apoptosis. *Cancer Res.* (1999).
249. Assersohn, L. *et al.* Studies of the potential utility of Ki67 as a predictive molecular marker of clinical response in primary breast cancer. *Breast Cancer Res. Treat.* (2003). doi:10.1023/B:BREA.0000003968.45511.3f
250. Ellis, P. A. *et al.* Reduced apoptosis and proliferation and increased Bcl-2 in residual breast cancer following preoperative chemotherapy. *Breast Cancer Res. Treat.* (1998). doi:10.1023/A:1005933815809
251. Dowsett, M. *et al.* Short-term changes in Ki-67 during neoadjuvant treatment of primary breast cancer with anastrozole or tamoxifen alone or combined correlate with recurrence-free survival. in *Clinical Cancer Research* (2005).
252. Smith, I. E. *et al.* Neoadjuvant treatment of postmenopausal breast cancer with anastrozole, tamoxifen, or both in combination: The Immediate Preoperative Anastrozole, Tamoxifen, or Combined With Tamoxifen (IMPACT) multicenter double-blind randomized trial. *J. Clin. Oncol.* (2005). doi:10.1200/JCO.2005.04.005
253. Jovanovic, B. *et al.* A randomized phase II neoadjuvant study of cisplatin, paclitaxel with or without everolimus in patients with stage II/III triple-negative breast cancer (TNBC): Responses and long-term outcome correlated with increased frequency of DNA damage response gene. *Clin. Cancer Res.* (2017). doi:10.1158/1078-0432.CCR-16-3055
254. Keam, B. *et al.* Ki-67 can be used for further classification of triple negative breast cancer into two subtypes with different response and prognosis. *Breast Cancer Res.* (2011). doi:10.1186/bcr2834
255. Nishimura, R., Osako, T., Okumura, Y., Hayashi, M. & Arima, N. Clinical significance of Ki-67 in neoadjuvant chemotherapy for primary breast cancer as a predictor for chemosensitivity and for prognosis. *Breast Cancer* (2010). doi:10.1007/s12282-009-0161-5
256. Matsubara, N. *et al.* Survival outcome and reduction rate of Ki-67 between pre- and post-neoadjuvant chemotherapy in breast cancer patients with non-pCR. *Breast Cancer Res. Treat.* (2014). doi:10.1007/s10549-014-3084-6
257. Colleoni, M. *et al.* A risk score to predict disease-free survival in patients not achieving a pathological complete remission after preoperative chemotherapy for breast cancer. *Ann. Oncol.* (2009). doi:10.1093/annonc/mdn747

258. Jones, R. L. *et al.* The prognostic significance of Ki67 before and after neoadjuvant chemotherapy in breast cancer. *Breast Cancer Res. Treat.* (2009). doi:10.1007/s10549-008-0081-7
259. Dowsett, M. *et al.* Short-term changes in Ki-67 during neoadjuvant treatment of primary breast cancer with anastrozole or tamoxifen alone or combined correlate with recurrence-free survival. *Clin Cancer Res* **11**, 951s–8s (2005).
260. Pucci, B., Kasten, M. & Giordano, A. Cell cycle and apoptosis. *Neoplasia* (2000). doi:10.1038/sj.neo.7900101
261. Lipponen, P. Apoptosis in breast cancer: relationship with other pathological parameters. *Endocr. Relat. Cancer* **13–16** (1999). doi:10.1677/erc.0.0060013
262. Mitch Dowsett, 1Ian E. Smith, 2 Steve R. Ebbs, 3 J. Michael Dixon, 4 Anthony Skene, 5 Clive Griffith, 6 Irene Boeddinghaus, 1, 2 Janine Salter, 1Simone Detre, 1Margaret Hills, 1Susan Ashley, 2 Stephen Francis, 7 Geraldine Walsh, 2 and Roger A'Hern¹. Proliferation and apoptosis as markers of benefit in neoadjuvant endocrine therapy of breast cancer. *Clin Cancer Res* **12**, 1024–1030 (2006).
263. Parkinson, C. A. *et al.* Exploratory Analysis of TP53 Mutations in Circulating Tumour DNA as Biomarkers of Treatment Response for Patients with Relapsed High-Grade Serous Ovarian Carcinoma: A Retrospective Study. *PLoS Med.* (2016). doi:10.1371/journal.pmed.1002198
264. Schreuer, M. *et al.* Quantitative assessment of BRAF V600 mutant circulating cell-free tumor DNA as a tool for therapeutic monitoring in metastatic melanoma patients treated with BRAF/MEK inhibitors. *J. Transl. Med.* (2016). doi:10.1186/s12967-016-0852-6
265. Lee, J. H. *et al.* Circulating tumour DNA predicts response to anti-PD1 antibodies in metastatic melanoma. *Ann. Oncol. Off. J. Eur. Soc. Med. Oncol.* (2017). doi:10.1093/annonc/mdx026
266. Tie, J. *et al.* Circulating tumor DNA as an early marker of therapeutic response in patients with metastatic colorectal cancer. *Ann. Oncol.* (2015). doi:10.1093/annonc/mdv177
267. Garlan, F. *et al.* Early evaluation of circulating tumor DNA as marker of therapeutic efficacy in metastatic colorectal cancer patients (PLACOL study). *Clin. Cancer Res.* (2017). doi:10.1158/1078-0432.CCR-16-3155
268. Raja, R. *et al.* Early reduction in ctDNA predicts survival in patients with lung

- and bladder cancer treated with durvalumab. *Clin. Cancer Res.* (2018). doi:10.1158/1078-0432.CCR-18-0386
269. Mok, T. *et al.* Detection and dynamic changes of EGFR mutations from circulating tumor DNA as a predictor of survival outcomes in NSCLC Patients treated with first-line intercalated erlotinib and chemotherapy. *Clin. Cancer Res.* (2015). doi:10.1158/1078-0432.CCR-14-2594
270. Marchetti, A. *et al.* Early prediction of response to tyrosine kinase inhibitors by quantification of EGFR mutations in plasma of NSCLC patients. *J. Thorac. Oncol.* (2015). doi:10.1097/JTO.0000000000000643
271. Cabel, L. *et al.* Circulating tumor DNA changes for early monitoring of anti-PD1 immunotherapy: A proof-of-concept study. *Ann. Oncol.* (2017). doi:10.1093/annonc/mdx212
272. Kato, K. *et al.* Numerical indices based on circulating tumor DNA for the evaluation of therapeutic response and disease progression in lung cancer patients. *Sci. Rep.* (2016). doi:10.1038/srep29093
273. Garcia-Murillas, I. *et al.* Assessment of Molecular Relapse Detection in Early-Stage Breast Cancer. *JAMA Oncol.* (2019). doi:10.1001/jamaoncol.2019.1838
274. Garcia-Murillas, I. *et al.* Mutation tracking in circulating tumor DNA predicts relapse in early breast cancer. *Sci. Transl. Med.* (2015). doi:10.1126/scitranslmed.aab0021
275. Fribbens, C. *et al.* Tracking evolution of aromatase inhibitor resistance with circulating tumour DNA analysis in metastatic breast cancer. *Ann. Oncol.* (2018). doi:10.1093/annonc/mdx483
276. Abbosh, C., Swanton, C. & Birkbak, N. J. Clonal haematopoiesis: A source of biological noise in cell-free DNA analyses. *Annals of Oncology* (2019). doi:10.1093/annonc/mdy552
277. Chang, J. *et al.* Biologic markers as predictors of clinical outcome from systemic therapy for primary operable breast cancer. *J. Clin. Oncol.* (1999). doi:10.1200/JCO.1999.17.10.3058
278. Dowsett, M. *et al.* Proliferation and apoptosis as markers of benefit in neoadjuvant endocrine therapy of breast cancer. *Clin Cancer Res* **12**, 1024s-1030s (2006).
279. Harper-Wynne, C. L. *et al.* Comparison of the systemic and intratumoral effects of tamoxifen and the aromatase inhibitor vorozole in postmenopausal patients

- with primary breast cancer. *J. Clin. Oncol.* (2002). doi:10.1200/JCO.20.4.1026
280. Cerami, E. *et al.* The cBio Cancer Genomics Portal: An open platform for exploring multidimensional cancer genomics data. *Cancer Discov.* (2012). doi:10.1158/2159-8290.CD-12-0095
281. Shah, S. P. *et al.* The clonal and mutational evolution spectrum of primary triple-negative breast cancers. *Nature* **486**, 395–399 (2012).
282. Olsson, E. *et al.* Serial monitoring of circulating tumor DNA in patients with primary breast cancer for detection of occult metastatic disease. *EMBO Mol Med* **7**, 1034–1047 (2015).
283. Osumi, H., Shinozaki, E., Yamaguchi, K. & Zembutsu, H. Early change in circulating tumor DNA as a potential predictor of response to chemotherapy in patients with metastatic colorectal cancer. *Sci. Rep.* (2019). doi:10.1038/s41598-019-53711-3
284. Gale, D. *et al.* Development of a highly sensitive liquid biopsy platform to detect clinically-relevant cancer mutations at low allele fractions in cellfree DNA. *PLoS One* (2018). doi:10.1371/journal.pone.0194630
285. Chen, M. & Zhao, H. Next-generation sequencing in liquid biopsy: cancer screening and early detection. *Human genomics* (2019). doi:10.1186/s40246-019-0220-8
286. Garcia-Murillas, I. *et al.* Abstract 2743: Comparison of enhanced Tagged-Amplicon Sequencing and digital PCR for circulating tumor DNA analysis in advanced breast cancer. in (2017). doi:10.1158/1538-7445.am2017-2743
287. Brown, J. R., Digiovanna, M. P., Killelea, B., Lannin, D. R. & Rimm, D. L. Quantitative assessment Ki-67 score for prediction of response to neoadjuvant chemotherapy in breast cancer. *Lab. Investig.* (2014). doi:10.1038/labinvest.2013.128
288. Von Minckwitz, G. *et al.* Ki67 measured after neoadjuvant chemotherapy for primary breast cancer. *Clin. Cancer Res.* (2013). doi:10.1158/1078-0432.CCR-12-3628
289. Leung, S. C. Y. *et al.* Analytical validation of a standardised scoring protocol for Ki67 immunohistochemistry on breast cancer excision whole sections: an international multicentre collaboration. *Histopathology* (2019). doi:10.1111/his.13880
290. Al-Kateb, H., Nguyen, T. D. T., Steger-May, K. & Pfeifer, J. D. Identification of

- major factors associated with failed clinical molecular oncology testing performed by next generation sequencing (NGS). *Mol. Oncol.* (2015). doi:10.1016/j.molonc.2015.05.004
291. Postel, M., Roosen, A., Laurent-Puig, P., Taly, V. & Wang-Renault, S. F. Droplet-based digital PCR and next generation sequencing for monitoring circulating tumor DNA: a cancer diagnostic perspective. *Expert Rev. Mol. Diagn.* (2018). doi:10.1080/14737159.2018.1400384
292. Riva, F. *et al.* Patient-specific circulating tumor DNA detection during neoadjuvant chemotherapy in triple-negative breast cancer. *Clin. Chem.* (2017). doi:10.1373/clinchem.2016.262337
293. Ding, P. N. *et al.* Plasma next generation sequencing and droplet digital PCR-based detection of epidermal growth factor receptor (EGFR) mutations in patients with advanced lung cancer treated with subsequent-line osimertinib. *Thorac. Cancer* (2019). doi:10.1111/1759-7714.13154
294. Lettig, L. *et al.* EGFR T790M detection rate in lung adenocarcinomas at baseline using droplet digital PCR and validation by ultra-deep next generation sequencing. *Transl. Lung Cancer Res.* (2019). doi:10.21037/tlcr.2019.09.18
295. Balko, J. M. *et al.* Molecular profiling of the residual disease of triple-negative breast cancers after neoadjuvant chemotherapy identifies actionable therapeutic targets. *Cancer Discov.* (2014). doi:10.1158/2159-8290.CD-13-0286
296. Tie, J. *et al.* Circulating tumor DNA analysis detects minimal residual disease and predicts recurrence in patients with stage II colon cancer. *Sci Transl Med* **8**, 346ra92 (2016).
297. Meijer, T. G. *et al.* Direct Ex Vivo Observation of Homologous Recombination Defect Reversal After DNA-Damaging Chemotherapy in Patients With Metastatic Breast Cancer. *JCO Precis. Oncol.* 1–12 (2019). doi:10.1200/PO.18.00268
298. Mutter, R. W. *et al.* Bi-allelic alterations in DNA repair genes underpin homologous recombination DNA repair defects in breast cancer. *J. Pathol.* (2017). doi:10.1002/path.4890
299. Meijer, T. *et al.* Abstract P6-06-02: Functional homologous recombination REpair CAPacity (RECAP) test in metastatic breast cancer biopsies. *Cancer Res.* **78**, P6-06-02-P6-06–02 (2018).

300. Wei, M. *et al.* BRCA1 promoter methylation in sporadic breast cancer is associated with reduced BRCA1 copy number and chromosome 17 aneusomy. *Cancer Res.* (2005). doi:10.1158/0008-5472.CAN-05-1277
301. Sharma, P. *et al.* The prognostic value of BRCA1 promoter methylation in early stage triple negative breast cancer. *J. Cancer Ther. Res.* (2014). doi:10.7243/2049-7962-3-2
302. Grushko, T. A. *et al.* Evaluation of BRCA1 inactivation by promoter methylation as a marker of triple-negative and basal-like breast cancers. *J. Clin. Oncol.* (2010). doi:10.1200/jco.2010.28.15_suppl.10510
303. Veeck, J. *et al.* BRCA1 CpG island hypermethylation predicts sensitivity to poly(adenosine diphosphate)-ribose polymerase inhibitors. *Journal of Clinical Oncology* (2010). doi:10.1200/JCO.2010.30.1010
304. Xu, X. *et al.* Gene promoter methylation is associated with increased mortality among women with breast cancer. *Breast Cancer Res. Treat.* (2010). doi:10.1007/s10549-009-0628-2
305. Tabano, S. *et al.* Analysis of BRCA1 and RAD51C promoter methylation in Italian families at high-risk of breast and ovarian cancer. *Cancers (Basel)*. (2020). doi:10.3390/cancers12040910
306. Stefansson, O. A. *et al.* BRCA1 Promoter Methylation Status in 1031 Primary Breast Cancers Predicts Favorable Outcomes Following Chemotherapy. *JNCI Cancer Spectr.* (2020). doi:10.1093/jncics/pkz100
307. O’Kane, G. M. *et al.* Outcomes and Immunogenicity of pancreatic cancer stratified by the HRDetect score. *J. Clin. Oncol.* (2020). doi:10.1200/jco.2020.38.15_suppl.4630
308. Zhu, X. *et al.* The prognostic and predictive potential of Ki-67 in triple-negative breast cancer. *Sci. Rep.* (2020). doi:10.1038/s41598-019-57094-3
309. Garcia-Murillas, I. *et al.* Assessment of Molecular Relapse Detection in Early-Stage Breast Cancer. *JAMA Oncol.* (2019). doi:10.1001/jamaoncol.2019.1838
310. Ma, C. X. *et al.* Neratinib efficacy and circulating tumor DNA detection of HER2 mutations in HER2 nonamplified metastatic breast cancer. *Clin. Cancer Res.* (2017). doi:10.1158/1078-0432.CCR-17-0900
311. Chen, Y. H. *et al.* Next-generation sequencing of circulating tumor DNA to predict recurrence in triple-negative breast cancer patients with residual disease after neoadjuvant chemotherapy. *npj Breast Cancer* **3**, 1–5 (2017).

Appendix 1 Rad51 GMNN double staining on FFPE

Antibodies

Rad51: Genetex GTX70230 (Mouse)

GMNN: Proteintech 10802-1-AA (Rabbit)

Method

- Dewax sections in xylene and rehydrate through graded alcohols (100%, 90% 70%) to water.
- Place sections in Dako PT module containing Dako pH9 pretreatment buffer (K8004) for 20 mins at 97°C followed by 20 mins cool down.
- Remove slides from PT module and place in Dako wash buffer (K8002) for 5 mins
- Rinse well in tap water
- Circle sections with resin pen and rinse with Dako wash buffer
- Remove excess fluid from slides and apply Dako H₂O₂ peroxidase blocking reagent for 5 mins
- Wash well in wash buffer 5 mins
- Remove excess fluid and apply Dako protein block (X0909) for 5 mins
- Remove excess fluid (**Do not wash**) and apply Rad51 primary antibody diluted 1/200 in Dako antibody diluent (K8006) for 1 hr at RT
- Wash well in 3 changes of wash buffer
- Remove excess fluid and apply Dako Envision Flex HRP (K8002) for 30mins
- Wash well in 3 changes of wash buffer
- Remove excess fluid and apply Dako DAB (1 drop of DAB/ml of substrate buffer) for 2-5 mins. Check for colour development after 2 mins but **DO NOT** leave for substrate on for more than 5 mins
- Wash well in wash buffer
- Place sections in boiling pH6 citrate buffer for 1min to remove excess antibody
- Wash in water and wash buffer
- Remove excess fluid and apply Dako protein block (X0909) for 5 mins

- Remove excess fluid (Do not wash) and apply GMNN antibody diluted 1/1500 in Dako antibody diluent for 45 mins at RT
- Wash well in 3 changes of wash buffer
- Remove excess fluid and apply Dako Envision Flex HRP (K8002) for 30mins
- Wash well in 3 changes of wash buffer
- Remove excess fluid and apply Vector TMB blue (SK4400) substrate made up as per kit instructions for 2-5 mins. Check microscopically for optimal staining. Reapply substrate if desired intensity of staining is not reached (*It may be necessary to leave this substrate to develop for up to 20 mins in certain cases*).
- Counterstain with 1% aqueous Neutral red if desired
- Dehydrate in grade alcohols, clear in xylene and mount in Vectamount.

Results

Rad51: Brown

GMNN: Blue/Green

Appendix 2 Immunofluorescence for RAD51/GMNN

Immunofluorescence for RAD51/Geminin foci

Fixing the cells:

- Plate cells on poly-lysine treated cover slips.
- Irradiate cells at 10Gy and incubate for 6h at 37°C.
- Aspirate the medium and wash in PBS
- Fix in PFA 4% for 30' at RT
- Wash in PBS
- Either use the cells or cover the plate with parafilm and leave at 4°C.

For FFPE cells and tumours:

- Cut 3µm, deparaffinise and rehydrate
- Antigen retrieve the samples using micro-waving at pH 9 (DAKO pH 9 buffer) for 18 min, let stand for 20 min (alternatively: pressure cook in **MenaPath** Antigen Access Unit at 125°C)

Immunofluorescence:

- Permeabilize with Triton 0.2% for 20' at RT
- Wash in PBS
- Treat with 100ul of DNase I (Roche, stock 10000u/ml to be diluted 1/10 in PBS) for 1h at 37°C in humidified chamber.
- Wash in PBS
- Block with IFF (PBS + 1% BSA + 2% FBS) for at least 30'
- Stain with anti-Rabbit Geminin antibody (dil 1/400; Proteintech) or anti-mouse RAD51 antibody (dil 1/200; Genetex –clone 14B4) at RT for 1 hour
- Wash in PBS – 3X5 minutes
- Add secondary antibodies (anti-rabbit 488 conjugate or anti-mouse 555 conjugate -1/1000 dilution in IFF) for 1 hour at RT
- Wash in PBS with Dapi (1/10000 in PBS) – 3X5 minutes
- Wash in PBS
- Fix in 4% PFA for 15 minutes
- Wash in PBS

- Wash in water and mount in vectashield




For the double Immunofluorescence:

- Permeabilize with Triton 0.2% for 20' at RT
- Wash in PBS
- Treat with 100ul of DNase I (Roche, stock 10000u/ml to be diluted 1/10 in PBS) for 1h at 37°C in humidified chamber.
- Wash in PBS
- Block with IFF (PBS + 1% BSA + 2% FBS) for at least 30 minutes.
- Incubate with anti-Rabbit Geminin antibody (dil 1/400; Proteintech) at RT for 1 hour
- Wash in PBS – 3X5 minutes
- Add secondary antibody (anti-rabbit 488 conjugate -1/1000 dilution in IFF) for 1 hour at RT
- Wash in PBS – 3X5 minutes
- Fix in 4% PFA for 15 minutes
- Incubate with anti-mouse RAD51 antibody (dil 1/200; Genetex –clone 14B4) for 1 hour at RT.
- Wash in PBS – 3X5 minutes
- Add secondary antibody (anti-mouse 555 conjugate -1/1000 dilution in IFF) for 1 hour at RT.
- Wash in PBS with Dapi (1/10000 in PBS) – 3X5 minutes
- Wash in PBS
- Fix in 4% PFA for 15 minutes
- Wash in PBS 2X2 minutes
- Wash in water and mount in vectashield

Appendix 3 SOP 031 RAD51 IHC

Standard Operating Procedure SOP 031: RAD51 analysis by Immunohistochemistry

Effective date: DD MMM YYYY

Version Author: (Neha Chopra)		Date 05 Jun 2017	Document SOP 031 Code: Issue No: 01 Version 01
Checked by: (Monee Shamsheer)		05 Jun 2017	No: Issue Date: 05/06/2017
Approved by: (Alex Pearson)		05 Jun 2017	Issued to: Molecular Oncology (Ralph Lauren/ICR)

Issue	Date	Comment
01	05/06/2017	First Issue

1. Purpose

The purpose of this SOP is for the assessment of RAD51 using double stained immunohistochemistry.

2. Principle

RAD51 expression is cell cycle-regulated, being lowest in resting cells and peaking in proliferating cells in the S/G2 phases of the cell cycle^{1,2}. RAD51 is a key enzyme for homologous recombination (HR) and critical for cell survival. When cells are exposed to genotoxic agents or irradiation, RAD51 protein transfers from the cytosol to the nucleus³, and recruits to sites of DNA damage mediating the search for a homologous sequence during homologous recombination^{4,5}.

The development of RAD51 nuclear foci at the sites of repair of DNA damage is the hallmark for HR-mediated DSB repair, and the levels of RAD51 nuclear foci reflect HR efficiency⁶. HR deficient cells fail to form DNA damage-induced RAD51 nuclear foci⁷.

Measurement of expression and nuclear foci formation of HR proteins for HR competence in patient tumors may identify effective and informative biomarkers that predict response and clinical outcome to treatment⁸.

Double staining with immunohistochemistry allows identification of cells in the S/G2 phase of the cell cycle by geminin (GMNN) nuclear staining (staining blue/green) and RAD51 foci (stain brown foci) within the nucleus.

3. SCOPE

Applicable for the assessment of RAD51 foci in FFPE tumours samples.

4. Associated COSHH

BIO1, BIO11.

5. Equipment AND consumables

Item description	Supplier	Cat No.
Rad51: (Monoclonal, Mouse)	Genetex	GTX70230
Geminin: (Polyclonal, Rabbit)	Proteintech	10802-1-AP
Dako PT module containing Dako pH9 pretreatment buffer	Agilent	K8004
Dako wash buffer	Agilent	K8002
Dako H2O2 peroxidase blocking reagent	Agilent	
Dako protein block	Agilent	K0909
Dako antibody diluent	Agilent	K8006
Dako Envision Flex HRP	Agilent	K8002
Dako DAB	Agilent	
Vector TMB blue substrate	Vector laboratories	SK4400
Vectamount	Vector laboratories	H-5501

6. PROCEDURE

Immunohistochemistry is a double stain with RAD51 and Geminin (GMNN) and is done by Breast Cancer Now Histopathology according to appendix 1.

Advanced preparation for immunohistochemistry staining

1. Discuss with Breast Cancer Now Histopathology in advance to ensure all reagents required for immunohistochemistry are available as per appendix 1.
2. If RAD51 and GMNN antibody are not available in Breast Cancer Now Histopathology this needs to be ordered in advance as per consumables list. This is not stock item in. The lot number for the RAD51 and GMNN antibody should be recorded in LAB-WS-SOP 031 SAMPLES worksheet in field P1 and P2 respectively.

Preparation of samples

3. Collect FFPE blocks from storage facility.
4. Ensure FFPE blocks are adequately labelled with trial ID (and histology block number if applicable).
5. Open LAB-WS-SOP 031 SAMPLES worksheet and complete columns A to E for each sample. Leave column F empty.
6. Place all FFPE blocks in a box with a printed copy of LAB-WS-SOP 031 SAMPLES worksheet. Ensure all samples are adequately labelled and correspond to the worksheet.
7. Samples should be given to Breast Cancer Now Histopathology for sectioning. Breast Cancer Now Histopathology should give each FFPE block a blinded number (MO-'Trial Name'-number (001...)) and complete the 'blinded number' column (F) in 'Samples' provided. The LAB-WS-SOP 031 SAMPLES worksheet with the completed blinded number should not be revealed to the scorer until the analysis has been completed. A paper copy should be retained in the trial specific folder and scanned onto the trial specific folder in the molecular oncology shared folder.

Rad51/gmmn staining with immunohistochemistry

8. A H&E section should be cut at 4 μ m to check for tumour content by a pathologist. If tumour is present proceed to step 2. If no tumour is present a further H&E section should be obtained to determine whether tumour is present. If no tumour is present, this should be annotated on LAB-WS-SOP 031 WORKSHEET 'Samples'.

9. Another section for RAD51/GMNN staining should be cut at 4µm and slide should be labelled with the corresponding blinded number as on LAB-WS-SOP 031 WORKSHEET 'Samples'.
10. RAD51/GMNN immunohistochemistry should be performed in accordance to Appendix 1.
11. RAD51/GMNN and H&E slides should be collected from Core Facility and stored in Molecular Laboratory Lab 2S8. FFPE blocks should be returned to the secured storage facility.

Upload of slides to hamamatzu nanozoomer

12. H&E and RAD51/GMNN slides should be scanned using the Hamamatzu Nanozoomer-XR digital slide scanner in 1S.... Ensure a login has been provided and a nanoscan folder has been created and linked to your profile.
13. Open 3.1 Nanozoomer program on the desktop and choose your profile.
14. Load the slides into the slide sorter and insert into the nanozoomer. Ensure you know where each slide is.
15. Using BATCH MODE enter in the slide identifier (enter the blinded number to ensure blinding for analysis). Ensure the organisation of the slide sorter represents the nanozoomer reference.
16. Scan slides using BATCH MODE.
17. Ensure images are scanned at 40X magnification.
18. When prompted set the area to be scanned and set focus points equally spaced within the tissue area. Scanned images out of focus should be rescanned in single mode and manually focused.
19. Images will be scanned and saved in nanoscans folder of the user.

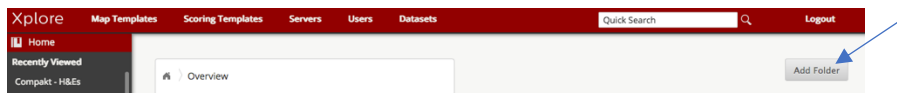
Upload of slides to path xl xplore

20. Images need to be uploaded to the ICR server on Path XL Xlpore
<https://breastcancernow.icr.ac.uk/> .

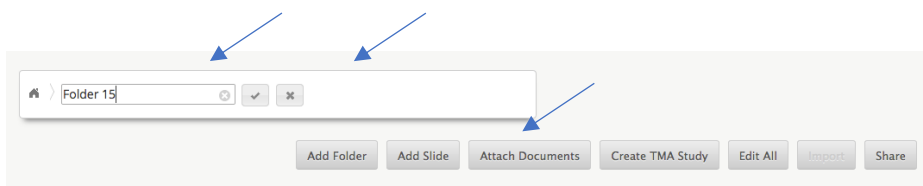
21. Open Path XL Xplore in the internet browser and log in with unique username and password.



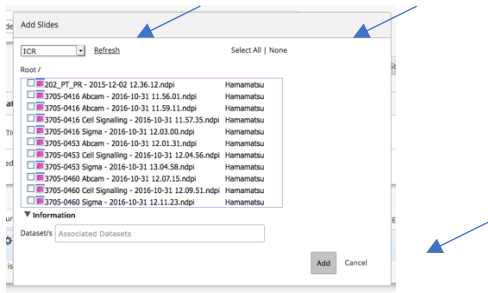
22. Click on 'Add Folder' icon



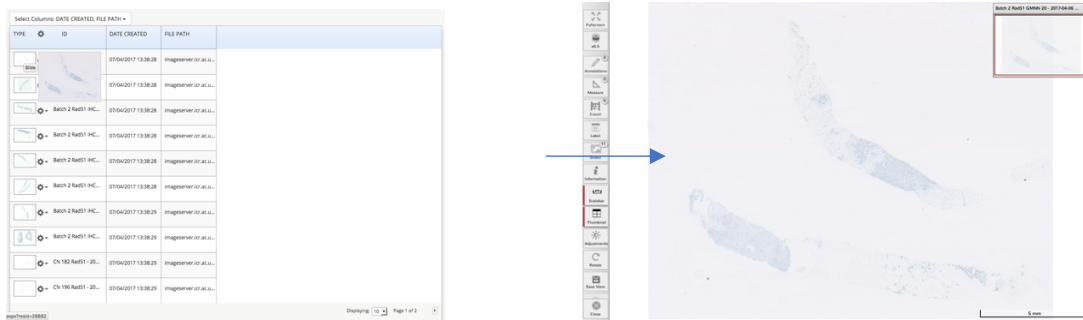
23. Name the folder by clicking on the 'home' picture → tick → add slide.



24. Ensure the root selected is ICR and find your folder. Then click Select All OR the images you require → click 'Add'.

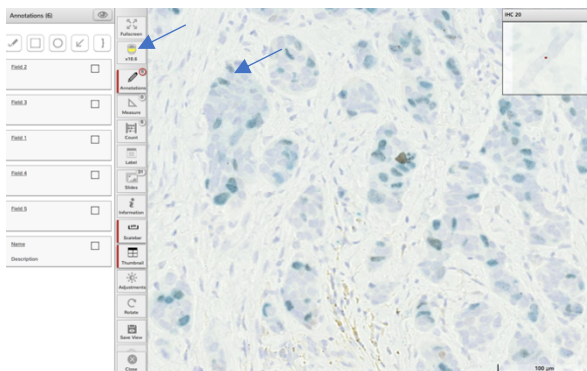


25. Your images will be added to your folder. Click on the image required to start the analysis.



Counting on path xl xplore

26. To select the field to analyse click on 'annotation' and use the icons to set the field. The of field should be approximately 77000mm².

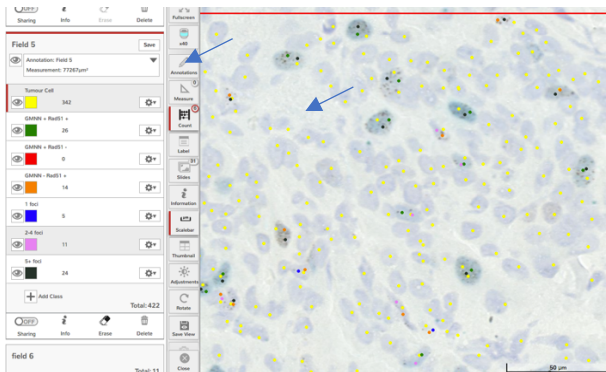


27. To increase the magnification to 40X use the numbers on the keyboard.

28. Click on 'Count' and set the indicators for identification of cells. Indicator colours can be user dependent. You should be able to count the number of

tumour cells, number of GMNN positive cells and number of RAD51 positive cells (with 5+ foci) that are GMNN +ve.

To count cells in each category ensure you are clicked onto the correct category required and then right click. A round spot in the correct colour to the category chosen should appear.



29. To score for proliferation fraction ($(\text{No of tumour cells} / \text{No of GMNN cells}) * 100$):

- a. A maximum of 100 tumour cells per field should be identified in 5 random fields giving a total count of 500 tumour cells.
- b. If less than 300 tumour cells are identified, additional areas of the tumour should be identified to reach a minimum of 300 tumour cells. If this is not possible the sample should be rejected for analysis and restained.
- c. If on restaining a minimum of 300 tumour cells cannot be counted the sample should be rejected from further analysis.

30. To score for RAD51 score ($(\text{No. of RAD51 AND No. of GMNN positive cells} / \text{No. of GMNN cells}) * 100$):

- a. All GMNN positive cells with 5+ RAD51 foci should be scored.
- b. If the number of GMNN positive cells is <30 more GMNN positive cells should be counted over the tumour area. Tumour cells without GMNN do not need to be counted.
- c. If no more than 30 GMNN positive cells can be identified the sample should be rejected for analysis and restained.

- d. Upon restraining every effort should be made to score >30 GMNN positive cells. If >30 GMNN positive cells cannot be reached the sample should be rejected for analysis.

7. Analysis

1. Raw data collected from Path XL Xplore should be entered into LAB-WS-SOP 031 WORKSHEET 'Raw Data'. Totals should be calculated to obtain the data for the whole sample that will be used for analysis
2. LAB-WS-SOP 031 WORKSHEET 'Raw Data' will transfer data to LAB-WS-SOP 031 WORKSHEET 'Analysis' to calculate:
3. Proliferation fraction should be calculated as:
4. $(\text{No. of GMNN positive cells} / \text{No. of tumour cells}) * 100$
5. RAD51 score should be calculates as:
6. $(\text{No. of RAD51 AND GMNN positive cells} / \text{No. of GMNN positive cells}) * 100$

Appendix 4 Ki67 Protocol

Academic Department of Biochemistry, Royal Marsden NHS Trust

Prepared by: Vera Martins

Reviewed by Doc Control or Designee: Dr Elizabeth Folkard

Approved by: Professor Mitch Dowsett

Manual: IMMUNO/GEN/MAN

Document Number: MET/017/7 Academic Department of Biochemistry

Title: **Immunohistochemical demonstration of Ki67 for assessment of proliferation in FFPE tissues using antibody clone MIB-1**

1. INTRODUCTION

The Ki67 antigen is a nuclear protein preferentially expressed during all active phases of the cell cycle (G1, S, G2 and M-phases), but not in resting cells (G0-phase). During interphase, the antigen can be exclusively detected within the nucleus. The mouse monoclonal antibody MIB-1 is widely regarded as the 'gold-standard' for the demonstration of Ki67-positive cells by immunohistochemistry (IHC).

2. OBJECTIVE

To describe the process for the demonstration by IHC of Ki67 in formalin fixed paraffin embedded (FFPE) material using antibody clone MIB-1 and the REAL detection system on the Autostainer (both Dako UK Ltd).

This SOP will describe:

- IHC staining procedure and conditions
- Controls
- Assay acceptance criteria
- Scoring method, including definition of positive staining
- Data recording and results reporting
- Review

3. SCOPE

Applicable to all FFPE patient tissue samples including those from patients in clinical studies.

4. RESPONSIBILITIES

It is the responsibility of laboratory staff trained in the demonstration of Ki67 by IHC to carry out the method and document results in accordance with this SOP.

All procedures should be performed in accordance with the local rules and users of this SOP should be familiar with appropriate COSHH assessments.

5. RELATED DOCUMENTS

5.1. Medicines and Healthcare Products Regulatory Agency (MHRA). Good Clinical Practice (GCP) guidance on the maintenance of regulatory compliance in laboratories that perform the analysis or evaluation of clinical trial samples can be found at: <https://www.gov.uk/good-clinical-practice-for-clinical-trials>

5.2. Control of Substances Hazardous to Health (COSHH) assessments. Information on COSHH can be found on the ICR intranet at: <http://ispace.icr.ac.uk/corporate/departments/facilities/HSEQ/hands/labsafety/menu/hazardoussubstances/COSHH/Pages/NewCOSHHSystem.aspx>

ICR COSHH assessments applicable to this SOP are:

BIO 1

BIO 2

BIO 11

BIO 14

5.3. The SOP for Laboratory Notebooks and other Forms of Raw Data should be understood and followed (LAB/001). Laboratory Notebook (ID/ABC/DATA/IHC Ki67/n) where ID is the assessor's initials, (ABC) is study identifier and n is the raw-data notebook series-number. Notebooks are not to be removed from departmental premises without permission of the Head of Department, and should be stored securely by the assessor while in use. Archived notebooks will be stored centrally in a designated departmental storage facility.

5.4. The Electronic Records and Data SOP QAU/011 is a generic guide to be used in conjunction with specific study related work instructions.

- 5.5. Computer data files (e.g. ID/ABC/001/DAT spreadsheet or ID/ABC/001/DATF final spreadsheet) are located in a departmental shared folder on BIOCHEM server *smb://biochem/BIOCHEM/shared/clinical trials (immuno)/study name*
- 5.6. Dako Autostainer Universal staining system (MET/028).
- 5.7. Solutions are made up fresh every run and labelled (REA/001) either by hand on the container or on pre-printed labels filled in manually.
- 5.8. Laboratory Housekeeping (LAB/002). IHA Staining Record (DOC/005) to be completed with every staining run.
- 5.9. Issues Log: Review & Action (DOC/004) in Reporting Laboratory Issues (QAU/010).
- 5.10. Immunohistochemistry Control Acceptability Ranges document (DOC/010).
- 5.11. Construction of Tissue Microarrays (TMA's) and TMA Templates/Formats (MET/029).
- 5.12. Applicable study specific work instructions.

6. PROCEDURE

This section gives details of procedures specific to the use of the MIB-1 antibody and the applicable IHC staining procedures.

Consumables details should be recorded in the IHA Staining Record (DOC/005). Should any product be discontinued by the supplier or otherwise become unavailable they should be replaced by a similar product of equivalent grade. If the primary antibody lot changes mid-study the new lot should be assayed with the appropriate control once and the result scored. If the result falls within pre-validated control range accept and record this in the IHA Staining Record (DOC/005). Should the result fall outside the pre-validated control range document this in the Issues Log (DOC/004) and consult with the project manager for resolution.

6.1. **Antigen retrieval conditions:** Low pH (pH6.0) Target Antigen Retrieval Solution (K8005, Dako UK Ltd), in Microwave Oven (Sanyo EM-G3597B, Serial Number SY08/0806028).

6.2. **Primary antibody dilution:** dilute the concentrated antibody solution 1:50 in EnVision Antibody Diluent (K8006, Dako UK Ltd) into an Autostainer Reagent Vial (S34253, Dako UK Ltd).

6.3. **Negative antibody control:** use EnVision Antibody Diluent (K8006, Dako UK Ltd) in an Autostainer Reagent Vial (S34253, Dako UK Ltd).

7. CONTROLS

FFPE samples of human breast cancer.

Anonymised human breast cancer samples, known to stain positive for Ki67 with differing levels of expression. The chosen tissue(s) will depend on the level of proliferation deemed appropriate for each study e.g. a high, medium and low proliferation rate may be desirable to cover the range of expected test results.

On first use a specific control sample is analysed **five** times on different occasions; the new control adopted if it shows consistent and specific staining in the expected pattern as outlined above.

The control is required to be accepted prior to scoring, and its 'visual acceptance' is noted on the IHA Staining Record (DOC/005) as 'Yes'. The source data for scoring controls will be documented in the study specific laboratory notebook (ID/ABC/DATA/IHC c-PARP/n). An acceptance range may be derived from the mean and SD using the chosen scoring system and/or according to study specific requirements. The range will be recorded in the Immunohistochemistry Control Acceptability Ranges document (DOC/010) and the average of all scorers' results in the study will be calculated to update the ranges approximately every 10 sections cut through a control block. Should the new control be deemed unsatisfactory, at the staining stage, this finding is referred to the project manager for discussion. The Staining Record is reviewed by the Project Manager (or delegated person) to help resolve the issue (DOC/004).

When the first control block of tissue contains only four assessable duplicate cores (4 x 2 = 8 QC cores), the putative new positive block will be prepared, cut and stained alongside the current control on **five** separate occasions. The same procedure will be followed if the architecture of the tumour(s) substantially changes as the TMA is cut through, such that a representative range of expression is no longer seen across the cores.

8. IMMUNOHISTOCHEMICAL STAINING PROCEDURE

8.1. WORKING SOLUTIONS (According to the manufacturer's instructions)

- Dako DAB Away DAB Chromogen Removal System (S1967) reagents to be used as described to clean the Autostainer when prompted on screen.
- Hazardous waste receptacle contains approximately 500mls diluted Milton (Laboratoire Rivadis): 1 tablet Milton dissolved in about 5000mls tap water.

- Low pH Target Retrieval Solution about pH 6.0 (Dako, S2031 or HercepTest K5207).
 - Wash Buffer (Dako, S3006 or K5207)
 - REAL Peroxidase-Blocking Solution (Dako, S2023) neat unless otherwise stated on the bottle or manufacturer's instructions.
 - Ki67 MIB-1 clone (Dako, M7240).
 - REAL Kit (Dako, K5001) use neat from bottles (A) & (B) and use 20ul from small bottle of DAB+Chromogen / 1ml HRP Substrate Buffer from bottle (D), unless otherwise stated on the bottle or manufacturer's instructions.
 - Antibody diluent (Dako, S2022).
 - Mayer's Haemalum (TCS Biosciences, HS315).
 - DPX (Merck, HX 808712-UN 1307).
 - IMS (Genta, CAS No 64-17-5).
 - Xylene (Genta, CAS No 1330-20-7).
- 8.2. Clean Autostainer, if prompted on screen, before starting a staining run.

8.3. Dewax sections in at least two changes of xylene for approximately 5mins. in each (coated/dipped slides will take at least 30 minutes to dewax).

8.4. Rehydrate sections and bring to water by immersing for 1-2mins. in each of decreasing grades of industrial methylated spirits (IMS) 100%, 90%, 80%, 70%.

8.5. Pre-heat 700ml of Target Retrieval Solution (TRS) low pH (pH 6.0) by microwaving on full power (900W) in plastic receptacle for 5mins.

8.6. Without delay place rehydrated sections in the pre-heated TRS and microwave on full power for 10 minutes. **It is important to place the antigen retrieval pot and rack of slides as directed in Figure 1.** Then, immediately remove pot from the microwave oven, remove lid, and place in sink of cold water to cool for about 20 minutes (water should not overflow into pot).

8.7. The Autostainer can be started at this stage, if not already done so, and the reagents could be pre-prepared whilst these slides are cooling.

8.8. Remove rack of sections from pot and rinse briefly in tap water and then soak in Wash Buffer (K8007, Dako UK Ltd).

8.9. Programme Autostainer according to SOP MET/028 up to step where protocol template is selected. Use "**abreal**". Then select "Use Template".

- 8.10. Go to AUTO and click on “program” upon which “abreal” will appear in a box at the bottom left hand corner of the screen. Click the “abreal” box, once for each slide.
- 8.11. If the position of the negative control is not already pre-programmed, add it now. Change “Program” back to AUTO and click on cell you want to alter.
- 8.12. The default programme for “abreal” is ER. To change primary antibody to MIB-1 click on PRIMARY ANTIBODY box on grid (Table 1). Select EDIT SLIDE from scroll down list and change antibody and time information to MIB-1 for 20 mins click OK. Repeat this for the number of MIB1 test slides.
- 8.13. ALTERNATIVE PROGRAMMING METHOD: Open the pre-programmed run for 47 slides available from the main menu and called “**realmib1**”. This run is for 46 test cases and one negative control at position 3.
- 8.14. Print out one copy of the program grid and keep with IHA Staining Record.
- 8.15. Press NEXT twice.
- 8.16. Run Time window will show “Probe Washes”, buffer and distilled water volumes required contained in labelled aspirators under bench).
- 8.17. Figure 2 will also show the volume of each reagent that is required.
- 8.18. Save program with Date, am or pm (start time if a night run) or any other information according to study specific work instructions.
- 8.19. Decant reagents/antibodies into labelled (REA/001) vials and place in the appropriate slots as indicated by the Autostainer reagent layout in Figure 2 which shows the co-ordinate position of each vial of reagent to go in the white rack. When opening a reagent pot for the first time hand-write “opened on date” on the pot, or mark the tube to indicate it is in use. This is helpful if there are several yet to be opened pots within the same kit.
- 8.20. Check the non-hazardous waste receptacle is empty. The hazardous waste receptacle contains approximately 500mls diluted “Milton” i.e. 1 Milton tablet dissolved in about 500mls tap water.
- 8.21. Remove the long black slide racks, which are able to hold a maximum of 12 slides each, and prop up temporarily for ease of loading. Place sections in the Autostainer racks (starting at the far left on front row of the machine) and cover with Dako Wash Buffer at regular intervals to prevent sections drying out whilst they are all loaded. Load slides with labelled end first. Re-position the loaded slide rack/s securely.
- 8.22. Click on NEXT twice.
- 8.23. Before starting run check machine’s arm pathway clear, then click “yes” and

continue as prompted.

8.24. Remove sections into vessel containing water on completion of the run. Ensure the sections do not dry out. Rinse approximately one minute in running tap water.

8.25. Sign off from the main menu and shut down the computer.

8.26. Counter-stain with Mayer's Haematoxylin solution for 1min.

8.27. Blue in running tap water for about 5 minutes.

8.28. Dehydrate, clear and mount.

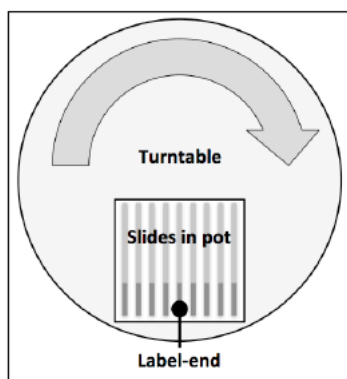


Figure 1. Orientation of antigen retrieval pot, the slides and the slide rack on the microwave oven turntable.

Fill plastic slide rack (holding 25 slides) with test and control slides (all orientated with label at same end).

Empty slots should be filled with plain slides so that all slides are equally exposed to heating.

Turn the end slide around with section is facing towards neighbour. This should ensure that the thermodynamic movement of the antigen retrieval solution is the same for all the sections.

Place the slide rack into the antigen retrieval pot and place the pot on the outer edge of the turning microwave plate, with label-end of slides facing out.

The rotation of the microwave plate maximizes the likelihood that all slides are exposed to the same amount and intensity of microwaves and hence thermic antigen retrieval.

Table 1. Grid run sequence of Autostainer (Realmib1 option).

RINSE	Avidin Block	RINSE	Biotin Block	RINSE	Endo. Enzyme Block	RINSE	MIB-1 1:50	RINSE	Biotin-ylated Link (A)	RINSE	Strept-ABC (B)	RINSE	RINSE	SWITCH	DAB Substrate (C+D)	RINSE
	15mins.		15mins.		5mins.		20mins.		15mins.		15mins.				10mins.	

Figure 2. Example of the Autostainer reagent grid. Always use the grid produced by the Autostainer for the specific run (colour-code relates to the colour of solutions).



9. TEST SAMPLES

Stain in sets with all the study time-points stained together in one run.

10. ASSAY ACCEPTANCE CRITERIA

The assay acceptance criteria are based on pre-validated positive controls. The control result in each staining batch must fall within the pre-defined range. Score the control first, if the control score is within range score the test samples. If the control does not fall within the pre-defined range consult with the Project Manager and colleagues in the team. It is only necessary to make a record in the Issues Log: Review and Action Document if Project Manager deems it necessary.

The positive antibody quality control for this assay is a TMA formed from cores taken from samples from human breast cancer tissues, (xenografts or FFPE pellets of cell lines may also be included). The cores should represent a range of expression levels, and generally 2 cores of each expression level should be assessed. Examples of control TMA formats are in MET/029. The specific arrangement of the Ki67 control TMA to be used in a clinical trial will be described in the study work instruction. One section from this TMA will be included in each antigen retrieval vessel.

The defined ranges will be used as the criteria for assessing the analysis of QC samples concurrently with study derived samples by those reviewing data. Assuming that QC

data follows a Gaussian distribution approximately 95% of values are expected to lie within a range of +/- two Standard Deviations (SD) from the mean value. Statistically, approximately a further 4% of values will be expected to fall within the ranges lying between 2 and 3 SD above or below the mean value.

The minimum requirements for the QC assay to be accepted are:

- not more than **two** samples with QC values falling outside the +/-2SD range (but inside +/-3SD) *with, in addition*
- not more than **one** sample with a QC value falling outside the +/-3SD range

If a QC TMA produces results that are not acceptable, a selection of 20% of tests in the batch shall be re-tested. If the results of the repeats are substantially in agreement with the failed batch then accept the 'failed' batch. When comparing the result of the 'failed' tests with the repeats of these tests apply the decision-making criteria as described in Section 14 of this SOP.

11. REPEAT ANALYSES: ATYPICAL RESULTS AND ANALYTICAL DEVIATIONS

Any atypical result or analytical deviation must be investigated and recorded according to prescribed procedures. This procedure describes how analytical deviations and atypical results are defined, reported, documented and investigated. This process applies to the Ki67 analysis of patients' samples conducted as part of a clinical trial in laboratories of the Academic Department of Biochemistry. Carry out investigations, together with the Project Manager, relating to the atypical result(s) and analytical deviation(s).

Ensure that an investigation has been carried out and documented before beginning any retesting. The Issues Log to be filled in and signed by the analyst and signed by the Project Manager or designated person after resolution of the problem.

Definitions

Atypical Result: result that falls outside the acceptance criteria as defined in the analytical method or where a result appears abnormal for example by excessive non-nuclear staining. An abnormal result might be one that is higher/lower than theoretically expected and includes QCs and test samples.

Analytical Deviation: where a process has deviated from the defined instructions. Examples would include an analytical run terminated early as a result of equipment malfunction, QCs or test materials not analysed in the defined sequence.

Resample: subsequent sample of the same original test sample (e.g. a second section from the FFPE original tissue block).

Re-analysis: additional testing performed on the re-sampled tissue section.

Responsibilities of the analyst: to check the results they have obtained. Should any atypical results occur to refer these and analytical deviations to the Project Manager.

Responsibilities of the project manager: to ensure that the atypical result and/or analytical deviation investigation is completed in accordance with this SOP, that the cause is defined where possible and any resulting actions are documented and carried out within the defined time scales.

Re-analysis of the original samples: the objective of re-analysis of a sample is to confirm or refute results whose validity is in doubt. It is not Laboratory Policy to perform re-analysis for every result falling outside of the expected range for the biomarker in question. The requirement for re-analysis may become apparent during the conduct of the analysis, or during review of the generated data.

SAMPLES WILL BE RE-ANALYSED UNDER THE FOLLOWING CIRCUMSTANCES:
Failure of the Quality Controls due to results outside the expected range or results are displaying excessive variance.

Abnormal pattern of staining is observed. This could include counter staining that does not allow scoring of positive or negative cells. Should the quality of the tissue be 'not assessable' then a full set of fresh sections from the batch shall be repeat stained. This repeat staining is noted in the original scorer's lab book and in the lab book of the person scoring the repeat sample. This can be the same person as long as notes and repeat batch number described in writing with the source data.

Reagent depletion or reagent addition failure is suspected.

A grossly atypical value is observed for the test sample under investigation, or a value highly unlikely or impossible.

If sample availability is limited the Project Manager must be informed before proceeding further in order that analytical priorities may be established and observed. The results generated by re-analysis will be compared with the original values, where these are not compromised by known analytical deficiencies.

If the results of re-analysis support the original value then the original value will be reported. If the results of re-analysis support each other but not the original result then the first re-analysed result will be reported.

If the results of re-analysis do not support each other or the original result, further re-analysis will not be undertaken without first consulting the Project Manager.

Repeat analysis may include accompanying samples from previously accepted batches to act as extra QCs.

Investigation

The likely cause and decisions taken regarding atypical results and deviations will be summarized and documented by the Project Manager or designated member of the study team.

The investigation is led by the Project Manager and may include a review of the analysis, e.g., method calculations and reagents used and instrumentation.

Corrective actions may be identified as part of the investigation. These must be documented and also recorded in the Issues Log: Review and Action document by writing on the back of the Issue Log sheet and adding further sheets stapled together. If an error or instrument problem has occurred a review must be performed to assess the effect of this error/ instrument problem on previous analyses.

12. SCORING

The following procedure describes the process for scoring. Also refer to specific study work instructions as applicable.

12.1. Equipment for scoring

1. Stained positive control tissue section. 2. Test sections. 3. Differential Cell Counter containing at least 2 key counters (for counting positive and negative cells), with alarm at 100 increments (e.g. Scientific Supplies and Technology, cat. no. CHESVDBC6TEA) 4. A bright-field microscope, equipped with a range of objectives (typically, x5, x10, x20, x40) and x10 ocular eyepieces, one of which should contain a 10 x 10mm graticule, with 1mm divisions.

12.2. Guidelines

Count only within the area overlain by the graticule using the x40 objective (equivalent to one high-power field, HPF).

The Ki67 %-positive (score) is calculated as a percentage to two decimal places and rounded to one decimal place:

$$\text{(Total number of Ki67-positive ITC's / Total number of ITC's) x 100}$$

12.3. Definition of positive staining

Ki67 is a nuclear protein and only invasive cells exhibiting brown nuclear staining are included in deriving the score. Cells staining in any of the categories 1 (faint), 2 (moderate) and 3 (strong) are considered positive. Cells showing an absence of brown nuclear staining are considered negative

Samples with poor fixation, preservation, etc. for which a score cannot be obtained should be reported as 'NA' (not assessable).

Samples where identification of invasive tumour areas is uncertain should be reviewed with a pathologist and temporarily reported as REV.

Samples where there are less than the required number of invasive cells available to count are called IIT (insufficient invasive tumour). A lowering of the minimum number of cells can only be approved by the Head of Department and supported by experimental evidence and validation.

12.4. Field selection using GLOBAL METHOD

Specify the percentages of invasive tumour in the sections that exhibit various levels of Ki67 scores ("levels" is defined below).

Specifying the percentages

Examine the entire glass slide section using low-power magnification (with 4x, 10x objectives).

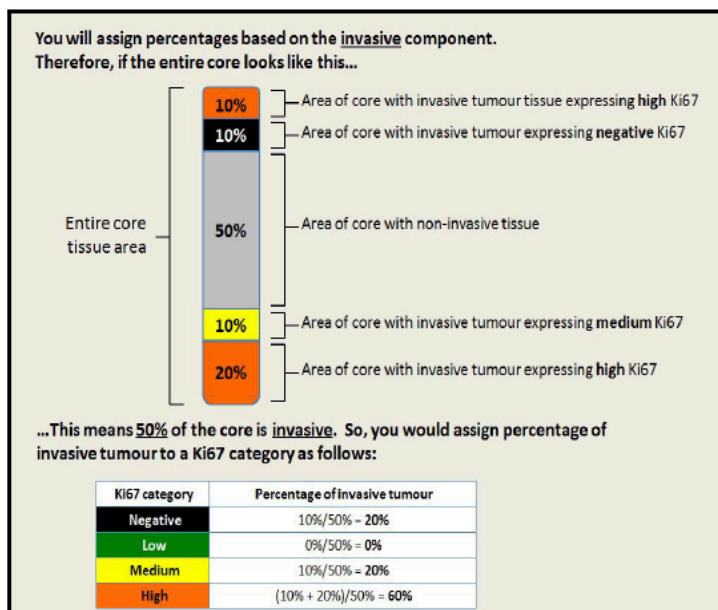
Estimate the percentages of the invasive tumour in the glass slide that exhibit the following Ki67 levels:

- Negative (i.e., contains invasive cells but a very low, including zero, percentage of positive invasive cells)
- Low
- Medium
- High

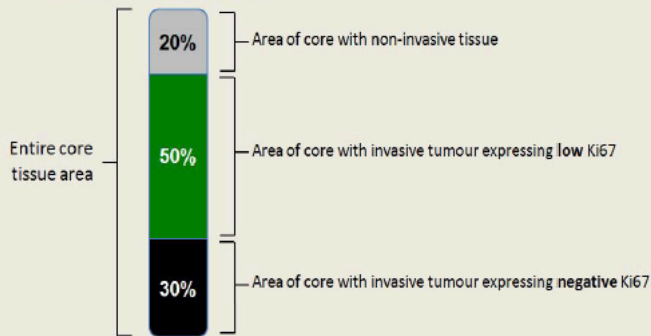
Areas with increased Ki67 positivity, including areas towards the edge of the tumour, as well as non-proliferating areas of invasive tumour cells, must be included in your assessment.

IMPORTANT: Heterogeneity of percentage of cells staining positive frequently occurs across a section. Therefore, scorers should select regions for scoring that are High, Medium, Low, or Negative in relation to the overall percentage positivity. Thus, “Negative”, “Low”, “Medium”, and “High” are meant to be relative determinations, based on each particular case, and do not reflect specific absolute values. Please see the examples provided below, which illustrate this concept.

Examples illustrating how to estimate the percentage of Ki67-stained invasive tumour nuclei



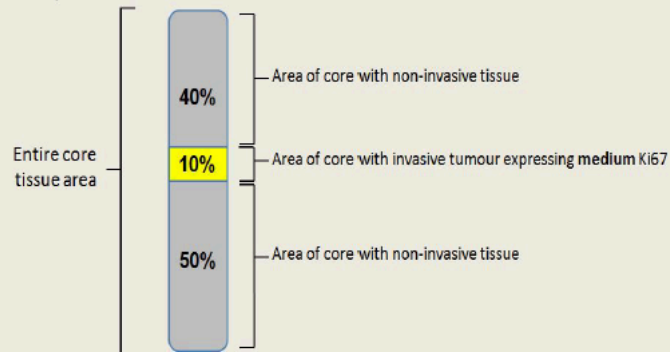
You will assign percentages based on the **invasive** component.
Therefore, if the entire core looks like this...



...This means **80%** of the core is **invasive**. So, you would assign percentage of invasive tumour to a Ki67 category as follows:

Ki67 category	Percentage of invasive tumour
Negative	$30\%/80\% = 37.5\%$
Low	$50\%/80\% = 62.5\%$
Medium	$0\%/80\% = 0\%$
High	$0\%/80\% = 0\%$

You will assign percentages based on the **invasive** component.
Therefore, if the entire core looks like this...



...This means **10%** of the core is **invasive**. So, you would assign percentage of invasive tumour to a Ki67 category as follows:

Ki67 category	Percentage of invasive tumour
Negative	$0\%/10\% = 0\%$
Low	$0\%/10\% = 0\%$
Medium	$10\%/10\% = 100\%$
High	$0\%/10\% = 0\%$

Assigning number of representative fields

Assignment of number of representative fields to score is done according to criteria shown in Table 2.

Table 2. Number of Ki67 levels represented

Number of Ki67 levels represented (High/Medium/Low/Negative)		Number of fields to score
One Level (e.g. 100% High Ki67)		4 fields are assigned to the one level Total number of fields to score: 4
Two Levels	• If the difference in the % representation of the two Ki67 levels is <25% (e.g. 40% high, 60% medium)	2 fields are assigned to each level Total number of fields to score: 4
	• If the difference in the % representation of the two Ki67 levels is >=25% (e.g. 20% high, 80% medium)	3 fields are assigned to the highest % level 1 fields is assigned to the lowest % level Total number of fields to score: 4
Three Levels	• If there are ties (e.g. 40% high, 40% medium, 20% low)	1 field is assigned to each level Total number of fields to score: 3
	• If there are no ties (e.g. 10% high, 65% medium, 25% negative)	2 fields are assigned to the highest % level and 1 field is assigned to each of the other two levels Total number of fields to score: 4
Four Levels		1 field is assigned to each level Total number of fields to score: 4

Scoring the representative fields

Identify representative fields using low-power magnification.

In selected field, using high-powered (40x) objective) microscope start scoring at the top of the grid.

Count nuclei in a “typewriter” pattern, until 100 invasive tumour nuclei in total are scored. When you reach 100 nuclei, the counter will sound.

Score as many fields as the number calculated according to Table 2 for each Ki67 level.

A maximum of 400 cells and a minimum of 200 cells are required to be scored in each core biopsies or excision/resection samples.

The fields selected must be representative of the biological heterogeneity observed across the sample, regardless of it being a core biopsy or a resection specimen. Any 'hot-spots' or areas of increased staining density towards the edge of tumours should be included. The fields to be included in the score are chosen on the basis of the observer's interpretation of the relative proportion of each of these areas within the sample.

13. DATA RECORDING AND RESULT REPORTING

Scores are recorded in a Study notebook (ID/ABC/DATA/IHC Ki67/1). ID is initials of observer, ABC is study identifier and 1 is raw data notebook number. Each case scored must be completed in one scoring session.

Result and report sheets are study specific. The result and report sheets may be designed in the Academic Department of Biochemistry or may be provided, in template form, by the sponsor of the clinical trial. Should the report form be an EXCEL spreadsheet for purely presenting the data, not for calculations, this has to be appropriately protected according to study specific work instructions. Should the Report Form be in a Word document then this has to be saved as a PDF. Certified hard copies have to be kept in an appropriately labelled secure Study File.

The observer should write alongside this raw data '*scored by "ID" (initials) on "date"*'. This constitutes the Source Data.

Any doubts about invasive content of samples are referred to team pathology review sessions or a pathologist review.

14. REVIEWING OF Ki67 BIOMARKER

Refer to Policy relating to Auditing (QSP/002) and to the specific study work instructions. Flag up problematic score to the project manager and discuss with colleagues in the team. Although specific study work instructions take preference, in the absence of these, the generic review summary workflow (Figure 3) is to be followed.

14. 1. 10% of the sections are to be visually assessed ie sample approximately every 10 slides in the scorebook in order to achieve at least 10% of the visual review of the slides within a study. Some studies may require all Ki67 slides to be reviewed therefore refer to study specific work instructions. Doubts about invasive content can be checked by a pathologist at a different time.

14.2. Re-scored score/s are source data and entered into Laboratory notebook/Notebook (ID/ABC/DATA/IHC Ki67/1). The Reviewer in the Academic Department of Biochemistry would be a member of the scoring team who had not scored the section before. **WHEN MAKING DECISIONS ABOUT ACCEPTABILITY OF THE SCORE REFER TO DECISION MAKING CRITERIA in 14.3.**

14.3. AT REVIEW – DECISION-MAKING CRITERIA:

14.3.1. In the event of a difference of opinion requiring re-scoring, and the original score is < 10 % and the reviewer re-scores the section and an absolute difference of less than 2% occurs between the assessor and the reviewer the original score is accepted. Example decisions at the 10% review process between 2 assessors, if %Ki67 score < 10 + 2 = Accept, are shown in Table 3 below.

Table 3

Eg	Assessor	Reviewer	Accept/Reject
1	7%	9%	Accept assessor's score
2	10%	12%	Accept assessor's score
3	10%	8%	Accept assessor's score
4	10%	14%	Reject score and follow workflow in Figure 3

14.3.2. In the event of a difference of opinion requiring re-scoring, and the original scores > 10 % and the reviewer re-scores the section and a relative difference of less than 20 % occurs between the assessor and the reviewer then that is an acceptable result. Refer to Table 4 for examples.

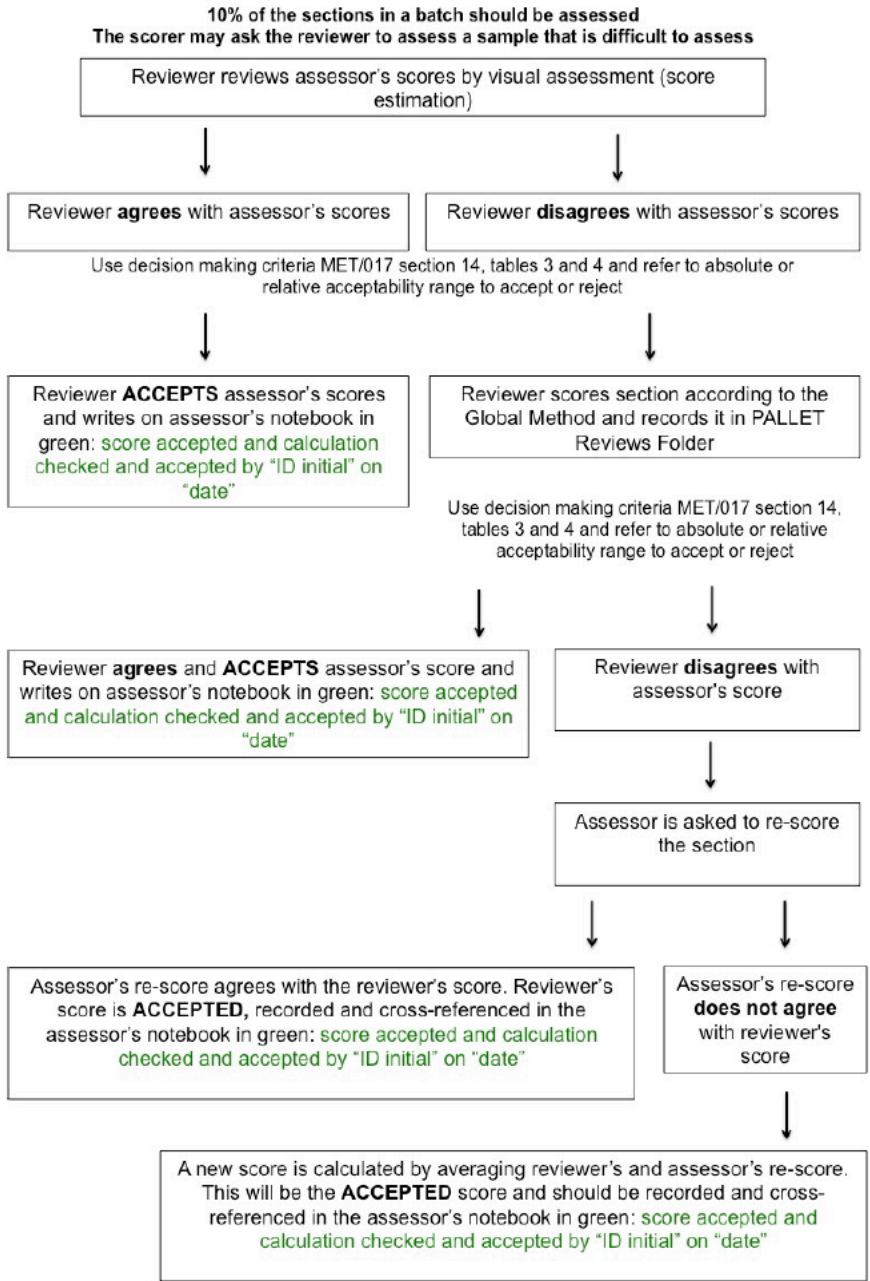
Table 4

Eg	Assessor	Reviewer	Accept/Reject
1	25%	20%	Accept assessor's score
2	11%	14%	Reject score and follow workflow in Figure 3
3	15%	12%	Accept assessor's score
4	50%	38%	Reject score and follow workflow in Figure 3

14.4. Periodically intra-observer checks to be instigated and reviewed by the Head of Department.

14.5. Ki67 results will also be subject to QA audit by the RMH QA and/or an External Auditor. The timing will be according to Study specific work instructions.

Figure 3. IHC score review workflow



Thanks

A special thanks to:

The patients and their families for their participation in the RIO trial.

Nick for believing RIO would be a success and directing the project in the right direction.

Alex for teaching me the science behind the project, I will be a better clinician for it. And for his cycling knowledge...I now have a great bike!

Ben and Inaki for their sequencing knowledge and always being available for questions no matter how small.

Matthew for always knowing where assays are and showing me the scientists way. And being an encouraging strava friend.

Molecular Oncology for being such a support when things were tough. Always reassuring me that research is slow but worth it at the end.

Breast Cancer Now and the ICR IT team for all the help with administration, constant MAC issues and the supply of cake.

And off course, Darpan and the kids, Aria, Veer and Leya who keep me going with their constant love and hugs.